AN INVESTIGATION OF CADMIUM, ZINC AND LEAD ISOTOPE SIGNATURES AND THEIR USE AS TRACERS IN THE ENVIRONMENT

by

Alyssa Erin Shiel

B.Sc., The University of Arizona, 2003

A THESIS SUBMITTED IN PARTIAL FULFILLMENT OF
THE REQUIREMENTS FOR THE DEGREE OF

DOCTOR OF PHILOSOPHY

in

The Faculty of Graduate Studies

(Oceanography)

THE UNIVERSITY OF BRITISH COLUMBIA
(Vancouver)

August 2010

Abstract

Environmental monitoring and remediation require techniques to identify the source and fate of metals emissions. In this study, Cd and Zn isotopes were evaluated as tools for the identification of metal sources through (1) the assessment of metallurgical processing as a source of Cd and Zn isotopic fractionation and (2) the measurement of isotopic compositions in bivalves from sites receiving variable metal contributions from natural and anthropogenic sources. This study was facilitated by the successful development of a technique to measure Cd and Zn isotopes (MC-ICP-MS) in environmental and anthropogenic samples.

Cadmium, Zn and Pb isotopic ratios were measured for samples from an integrated Zn–Pb smelting/refining complex in B.C. (British Columbia, Canada). Significant fractionation of Cd and Zn isotopes during processing is demonstrated by the total isotopic variation in $\delta^{114/110}$Cd (1.04‰) and $\delta^{66/64}$Zn (0.42‰) among smelter samples. Characterization of Cd and Zn isotopic compositions in emissions as fractionated relative to ores demonstrates the tracing capability of this new tool. Moreover, Pb isotopic signatures may be used to identify sources contributing metals to environmental samples.

Combined Cd, Zn and Pb isotope systematics were used to trace the source and distribution of these metals in bivalves from western Canada (B.C.), the USA and France. Variability in $\delta^{114/110}$Cd of bivalves (-1.20 to -0.09‰) is attributed to differences in the relative contributions of Cd from natural and anthropogenic (e.g., smelting) sources between sites. High Cd levels in B.C. oysters are identified as primarily natural, with some additional variability attributed to anthropogenic sources. In contrast, high Cd levels in French bivalves (Gironde estuary and Marennes-Oléron basin) are primarily anthropogenic. Variability in $\delta^{66/64}$Zn values exhibited by bivalve samples is small (0.28 to 0.46‰), with the exception of oysters from the polluted Gironde estuary (1.03 to 1.15‰). Lead isotopes are used to identify emissions from industrial processes and the consumption of unleaded gasoline and diesel fuel as metal sources to bivalve samples.

This study demonstrates the effective use of Cd and Zn isotopes to trace anthropogenic sources in the environment and the benefit of combining these tools with Pb "fingerprinting" techniques.

Table of Contents

List of Tables

List of Figures

CHAPTER 1

CHAPTER 2

CHAPTER 3

CHAPTER 4

Acknowledgements

There are many people I would like to thank for their support and encouragement, not only of my decision to pursue a Ph.D. but also during the journey, as all of them contributed to my success. First, I would like to thank my supervisors Dominique Weis and Kristin Orians for the opportunity to conduct this research and for their support throughout this project. I am especially grateful to Dominique, who, in addition to keeping my office stocked with Belgian chocolate, always had an open door, was available for scientific discussions and pushed me to progress. Her support and understanding, especially at the end, will not be forgotten. I would like to give a special thanks to Kristin for her contributions to this work, her advice and her commitment to my academic development. I would like to thank Roger Francois, who provided expertise and encouragement, especially when I was first undertaking work with Cd isotopes. I wish also to thank James Scoates for contributing to my overall academic growth, giving me advice and providing comments on my writing and presentations.

I am especially grateful to Jane Barling, who in addition to training me to operate the Nu and helping me set-up a Cd measurement method, has always shown a keen interest in my work and has asked probing questions that have benefited my research. My scientific writing has been improved greatly by comments from Jane. I am thankful for the help of Bert Mueller and Maureen Soon, who helped whenever asked, sharing a lot of their time and expertise. I am also grateful to many other talented researchers and support staff in EOS and PCIGR including Rich Friedman, Vivian Lai and Bruno Kieffer. I would like to thank George Kruzynski and Bill Heath for providing the B.C. oyster samples, for their interest in the Cd isotope study of B.C. oysters and for answering all my questions (especially while I was preparing for my candidacy exam). I would also like to thank all the EOS administrative staff for their friendliness and dedication, especially Cecilia Li, Carol Leven, Alex Allen and Cary Thomson.

I am thankful for the friendships of many other grad students in EOS and Chemistry, this experience would not have been the same without them. During my first few years, I was fortunate to share an office with Cheryl Wiramanaden, Sabrina Crispo and Anka Lekhi. I am grateful for their help in solving analytical problems, as well as

their friendships. Cheryl and Sabrina are especially thanked for teaching me how to work in a trace metal clean lab and how to survive as a grad student. After Cheryl, Sabrina and Anka graduated, I was welcomed into the "bowling alley" and I am grateful for the many supportive friends I have made during my residence there, especially Inês, Elspeth, Katrin, Caroline, Laure and Diane. Inês Nobre Silva and Elspeth Barnes helped ground me during the crazy period at the end and were there to congratulate me at each milestone (often with a glass of wine).

I am very thankful for the support of my family and friends. Very special thanks go to my parents, Wally and Holly, for raising me to work hard and to embrace challenges, and together with my sister, Diana, for the encouragement, frequent phone calls and visits. Another special thanks goes to Mike for his understanding and support, especially during the more stressful periods. Many thanks go to my very supportive extended family Anne, Arisia, Ajana and Alan Lee. Many of my best memories include them, including camping and backpacking trips, especially the trip to Europe, and their visits to Vancouver. I would like to extend my gratitude to Ann Marie Wolf and Anna Spitz, for allowing me to participate in the wonderful work being done at the Sonora Environmental Research Institute, Inc. (SERI) and for encouraging me to go to grad school. Last but not least, I would like to thank my best friends in the world, Mel, Mindie and Will in Tucson, Debbie and Eric in Austin and Leila and Jamie in London, for their friendships and support over the years, as well as for endless memories of good times.

Co-authorship Statement

This dissertation includes three manuscripts (Chapters 2, 3 and 4); I am the lead author of each of the three manuscripts. The three manuscripts are all co-authored by my supervisor, Dominique Weis, and my co-supervisor, Kristin J. Orians. They both provided financial support to the research carried out in this dissertation. Specific contributions to each manuscript are described below.

In preliminary efforts that facilitated the results presented in each of the manuscript chapters, the lead author:

- designed the set-up of the Cd isotopic method on the Nu Plasma MC-ICP-MS at PCIGR (UBC) with Jane Barling, based on a published method and adapted the method for the purpose of this dissertation;
- prepared samples for chemical analysis, including sample digestion and analytical separation techniques, as appropriate;
- performed all elemental and Cd, Zn and Pb isotopic analyses;
- interpreted all data;
- wrote up research results and prepared all figures and tables;
- prepared manuscripts for publication in peer-reviewed international scientific journals.

Chapter 2

Matrix effects on the multi-collector inductively coupled plasma mass spectrometric analysis of high-precision cadmium and zinc isotope ratios

Authors: Alyssa E. Shiel, Jane Barling, Kristin J. Orians and Dominique Weis

In addition to the above, the lead author:

- identified compromised Cd and Zn isotopic data quality;
- reviewed existing literature of matrix effects on MC-ICP-MS analysis;
- investigated the source of identified inaccuracies and imprecision through a series of experiments evaluating matrix effects on Cd and Zn isotopic analyses;

- developed and implemented solutions, including modifications to the Cd and Zn isotopic sample preparation techniques.

Jane Barling co-authored this manuscript; she and my supervisor, Dominique Weis, contributed to the development of this project, the interpretation of the results and provided comments on multiple versions of the manuscript. My co-supervisor, Kristin J. Orians, provided comments on the final version of the manuscript.

Chapter 3

Evaluation of zinc, cadmium and lead isotope fractionation during smelting and refining

Authors: Alyssa E. Shiel, Dominique Weis and Kristin J. Orians

In addition to the above, the lead author:

- identified the opportunity for unique study;
- initiated the participation of Teck;
- selected smelter samples;
- developed an understanding of smelting processes;
- undertook literature review of fractionation of Cd and Zn isotopes;
- evaluated smelting and refining operations as sources of isotopic fractionation.

I initiated this project with my supervisor, Dominique Weis, to assess the anthropogenic contribution to Cd and Zn isotope systematics in B.C. Smelter samples were provided by John F.H. Thompson (Teck Resources Ltd., VP Technology and Development). Michael Heximer (Teck Metals Ltd.) significantly contributed to this study by assisting with sample selection, providing expertise on smelting processes and reviewing the manuscript. My supervisor, Dominique Weis, provided comments on multiple manuscript versions. The manuscript significantly benefited from comments provided by Jane Barling. My co-supervisor, Kristin J. Orians, provided comments on the final version of the manuscript.

Chapter 4

Tracing cadmium, zinc and lead pollution in oysters from the coasts of western Canada, the USA and France using isotopes

Authors: Alyssa E. Shiel, Dominique Weis and Kristin J. Orians

The lead author:

- coordinated the participation of bivalve samples from the USA and France
- investigated natural variability of Cd and Zn isotopes and evaluated their use as tracers of anthropogenic emissions
- traced anthropogenic Pb using Pb isotopes.

The initial premise (B.C. part) for the study came from my co-supervisor, Kristin J. Orians, George M. Kruzynski (Fisheries and Oceans Canada) and my supervisor, Dominique Weis. The expansion of the study to include bivalves from France and the USA and to broaden the scope of the isotopic study by integrating Pb isotopic compositions (fingerprinting) was developed through my discussions with Dominique Weis.

B.C. oyster tissue samples, as well as assistance with sample selection, were provided by George M. Kruzynski, William Heath (B.C. Ministry of Agriculture Food and Fisheries) and Leah I. Bendell (Simon Fraser University). Didier Claisse and Daniel Cossa (IFREMER, France) from the French monitoring network (RNO) provided bivalve samples from coastal France. Gunnar Lauenstein (NOAA, U.S.A.) from the Mussel Watch Project of the U.S. National Status and Trends Program provided bivalve samples from the USA East Coast and Hawaii. This manuscript benefited from my discussions with Dominique Weis, Kristin J. Orians, George Kruzynski, William Heath and Daniel Cossa and the review of multiple manuscript versions by Dominique Weis. In addition, Kristin J. Orians and Jane Barling provided constructive reviews of this manuscript.

In addition to that provided by the supervisory committee, noteworthy academic support was provided regularly by James S. Scoates, who also reviewed portions of each manuscript chapter.

CHAPTER 1

Introduction

1.1 Introduction

Metal contamination of the environment poses a risk to the health of natural ecosystems and resident organisms and can have devastating implications for human health. Environmental monitoring and assessment techniques, which evaluate the source, transport and fate of metals in the environment, are instrumental in assessing the impact of metal emissions and maximizing the efficiency of remediation strategies. Some trace metals, e.g., zinc (Zn), are essential micronutrients (biologically necessary), whereas, cadmium (Cd), and lead (Pb) are non-essential metals and may be toxic even at low concentrations. The concentration of the micronutrient Zn is much higher than those of Cd and Pb in human blood (Table 1.1), reflecting its significance in human nutrition and health. Cadmium and Pb compounds are carcinogenic and can cause birth defects (Emsley, 1998). There is a low risk of severe or fatal Cd poisoning from ingestion due to the associated emetic action (i.e., induces vomiting). However, cumulative exposures to Cd cause accumulation in the kidneys and eventually renal dysfunction (Elinder and Järup, 1996). Endemic outbreaks of renal disease have been reported in areas of Japan from repeated Cd exposures consequent to the consumption of rice grown on soils polluted by mining and ore processing (Nogawa and Ishizaki, 1979). In the case of Pb ingestion, most Pb passes through the body without being absorbed but Pb poisoning is cumulative; e.g., Pb poisoning is reported in children from exposures to soil and dust contaminated with Pb from leaded gasoline and lead-based paints (Mielke and Reagan, 1998).

Cadmium, Zn and Pb are present in the natural environment (e.g., continental crust and seawater) at trace levels (Table 1.1), with the exception of the much higher concentrations found in ores. Environmental sources of these metals include natural sources (e.g., for all these metals, the weathering of rocks and volcanic activity, and in the case of Pb, radioactive decay) and anthropogenic sources. Major metal pollution results from the combustion of fossil-fuels by stationary (e.g., power plants) and mobile (e.g., automobiles and air planes) sources, mining, smelting, manufacturing and waste incineration. In the USA, national emission standards exist for the release of hazardous air pollutants (Clean Air Act) and Priority Pollutants (Clean Water Act), which include

Cd, Zn and Pb. In addition, industrial and federal facilities must report releases of chemicals on the toxic release inventory list (e.g., Cd, Zn and Pb) to the US Environmental Protection Agency (US EPA).

1.1.1 Anthropogenic perturbations of natural Cd, Zn and Pb distributions

Significant anthropogenic emissions may be much larger than natural inputs and thus greatly impact the natural geochemical cycling of heavy metals. Anthropogenic activities have long lead to disturbances in natural Pb levels and distributions. At least 5,000 years ago, Pb was produced as a by-product of silver metal production, which was refined from sulfide ores using smelting and cupeling techniques (Settle and Patterson, 1980). Mining and smelting operations, for the sole intention of refining Pb, have represented a significant portion of total Pb production only during the past century (Settle and Patterson, 1980). Globally, modern anthropogenic sources account for ~91% of total (sum of natural and anthropogenic) atmospheric Pb emissions to the environment (Pacyna and Pacyna, 2001).

In 1976, Pb concentrations in the bones of Americans were revealed to be ~500× higher than those measured in the bones of Ancient Peruvians (Ericson et al., 1979). Between the early 1980s and mid-1990s, a global decline (~64%) in Pb emissions to the atmosphere was observed (Pacyna and Pacyna, 2001). Reductions in atmospheric Pb emissions are related primarily to the introduction of unleaded gasoline and the phase-out of leaded gasoline for use in automobiles in Canada (banned in 1990), the USA (banned in 1996), and Europe (e.g., banned in France in 2000). In the USA, Pb consumption was 10× larger when Pb was used as antiknock additive in gasoline (Reuer and Weiss, 2002). Combustion of unleaded and leaded gasoline (the latter being gasoline treated with an organolead compound, most commonly tetraethyl lead) remains the major source of global atmospheric Pb emissions, accounting for approximately 74% of total anthropogenic Pb emissions (Pacyna and Pacyna, 2001).

Similarly, global anthropogenic emissions of Cd and Zn to the atmosphere are estimated to account for the majority (70% for Cd and 56% for Zn) of total (i.e., sum of natural and anthropogenic) emissions of these metals (Pacyna and Pacyna, 2001). The largest source of Cd and Zn emissions to the atmosphere is non-ferrous metal smelting

and refining, accounting for approximately 72–73% of anthropogenic emissions of these metals (Pacyna and Pacyna, 2001). Emissions of trace metals, including Cd and Zn, to the atmosphere from non-ferrous metal smelting and refining in North America and Europe decreased during the 1980/90s due to increasingly strict government regulations and the establishment of more efficient technologies for emission control. As a result, between the early 1980s and mid-1990s, a global decline (~61 or 57%, respectively) in atmospheric emissions of Cd and Zn was observed (Pacyna and Pacyna, 2001).

Recent studies have demonstrated the global impact of anthropogenic trace metal emissions to the atmosphere. In a study examining metal levels in ice from Greenland, Candelone et al. (1995) reported that levels of Cd and Zn were undetectable before the Industrial Revolution, in contrast, recorded Pb levels were already an order of magnitude above natural levels (compared with levels in ice deposited ~7760 yrs BP) by the late 18th century. Levels of Cd, Zn and Pb were reported to have increased from the beginning of the record (1774) until the 1960/70s and then to decrease during the following decades (Candelone et al., 1995). Planchon et al. (2002) measured trace metals in Antarctic snow/ice deposited from 1834 to 1990. They report enhancements during recent decades of Cr, Cu, Zn, Ag, Pb, Bi and U related to anthropogenic activities (largely non-ferrous metal smelting and refining) in the Southern Hemisphere, especially in South America, Southern Africa and Australia. They found no clear temporal trend for Cd.

Potential exists for the measurement of metal isotopic compositions to unequivocally trace the source of metal emissions. Identification of the source and fate of these anthropogenic metal emissions, and differentiation between natural and anthropogenic metals in the environment will aid in reducing environmental exposures and lead to improved environmental and human health.

1.1.2 Radiogenic isotope tracer– Pb stable isotopes

Lead has four stable isotopes with masses between 204 and 208, three (^{206}Pb, ^{207}Pb and ^{208}Pb) are the stable end products of radioactive decay chains (^{238}U, ^{235}U and ^{232}Th, respectively), while one is a non-radiogenic isotope (^{204}Pb). The Pb isotopic composition of anthropogenic emissions resulting from high temperature processes (e.g., fossil fuel combustion, smelting and refining) reflects the isotopic composition of the source

materials. As a result, Pb isotopic composition can be used to trace the source of Pb emissions in a technique called "fingerprinting". In addition, the relative contributions of both natural and anthropogenic Pb sources may be determined when the isotopic compositions of the sources are well constrained. This fingerprinting technique has proven to be a very useful tracer of Pb pollution (and other associated metals) in the environment for over the past three decades.

The utility of Pb isotopes as a tracer of anthropogenic emissions was first suggested by the work of Chow and co-workers (i.e., Chow et al., 1975), which demonstrated the large range in Pb isotopic composition found in leaded gasoline (i.e., ores), coals and aerosols (Reuer and Weiss, 2002). In an early study, Shirahata et al. (1980) discovered chronological co-related variations in both Pb concentration and isotopic composition; elevated Pb concentrations in surface sediment layers (~4× higher than the levels found in layers 130 yr old) were linked to industrial sources using Pb isotopes. Lead isotopes have been used to trace the source of Pb in, e.g., blood, animal tissues, groundwater, seawater and soils (see the review article: Weiss et al., 1999). In addition, Pb isotope measurements of various environmental archives (e.g., ice, peat bogs, sediments, corals, trees and lichens) have provided records of temporal changes in Pb emission sources (Weiss et al., 1999).

1.1.3 Mass-dependent fractionation

Although the isotopic compositions of other heavy metals, e.g., Cd and Zn, are not controlled by radioactive decay, mass-dependent fractionation of these elements may be used to trace the source of these elements in the environment. For elements with more than one isotope, mass-dependent fractionation can lead to natural variations in the isotopic composition of the element. The stable isotopic composition of a sample reflects that of the source plus any isotopic fractionation introduced by physical and chemical reactions (Peterson and Fry, 1987). Mass-dependent fractionation for an element is dependent on the relative mass difference for the isotope pair (the difference in mass between the isotopes, Δm, relative to the average mass of the element's isotopes). As a result, the relative mass difference decreases with increasing mass for $\Delta m=1$. For the traditional light stable isotopes, C and N, the relative mass differences for $\Delta m=1$ are 8%

and 7%, respectively. For heavier elements, such as Zn and Cd, the relative mass differences for Δm=1 are much smaller, 1.5% and 0.9%, respectively.

The light stable isotope systems, such as H, C, N, O and S, have been traditionally studied using isotope ratio mass spectrometry instruments; however, use of this technique is limited to light elements, which can easily be converted to common gases. Heavy isotope systems, both radiogenic and stable, have been studied using thermal ionization mass spectrometry (TIMS); recent TIMS instruments are equipped with multiple moveable collectors allowing the simultaneous collection of several masses, overcoming some earlier limitations associated with temporal stability of the ion beam. Isotopic analysis using TIMS instruments is limited to elements that can be ionized using the thermal source, which has a low ion yield (much less than 1%, usually less than 0.3%) (Felton, 2003). The ICP source, which can ionize 95% of the periodic table (Felton, 2003), affords the high ionization efficiency needed for the measurement of elements with high ionization potentials such as Zn and Cd.

The precision needed to measure the small natural variations in the isotopic compositions of heavy elements (produced by mass-dependent fractionation) has only been feasible in the last 15 yrs since the first multi-collector inductively coupled plasma mass spectrometry (MC-ICP-MS) instrument was introduced (Halliday et al., 1995). Prior to the MC-ICP-MS instrument, detection of the small variations in the isotopic compositions of elements with masses >40 was difficult or impossible (Weiss et al., 2008). MC-ICP-MS has become the preferred method for non-traditional stable isotope analysis and has facilitated the measurement of the small isotopic variations of most non-traditional stable elements (e.g., Zn and Cd) in terrestrial materials. Elements reported as under investigation using MC-ICP-MS include all elements, with two or more stable isotopes (i.e., excludes the listed elements: As, Be, Co and Mn), listed by the US EPA as hazardous air pollutants (Sb, Cd, Cr, Pb, Hg, Ni, Se) under the Clean Air Act and/or as Priority Pollutants (Sb, Cd, Cr, Cu, Pb, Hg, Ni, Se, Ag, Tl and Zn) under the Clean Water Act.

1.1.4 Cd and Zn isotope variations in the environment

Variations in the Cd and Zn isotopic compositions[1] of select geological, marine and anthropogenic samples are shown in Fig. 1.1 and 1.2, respectively. Maréchal et al. (1999) and Wombacher et al. (2003) developed MC-ICP-MS techniques for the accurate and precise determination of Zn and Cd isotopic compositions, respectively, laying the foundation for the numerous MC-ICP-MS studies of these elements that have followed. At the time this Ph.D. project was proposed, few studies had looked at natural variations in Cd isotopes using MC-ICP-MS. Terrestrial rock and mineral samples were reported to exhibit only small variations ($\Delta\delta^{114/110}$Cd = 0.88‰; Fig. 1.1) in Cd isotopic composition (Wombacher et al., 2003) with the exception of the value reported for a layered tektite (impact-related rock) ($\delta^{114/110}$Cd = 3.04‰; not shown in Fig. 1.1). High temperature processes (i.e., evaporation of Cd) were identified as a source of Cd isotopic fractionation (Wombacher et al., 2004). Cloquet et al. (2005) measured Cd isotopic variations in geological materials as well as anthropogenic samples (the latter shown in Fig. 1.1). A significant difference was reported (Cloquet et al., 2005) between the Cd isotopic compositions of smelter produced dust and slag ($\Delta\delta^{114/110}$Cd = 1.00‰; Fig. 1.1).

More recent work has included the determination of the Cd isotopic composition of seawater; first by Lacan et al. (2006) who measured Cd isotopes in depth profiles from the Northwest Pacific Ocean and Northwest Mediterranean Sea, and then by Ripperger et al. (2007), who measured seawater samples from the Atlantic, Southern, Pacific and Arctic Oceans (samples from the Atlantic and Pacific Oceans and the Mediterranean Sea are shown in Fig. 1.1). In addition, Lacan et al. (2006) demonstrated the preferential uptake of light Cd by phytoplankton in culture experiments ($\Delta\delta^{114/110}$Cd = -1.35‰). Schmitt et al. (2009) and Horner et al. (2010) measured the Cd isotopic compositions in ferromanganese crusts in an evaluation of their archiving of deep-water Cd isotopic

[1] Cd and Zn isotopic compositions of samples are reported in the standard delta (δ) per mil (‰) notation relative to the JMC Cd (Wombacher and Rehkämper, 2004) and "Lyon-JMC" Zn reference standards (Maréchal et al., 1999):

$$\delta^{114/110}\text{Cd} = \left(\frac{(^{114/110}Cd)_{\text{sample}}}{(^{114/110}Cd)_{\text{standard}}} - 1 \right) \text{x } 1{,}000$$

$$\delta^{66/64}\text{Zn} = \left(\frac{(^{66/64}Zn)_{\text{sample}}}{(^{66/64}Zn)_{\text{standard}}} - 1 \right) \text{x } 1{,}000$$

composition. The large study by A.-D. Schmitt et al. (2009) also measured Cd isotopes in MORB, OIB, loess and sphalerite (select samples are shown in Fig. 1.1). Systematic variations in Cd isotopic composition (Fig. 1.1) were reported for polluted topsoil near a Pb smelter and refinery in Northeast France (Cloquet et al., 2006b) and allowed the authors to trace the Cd source. Gao et al. (2008) used Cd isotopes to identify sediments as smelting polluted (Fig. 1.1).

Early work on Zn isotopes included measurements of marine samples, e.g., ferromanganese nodules (representative of overlying waters; Fig. 1.2) and sediment trap material (Maréchal et al., 2000) (Fig. 1.2). Large variations in the Zn isotopic composition of the carbonate fraction of a sediment core from the equatorial Pacific deep-ocean suggested potential for use as a paleoceanography proxy for surface productivity (Pichat et al., 2003). More recently, Zn isotopes have been measured in seawater from the North Pacific (Bermin et al., 2006; John, 2007) and the North Atlantic (John, 2007) and in seafloor hydrothermal vent fluids and chimneys (John et al., 2008) (Fig. 1.2). Heavy Zn isotopes have been demonstrated to preferentially absorb onto diatom frustules in culturing experiments (Gélabert et al., 2006; John et al., 2007a).

A restricted range of Zn isotopic composition (Fig. 1.2) has been established for sphalerite samples (ZnS) of worldwide origin (Albarède, 2004; Wilkinson et al., 2005; Mason et al., 2005; Sonke et al., 2008). In an attempt to quantify Zn isotopic fractionation introduced by industrial processes, Zn isotopes have been measured in anthropogenic samples (Fig. 1.2), e.g., polluted lichens, urban waste incineration flue gases and urban aerosols from Northeast France (Cloquet et al., 2006a); Zn metals, health products and hardware (John et al., 2007b) and polluted sediments, soils and tailings from a now-closed Zn ore processing facility in Southwest France (Sivry et al., 2008). Sonke et al., (2008) measured historical variations of Zn isotopes in two sediment cores from Northeast Belgium. Mattielli et al. (2009) examined process samples from a Pb–Zn smelter and refinery in Northeast France (Fig. 1.2) in an evaluation of anthropogenic fractionation processes of Zn isotopes and their subsequent tracing in the environment.

1.1.5 Metal Pollution in British Columbia (Canada)

British Columbia is home to one of the world's largest fully integrated Zn and Pb smelting and refining complexes (Trail, B.C.). In 2008, this facility (Teck) reported the largest provincial on-site releases to air and water of the metals, Cd, Zn and Pb, and their compounds (235 kg, 97 tonnes, 3,065 kg; respectively) (Environment Canada, 2009). Even so, the quantities of Cd, Zn and Pb released from the smelting and refining operations in Trail declined considerably, by a factor of 21, between 1994 and 2008 (in 1994: 11 tonnes, 4,466 tonnes, 246 tonnes; respectively) (Environment Canada, 2009). Decreasing metal emissions levels from Teck's Trail facility reflect the vast improvement in efficiency of emission control technologies employed at the facility in an to improve their environmental performance.

1.1.6 High Cd levels in oysters from British Columbia

High Cd levels have been found in oysters (*Crassostrea gigas*) along the coasts of British Columbia (B.C.), western Canada (Kruzynski, 2001, 2004; Lekhi et al., 2008; Bendell and Feng, 2009). High Cd levels are found not only in oysters but also in other resident shellfish, e.g., scallops and mussels (Lares and Orians, 1997; Kruzynski, 2004). Coastal communities (including First Nations communities) are concerned about the potential health problems associated with the consumption of these shellfish (which may represent a significant proportion of their diet) and the potential loss of markets that support local shellfish aquaculture (Kruzynski, 2004). In B.C., the expansion of the aquaculture industry has the potential to create jobs and build revenue for the Province where declines in the forestry industry and natural fisheries have meant the losses of both (Kruzynski, 2004). In an effort to promote the expansion of shellfish aquaculture in B.C., the Provincial Government announced the Shellfish Development Initiative, in 1997, which doubled the amount of crown land made available for shellfish aquaculture (Kruzynski, 2004). At this time, the largest export markets of B.C. bivalve shellfish were the US (~80%) and Hong Kong (~10%) (Carswell, 2001). In 1999/2000, Hong Kong rejected several shipments of B.C. oysters for exceeding their Cd limit of 2 $\mu g\ g^{-1}$ (tissue, wet weight). As a result, the Canadian Food Inspection Agency (CFIA) conducted a survey of B.C. oysters and found a mean Cd concentration of 2.6 $\mu g\ g^{-1}$ (tissue, wet

weight) (Schallié, 2001). Over 60% of the oyster samples, as well as the means of major oyster farming areas had Cd levels exceeding 2 μg g^{-1} (tissue, wet weight); oysters with relatively high Cd levels were not limited to populated areas but rather included those harvested from sparsely inhibited or "pristine" areas (Schallié, 2001). In contrast, a complimentary study by the CFIA reported a mean Cd concentration of 0.33 μg g^{-1} (tissue, wet weight) for oysters (*C. virginica*) collected from the eastern coast of Canada (Schallié, 2001). In addition, no change has been observed in the Cd concentrations of B.C. oysters (*C. gigas*) over the past 30 years (Kruzynski et al., 2002). This is in contrast to reports of declining Cd concentrations of oysters (*C. virginica*) collected from the Southeastern USA (Gulf of Mexico) which are attributed to decreasing inputs of industrial and urban waste to those waters (Beliaeff et al. 1997).

Potential sources of high Cd levels found in B.C. bivalves include natural sources, primarily the upwelling of nutrient-rich deep-waters found in the North Pacific Ocean, and anthropogenic sources (e.g., smelting and refining operations in B.C.).

1.2 Overview of the dissertation

This dissertation was written in manuscript-style format, where each of the three manuscript chapters was prepared for publication in international scientific journals. As a result, a few repetitions exist between chapters, especially between the methods sections of Chapters 2, 3 and 4. Chapter 2 is published in Analytica Chimica Acta under the title "Matrix effects on the multi-collector inductively coupled plasma mass spectrometric analysis of high-precision cadmium and zinc isotope ratios." Chapter 3 is published in Science of the Total Environment under the title "Evaluation of zinc, cadmium and lead isotope fractionation during smelting and refining." Aspects of this study have also been presented at international and national scientific conferences as oral and poster presentations. A list of peer-reviewed publications (including those listed above) and conference abstracts related to this study is provided in Appendix A. Contributions to each manuscript by Alyssa E. Shiel, her co-authors (including her supervisor, Dominique Weis, and co-supervisor, Kristin J. Orians) and other individuals are detailed in the Co-authorship Statement.

All chemical and analytical work in this study was performed by Alyssa E. Shiel at the Pacific Centre for Isotopic and Geochemical Research (PCIGR) at the University of British Columbia (UBC). Elemental analyses were performed on the ELEMENT2 (Thermo Finnigan, Germany) High Resolution Inductively Coupled Mass Spectrometer (HR-ICP-MS) and the Varian 725-ES (Varian, Inc., USA) Inductively Coupled Plasma Optical Emission Spectrometer. Isotopic analyses were performed on the Nu Plasma (Nu 021; Nu Instruments, UK). Multi-collector Inductively Coupled Plasma Mass Spectrometer. Jane Barling (MC-ICP-MS), Bert Mueller (HR-ICP-MS) and Maureen Soon (ICP-OES) provided assistance with the operation of the instruments, as well as training.

In Chapter 2, an investigation is undertaken of non-spectral interferences, or matrix effects, on Cd and Zn isotope measurements by MC-ICP-MS resulting from the presence of (1) resin-derived contaminants (both organics and inorganic elements) added to samples during chromatographic separations and (2) inorganic elements in relatively large quantities (matrix element molar concentration is 5× that of the analyte). In addition to the results of these matrix experiments, the analytical results include elemental concentrations (ICP-MS) of chromatographic column blanks, evaluating the cleanliness of different batches of the same resin and the effectiveness of on-column and batch resin cleaning methods. This study was motivated by the need to measure high-precision, accurate Cd and Zn isotopic ratios. Identification of potentially compromised data quality, related to matrix effects on Cd and Zn isotopic measurements, made this study highly relevant, especially with the organic matrix of our samples. The results of this study were used to improve the quality of Cd and Zn isotopic measurements explored in the following two chapters.

In Chapter 3, in the light of the regional importance of the smelting and refining complex in Trail, B.C., metallurgical processing is evaluated as a source of Cd, Zn and Pb isotope fractionation and dispersion into the environment. The analytical results include Cd, Zn and Pb concentrations (ICP-OES) and isotopic compositions (MC-ICP-MS) of smelter process samples, recycled Cd metal and CdS pigments. Cd and Zn isotopes are identified as effective tracers of smelting and refining air emissions and effluent. The combined use of Pb isotopes allows the identification of source ores. The

results demonstrated the closed nature of the integrating processing, with the exception of the reported emissions. The characterization of the isotopic compositions of anthropogenic sources allows tracing of these signals in natural samples, e.g., bivalves, in the next chapter.

In Chapter 4, Cd, Zn and Pb concentrations and isotopic compositions are used to trace anthropogenic metal pollution in bivalves from western Canada, the USA and France. This study evaluates the usefulness of these isotopic tracers individually and in combination. The analytical results include Cd, Zn and Pb concentrations (ICP-MS) and isotopic compositions (MC-ICP-MS) of bivalve (oyster and mussel) tissue samples. The original motivation for this study was the high Cd content of B.C. oysters; the sources of this high Cd are evaluated through the combined use of Cd, Zn and Pb isotopes in this study and shown to be mostly natural. The study was then extended to include oysters and other bivalves collected from France and the USA East Coast to broaden the scope of the study to include locations with different anthropogenic processes at play.

In Chapter 5, significant findings presented in each manuscript chapter are summarized and implications from the entire study are discussed. Finally, suggestions for further research are made.

Table 1.1. Metal (Zn, Cd and Pb) abundances in continental crust, ocean seawater and human blood.

Element	**Zn**	**Cd**	**Pb**
Atomic number	30	48	82
Atomic weight	65.39	112.4	207.2
Upper continental crust abundance (ppm)[a]	52	0.102	17
Surface ocean seawater concentration (ppm)[b]	0.8-314 x 10^{-6}	0.08-19 x 10^{-6}	2.3-21 x 10^{-6}
Human blood (mg dm^{-3})[c]	7.0	0.0052	0.21

[a]Wedepohl, 1995.

[b]Surface water concentrations for both the Atlantic and Pacific Oceans; [Zn] and [Cd] in the Pacific Ocean (Bruland, 1980); [Pb] in the Pacific Ocean (Boyle et al., 2005) and [Zn], [Cd] and [Pb] in the Atlantic Ocean (Kremling and Streu, 2001).

[c]Emsley, 1998, and references within.

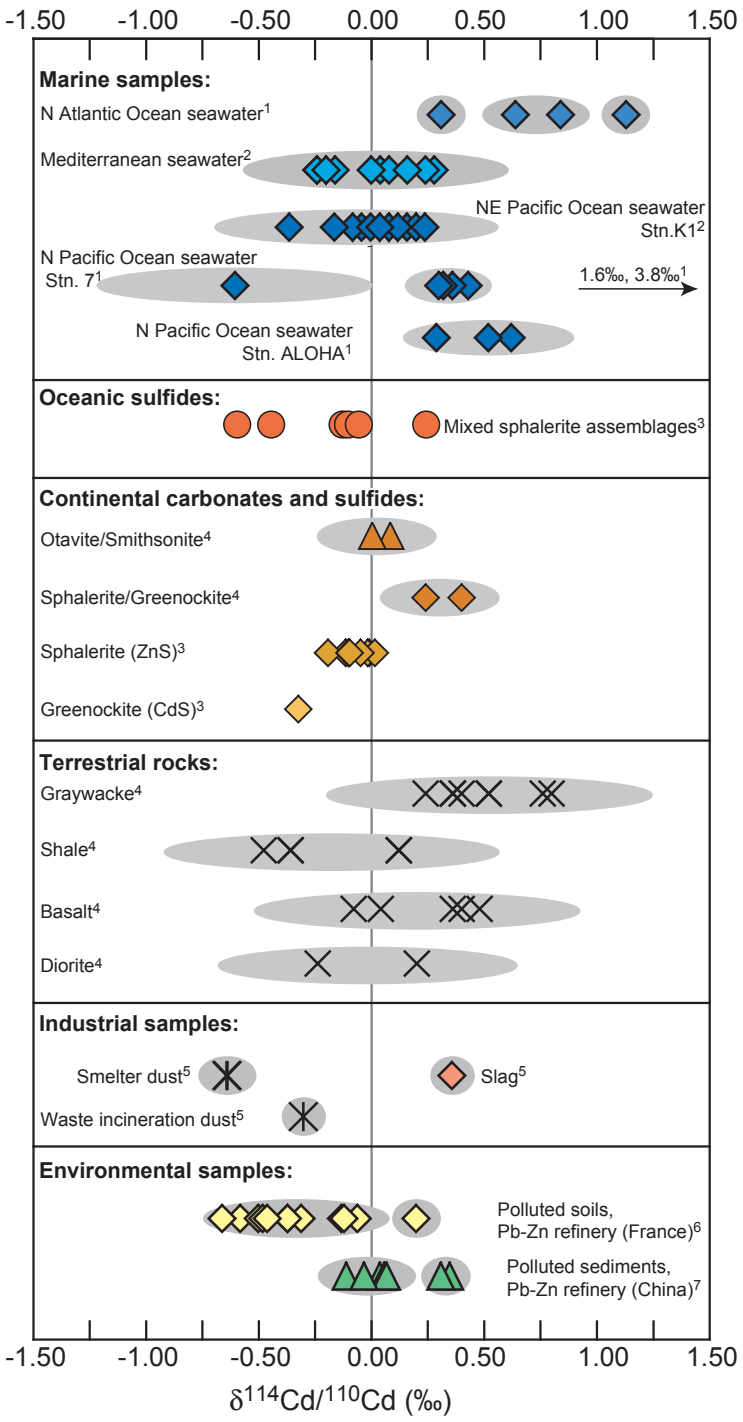

Fig. 1.1. Variations in the Cd isotopic composition of select geological, marine and anthropogenic samples. The grey ellipses indicate error as reported by referenced authors. In several cases the error is smaller than the symbol. Data sources: [1]Ripperger et al., 2007; [2]Lacan et al., 2006; [3]Schmitt et al., 2009; [4]Wombacher et al., 2003; [5]Cloquet et al., 2005; [6]Cloquet et al., 2006b; [7]Gao et al., 2008.

Fig. 1.2. Variations in the Zn isotopic composition of select geological, marine and anthropogenic samples. The grey ellipses indicate error as reported by referenced authors. In several cases the error is smaller than the symbol. Data sources: [1]Bermin et al., 2006; [2]John, 2007; [3]Maréchal et al., 1999; [4]John et al., 2008; [5]Sonke et al., 2008; [6]Mason et al., 2005; [7]Albarède, 2004; [8]Wilkinson et al., 2005; [9]Mattielli et al., 2009; [10]Sivry et al., 2008; [11]Cloquet et al., 2006a; [12]John et al., 2007b.

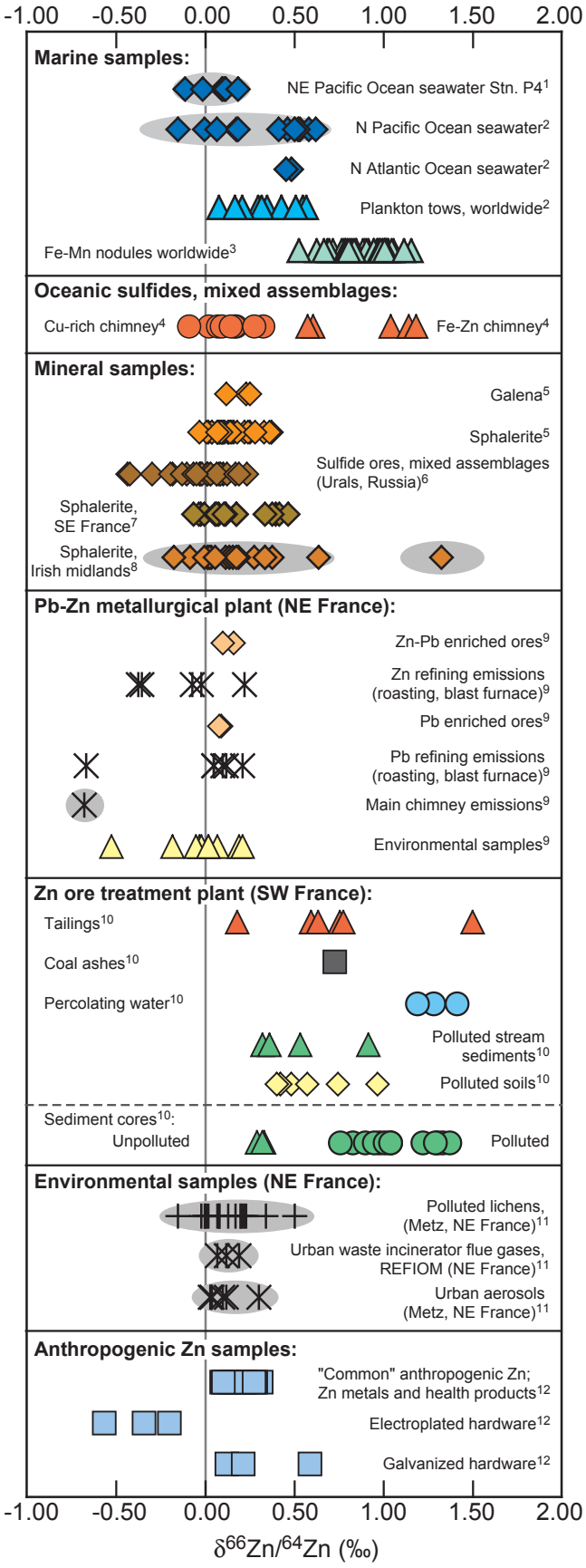
-1.00
-0.50
0.00
0.50
1.00
1.50
2.00
Marine samples:
NE Pacific Ocean seawater Stn. P4[1]
N Pacific Ocean seawater[2]
N Atlantic Ocean seawater[2]
Plankton tows, worldwide[2]
Fe-Mn nodules worldwide[3]
Oceanic sulfides, mixed assemblages:
Cu-rich chimney[4]
Fe-Zn chimney[4]
Mineral samples:
Galena[5]
Sphalerite[5]
Sulfide ores, mixed assemblages (Urals, Russia)[6]
Sphalerite, SE France[7]
Sphalerite, Irish midlands[8]
Pb-Zn metallurgical plant (NE France):
Zn-Pb enriched ores[9]
Zn refining emissions (roasting, blast furnace)[9]
Pb enriched ores[9]
Pb refining emissions (roasting, blast furnace)[9]
Main chimney emissions[9]
Environmental samples[9]
Zn ore treatment plant (SW France):
Tailings[10]
Coal ashes[10]
Percolating water[10]
Polluted stream sediments[10]
Polluted soils[10]
Sediment cores[10]:
Unpolluted
Polluted
Environmental samples (NE France):
Polluted lichens, (Metz, NE France)[11]
Urban waste incinerator flue gases, REFIOM (NE France)[11]
Urban aerosols (Metz, NE France)[11]
Anthropogenic Zn samples:
"Common" anthropogenic Zn; Zn metals and health products[12]
Electroplated hardware[12]
Galvanized hardware[12]
-1.00
-0.50
0.00
0.50
1.00
1.50
2.00
δ66Zn/64Zn (‰)

1.3 References

Albarède, F. (2004) The stable isotope geochemistry of copper and zinc. Reviews in Mineralogy and Geochemistry 55: 409–427.

Beliaeff, B., O'Connor, T.P., Daskalakis, D.K., Smith, P.J. (1997) US Mussel Watch data from 1986 to 1994: Temporal trend detection at large spatial scales. Environmental Science & Technology 31: 1411–1415.

Bendell, L.I., Feng, C. (2009) Spatial and temporal variations in cadmium concentrations and burdens in the Pacific oyster (*Crassostrea gigas*) sampled from the Pacific north-west. Marine Pollution Bulletin 58: 1137–1143.

Bermin, J., Vance, D., Archer, C., Statham, P.J. (2006) The determination of the isotopic composition of Cu and Zn in seawater. Chemical Geology 226: 280–297.

Boyle, E.A., Bergquist, B.A., Kayser, R.A., Mahowald, N. (2005) Iron, manganese, and lead at Hawaii Ocean Time-series station ALOHA: Temporal variability and an intermediate water hydrothermal plume. Geochimica et Cosmochimica Acta 69: 933–952.

Boyle, E.A., Sherrell, R.M., Bacon, M.P. (1994) Lead Variability in the Western North-Atlantic Ocean and Central Greenland Ice - Implications for the Search for Decadal Trends in Anthropogenic Emissions. Geochimica et Cosmochimica Acta 58: 3227–3238.

Bruland, K.W. (1980) Oceanographic Distributions of Cadmium, Zinc, Nickel, and Copper in the North Pacific. Earth and Planetary Science Letters 47: 176-198.

Candelone, J.P., Hong, S.M., Pellone, C., Boutron, C.F. (1995) Postindustrial Revolution Changes in Large-Scale Atmospheric-Pollution of the Northern-Hemisphere by Heavy-Metals as Documented in Central Greenland Snow and Ice. Journal of Geophysical Research-Atmospheres 100: 16605–16616.

Carswell, B. (2001) Shellfish aquaculture: industry snapshot and the shellfish development initiative. In: Kruzynski, G.M., Addison, R.F., MacDonald, R.W. (Eds.) (2002) Proceedings of a workshop on possible pathways of cadmium into the Pacific oyster *Crassostrea gigas* as cultured on the coast of British Columbia,

Institute of Ocean Sciences, Mar. 6–7, 2001, pp. 27–28. Canadian Technical Report of Fisheries and Aquatic Science 2405: pp. 65.

Chow, T.J., Synder, C.B., Earl, J.L. (1975) Isotope ratios of lead as pollutant source indicators. In Proc. United Nations FAO and International Atomic Energy Association Symposium, Vienna, Austria, paper no. IAEA-SM-191/4, pp. 95–108.

Cloquet, C., Carignan, J., Libourel, G. (2006a) Isotopic composition of Zn and Pb atmospheric depositions in an urban/periurban area of northeastern France. Environmental Science & Technology 40: 6594–6600.

Cloquet, C., Carignan, J., Libourel, G., Sterckeman, T., Perdrix, E. (2006b) Tracing source pollution in soils using cadmium and lead isotopes. Environmental Science & Technology 40: 2525–2530.

Cloquet, C., Rouxel, O., Carignan, J., Libourel, G. (2005) Natural cadmium isotopic variations in eight geological reference materials (NIST SRM 2711, BCR 176, GSS-1, GXR-1, GXR-2, GSD-12, Nod-P-1, Nod-A-1) and anthropogenic samples, measured by MC-ICP-MS. Geostandards and Geoanalytical Research 29: 95–106.

Elinder, C.G., Järup, L. (1996) Cadmium exposure and health risks: Recent findings. Ambio 25: 370–373.

Emsley, J. (1998) The Elements, third edition. New York: Oxford University Press, pp. 292.

Environment Canada. (2009) National Pollutant Release Inventory, Pollution Data Library, 2008 Revised Facility Data Release: http://www.ec.gc.ca/npri/.

Ericson, J.E., Shirahata, H., Patterson, C.C. (1979) Skeletal Concentrations of Lead in Ancient Peruvians. New England Journal of Medicine 300: 946–951.

Felton, M.J. (2003) Plasma opens new doors in isotope ratio MS. Analytical Chemistry 75: 119A–123A.

Gao, B., Liu, Y., Sun, K., Liang, X., Peng, P., Sheng, G., Fu, J. (2008) Precise determination of cadmium and lead isotopic compositions in river sediments. Analytica Chimica Acta 612: 114–120.

Gélabert, A., Pokrovsky, O.S., Viers, J., Schott, J., Boudou, A., Feurtet-Mazel, A. (2006) Interaction between zinc and freshwater and marine diatom species: Surface complexation and Zn isotope fractionation. Geochimica et Cosmochimica Acta 70: 839–857.

Halliday, A.N., Lee, D.C., Christensen, J.N., Walder, A.J., Freedman, P.A., Jones, C.E., Hall, C.M., Yi, W., Teagle, D. (1995) Recent Developments in Inductively-Coupled Plasma Magnetic-Sector Multiple Collector Mass-Spectrometry. International Journal of Mass Spectrometry and Ion Processes 146: 21–33.

Horner, T.J., Schönbächler, M., Rehkämper, M., Nielsen, S.G., Williams, H., Halliday, A.N., Xue, Z., Hein, J.R. (2010) Ferromanganese crusts as archives of deep water Cd isotope compositions. Geochemistry Geophysics Geosystems 11, Q04001, doi: 04010.01029/02009GC002987.

John, S.G. (2007) The Marine Biogeochemistry of Zinc Isotopes. Ph.D. thesis, Massachusetts Institute of Technology, pp. 142.

John, S.G., Geis, R.W., Saito, M.A., Boyle, E.A. (2007a) Zinc isotope fractionation during high-affinity and low-affinity zinc transport by the marine diatom *Thalassiosira oceanica*. Limnology and Oceanography 52: 2710–2714.

John, S.G., Park, G., Zhang, Z., Boyle, E.A. (2007b) The isotopic composition of some common forms of anthropogenic zinc. Chemical Geology 245: 61–69.

John, S.G., Rouxel, O.J., Craddock, P.R., Engwall, A.M., Boyle, E.A. (2008) Zinc stable isotopes in seafloor hydrothermal vent fluids and chimneys. Earth and Planetary Science Letters 269: 17–28.

Kremling, K., Streu, P. (2001) The behaviour of dissolved Cd, Co, Zn, and Pb in North Atlantic near-surface waters (30 degrees N/60 degrees W-60 degrees N/2 degrees W). Deep-Sea Research Part I-Oceanographic Research Papers 48: 2541-2567.

Kruzynski, G.M. (2001) Cadmium in BC farmed oysters: a review of available data, potential sources, health considerations, and research needs. In: Kruzynski, G.M., Addison, R.F., MacDonald, R.W. (Eds.) (2002) Proceedings of a workshop on possible pathways of cadmium into the Pacific oyster *Crassostrea gigas* as cultured on the coast of British Columbia, Institute of Ocean Sciences, Mar. 6–7,

2001, pp. 21–22. Canadian Technical Report of Fisheries and Aquatic Science 2405: pp. 65.

Kruzynski, G.M. (2004) Cadmium in oysters and scallops: the BC experience. Toxicology Letters 148: 159–169.

Kruzynski, G.M., Addison, R.F., MacDonald, R.W. (2002) Proceedings of a workshop on possible pathways of cadmium into the Pacific oyster *Crassostrea gigas* as cultured on the coast of British Columbia, Institute of Ocean Sciences, Mar. 6–7, 2001, pp. 21–22. Canadian Technical Report of Fisheries and Aquatic Science 2405: pp. 65. (Available at http://www.dfo-mpo.gc.ca/Library/262960.pdf)

Lacan, F., Francois, R., Ji, Y.C., Sherrell, R.M. (2006) Cadmium isotopic composition in the ocean. Geochimica et Cosmochimica Acta 70: 5104–5118.

Lares, M.L., Orians, K.J. (1997) Natural Cd and Pb variations in *Mytilus californianus* during the upwelling season. Science of the Total Environment 197: 177–195.

Lekhi, P., Cassis, D., Pearce, C.M., Ebell, N., Maldonado, M.T., Orians, K. (2008) Role of dissolved and particulate cadmium in the accumulation of cadmium in cultured oysters (*Crassostrea gigas*). Science of the Total Environment 393: 309–325.

Maréchal, C.N., Nicolas, E., Douchet, C., Albarède, F. (2000) Abundance of zinc isotopes as a marine biogeochemical tracer. Geochemistry Geophysics Geosystems 1, 1015, doi: 10.1029/1999GC000029.

Maréchal, C.N., Télouk, P., Albarède, F. (1999) Precise analysis of copper and zinc isotopic compositions by plasma-source mass spectrometry. Chemical Geology 156: 251–273.

Mason, T.F.D., Weiss, D.J., Chapman, J.B., Wilkinson, J.J., Tessalina, S.G., Spiro, B., Horstwood, M.S.A., Spratt, J., Coles, B.J. (2005) Zn and Cu isotopic variability in the Alexandrinka volcanic-hosted massive sulphide (VHMS) ore deposit, Urals, Russia. Chemical Geology 221: 170–187.

Mattielli, N., Petit, J.C.J., Deboudt, K., Flament, P., Perdrix, E., Taillez, A., Rimetz-Planchon, J., Weis, D. (2009) Zn isotope study of atmospheric emissions and dry depositions within a 5 km radius of a Pb-Zn refinery. Atmospheric Environment 43: 1265–1272.

Mielke, H.W., Reagan, P.L. (1998) Soil is an important pathway of human lead exposure. Environmental Health Perspectives 106: 217–229.

Nogawa, K., Ishizaki, A. (1979) Comparison between Cadmium in Rice and Renal Effects among Inhabitants of the Jinzu River Basin. Environmental Research 18: 410–420.

Pacyna, J.M., Pacyna, E.G. (2001) An assessment of global and regional emissions of trace metals to the atmosphere from anthropogenic sources worldwide. Environmental Reviews 9: 269–298.

Peterson, B.J., Fry, B. (1987) Stable isotopes in ecosystem studies. Annual Review of Ecology and Systematics 18: 293–320.

Pichat, S., Douchet, C., Albarède, F. (2003) Zinc isotope variations in deep-sea carbonates from the eastern equatorial Pacific over the last 175 ka. Earth and Planetary Science Letters 210: 167–178.

Planchon, F.A.M., Boutron, C.F., Barbante, C., Cozzi, G., Gaspari, V., Wolff, E.W., Ferrari, C.P., Cescon, P. (2002) Changes in heavy metals in Antarctic snow from Coats Land since the mid-19th to the late-20th century. Earth and Planetary Science Letters 200: 207–222.

Reuer, M.K., Weiss, D.J. (2002) Anthropogenic lead dynamics in the terrestrial and marine environment. Philosophical Transactions of the Royal Society of London Series a-Mathematical Physical and Engineering Sciences 360: 2889–2904.

Ripperger, S., Rehkämper, M., Porcelli, D., Halliday, A.N. (2007) Cadmium isotope fractionation in seawater - A signature of biological activity. Earth and Planetary Science Letters 261: 670–684.

Schallié, K. (2001) Results of the 2000 survey of cadmium in B.C. oysters. In: Kruzynski, G.M., Addison, R.F., MacDonald, R.W. (Eds.) (2002) Proceedings of a workshop on possible pathways of cadmium into the Pacific oyster *Crassostrea gigas* as cultured on the coast of British Columbia, Institute of Ocean Sciences, Mar. 6–7, 2001, pp. 31–32. Canadian Technical Report of Fisheries and Aquatic Science 2405: pp. 65.

Schmitt, A.D., Galer, S.J.G., Abouchami, W. (2009) Mass-dependent cadmium isotopic variations in nature with emphasis on the marine environment. Earth and Planetary Science Letters 277: 262–272.

Settle, D.M., Patterson, C.C. (1980) Lead in albacore: guide to lead pollution in Americans. Science 207, 1167–1176.

Sivry, Y., Riotte, J., Sonke, J.E., Audry, S., Schäfer, J., Viers, J., Blanc, G., Freydier, R., Dupré, B. (2008) Zn isotopes as tracers of anthropogenic pollution from Zn-ore smelters The Riou Mort-Lot River system. Chemical Geology 255: 295–304.

Sonke, J.E., Sivry, Y., Viers, J., Freydier, R., Dejonghe, L., Andre, L., Aggarwal, J.K., Fontan, F., Dupré, B. (2008) Historical variations in the isotopic composition of atmospheric zinc deposition from a zinc smelter. Chemical Geology 252: 145–157.

Wedepohl, K.H. (1995) The Composition of the Continental-Crust. Geochimica et Cosmochimica Acta 59: 1217–1232.

Weiss, D.J., Rehkämper, M., Schoenberg, R., McLaughlin, M., Kirby, J., Campbell, P.G.C., Arnold, T., Chapman, J., Peel, K., Gioia, S. (2008) Application of Nontraditional Stable-Isotope Systems to the Study of Sources and Fate of Metals in the Environment. Environmental Science and Technology 42: 655–664.

Weiss, D.J., Shotyk, W., Kempf, O. (1999) Archives of atmospheric lead pollution. Naturwissenschaften 86: 262–275.

Wilkinson, J.J., Weiss, D.J., Mason, T.F.D., Coles, B.J. (2005) Zinc isotope variation in hydrothermal systems: Preliminary evidence from the Irish Midlands ore field. Economic Geology 100: 583–590.

Wombacher, F., Rehkämper, M. (2004) Problems and suggestions concerning the notation of cadmium stable isotope compositions and the use of reference materials. Geostandards and Geoanalytical Research 28: 173–178.

Wombacher, F., Rehkämper, M., Mezger, K. (2004) Determination of the mass-dependence of cadmium isotope fractionation during evaporation. Geochimica et Cosmochimica Acta 68: 2349–2357.

Wombacher, F., Rehkämper, M., Mezger, K., Munker, C. (2003) Stable isotope compositions of cadmium in geological materials and meteorites determined by multiple-collector ICPMS. Geochimica et Cosmochimica Acta 67: 4639–4654.

CHAPTER 2

Matrix effects on the multi-collector inductively coupled plasma mass spectrometric analysis of high-precision cadmium and zinc isotope ratios[1]

[1]A version of this chapter has been published. Shiel, A.E., Barling, B., Orians, K.J., Weis, D. (2009) Matrix effects on the multi-collector inductively coupled plasma mass spectrometric analysis of high-precision cadmium and zinc isotope ratios. Analytica Chimica Acta 633: 29–37.

2.1 Introduction

The multi-collector inductively coupled plasma mass spectrometer (MC-ICP-MS) has enabled the measurement of small differences in the isotopic composition of many heavy stable elements. In particular, the enhanced ionization efficiency inherent to the inductively coupled plasma source has enabled the ionization of elements, such as Cd and Zn, that have been difficult to ionize by other methods, e.g., TIMS (Rosman and de Laeter, 1976; Rosman et al., 1980; Rosman and de Laeter, 1988; Loss et al., 1990). Recent MC-ICP-MS investigations have revealed small Cd and Zn isotopic variations in terrestrial (Maréchal et al., 1999; Maréchal et al., 2000; Wombacher et al., 2003; Cloquet et al., 2005; Weiss et al., 2005; Wilkinson et al., 2005; Dolgopolova et al., 2006; Weiss et al., 2007), marine (Maréchal et al., 1999; Maréchal et al., 2000; Pichat et al., 2003; Bermin et al., 2006; Lacan et al., 2006; Ripperger et al., 2007; John, 2007; Shiel et al., 2007; John et al., 2008; Shiel et al., 2008), anthropogenic (Cloquet et al., 2005; Dolgopolova et al., 2006; Shiel et al., 2007; Shiel et al., 2008; Cloquet et al., 2006a; Cloquet et al., 2006b; Sivry et al., 2006; John et al., 2007; Sivry et al., 2008; Sonke et al., 2008) and extraterrestrial samples (Wombacher et al., 2003; Luck et al., 2005; Moynier et al., 2006). The largest isotopic variations are of anthropogenic (e.g., ore processing and smelting) and extraterrestrial (e.g., chondrites, meteorites and lunar samples) origins. Reported isotopic variations range from $\delta^{114/110}$Cd = -7.8 to +14.8‰ (Wombacher et al., 2003; Cloquet et al., 2005; Lacan et al., 2006; Ripperger et al., 2007; Shiel et al., 2007; Shiel et al., 2008; Cloquet et al., 2006b; Sivry et al., 2006) relative to the "JMC Cd" reference standard (Johnson Matthey Company) (Wombacher and Rehkämper, 2004) and from $\delta^{66/64}$Zn = -3.83 to +6.39‰ (Maréchal et al., 1999; Maréchal et al., 2000; Weiss et al., 2005 Wilkinson et al., 2005; Dolgopolova et al., 2006; Weiss et al., 2007; Pichat et al., 2003; Bermin et al., 2006; John, 2007; John et al., 2008; Shiel et al., 2008; Cloquet et al., 2006a; John et al., 2007; Sivry et al., 2008; Sonke et al., 2008; Luck et al., 2005; Moynier et al., 2006) relative to the "JMC Zn-Lyon" reference standard (Maréchal et al., 1999).

Resolution of these small differences in Cd and Zn isotopic compositions requires a high degree of accuracy and precision and therefore careful attention must be paid to

potential spectral and non-spectral interferences (Evans and Giglio, 1993; Douglas and Tanner, 1998; Horlick and Montaser, 1998; Rehkämper et al., 2004). Spectral interferences include isobaric interferences of singly (e.g., $^{114}Sn^{+}$ on $^{114}Cd^{+}$) and doubly (e.g., $^{136}Ba^{2+}$ on $^{68}Zn^{+}$) charged elements and polyatomic species from the recombination of argon, atmospheric gases, solvents and sample matrix (e.g., $^{68}Zn^{40}Ar^{+}$ on $^{108}Cd^{+}$) (Douglas and Tanner, 1998; Tan and Horlick, 1986). These interferences on isotopes of the analyte result in non-mass-dependent isotopic variations that are readily identified by comparing the per amu delta values calculated from the different analyte isotope ratios. Non-spectral interferences, or 'matrix effects', are changes in the instrument response (signal intensity and mass bias) to the analyte resulting from the presence of matrix components (Rehkämper et al., 2004; Carlson et al., 2001; Galy et al., 2001). In contrast to spectral interferences, these interferences are difficult to identify because the effects are mass-dependent and may obscure small natural mass-dependent fractionations (Carlson et al., 2001). Recently, efforts have been made to evaluate non-spectral interferences in the analysis of non-traditional stable isotopes by MC-ICP-MS; e.g., Ir on Ag–Pd (Carlson et al., 2001); Na, Al, Ca on Mg (Galy et al., 2001); Nb, Cd, Sb, W, Tl, Na, Mg on Mo–Zr (Pietruszka et al., 2006. However, their origin and mode of occurrence and formation are not yet well understood.

Correction of measured ratios for instrumental mass-dependent fractionation or mass bias (f) is required to resolve small natural mass-dependent isotopic variations (e.g., Rehkämper et al., 2004). Two methods for mass bias correction were used in this study: (1) sample-standard bracketing of measured ratios (SSB) and (2) combined external normalization–SSB (Ag-corrected for Cd, Cu-corrected for Zn) (Maréchal et al., 1999; Wombacher et al., 2003; Rehkämper et al., 2004; Longerich et al., 1987). The first method, SSB requires that instrumental mass bias remains stable or varies systematically with time and that mass bias behavior is the same for the samples and bracketing standards (Albarède and Beard, 2004). The second method, combined external normalization–SSB, assumes that the mass bias response of the analyte (Cd or Zn) varies systematically with the mass bias response of the mass bias-correcting element (Ag or Cu) (Maréchal et al., 1999). For reliable external normalization data f(Ag)/f(Cd) and f(Cu)/f(Zn) must be constant in samples and standards during an analytical session.

Therefore, any matrix effect that causes mass bias variations in samples relative to standards must be investigated.

This study was motivated by observations made during the investigation of Cd and Zn isotopic variation in biological samples (Shiel et al., 2007; Shiel et al., 2008). Namely: (1) ion signal intensity enhancement in samples of known concentration, (2) differences in mass bias of normalizing elements between samples and bracketing standards and (3) isotopic signatures in samples that varied depending on the dilution factor of the analyzed solution. This latter observation strongly suggested a matrix effect related to column-derived material and motivated this study of non-spectral matrix effects associated with column-derived matrix. These experiments were designed to separate the matrix effects resulting from the inorganic and organic components of the column blank. To do this, Cd and Zn cuts, eluted from blank column loads, were used to dope pure standard solutions in proportions reflecting the presence of eluted column blank in diluted samples. This methodology is in contrast to experiments comparing pure standards to standards that have been passed through chemistry in that a single column blank is used to dope standards in a sequence of dilutions similar to those found in chromatographically processed samples. Although the experiments described here are specific to Cd and Zn, the results may be applicable to any isotopic system where samples are purified by ion exchange chromatography and analyzed by MC-ICP-MS.

2.2 Experimental

Experimental work was carried out in metal-free Class 1,000 clean labs at the Pacific Centre for Isotopic and Geochemical Research (PCIGR), University of British Columbia. The high resolution inductively coupled plasma mass spectrometer (HR-ICP-MS) and MC-ICP-MS are housed in Class 10,000 labs. Sample preparation for trace element and isotopic analysis was performed in Class 100 laminar flow hoods, in both the clean labs and instrument rooms.

2.2.1 Reagents and standards

Nitric (HNO_3) and hydrofluoric (HF) acids used in this study were purified in-house from concentrated reagent grade acids by sub-boiling distillation. Baseline® hydrobromic (HBr), hydrochloric (HCl) and perchloric ($HClO_4$) acids produced by Seastar Chemicals Inc. (Canada) were also utilized. Standard solutions used for trace element concentration determination by HR-ICP-MS were prepared from 1,000 μg mL^{-1} single-element solutions from High Purity Standards, Inc. (USA) and Specpure® Plasma (Alfa Aesar®, Johnson Matthey Company, USA). These single-element standards were also used in the matrix experiments on the MC-ICP-MS. Ultrapure water (≥18.2 MΩ cm), prepared by de-ionization of reverse osmosis water using a Milli-Q® system (Millipore, USA), was used to prepare all solutions. All labware was washed successively with a ~2% extran® 300 (Merck KGaA, Germany) solution (alkaline cleanser), analytical grade HCl and environmental grade HNO_3.

2.2.2 Isotopic standards

The in-house primary and secondary Cd reference standards (PCIGR-1 Cd and PCIGR-2 Cd) are from High Purity Standards, Inc. (USA) (lots 291012 and 502624, respectively). The "JMC Cd" (Wombacher et al., 2003; Wombacher and Rehkämper, 2004), "Münster Cd" (Wombacher and Rehkämper, 2004) and BAM-1012 Cd (Federal Institute for Materials Research and Testing, Germany) (Wombacher and Rehkämper, 2004) reference materials were also analyzed. All Cd isotopic solutions were prepared as 2:1 Cd and Ag solutions, with a single analysis consuming 150 ng Cd.

The in-house primary and secondary Zn reference standards (PCIGR-1 Zn and PCIGR-2 Zn) are from High Purity Standards, Inc. and Specpure® (lots 505326 and 011075A, respectively). Zinc isotopic solutions were prepared as 3:1 Zn to Cu solutions, with a single analysis consuming 100 ng Zn.

2.2.3 Ion exchange chemistry

Column blanks for the matrix experiments were prepared using the Cd and Zn anion exchange chromatography purification procedure of Mason (2003), identically to real samples (Appendix B). The Cd and Zn eluate cuts were collected in Savillex® PFA

vials, dried, treated with 0.100 mL ~15 M HNO_3 (standard treatment) in an effort to digest organic column residue, then redried and dissolved in 1 mL 0.05 M HNO_3 in preparation for isotopic analysis. Alternative refluxed HNO_3 and $HClO_4/HNO_3$ digestions for removal of organic residue were also tested. Column blanks for Cd and Zn are negligible (Table 2.1). However, HR-ICP-MS analysis of these blanks identified a number of non-coeluting elements present at levels that cannot be attributed to the acids used in the procedure (Table 2.1) but rather derive from the resin (Straßburg et al., 1998; personal communication, D. Hardy, Bio-Rad Laboratories, 2008).

Magnesium was the most significant contaminant element in the Cd eluate cut of the column blank, with Ca, Fe, Al and Zn all present at ng levels (Table 2.1). Of these the only potential Cd or Ag spectral interference was Zn ($^{67}Zn^{40}Ar^+$, $^{70}Zn^{40}Ar^+$). The most significant contaminant element in the Zn eluate cut of the column blank was Al followed by Fe, Mg, Ca and Cr at ng levels (Table 2.1). Aluminum ($^{27}Al^{36}Ar^+$, $^{27}Al^{38}Ar^+$, $^{27}Al^{40}Ar^+$) was the only potential Zn or Cu spectral interference.

Inorganic contaminants in both the Cd and Zn eluate cuts, despite careful cleaning, were variable (Table 2.1). We therefore investigated three resin-cleaning protocols. In the first method, the resin was cleaned on-column using the routine on-column cleaning (Appendix B). Two other resin-cleaning methods (used in addition to the routine on-column cleaning) were tested to see if the inorganic content of the column blanks could be reduced: (1) an on-column cleaning method utilizing 10 mL each of the eluting acids (full clean) and (2) the batch cleaning method of De Jong et al. (2007). Neither cleaning procedure significantly reduced the inorganic content of the blanks (Table 2.1). Previously, Straßburg et al. (1998) reported that Na, Mg, Al, K, Cr, Fe, Zn and Ba occur as contaminants in the anion exchange resin AG 1-X8 (Bio-Rad Laboratories, Inc., USA). Bio-Rad Laboratories AG (Analytical Grade) resins are generated by extensive acid and base cleaning of technical grade Dowex resins. However, even after this cleaning, a background of elements persists due to variable purity of components used in the initial manufacture of the technical grade resin [personal communication, D. Hardy, Bio-Rad Laboratories, 2008]. As a result, resin-derived inorganic elements and organics (e.g., styrene divinylbenzene; personal communication,

D. Hardy, Bio-Rad Laboratories, 2008) may be leached out during column chemistry producing non-reproducible blanks.

2.2.4 Mass spectrometry

2.2.4.1 Trace element analyses

Trace element analyses of column blanks were performed on an ELEMENT2 (Thermo Finnigan, Germany) HR-ICP-MS. Measurements were made using a Conikal glass concentric nebulizer (Glass Expansion, USA) and a Scott-type glass spray chamber. Elemental concentrations were quantified using multi-element calibration curves with indium, measured at mass 115, as an internal standard. All solutions were prepared with 0.15 M HNO_3.

2.2.4.2 Isotopic analyses

Isotope ratios were measured by multi-collection on a Nu Plasma MC-ICP-MS (Nu 021; Nu Instruments, UK) using the DSN-100 (Nu Instruments, UK) membrane desolvator for sample introduction. The standard dry plasma cones (type B; Nu Instruments, UK) were used, with the exception of one experiment, where the standard wet plasma cones (type A; Nu Instruments, UK) were used. A standard SSB measurement protocol (Rehkämper et al., 2004) was followed, where samples were run alternately with standards.

The Cd isotope measurement method was adapted from Wombacher et al. (2003) and consisted of a dynamic run with main and interference cycles that enabled collection of masses 106 to 118 (isotopes of Cd, Ag and Sn). Correction of the Sn interference on ^{112}Cd, ^{114}Cd and ^{116}Cd was enabled by measurement of ^{118}Sn. An analysis comprised 2 blocks of 15 × 5 s integrations with a 20 s ESA deflected baseline before each block.

Zinc isotope measurements consisted of a single cycle to collect masses 62 to 68 (isotopes of Zn, Cu and Ni). Correction of the Ni interference on ^{64}Zn was permitted by collection of ^{62}Ni. Each measured ratio comprised 2 blocks of 15 × 10 s integrations. An on-peak zero was measured before each Zn analysis in order to correct for background signal.

2.2.5 Isotope data presentation

Cadmium and Zn isotopic compositions are expressed relative to the PCIGR-1 Cd and PCIGR-1 Zn reference standards in the standard delta (δ) notation as follows:

$$\delta^{i}\mathrm{Cd} = \left(\frac{(^{i}Cd)_{\text{sample}}}{(^{i}Cd)_{\text{standard}}} - 1 \right) \text{x } 1{,}000$$

$$\delta^{j}\mathrm{Zn} = \left(\frac{(^{j}Zn)_{\text{sample}}}{(^{j}Zn)_{\text{standard}}} - 1 \right) \text{x } 1{,}000$$

where i and j are the measured isotope ratios, for Cd i = 111/110, 112/110, 113/110 or 114/110 and for Zn j = 66/64, 67/64, 68/64 or 68/66. Isotopic compositions are reported in terms of $\delta^{114/110}$Cd (‰) and $\delta^{66/64}$Zn (‰). However, these and the other isotope ratios are also reported as delta values per atomic mass unit (amu) in Appendices C, D, E, F, G; these values are used for diagnostic purposes to (1) control quality and (2) monitor for spectral interferences. Delta values per amu are calculated by dividing the delta value by the difference in mass of the two isotopes. Although monitored, low abundance Cd isotopes, ^{106}Cd (1.25%) and ^{108}Cd (0.89%), are not reported, as they are associated with poor precision. Although relatively abundant, ^{116}Cd (7.49%) is omitted because it is not measured in the same cycle as the mass bias–correcting element (Ag).

Delta values are reported as (1) SSB and (2) combined external normalization–SSB corrected. For SSB, delta values are calculated from measured ratios in samples referenced to the mean of their two bracketing standards (Rehkämper et al., 2004). For combined external normalization–SSB, the external normalization of Cd or Zn samples and standards was made using Ag or Cu, respectively. The measured ^{107}Ag/^{109}Ag or ^{65}Cu/^{63}Cu ratios are then used to calculate the instrumental mass bias, f(Ag) and f(Cu), and these values are used to correct the measured Cd and Zn ratios using the exponential form of the General Power Law (GPL) (Maréchal et al., 1999; Rehkämper et al., 2004). Delta values were then calculated by referencing exponentially corrected sample ratios to exponentially corrected standard ratios using the SSB method. The graphical normalization method of Maréchal et al. (1999) was not used here because there was insufficient instrumental mass bias drift during Cd and Zn measurement sessions.

Reproducibility of measurements of in-house Cd and Zn secondary standards and a zero-delta by back-to-back measurement of the PCIGR-1 Cd and PCIGR-1 Zn standards is reported in Tables 2.2 and 2.3, respectively. In-house secondary standard measurements were made systematically before and during each analytical session. Delta values for Cd reference standards (Table 2.2) agreed within uncertainty with $\delta^{114/110}$Cd values in the literature.

2.2.6 Description of the matrix experiments

The pure Cd and Zn standards (PCIGR-1) and doped standard solutions for isotopic analysis were prepared daily. Three categories of dopant were investigated: (1) bulk organic and inorganic column-derived components, (2) mock column-derived inorganic components prepared from pure standard solutions and (3) various single metallic element matrix components. All doped standards were treated as samples.

Matrix effects were assessed by examining changes in signal intensities (^{110}Cd, ^{109}Ag, ^{64}Zn and ^{63}Cu), mass biases (f(Cd), f(Ag), f(Zn), f(Cu)) and delta values between doped and undoped standards. Matrix effects on the $\delta^{114/110}$Cd and $\delta^{66/64}$Zn values were deemed significant when they were outside the 2S.D. reproducibility of the in-house secondary standards; i.e., for $\delta^{114/110}Cd_{SSB}$ ± 0.33‰, $\delta^{114/110}Cd_{Ag\text{-}corr.}$ ± 0.14‰, $\delta^{66/64}Zn_{SSB}$ ± 0.06‰ and $\delta^{66/64}Zn_{Cu\text{-}corr.}$ ± 0.19‰ (Tables 2.2 and 2.3, respectively).

2.2.7 Matrix components

Bulk column blank material (i.e., organic and inorganic) was added to pure Cd and Zn standards in proportions (0.2–50%) consistent with the range of dilutions needed for the real samples that motivated this study. For example, typical digested bivalve samples contain 300 ng of Cd and 5,000 ng Zn, while 150 ng of Cd and 100 ng of Zn are required for a MC-ICP-MS isotopic analysis. Therefore, with 100% column yield, 50% of the Cd eluate cut or 2% of the Zn eluate cut are present in the analyzed solution.

In order to investigate the effect of the inorganic component of the bulk column blank, two doping experiments were performed for Cd. In the first, the matrix effect induced by Mg (the major component of the blank) was determined. In the second, the combined effect of the major contaminant elements was investigated using a “mock

column inorganic matrix" solution. In both experiments, elements were doped at the highest quantities measured in the blanks (October 2006, Table 2.1). Therefore, the Cd standard (150 ng mL^{-1}) was doped with 42 ng mL^{-1} of Mg corresponding to a molar concentration of 1.3 times the molar concentration of Cd. The "mock column inorganic matrix" was prepared similarly resulting in a total matrix element concentration of 1.7 times the molar concentration of Cd.

In the final set of experiments, large quantities of metallic elements, five times the molar concentration of Cd or Zn, were added to the Cd and Zn standards to approximate sample-derived inorganic matrix components and characterize the matrix effects associated with individual inorganic element additions. The matrix elements in these experiments were chosen on the basis of their abundance in biological or geological materials as well as to cover a wide range in mass and ionization potential (IP) (Table 2.4; Sansonetti and Martin, 2005).

2.3 Results and discussion

The results for the bulk column blank matrix addition experiments for Cd and Zn are given in tables in Appendices C and D, respectively. The results for the inorganic column blank matrix addition experiments are given in Appendix E with results of the metallic elements doping experiments for Cd and Zn in Appendices F and G, respectively.

2.3.1 Bulk column blank matrix addition

Ion signal enhancement relative to the undoped standards results from the presence of bulk column blank matrix during isotopic analysis by MC-ICP-MS. Ion signal intensity changes, for Cd–Ag (Fig. 2.1a and b) and for Zn–Cu (Fig. 2.2a and b), vary considerably from run to run but are generally somewhat larger for the element pair Zn–Cu as compared to the pair Cd–Ag. For both pairs the mass bias-correcting elements (Ag and Cu) (Figs. 2.1b and 2.2b) generally experience larger signal enhancement than the analytes (Cd and Zn) (Figs. 2.1a and 2.2a).

More importantly, column matrix induces changes in the instrumental mass bias of both analytes and mass bias-correcting elements, resulting in inaccurate Cd and Zn isotope ratios (Figs. 2.1c, d and 2.2c, d). These effects, like the ion signal intensity enhancement, vary from one session to the next.

For SSB corrected Cd delta values, with the addition of up to 20% matrix to standards, mass bias changes are insignificant and $\delta^{114/110}Cd_{SSB}$ values are within error of undoped standard values (Fig. 2.1c). However, column matrix concentrations of 50% result in heavy $\delta^{114/110}Cd_{SSB}$ values due to higher f(Cd) in the presence of matrix (Fig. 2.1c). Use of the wet plasma cones (A cones) for Cd isotopic analysis does not reduce this mass bias change. Low matrix levels (0.2–2%) have little effect on f(Zn) and thus $\delta^{66/64}Zn_{SSB}$ values are within error of matrix-free values (Fig. 2.2c). However as with Cd, mass bias effects result in heavy $\delta^{66/64}Zn_{SSB}$ values for 10% and 50% column matrix (Fig. 2.2c).

For the combined external normalization–SSB (instrumental mass bias correction using f(Ag) and f(Cu)) f(Ag) and f(Cu) overcorrect the measured Cd and Zn isotopic ratios, i.e., f(Ag)>f(Cd) and f(Cu)>f(Zn), resulting in light $\delta^{114/110}Cd_{Ag\text{-}corr.}$ (Fig. 2.1d) and $\delta^{66/64}Zn_{Cu\text{-}corr.}$ (Fig. 2.2d) values even at low matrix levels. The $\delta^{114/110}Cd_{Ag\text{-}corr.}$ and $\delta^{66/64}Zn_{Cu\text{-}corr.}$ values per amu are similar in magnitude, suggesting the matrix-induced mass bias effects may be largely related to the relative ionization potentials of the element pairs, Cd–Ag and Zn–Cu, which unlike mass are similar (Table 2.4).

Differences in mass bias between analytes and their mass bias-correcting elements, such as these, have been reported in previous studies (Wombacher et al., 2003; Carlson et al., 2001; Pietruszka et al., 2006) and result in discrepancies between the delta values derived from the SSB and the combined external normalization–SSB instrumental mass bias correction methods. Such discrepancies may be used to identify the presence of matrix effects. Importantly, as we demonstrate here, it cannot be assumed that the combined external normalization–SSB correction produces more accurate results than SSB correction alone.

2.3.2 Inorganic elements introduced during cadmium column chemistry

Although the relative contribution of inorganic elements is small, their effect on ion signal intensity and mass bias can be significant. Doping with Mg (column blank level) increases the ion signal intensities of both Cd and Ag (4.5–14.9%) as does doping with "mock column inorganic matrix" (8.6–15.7%) (Appendix E). Doping with Mg alone leads to insignificant changes in mass bias and delta values for both mass bias correction methods. The "mock column inorganic matrix" produces changes in f(Cd) that are insignificant or, in one of four tests, result in a heavy delta value ($\delta^{114/110}Cd_{SSB} = 0.47‰$). This suggests that the larger changes in f(Cd) introduced by bulk column blank matrix are largely related to resin-derived organics.

The combined external normalization–SSB mass bias correction method using f(Ag) results in $\delta^{114/110}Cd_{Ag\text{-}corr.}$ values that are heavy in two tests ($\delta^{114/110}Cd_{Ag\text{-}corr.} = 0.24‰$, 0.37‰) and light in one test ($\delta^{114/110}Cd_{Ag\text{-}corr.} = -0.26‰$). For these three tests, the magnitude of the change in the $\delta^{114/110}Cd_{Ag\text{-}corr.}$ values is 28–71% of that observed for the bulk column blank matrix, again suggesting inorganic elements alone are not responsible for the mass bias effects introduced by bulk column blank matrix.

2.3.3 Inorganic matrix effects

Additions of metallic matrix elements to the analyte in larger quantities than are present in the "mock column inorganic matrix" cause ion signal intensity enhancement in the majority of cases and suppression in a few cases. In contrast to bulk column blank matrix, ion signal intensity changes are greater for the higher mass pair Cd–Ag than for Zn–Cu. Both Cd and Zn ion signals are suppressed by Al and enhanced by Sr (two of three results for Sr-doped Cd standards), Ba and Pb (Fig. 2.3a and b). Aluminum, Sr and Ba enhance both Ag and Cu ion signal intensities (Fig. 2.3a and b), while Pb causes suppression of the Cu ion signal, but not of the Ag ion signal, suggesting that the mechanism for suppression is more effective for lower mass analyte ions (Fig. 2.3a and b). Silver ion signal intensity is always more enhanced than Cd and Cu ion signal intensity is usually more enhanced than Zn perhaps due to the lower ionization potentials of the mass bias-correcting elements (Table 2.4).

With few exceptions, both mass bias correction methods produce light Cd and Zn delta values indicating that f(Cd), f(Ag), f(Zn) and f(Cu) are all reduced when metallic elements are present. Correction of measured Cd with SSB alone produces light delta values with few exceptions (one heavy result each for Al, Ir and Pb) (Fig. 2.4a). Fractionation correction using f(Ag) for doped Cd runs only partially compensates for the matrix effect on f(Cd) (i.e., f(Cd) > f(Ag)) and $\delta^{114/110}Cd_{Ag\text{-}corr.}$ values are still all light. One exception is for Sr-doped Cd standards (two of three results), where the resulting $\delta^{114/110}Cd_{Ag\text{-}corr.}$ value is within error of the undoped Cd standard. The lightest $\delta^{114/110}Cd_{SSB}$ and $\delta^{114/110}Cd_{Ag\text{-}corr.}$ values (Fig. 2.4a) result from the tested matrix elements with the lowest ionization potentials, Rb and Cs (Table 2.4). Changes in the ion signal intensity of ^{110}Cd and the calculated $\delta^{114/110}Cd_{SSB}$ and $\delta^{114/110}Cd_{Ag\text{-}corr.}$ values for Zn-doped solutions are in part due to the formation of $ZnAr^+$ ((*m*/*z*) = 107, 110) from minor isotopes of Zn (Figs. 2.3a and 2.4a). However, the small contributions from $ZnAr^+$ do not significantly change either the magnitude of the delta values or the difference between the $\delta^{114/110}Cd_{SSB}$ and $\delta^{114/110}Cd_{Ag\text{-}corr.}$ values (Appendix F).

All doped Zn standard runs are isotopically light (Fig. 2.4b), with the exception of the Ba-doped Zn standards where heavy isotopic values for some isotope ratios can be attributed to the isobaric interference of Ba^{2+} on ^{65}Cu, ^{66}Zn, ^{67}Zn and ^{68}Zn (Appendix G). The apparently light Zn isotope ratios observed for Sr-doped Zn standards (Fig. 2.4b) are largely attributed to a spectral interference ($SrAr^{2+}$) that affects ^{63}Cu and ^{64}Zn (Appendix G). The lightest $\delta^{66/64}Zn_{SSB}$ values result from doping with Al and Ca, elements with ionization potentials lower than those of both Zn and Cu (Table 2.4). In contrast to Cd–Ag, fractionation correction using f(Cu) produces $\delta^{66/64}Zn_{Cu\text{-}corr.}$ values that are overcorrected and are even lighter than $\delta^{66/64}Zn_{SSB}$ values for Al, Ca, Cd and Pb (i.e., f(Zn) < f(Cu)) (Fig. 2.4b).

2.3.4 Chemical treatment of resin-derived organics

The magnitude of the matrix effect varied with analytical session and so comparisons between our standard column matrix treatment and the refluxed HNO_3 and $HClO_4/HNO_3$ treatments are made for experiments run in the same session (see Appendices C and D). Chemical treatment with refluxed HNO_3 (Blank 5 compared to

standard treatment Blank 2) or $HClO_4/HNO_3$ (Blank 6 compared to standard treatment Blank 4) does not reduce signal enhancement but column blank matrix-induced mass bias variation and associated inaccuracy in $\delta^{114/110}Cd$ values are reduced (Fig. 2.1c and d). The $HClO_4/HNO_3$-treated column matrix results in signal enhancements and delta values identical to those of the $HClO_4/HNO_3$ acid blank, suggesting residual $HClO_4$ or inorganic elements introduced with the $HClO_4$ are the source of the mass bias effect. Similarly for Zn, chemical treatment with refluxed HNO_3 (Blank 3 compared to standard treatment Blank 1) or $HClO_4/HNO_3$ (Blank 4 compared to standard treatment Blank 1) reduces the matrix effect on the mass bias (Fig. 2.2c and d) and in the case of the refluxed HNO_3-treated column blank the matrix effect on the mass bias is insignificant.

After refluxed HNO_3 digestion, remaining matrix effects are attributed to the presence of residual refractory organics and the inorganic column matrix. The $HClO_4$ treatment should remove residual organics, but introduces additional inorganic contamination (Table 2.1). In addition, residual $HClO_4$ may be present, due to its high boiling point (~203 °C), and may itself be the source of mass bias effects.

The reduction of the mass bias effects, observed for bulk column blanks that have undergone more oxidizing treatments than our standard column blank treatment, supports the conclusion that organics are partially responsible for the observed matrix effects. The remaining mass bias effects, observed as delta values, for the more aggressively digested column blanks are approximately equal to the effect observed for the "mock column inorganic matrix." Therefore, inaccurate delta values from column matrix treated by our standard digestion are attributed to a combination of organics and inorganic elements leached from the resin.

2.3.5 Correction of delta values

Correction of delta values may be possible if delta values resulting from the presence of column matrix are consistent over time (during a given run or between runs). Archer and Vance (2004) suggested (for Zn) that referencing samples to standards, which themselves have been through columns, could effectively compensate for a column matrix effect. Our experiments show that the magnitude of the matrix effect is dependent on the dilution of the column matrix and the associated organic and inorganic

contaminants, and that the column blank itself is variable. Therefore, for this method to work column blank would need to be added to standards in similar proportions to column matrix present in the samples and even so some variability would be expected due to the variability of the inorganic component of the column blank.

2.3.6 Consequences for natural samples

These experiments demonstrate that resin-derived organics and inorganic elements, introduced to the sample during column chemistry, create a mismatch between sample and bracketing standard matrices leading to inaccurate delta values. The degree of inaccuracy increases with the amount of column blank matrix added to the pure standard solutions. One of the original motivations for this investigation was the observation that isotopic signatures in samples varied depending on the dilution factor of the analyzed solution. In order to test whether the observed inaccuracy could be accounted for by the column blank matrix effect, an experiment was devised in which replicate purifications of variable column loads enabled variable dilution of the Cd eluate cut (Fig. 2.5). The degree of inaccuracy introduced by our matrix experiment was identical in magnitude to that seen in our natural samples (cf. Fig. 2.1c and d).

The range of dilutions investigated in these experiments is not necessarily restricted to biological materials. For example, at one extreme samples may contain high Cd and/or Zn concentrations but be limited in availability (e.g., lunar samples; Moynier et al., 2006). Also, there are samples with extremely low Cd and/or Zn concentrations where large quantities of sample are needed for a single analysis (e.g., seawater; Lacan et al., 2006; John, 2007). In both these scenarios sample dilution may be limited, resulting in analyses vulnerable to the type of matrix effects described here. However, for many sample materials (e.g., anthropogenic materials; Cloquet et al., 2006b; Sivry et al., 2008; Sonke et al., 2008 and Zn ores; Wilkinson et al., 2005; Dolgopolova et al., 2006), sample size and analyte concentration do not limit dilution and these materials are not expected to be subject to these matrix effects as long as sufficient sample material is loaded on the column.

Inorganic and organic resin-derived contaminants and associated matrix effects are expected to vary with the resin, volume of the resin bed, eluents and volumes of

eluents used in the column chemistry. Similar chemistries using AG MP-1M resin, employed for the purification of Zn, Cu and Fe (e.g., Maréchal et al., 1999), may produce purified samples susceptible to these matrix effects during MC-ICP-MS analysis. In addition, chromatography procedures utilizing other resins, including the Bio-Rad AG 1 anion exchange resins, are expected to introduce similar matrix effects. Indeed, the only similar study to this one has found that AG 1-X8 resin-derived contaminants cause matrix effects in MC-ICP-MS analysis of Mo isotopes (Pietruszka and Reznik, 2008). Ultimately, each ion exchange purification method will need to be assessed individually. Based on our experiments, we recommend, that for accurate delta values, sufficient quantities of sample material be loaded on the column so that no more than 20% of the Cd or Zn eluate cut is in the analyzed solution.

2.4 Conclusions

Matrix effects are particularly significant in the measurement of isotopic fractionation in systems with small natural variations, such as Cd and Zn. Our study demonstrates that column matrix and even low-levels of metallic elements must be evaluated as potential sources of error during Cd and Zn isotopic analysis. The main findings of our investigation are:

(1) Bulk column blank matrix and metallic elements cause signal enhancement. In both Cd–Ag and Zn–Cu systems, enhancements are greater for the lower ionization potential mass bias-correcting elements (Ag and Cu) than for the analytes (Cd and Zn). Signal enhancement and suppression indicate matrix problems and are associated with inaccurate Cd and Zn isotope ratios.
(2) Mass bias changes result from bulk column blank matrix introduced during standard column chemistry. For both Cd and Zn these mass bias changes result in heavy SSB corrected delta values and light combined external normalization–SSB corrected delta values.

(3) The inorganic content of bulk column blank matrix is variable and even small quantities can cause significant effects. However, the effects are not large enough to account for those of the bulk column blank matrix.
(4) Residual resin-derived organics are a significant source of column-induced matrix effects.
(5) Chemical treatment of column blanks, aimed at destroying resin-derived organics, with either refluxed HNO_3 or $HClO_4$/ HNO_3 reduced the mass bias effect relative to the standard HNO_3 dry down.
(6) In both Cd–Ag and Zn–Cu systems, the mass bias responses of the analyte and mass bias-correcting element differ in the presence of matrix. This results in disagreement between $\delta^{114/110}Cd_{SSB}$ and $\delta^{114/110}Cd_{Ag\text{-}corr.}$ and $\delta^{66/64}Zn_{SSB}$ and $\delta^{66/64}Zn_{Cu\text{-}corr.}$ values. In such cases the externally normalized values cannot be assumed to give the more accurate result.

2.5 Acknowledgements

This work benefited from discussions on matrix effects with Bert Mueller and we also thank him for his assistance with the ELEMENT2 HR-ICP-MS. We are grateful to James Scoates, Laure Aimoz and six anonymous reviewers for comments on various versions of this manuscript. We also thank Frank Wombacher for providing aliquots of the “JMC Cd”, the “Münster Cd” and the BAM-1012 Cd reference standards. This study was funded by NSERC Discovery grants to Dominique Weis and Kristin J. Orians.

Table 2.1. Inorganic contents of column chemistry blanks are shown for three resin cleaning methods, the routine clean was used in this study (see Appendix B). Perchloric treatment of a column blank after routine cleaning (Cd Blank 6 and Zn Blank 4) was evaluated for additional contamination.

	Routine clean			Full clean	Batch clean	$HClO_4$-treated	[Matrix element][5]/ [Cd][6] or [Zn][7]
Element (ng)	Oct 06	Jun 07	Apr 08	Jun 07	Apr 08	Jun 07	in real samples
Cd fraction (0.5 M HNO_3)							
Mg[1]	42	17	0.2	21	2.7	74	0.095-0.447
Al[1]	3.3	0.83	1.1	2.1	1.1	2.5	0.007-0.032
Ca[1]	8.2	ND	0.46	3.3	0.97	7.3	0.011-0.053
Cr[1]	0.7	0.33	0.2	0.61	0.15	41	0.001-0.003
Fe[2]	3.8	1.5	0.61	1.3	0.44	2.8	0.003-0.015
Zn[3]	1.9	1	0.14	0.67	0.43	1.6	0.001-0.004
Cd[4]	ND	ND	ND	ND	ND	ND	
Zn fraction (0.1 M HBr + 0.5 M HNO_3)							
Mg[1]	1.7	ND	4.2	19	ND	11	0.002-0.011
Al[1]	66	42	21	108	10	42	0.078-0.368
Ca[1]	1.7	ND	0.15	5.3	ND	3.5	0.001-0.006
Cr[1]	1.3	1.9	0.92	1.5	0.47	42	0.001-0.003
Fe[2]	5.2	4.4	7.6	8.6	4.4	5.0	0.003-0.012
Zn[3]	1.4	2.6	0.67	0.60	3.7	0.90	0.000-0.002

Not Detected (ND)
Element should elute in [1]the first 10 mL of 7 M HCl, [2]8 M HF + 2 M HCl, [3]0.1 M HBr + 0.5 M HNO_3 or [4]0.5 M HNO_3.
[5]Molar concentrations of matrix elements in the highest blank, chemistry performed Oct. 2006.
B.C. oyster Cd[6] (2.9-13.7 ppm dry weight) and Zn[7] (197-1082 ppm dry weight) concentrations used in calculation, assume 0.150 g tissue digested and loaded on column.

Table 2.2. Cadmium isotope data for secondary Cd isotopic standards and for measurement of a "zero-delta" by back-to-back analysis of the PCIGR-1 Cd standard.

	Sample-standard bracketing		External normalization with sample-standard bracketing	
Sample	δCd/amu[a]	$\delta^{114/110}$Cd	δCd/amu[a]	$\delta^{114/110}$Cd
PCIGR-1 Cd relative to PCIGR-1 Cd				
mean (n=33)	-0.00	-0.01	0.00	0.00
2SD	0.04	0.17	0.03	0.08
PCIGR-2 Cd relative to PCIGR-1 Cd				
mean (n=42)	-0.37	-1.43	-0.37	-1.47
2SD	0.08	0.33	0.04	0.14
JMC Cd relative to PCIGR-1 Cd				
mean (n=3)	-0.02	-0.07	-0.01	-0.03
2SD	0.03	0.11	0.02	0.05
BAM-1012 relative to PCIGR-1 Cd				
mean (n=4)	-0.33	-1.29	-0.38	-1.47
2SD	0.10	0.35	0.04	0.12
BAM-1012 relative to JMC Cd – literature		-1.08[b]		
mean (n=5)	-0.28	-1.11	-0.34	-1.37
2SD	0.08	0.36	0.08	0.25
Münster Cd relative to JMC Cd-literature		4.65[b], 4.48[c]		
mean (n=4)	1.13	4.50	1.13	4.50
2SD	0.06	0.27	0.02	0.03
Münster Cd relative to BAM-1012-literature		5.74[b]		
mean (n=3)	1.44	5.75	1.44	5.76
2SD	0.03	0.13	0.02	0.09

[a] δCd/amu is calculated from the mean of 4 ratios (^{111}Cd/^{110}Cd, ^{112}Cd/^{110}Cd, ^{113}Cd/^{110}Cd, ^{114}Cd/^{110}Cd).
[b] Wombacher and Rehkämper (2004).
[c] Cloquet et al. (2005).

Table 2.3. Zinc isotope data for the in-house secondary Zn isotopic standard and for measurement of a "zero-delta" by back-to-back analysis of the PCIGR-1 Zn standard.

	Sample-standard bracketing		External normalization with sample-standard bracketing	
Sample	δZn/amu[a]	$\delta^{66/64}$Zn	δZn/amu[a]	$\delta^{66/64}$Zn
PCIGR-1 Zn relative to PCIGR-1 Zn				
mean (n=52)	0.001	0.00	0.00	0.00
2SD	0.020	0.05	0.03	0.05
PCIGR-2 Zn relative to PCIGR-1 Zn				
mean (n=18)	-5.15	-10.37	-5.10	-10.28
2SD	0.03	0.06	0.10	0.19

[a] δZn/amu is calculated from the mean of 4 ratios (^{66}Zn/^{64}Zn, ^{67}Zn/^{64}Zn, ^{68}Zn/^{64}Zn).

Table 2.4. First and second ionization energies (eV) and atomic weights for analytes and matrix elements relevant in this study (Sansonetti and Martin, 2005).

Atomic Weight	Element	1st IP	2nd IP
24.3	Mg	7.65	15.04
27.0	Al	5.98	18.83
40.1	Ca	6.11	11.87
63.6	Cu	7.73	20.29
65.4	Zn	9.39	17.96
85.5	Rb	4.18	27.29
87.6	Sr	5.69	11.03
107.9	Ag	7.58	21.48
112.4	Cd	8.99	16.91
132.9	Cs	3.89	23.16
137.3	Ba	5.21	10.00
175.0	Lu	5.43	13.9
192.2	Ir	8.97	
207.2	Pb	7.42	15.03

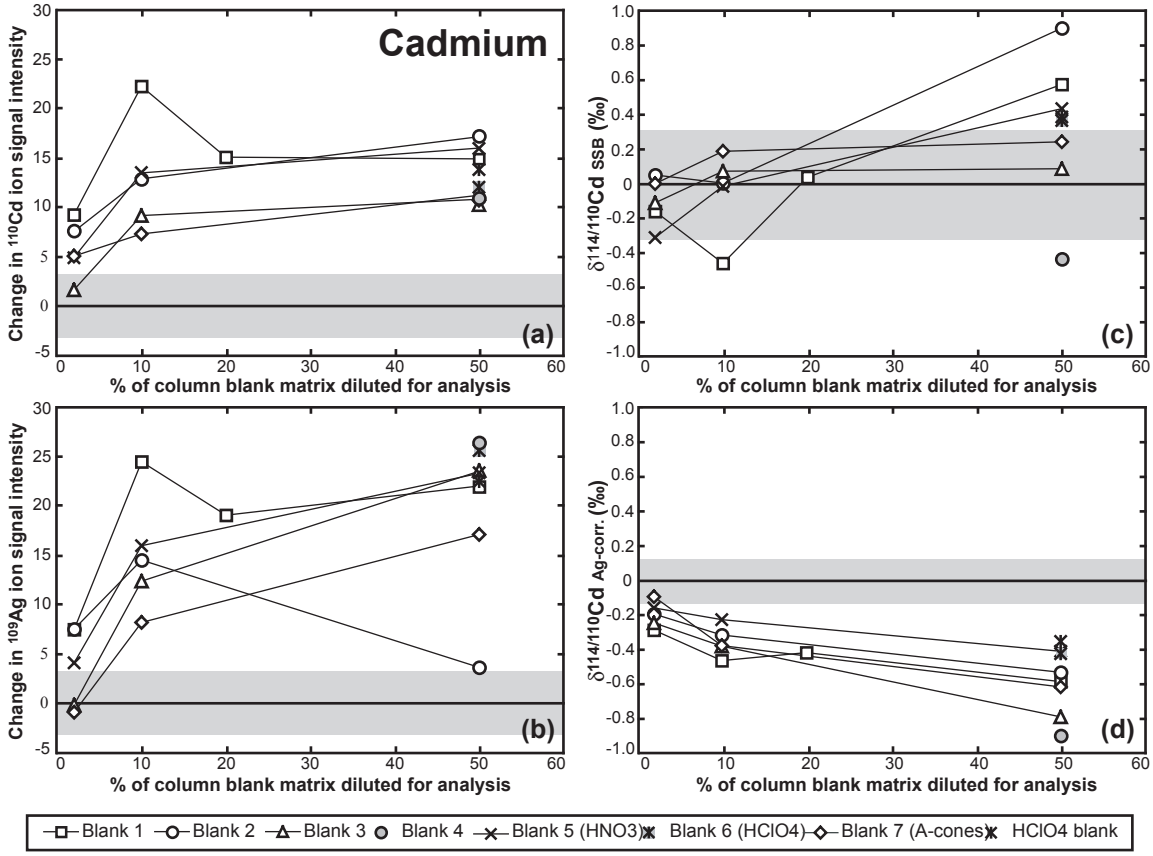

Fig. 2.1. Matrix effects on Cd isotope ratio measurements as a function of bulk column blank matrix addition: (a) percent changes in ^{110}Cd ion signal intensity, (b) percent changes in ^{109}Ag ion signal intensity, (c) $\delta^{114/110}Cd_{SSB}$ and (d) $\delta^{114/110}Cd_{Ag\text{-}corr.}$ values. For (a) and (b), the grey areas denote 2 standard deviation (SD) on the mean ^{110}Cd and ^{109}Ag ion signal intensities during measurement of a "zero-delta" by back-to-back analysis of the PCIGR-1 Cd standard (n = 33). For (c) and (d), the grey areas denote 2SD on the mean $\delta^{114/110}Cd_{SSB}$ and $\delta^{114/110}Cd_{Ag\text{-}corr.}$ values for the in-house secondary Cd standard (Table 2.2). Note that in (b) for Blanks 1 and 2 with 2% matrix, the values (7.48% and 7.51%, respectively) are overlapping.

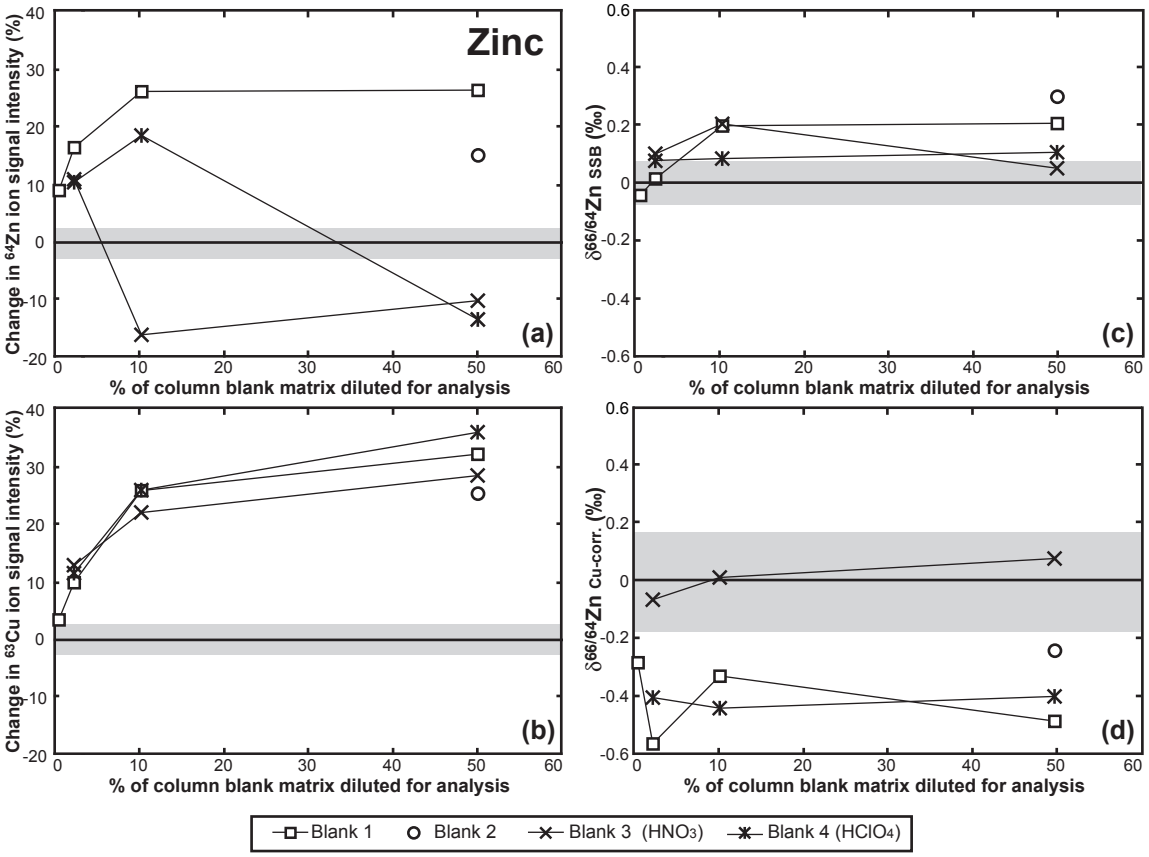

Fig. 2.2. Matrix effects on Zn isotope ratio measurements as a function of bulk column blank matrix addition: (a) percent changes in ^{64}Zn ion signal intensity, (b) percent changes in ^{63}Cu ion signal intensity, (c) $\delta^{66/64}Zn_{SSB}$ and (d) $\delta^{66/64}Zn_{Cu\text{-}corr.}$ values. For (a) and (b), the grey areas denote 2 standard deviation (SD) on the mean ^{64}Zn and ^{63}Cu ion signal intensities during measurement of a "zero-delta" by back-to-back analysis of the PCIGR-1 Zn standard (n = 52). For (c) and (d), the grey areas denote 2SD on the mean $\delta^{66/64}Zn_{SSB}$ and $\delta^{66/64}Zn_{Cu\text{-}corr.}$ values for the in-house secondary Zn standard (Table 2.3).

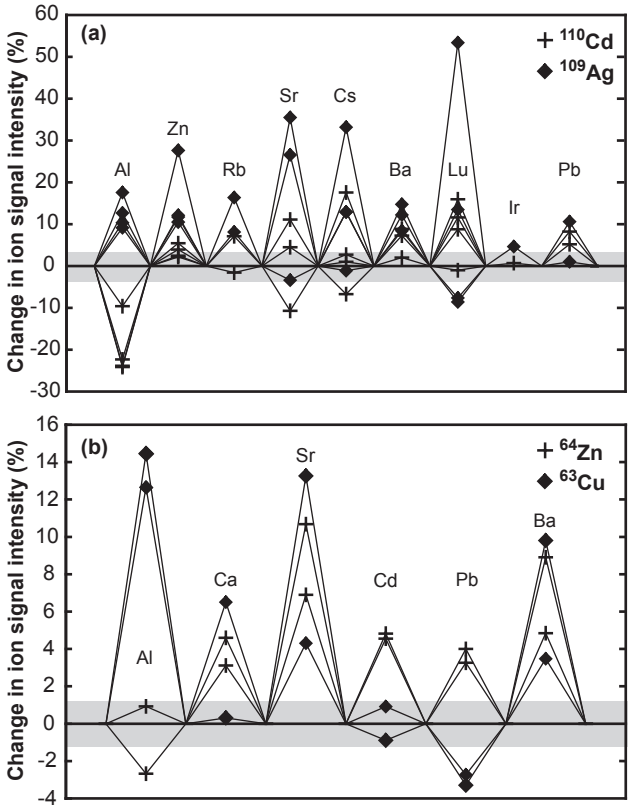

Fig. 2.3. Matrix effects for solutions doped with metallic elements: (a) ^{110}Cd and ^{109}Ag ion signal intensities and (b) ^{64}Zn and ^{63}Cu ion signal intensities, calculated as the variation (%) of the doped solution ion signal intensity from the mean ion signal intensity of the two bracketing undoped standards. For (a), the grey area denotes 2 standard deviation (SD) on the mean ^{110}Cd and ^{109}Ag ion signal intensities during measurement of a "zero-delta" by back-to-back analysis of the PCIGR-1 Cd standard (n = 33). For (b), the grey area denotes 2SD on the mean ^{64}Zn and ^{63}Cu ion signal intensities during measurement of a "zero-delta" by back-to-back analysis of the PCIGR-1 Zn standard (n = 52).

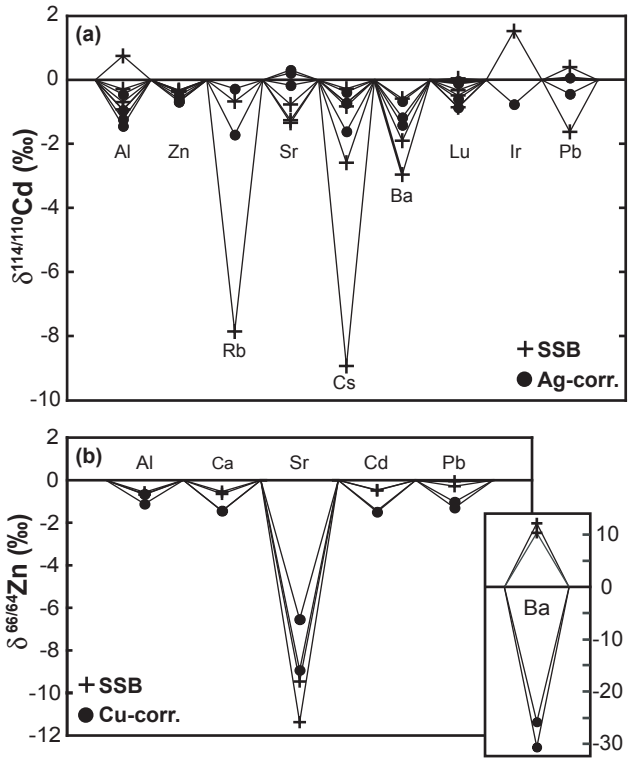

Fig. 2.4. Matrix effects for solutions doped with metallic elements: (a) $\delta^{114/110}Cd_{SSB}$ and $\delta^{114/110}Cd_{Ag\text{-}corr.}$ values and (b) $\delta^{66/64}Zn_{SSB}$ and $\delta^{66/64}Zn_{Cu\ corr.}$ values. Matrix effects on the $\delta^{114/110}Cd$ and $\delta^{66/64}Zn$ values are discussed as significant when outside the 2 standard deviation (SD) of the in-house secondary Cd and Zn standards (Tables 2.2 and 2.3, respectively), not shown in (a) and (b).

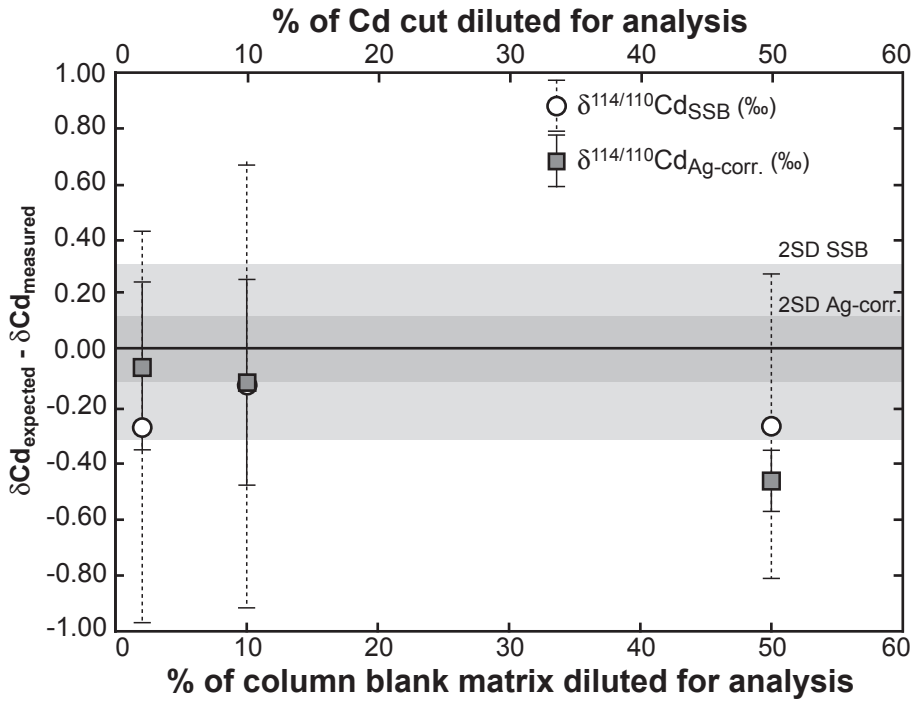

Fig. 2.5. Matrix effects as a function of the dilution of the Cd eluate cut for a bivalve sample. For this experiment, variable quantities of a single bivalve digest were loaded on columns such that the analyzed solutions contained 2–50% of the eluted Cd and column matrix. The shift from the expected delta value is represented by $\delta^{114/110}Cd_{expected}$ - $\delta^{114/110}Cd_{measured}$. The $\delta^{114/110}Cd$ measured values are the mean of three measurements (performed during two analytical sessions), where the error bars signify 2 standard deviation (SD). The grey areas denote 2SD on the mean $\delta^{114/110}Cd_{SSB}$ and $\delta^{114/110}Cd_{Ag\text{-}corr.}$ values for the in-house secondary Cd standard (Table 2.2).

2.6 References

Albarède, F., Beard, B.L. (2004) Analytical methods for non-traditional isotopes. Reviews in Mineralogy and Geochemistry 55: 113–152.

Archer, C., Vance, D. (2004) Mass discrimination correction in multiple-collector plasma source mass spectrometry: an example using Cu and Zn isotopes. Journal of Analytical Atomic Spectrometry 19: 656–665.

Bermin, J., Vance, D., Archer, C., Statham, P.J. (2006) The determination of the isotopic composition of Cu and Zn in seawater. Chemical Geology 226: 280–297.

Carlson, R.W., Hauri, E.H., Alexander, C.M.O'D. (2001) Matrix-induced isotopic mass fractionation in the ICP-MS. In: Holland, G., Tanner, S.D. (eds) Plasma Source Mass Spectrometry: The New Millennium. Cambridge: The Royal Society of Chemistry, pp. 288–297.

Cloquet, C., Carignan, J., Libourel, G. (2006a) Isotopic composition of Zn and Pb atmospheric depositions in an urban/periurban area of northeastern France. Environmental Science & Technology 40: 6594–6600.

Cloquet, C., Carignan, J., Libourel, G., Sterckeman, T., Perdrix, E. (2006b) Tracing source pollution in soils using cadmium and lead isotopes. Environmental Science & Technology 40: 2525–2530.

Cloquet, C., Rouxel, O., Carignan, J., Libourel, G. (2005) Natural cadmium isotopic variations in eight geological reference materials (NIST SRM 2711, BCR 176, GSS-1, GXR-1, GXR-2, GSD-12, Nod-P-1, Nod-A-1) and anthropogenic samples, measured by MC-ICP-MS. Geostandards and Geoanalytical Research 29: 95–106.

De Jong, J., Schoemann, V., Tison, J.L., Becquevort, S., Masson, F., Lannuzel, D., Petit, J., Chou, L., Weis, D., Mattielli, N. (2007) Precise measurement of Fe isotopes in marine samples by multi-collector inductively coupled plasma mass spectrometry (MC-ICP-MS). Analytica Chimica Acta 589: 105–119.

Dolgopolova, A., Weiss, D.J., Seltmann, R., Kober, B., Mason, T.F.D., Coles, B., Stanley, C.J. (2006) Use of isotope ratios to assess sources of Pb and Zn dispersed

in the environment during mining and ore processing within the Orlovka-Spokoinoe mining site (Russia). Applied Geochemistry 21: 563–579.

Douglas, D.J., Tanner, S.D. (1998) Fundamental Considerations in ICPMS. In: Montaser, A. (ed) Inductively Coupled Plasma Mass Spectrometry. Wiley-VCH, pp. 615–679.

Evans, E.H., Giglio, J.J. (1993) Interferences in Inductively Coupled Plasma Mass-Spectrometry - a Review. Journal of Analytical Atomic Spectrometry 8: 1–18.

Galy, A., Belshaw, N.S., Halicz, L., O'Nions, R.K. (2001) High-precision measurement of magnesium isotopes by multiple-collector inductively coupled plasma mass spectrometry. International Journal of Mass Spectrometry 208: 89–98.

Horlick, G., Montaser, A. (1998) Analytical Characteristics of ICPMS. In: Montaser, A. (ed) Inductively Coupled Plasma Mass Spectrometry. Wiley-VCH, pp. 503–588.

John, S.G. (2007) The Marine Biogeochemistry of Zinc Isotopes. Ph.D. thesis, Massachusetts Institute of Technology, pp. 142.

John, S.G., Park, G., Zhang, Z., Boyle, E.A. (2007) The isotopic composition of some common forms of anthropogenic zinc. Chemical Geology 245: 61–69.

John, S.G., Rouxel, O.J., Craddock, P.R., Engwall, A.M., Boyle, E.A. (2008) Zinc stable isotopes in seafloor hydrothermal vent fluids and chinmeys. Earth and Planetary Science Letters 269: 17–28.

Lacan, F., Francois, R., Ji, Y., Sherrell, R.M. (2006) Cadmium isotopic composition in the ocean. Geochimica et Cosmochimica Acta 70: 5104–5118.

Longerich, H.P., Fryer, B.J., Strong, D.F. (1987) Determination of Lead Isotope Ratios by Inductively Coupled Plasma-Mass Spectrometry (ICP-MS). Spectrochimica Acta Part B-Atomic Spectroscopy 42: 39–48.

Loss, R.D., Rosman, K.J.R., de Laeter, J.R. (1990) The Isotopic Composition of Zinc, Palladium, Silver, Cadmium, Tin, and Tellurium in Acid-Etched Residues of the Allende Meteorite. Geochimica et Cosmochimica Acta 54: 3525–3536.

Luck, J.-M., Ben Othman, D., Albarède, F. (2005) Zn and Cu isotopic variations in chondrites and iron meteorites: Early solar nebula reservoirs and parent-body processes. Geochimica et Cosmochimica Acta 69: 5351–5363.

Maréchal, C.N., Nicolas, E., Douchet, C., Albarède, F. (2000) Abundance of zinc isotopes as a marine biogeochemical tracer. Geochemistry Geophysics Geosystems 1, 1015, doi: 10.1029/1999GC000029.

Maréchal, C.N., Télouk, P., Albarède, F. (1999) Precise analysis of copper and zinc isotopic compositions by plasma-source mass spectrometry. Chemical Geology 156: 251–273.

Mason, T.F.D. (2003) High-precision transition metal isotope analysis by plasma-source mass spectrometry and implications for low temperature geochemistry. Ph.D. thesis, University of London, pp. 287.

Moynier, F., Albarede, F., Herzog, G.F. (2006) Isotopic composition of zinc, copper, and iron in lunar samples. Geochimica et Cosmochimica Acta 70: 6103–6117.

Pichat, S., Douchet, C., Albarède, F. (2003) Zinc isotope variations in deep-sea carbonates from the eastern equatorial Pacific over the last 175 ka. Earth and Planetary Science Letters 210: 167–178.

Pietruszka, A.J., Reznik, A.D. (2008) Identification of a matrix effect in the MC-ICP-MS due to sample purification using ion exchange resin: An isotopic case study of molybdenum. International Journal of Mass Spectrometry 270: 23–30.

Pietruszka, A.J., Walker, R.J., Candela, P.A. (2006) Determination of mass-dependent molybdenum isotopic variations by MC-ICP-MS: An evaluation of matrix effects. Chemical Geology 225: 121–136.

Rehkämper, M., Wombacher, F., Aggarwal, J.K. (2004) Stable Isotope Analysis by Multiple Collector ICP-MS. In: de Groot, P.A. (ed) Handbook of Stable Isotope Analytical Techniques, Vol 1. Elsevier, pp. 692–725.

Ripperger, S., Rehkämper, M., Porcelli, D., Halliday, A.N. (2007) Cadmium isotope fractionation in seawater - A signature of biological activity. Earth and Planetary Science Letters 261: 670–684.

Rosman, K.J.R., Barnes, I.L., Moore, L.J., Gramlich, J.W. (1980) Isotope Composition of Cd, Ca and Mg in the Brownfield Chondrite. Geochemical Journal 14: 269–277.

Rosman, K.J.R., de Laeter, J.R. (1976) Isotopic Fractionation in Meteoritic Cadmium. Nature 261: 216–218.

Rosman, K.J.R., De Laeter, J.R. (1988) Cadmium Mass Fractionation in Unequilibrated Ordinary Chondrites. Earth and Planetary Science Letters 89: 163–169.

Sansonetti, J.E., Martin, W.C. (2005) Handbook of basic atomic spectroscopic data. Journal of Physical and Chemical Reference Data 34: 1559–2259.

Shiel, A.E., Orians, K.J., Cossa, D., Weis, D. (2007) Anthropogenic contamination of bivalves revealed by Cd isotopes. Geochimica et Cosmochimica Acta 71, Supplement 1: A928.

Shiel, A.E., Orians, K.J., Cossa, D., Weis, D. (2008) Sourcing metals in bivalves using combined Pb, Zn and Cd isotopic compositions. Geochimica et Cosmochimica Acta 72, Supplement 1: A859.

Sivry, Y., Dupré, B., Sonke, J., Viers, J., Audry, S., Schäfer, J., Blanc, G., Riotte, J. (2006) Use of Cd and Zn isotopic variations in a sedimentary core to trace anthropogenic contamination. Geochimica et Cosmochimica Acta 70: A595.

Sivry, Y., Riotte, J., Sonke, J.E., Audry, S., Schäfer, J., Viers, J., Blanc, G., Freydier, R., Dupré, B. (2008) Zn isotopes as tracers of anthropogenic pollution from Zn-ore smelters The Riou Mort-Lot River system. Chemical Geology 255: 295–304.

Sonke, J.E., Sivry, Y., Viers, J., Freydier, R., Dejonghe, L., André, L., Aggarwal, J.K., Fontan, F., Dupré, B. (2008) Historical variations in the isotopic composition of atmospheric zinc deposition from a zinc smelter. Chemical Geology 252: 145–157.

Straßburg, S., Wollenweber, D., Wünsch, G. (1998) Contamination caused by ion-exchange resin!? Consequences for ultra-trace analysis. Fresenius Journal of Analytical Chemistry 360: 792–794.

Tan, S.H., Horlick, G. (1986) Background Spectral Features in Inductively Coupled Plasma Mass-Spectrometry. Applied Spectroscopy 40: 445–460.

Weiss, D.J., Mason, T.F.D., Zhao, F.J., Kirk, G.J.D., Coles, B.J., Horstwood, M.S.A. (2005) Isotopic discrimination of zinc in higher plants. New Phytologist 165: 703–710.

Weiss, D.J., Rausch, N., Mason, T.F.D., Coles, B.J., Wilkinson, J.J., Ukonmaanaho, L., Arnold, T., Nieminen, T.M. (2007) Atmospheric deposition and isotope

biogeochemistry of zinc in ombrotrophic peat. Geochimica et Cosmochimica Acta 71: 3498–3517.

Wilkinson, J.J., Weiss, D.J., Mason, T.F.D., Coles, B.J. (2005) Zinc isotope variation in hydrothermal systems: Preliminary evidence from the Irish Midlands ore field. Economic Geology 100: 583–590.

Wombacher, F., Rehkämper, M. (2004) Problems and suggestions concerning the notation of cadmium stable isotope compositions and the use of reference materials. Geostandards and Geoanalytical Research 28: 173–178.

Wombacher, F., Rehkämper, M., Mezger, K., Munker, C. (2003) Stable isotope compositions of cadmium in geological materials and meteorites determined by multiple-collector ICPMS. Geochimica et Cosmochimica Acta 67: 4639–4654.

CHAPTER 3

Evaluation of zinc, cadmium and lead isotope fractionation during smelting and refining [1]

[1]A version of this chapter has been published. Shiel, A.E., Weis, D., Orians, K.J. (2010) Evaluation of zinc, cadmium and lead isotope fractionation during smelting and refining. Science of the Total Environment 408: 2357–2368.

3.1 Introduction

Worldwide production of refined Zn, Cd and Pb metals in 2007 was 11,500,000 t (Tolcin, 2009), 20,400 t (Tolcin, 2008) and 8,280,000 t (Guberman, 2009), respectively. The majority of Zn is used as an anti-corrosion coating (40%), e.g., galvanized steel (Greenwood and Earnshaw, 2001). The majority of Cd is used to produce the metallic Cd electrode plate found in nickel-cadmium (Ni-Cd) batteries (67%); significant Cd is also used in pigments (15%), plastic stabilizers (10%) and coatings (7%) (Greenwood and Earnshaw, 2001). Today, lead-acid battery production accounts for the largest use of Pb; Pb is also used to produce ammunition, building construction materials, communication and power cable coverings and leaded gasoline (still sold for use in automobiles in parts of Eastern Europe, Africa, the Middle East, Asia and Latin America and used to fuel small general aviation aircrafts) (Greenwood and Earnshaw, 2001).

Zinc, Cd and Pb are all chalcophile elements. Zinc and Pb are the major constituents of the ore minerals sphalerite (ZnS) and galena (PbS). Cadmium is the constituent element of the mineral greenockite (CdS) and also occurs as a significant impurity (usually ~0.2–0.4%) in the ore mineral sphalerite, sphalerite being the important commercial source (Greenwood and Earnshaw, 2001). Sphalerite and galena ores are commonly associated and mined together. The main metallic Zn and Pb components of these ores are separated from other ore and gangue minerals, using methods such as grinding and sulfide flotation, to produce Zn and Pb ore concentrates. These ore concentrates undergo smelting and refining to produce high purity metals. Most of the world's refined Zn is produced from Zn ore concentrates using an electrowinning process, while most Pb is produced from Pb ore concentrates and secondary Pb materials (e.g., spent Pb-acid batteries) using pyrometallurgical processes. Cadmium is recovered primarily as a byproduct of Zn smelting and refining and from the recycling of spent Ni-Cd batteries, alloys and electric arc furnace dust.

In 2007, Canada was the second largest producer of refined Zn and the fourth largest producer of refined Cd in the world, producing ~7% (Tolcin, 2009) and ~10% (Tolcin, 2008), respectively. Canada also produced ~3% of the world's Pb (Guberman, 2009). Teck is Canada's largest mining, mineral processing and metallurgical company.

Their operations in Trail, British Columbia (B.C.) include one of the world's largest fully integrated Zn and Pb smelting and refining complexes, which contributed an estimated 36%, 33% and 67% of Canada's Zn, Pb and Cd metals production in 2007, respectively (calculated from Fthenakis, 2004; Teck Cominco Ltd., 2008; Tolcin, 2008, 2009; Guberman, 2009).

Zinc and Pb smelters, together with refineries, are large contributors to anthropogenic Zn, Cd and Pb emissions. Releases to air and water vary with the Zn and Pb ores used, type of metallurgical processing and the abatement measures in place. In this contribution, we endeavor to better understand the behavior of Zn, Cd and Pb isotopes during metallurgical processing and we explore the potential use of new geochemical tools, such as Zn and Cd isotopes, to source and trace these metals in the environment.

For elements with two or more stable isotopes, physical and chemical reactions may result in mass-dependent isotopic fractionation. This leads to natural variations in the isotopic compositions of many elements. The stable isotopic composition of a sample reflects that of the source and/or isotopic fractionation introduced by physiochemical reactions (Peterson and Fry, 1987). The extent of natural isotopic variability for an element is primarily determined by the relative mass difference for isotopes of that element (i.e., the mass difference for an isotope pair, Δm, relative to the average mass of the isotopes of the element) (Johnson et al., 2004). The extent of isotopic variability for an element will decrease with increasing atomic weight; for $\Delta m = 1$, the relative mass difference is, e.g., 8.0% for C, 1.5% for Zn, 0.9% for Cd and 0.5% for Pb. However, heavier elements tend to have more isotopes, and so the Δm, and subsequently the relative mass difference, for two isotopes of an element, may be much larger than that for $\Delta m = 1$. Due to the extended mass range of Cd isotopes relative to that of Zn isotopes, both Zn and Cd have total relative mass differences of 9.0% for $\Delta m = 6$ and $\Delta m = 10$ (i.e., Δm = mass range for all isotopes of the given element), respectively, despite the heavier mass of Cd. For Pb, this total relative mass difference is significantly smaller, 1.9% for $\Delta m = 4$. Only with modern instruments, primarily the multi-collector inductively coupled plasma mass spectrometer (MC-ICP-MS) with its enhanced ionization efficiency, has the precision needed to measure the small isotopic variations of

most heavy stable elements (e.g., Zn and Cd) in terrestrial materials been available. In the case of Pb, any isotopic mass-dependent fractionation is very small in contrast to the variation in isotopic abundance among the world's ore deposits (0.61% for ^{204}Pb, 6.64% for ^{206}Pb, 6.03% for ^{207}Pb and 4.93% for ^{208}Pb; Böhlke et al., 2005). Lead has four stable isotopes, three (^{206}Pb, ^{207}Pb and ^{208}Pb) the stable end products of radioactive decay chains (^{238}U, ^{235}U and ^{232}Th, respectively) and one non-radiogenic isotope (^{204}Pb). The Pb isotopic composition of an ore deposit is that of the initial Pb-isotopic composition of the host-rock/source material at the time of formation, plus new radiogenic Pb if any, which would have accumulated from the radioactive decay of U and Th since the time of formation (i.e., the age of the deposit; Faure and Mensing, 2005). The Pb isotopic composition of anthropogenic emissions resulting from high temperature processes (e.g., fossil fuel combustion, smelting and refining) reflects the isotopic composition of the source. As a result, Pb isotopic composition can be used to trace the source of Pb emissions in a technique called Pb isotope fingerprinting.

A few previous studies have examined the Zn and Cd isotopic variability among sulfide ores (Wombacher et al., 2003; Mason et al., 2005; Sonke et al., 2008; Mattielli et al., 2009; Schmitt et al., 2009), constraining the range in isotopic compositions of smelter source materials. Potential use of Zn and Cd isotopes as tracers has been increasingly explored since Wombacher et al. (2004) and Cloquet et al. (2005) identified that high temperature processes (e.g., evaporation of Cd) cause isotopic fractionation. More recently, Mattielli et al. (2009) identified successive steps of pyrometallurgical processing, particularly evaporation, as a source of Zn isotopic fractionation in resulting airborne particles. Zinc isotopes can therefore be used as a tracer of atmospheric Zn emissions released from these processing plants. Most recent studies have focused on the isotopic fractionation imparted to environmental samples taken from the vicinity of ore processing plants (Dolgopolova et al., 2006) and refineries (Cloquet et al., 2006b; Gao et al., 2008; Sivry et al., 2008; Sonke et al., 2008; Mattielli et al., 2009). By contrast, process samples have been the focus of fewer studies (Cloquet et al., 2005; Sivry et al., 2008; Mattielli et al., 2009).

Several studies have evaluated the use of Zn or Cd isotopes to source anthropogenic emissions of these elements in the environment. The coupled use of Zn

and Pb isotopes traced the source of enriched Zn in lichens and leaves (Russia) to local activities related to mining and ore processing as well as long-range transport of dust from other anthropogenic activities or natural processes (Dolgopolova et al., 2006). Enriched Zn in sediments and soils was traced using Zn isotopes to emissions from local metallurgical processing plants in the polluted Lot watershed in SW France (Sivry et al., 2008) and in a peat bog lake near Lommel, Belgium (Sonke et al., 2008). A trend between proximity to a Pb and Zn refinery plant (N France) and Cd isotopic composition was identified in topsoils (from proximal and a light Cd isotopic composition consistent with emissions from the refinery, to distal and a heavier isotopic composition consistent with natural sources) demonstrating Cd isotopes can be used as an environmental tracer (Cloquet et al., 2006b).

The primary focus of this study is to determine the presence and degree of Zn, Cd and Pb isotopic fractionation introduced during the metallurgical processing of Zn and Pb ore concentrates in one of the world's largest integrated Zn and Pb processing plants (Teck's operations in Trail, B.C.). We obtained samples of source materials, end products and intermediate products (e.g., roaster calcine) chosen to represent significant steps in processing (especially high temperature processes), which may result in isotopic fractionation. The thermal recovery of Cd in the recycling of Ni-Cd batteries was evaluated as a source of Cd isotopic fractionation by comparing the Cd isotopic compositions of recycled Cd metal, recovered from Ni-Cd batteries at INMETCO's Cd recovery plant (Ellwood City, PA), and refined Cd metal (Teck), chosen to exemplify the refined Cd metal used to make the metallic Cd electrode plate found in Ni-Cd batteries. The process of calcination, used to produce CdS pigments, was evaluated as a source of isotopic fractionation by comparing the Cd isotopic compositions of CdS pigment and Cd bearing minerals.

3.2 Materials and methods

3.2.1 Sample materials and collection

Samples were collected from the Zn and Pb operations at Teck's integrated Zn and Pb smelting and refining complex in Trail, B.C. in December 2008. Teck's Trail

facility also produces Cd, Ge and In as byproducts of Zn production and Ag, Au, Bi, Cu and As as byproducts of Pb production and sulfuric acid (H_2SO_4) produced from SO_2 off-gases. Zinc and Pb ore concentrates comprise the primary feeds for Zn and Pb operations. These ore concentrates are produced at mining sites from ores using crushing, grinding and selective flotation to isolate ZnS and PbS and reject gangue minerals (including FeS) to mine tailings (Fthenakis, 2004). Although the focus of this paper is to study the Zn, Cd and Pb isotopic fractionation imparted by smelting and refining of Zn and Cd, due to the integrated nature of the processing at Teck's Trail facility, both Zn and Pb processing must be considered as sources of Zn, Cd and Pb isotopic fractionation in smelting and refining products and emissions.

Zinc and Cd refining, as relevant to this study, is summarized in Fig. 3.1. For Zn, Teck's Trail facility employs an electrolytic Zn process, which consists of parallel high temperature roasting (Z1) and pressure leaching (not shown in Fig. 3.1), leaching with H_2SO_4 (Z2), purification (Z4), electrodeposition (Z5) and melting/casting (Z6) (Fthenakis, 2004). Although, Zn ore concentrates are normally treated in parallel with two processes, roasting (80–85%) and pressure leaching (20–25%), the pressure leaching plant was not in operation during the sampling period and any contributions from previously processed inventory are negligible (personal communication, M. Heximer, Teck Metals Ltd., 2009). During roasting (Z1), much of the Zn in the ZnS ore concentrate is oxidized to form ZnO (calcine). The sulfur in the ZnS is converted to SO_2 gas, which is isolated in the SO_2 gas treatment plant and converted to H_2SO_4. Iron impurities present in the Zn ore concentrates form Zn ferrite ($ZnFe_2O_4$; Graydon and Kirk, 1988) (~11% of the Zn; personal communication, M. Heximer, Teck Metals Ltd., 2009). The roaster calcine is leached in H_2SO_4 (Z2) to dissolve the ZnO (~89% of the Zn; personal communication, M. Heximer, Teck Metals Ltd., 2009) and form a $ZnSO_4$ solution, while the $ZnFe_2O_4$ is separated as a solid and directed to Pb operations for treatment. The $ZnSO_4$ solution is sent to the purification circuit (Z4), where cementation is used to remove other metals. Zn metal is recovered from the sulfate solution by electrowinning (Z5). The Zn stripped off the cathodes is melted and cast (99.995% Zn or different Zn alloys; Z6). Cadmium cake, resulting from the purification of the $ZnSO_4$ solution, is directed to the Cd plant (Z7), where additional leaching and vacuum distillation are used to purify the Cd metal (≥

99.99% Cd). Residues from the Cd plant (Z7) are directed to the sulfide leaching plant (Z2), these residues result from the Cd plant processes of leaching and prilling (used to form Cd pellets), which take place before the distillation step. The effluent from Zn operations is treated with milk of lime ($Ca(OH)_2$), to precipitate out dissolved metals as hydroxides, filtered (Z8) and reprocessed in Zn and Pb operations for metal recovery.

For Pb, Teck's Trail facility uses a Kivcet (flash smelting technology) furnace to produce Pb bullion and slag (P2). This smelting furnace is fed a mixed feed comprised of Pb ore concentrates and residues from Zn operations; this feed mixture is prepared in the feed plant (P1). Smelting separates impure Pb bullion from the slag metals (P2). The Pb bullion is directed to the drossing plant and Pb refinery (not shown in Fig. 3.1), while the molten slag is treated in a slag-fuming furnace (P3) to remove Zn as ZnO fume (also removing Cd as CdO). The remaining fumed slag is sold as ferrous granules for use as an iron supplement in cement production. The ZnO fume is dehalogenated (F and Cl are removed) in a fume leach plant (P4) and then fed into the oxide leaching plant (Z3). In the oxide leaching plant the fume is treated with H_2SO_4 to remove impurities of In and Ge, which are directed to the In/Ge Plant (not shown in Fig. 3.1), and impurities of Pb, As and Sb, which are recycled back into Pb operations. The $ZnSO_4$ and $CdSO_4$ solution is fed into the sulfide leaching plant (Z2).

Samples include a variety of Zn smelting operation feeds: Zn ore concentrates (primarily ZnS) (S1) produced at (a) the black shale hosted Red Dog Zn–Pb mine (Alaska, USA), the world's largest source of Zn and the primary source of Zn ore concentrate for Teck's Trail facility; (b) the carbonate hosted Pend Oreille Zn–Pb mine (Washington, USA) and (c) Bolivian Zn–Pb mines in the Oruro and Potosi regions. The roaster (Z1) feed typically comprises: Red Dog Zn ore concentrates (40–60%), Pend Oreille Zn ore concentrates (20%) and other Zn ore concentrates (20–40%), e.g., the Bolivian blend. In addition to the three Zn ore concentrate samples, six samples from Zn and Pb smelting operations were included in this study: (S2) calcine, primarily zinc oxide (ZnO), produced by roasting the Zn ore concentrates (965–980 °C; Z1); (S3) Pb smelter mixed feed, produced in the feed plant (P1), includes Pb ore concentrates and residues from Zn operations (effluent treatment plant, Z8; sulfide leaching plant, Z2; oxide leaching plant, Z3); (S4) ZnO fume, resulting from slag fuming (P3), before

dehalogenation (P4); (S5) refined zinc metal and (S6) refined cadmium metal products and (S7) effluent from Zn smelting operations, primarily originating from the roasters (Z1) and associated SO_2 gas treatment, sampled prior to treatment at the Effluent Treatment Plant (Z8).

In addition, recycled cadmium metal (S8), reclaimed primarily from Ni-Cd batteries (not shown in Fig. 3.1), was obtained from The International Metals Reclamation Company, Inc. (INMETCO) in Ellwood City, PA, USA. INMETCO recycles consumer and commercial Ni-Cd batteries by thermal recovery in their Cd recovery plant, which came on line in December 1995. In the Cd recovery process, Cd materials are reduced, using carbon, to Cd metal, vaporized and condensed into Cd metal shot (99.750–99.999% Cd; Hanewald et al., 1996). Cadmium sulfide (CdS) pigment (S9; not shown in Fig. 3.1) was obtained as true cadmium yellow light pigment (Pébéo Fragonard, France) manufactured from zinc salts calcinated at 600 ºC (personal communication, Pébéo Fragonard, 2009).

3.2.2 Sample preparation

Experimental work was carried out in metal-free Class 1,000 clean labs at the Pacific Centre for Isotopic and Geochemical Research (PCIGR), University of British Columbia (UBC). Sample preparation for elemental and isotopic analyses was performed in Class 100 laminar flow hoods in the clean labs and instrument rooms.

3.2.2.1 Reagents

Nitric (HNO_3), hydrochloric (HCl) and hydrofluoric (HF) acids used in this study were purified in-house from concentrated reagent grade acids by sub-boiling distillation. Baseline® hydrobromic (HBr) acid and hydrogen peroxide (H_2O_2) produced by Seastar Chemicals Inc. (Canada) were also utilized. Ultra-pure water (≥ 18.2 MΩ cm), prepared by de-ionization of reverse osmosis water using a Milli-Q® system (Millipore, USA), was used to prepare all solutions. All labware was washed successively with a ~2% extran® 300 (Merck KGaA, Germany) solution (alkaline cleanser), analytical grade HCl and environmental grade HNO_3.

3.2.2.2 Sample digestion

For powdered smelter samples, between 9.63 and 25.5 mg was weighed out into Savillex® PFA vials. For the CdS pigment, 0.5 mg was weighed out. Refined Cd and Zn metals were cleaned with Citranox® detergent (Alconox, Inc., USA), leached with 1 M HCl and resulting leachates were collected to represent the metals. Powdered samples (S1, S2, S3, S4, S9), metal leachates (S5, S6, S8) and effluent (S7) were digested in two steps: (1) 3 mL ~15 M HNO_3 and 2 mL ~29 M HF and (2) 5 mL ~6 M HCl. Digestion was carried out on a hotplate except in the case of the Pb smelter mixed feed (S3, highly refractory sample) for which digestion was carried out in an oven at 190 °C in a steel-jacketed high-pressure PTFE bomb. From each digested sample solution, three separate aliquots were taken for (1) elemental analysis, (2) the isolation of Cd and Zn and (3) the isolation of Pb.

3.2.2.3 Anion exchange chromatography

The anion exchange chromatography procedure used to isolate Zn and Cd follows the method of Mason (2003) and is presented in Shiel et al. (2009). Column blanks for Zn and Cd are negligible (Zn detected in the column blank corresponds to 8.5×10^{-5}% or 9.4×10^{-4}% of the total sample Zn loaded on the column; calculated using the Zn content of two different column blanks and the smallest quantity of sample Zn loaded on the column; Cd was not detected in the column blanks). In this study, the resin was batch cleaned using the method of De Jong et al. (2007) prior to packing the column. The resin was then cleaned in the column before loading and purifying samples. Fresh resin was used for each sample. The Cd and Zn eluate cuts were collected in Savillex® PFA vials, dried, treated with HNO_3 and H_2O_2 and close-vessel digested on a hotplate in an effort to digest any resin-derived organics (Shiel et al., 2009), then dried again driving off any traces of eluent acids (i.e., trace HF, HCl or HBr), and redissolved in 1 mL 0.05 M HNO_3 in preparation for isotopic analysis. Recovery of Cd and Zn was monitored to ensure ~100%, in order to avoid introduction of isotopic fractionation associated with chromatographic separation (as observed for numerous ion exchange chromatography procedures: Maréchal et al., 1999; Anbar et al., 2000; Maréchal and Albarède, 2002;

Wombacher et al., 2003; Schönbächler et al., 2007). Quantitative yields for Cd and Zn were 100 ± 4% and 100 ± 7%, respectively.

Sample Pb was isolated by anion exchange chromatography using the AG 1-X8 (100–200 mesh) resin (Bio-Rad Laboratories, Inc.), as previously described (Weis et al., 2006). Briefly, the sample is loaded onto the column in 0.5 M HBr and the resin absorbs Pb while bulk elements are eluted. Lead is then recovered using 6 M HCl. The Pb eluate cuts were collected in Savillex® PFA vials, dried, treated with HNO_3 and H_2O_2 and close-vessel digested on a hotplate in an effort to digest any resin-derived organics (Shiel et al., 2009), then dried again driving off any traces of eluent acids (i.e., trace HCl or HBr), and redissolved in 1 mL 0.05 M HNO_3 in preparation for isotopic analysis. Yield for Pb was ± 6%.

3.2.3 Standards

Standard solutions used for element concentration determination were prepared from 1,000 μg mL^{-1} single-element solutions from High Purity Standards, Inc. (USA), Specpure® Plasma (Alfa Aesar®, Johnson Matthey Company, USA) and PlasmaCAL (SCP Science, Canada).

The in-house primary and secondary reference Zn isotopic standards (PCIGR-1 Zn and PCIGR-2 Zn) are from High Purity Standards, Inc. and Specpure® (lots 505326 and 011075A, respectively). The "Lyon-JMC" Zn standard (Maréchal et al., 1999) was analyzed and is isotopically identical, within uncertainty, to the PCIGR-1 Zn standard ($\delta^{66/64}$Zn = -0.01 ± 0.22‰, n = 7). The in-house primary and secondary reference Cd isotopic standards (PCIGR-1 Cd and PCIGR-2 Cd) are from High Purity Standards, Inc. (USA) (lots 291012 and 502624, respectively). The JMC Cd, "Münster Cd" and BAM-1012 Cd (Federal Institute for Materials Research and Testing, Germany) reference materials (Wombacher and Rehkämper, 2004) were analyzed and results agree with values reported in the literature (Shiel et al., 2009). JMC Cd and PCIGR-1 Cd are identical within uncertainty ($\delta^{114/110}$Cd = -0.03 ± 0.05‰, n = 3). The NIST (USA) SRM 981 natural Pb (isotopic) standard is used for monitoring analytical run instrument drift and normalization of all measured Pb isotopic ratios.

3.2.4. Data presentation

Zinc and Cd isotopic compositions are expressed relative to the PCIGR-1 Zn and PCIGR-1 Cd reference standards in the standard delta (δ) per mil (‰) notation as follows:

$$\delta^{i}\mathrm{Zn} = \left(\frac{(^{i}Zn)_{\mathrm{sample}}}{(^{i}Zn)_{\mathrm{standard}}} - 1 \right) \text{ x } 1{,}000$$

$$\delta^{j}\mathrm{Cd} = \left(\frac{(^{j}Cd)_{\mathrm{sample}}}{(^{j}Cd)_{\mathrm{standard}}} - 1 \right) \text{ x } 1{,}000$$

where i and j are the measured isotope ratios, for Zn i = 66/64, 67/64 or 68/64 and for Cd j = 111/110, 112/110, 113/110 or 114/110. Isotopic compositions for all the ratios mentioned above are reported here, although discussion will revolve around $\delta^{114/110}$Cd and $\delta^{66/64}$Zn values, as these are the most widely reported. For Pb, the ^{206}Pb/^{204}Pb, ^{207}Pb/^{204}Pb, ^{208}Pb/^{204}Pb, ^{206}Pb/^{207}Pb and ^{208}Pb/^{206}Pb ratios are reported. To assess the importance of mass-dependent isotopic fractionation for Pb, some discussion for Pb will focus on deviations in a given Pb isotope ratio between two samples, expressed in delta (δ) per mil (‰) notation per atomic mass unit (amu) as follows:

$$\delta^{k}\mathrm{Pb} = \left(\frac{(^{k}Pb)_{\mathrm{A}}}{(^{k}Pb)_{\mathrm{B}}} - 1 \right) \text{ x } 1{,}000 \text{ x } (\mathrm{mass}_1 - \mathrm{mass}_2)^{-1}$$

where k is the measured isotope ratio, $\mathrm{mass}_1/\mathrm{mass}_2$ = 206/207 or 208/206, for two samples, A and B.

3.2.5 Analytical techniques

3.2.5.1 Elemental analysis

Element concentration analyses of sample digests and Zn, Cd and Pb eluate cuts were performed on a Varian 725-ES (Varian, Inc., USA) inductively coupled plasma optical emission spectrometer (ICP-OES) housed in the Earth and Ocean Sciences department, UBC. Emission line wavelengths of 213.857 nm, 226.502 nm and 220.353 nm were used to determine the concentrations of Zn, Cd and Pb, respectively. Element concentrations were quantified using multi-element calibration curves with europium (Eu), measured at 420.504 nm, as an internal standard. All solutions were prepared with

0.3 M HNO_3. Measured Zn, Cd and Pb concentrations agree with product composition information provided by Teck.

3.2.5.2 Isotopic analysis

Isotope ratios were measured by multi-collection on a Nu Plasma (Nu 021; Nu Instruments, UK) multi-collector inductively coupled plasma mass spectrometer (MC-ICP-MS) using the DSN-100 (Nu Instruments, UK) membrane desolvator for sample introduction. The MC-ICP-MS is housed in a Class 10,000 lab at the PCIGR, UBC. All standard and samples solutions were prepared fresh for each Zn, Cd and Pb measurement session by diluting with 0.05 M HNO_3. Copper, Ag and Tl were doped into all measured solutions of Zn, Cd and Pb, respectively, and used to monitor and correct for instrumental mass bias.

3.2.5.2.1 Zn and Cd isotopes

Zinc and cadmium isotope measurements were obtained following the procedures described by Shiel et al. (2009). In brief, a standard sample-standard bracketing (SSB) measurement protocol was followed, where samples were run alternately with standards. Each sample was measured a minimum of three times during at least two different analytical sessions. Zinc isotopic solutions were prepared as 3:1 Zn and Cu solutions, typically at 70 μg L^{-1} Zn and 23 μg L^{-1} Cu. Ion signal intensities were measured for masses 62–68 (isotopes of Zn, Cu and Ni). The isobaric Ni interference on ^{64}Zn was corrected by monitoring ^{62}Ni. Ion signal intensities for ^{62}Ni were ≤ 0.12 mV for all measurements (samples and standards), corresponding to ≤ 0.03 mV on mass 64 with a ^{64}Zn ion signal intensity ranging from 4.2 to 5.1 V, making the Ni contribution insignificant for all analyses. Cadmium isotopic solutions were prepared as 2:1 Cd and Ag solutions, typically at 60 μg L^{-1} Cd and 30 μg L^{-1} Ag. Ion signal intensities were measured for masses 106–118 (isotopes of Cd, Ag and Sn) in two cycles. The contribution of Sn on Cd isotopes 112 and 114 was corrected by monitoring the intensity of ^{118}Sn. Ion signal intensities for ^{118}Sn were ≤ 0.40 mV for all samples and standards, excluding the Pb smelter mixed feed (S3), corresponding to ≤ 0.01 mV on mass 114 with a ^{114}Cd ion signal intensity ranging from 3.3 to 5.4 V, making the Sn contribution

insignificant even before correction. For the Pb smelter mixed feed, a ^{118}Sn ion signal intensity of 36 mV was measured and used to correct for the corresponding 0.98 mV on mass 114 with a ^{114}Cd ion signal intensity of ~ 5.1 V.

Two methods were used to correct for instrumental mass bias: (1) SSB of measured ratios and (2) combined external normalization–SSB. For Zn, the SSB method resulted in more precise results and is reported. This can be attributed to differences in the behaviors of Zn and Cu in the presence of residual sample matrix (Shiel et al., 2009). For Cd, combined external normalization–SSB corrected delta values are reported because they are the most reproducible. This can be attributed to similar behaviors of Cd and Ag in the presence of residual sample matrix (Shiel et al., 2009).

3.2.5.2.2 Pb isotopes

Lead isotope measurements were obtained following the procedures described in more detail elsewhere (Weis et al., 2006; Barling and Weis, 2008). At the start of each analytical session a batch (≥ 5) of the NIST SRM 981 standard was run. Samples were run following a modified SSB measurement protocol, where the standard was run after every two samples. Lead isotopic solutions, both samples and standards, were prepared as 4:1 Pb and Tl solutions, typically at 15 μg L^{-1} Pb and 3.75 μg L^{-1} Tl. Ion signal intensities were measured for masses 202–208 (isotopes of Pb, Tl and Hg). Instrumental mass fractionation was corrected using a Tl standard (Specpure®, lot 205081F) with a ^{205}Tl/^{203}Tl ratio of 2.3885 (Weis et al., 2006). Corrected Pb ratios for the NIST SRM 981 standard were within error of the triple spike Pb ratios (Galer and Abouchami, 1998). The isobaric Hg interference on ^{204}Pb was corrected by monitoring ^{202}Hg and assuming natural abundances, ^{202}Hg/^{204}Hg = 4.350 (de Laeter et al., 2003). Ion signal intensities for ^{202}Hg were ≤ 0.24 mV for all measurements (samples and standards), corresponding to ≤ 0.05 mV on mass 204 with a ^{204}Pb ion signal intensity ranging from 0.12 to 0.15 V, making the Hg contribution insignificant for all analyses. The ion signal intensity for ^{208}Pb was between 4.6 and 6.1 V and for ^{204}Pb was ≥ 0.12 V for all analyzed samples. Measured, instrumental mass bias corrected ratios were normalized to the triple spike values of Galer and Abouchami (1998) using the ln–ln method or the SSB normalization method

(White et al., 2000; Albarède and Beard, 2004), depending on the level of instrumental mass bias drift during the analytical session.

3.2.5.2.3 Spectral and non-spectral interferences

Care was taken to avoid spectral and non-spectral interferences on measured isotopes. All samples were processed through chromatography columns to isolate the analytes as described in Section 3.2.2.3. The high analyte concentrations of these samples meant that it was possible to dilute the purified samples by at least 4,600×, 35× or 73× for Zn, Cd or Pb, respectively. By measuring these dilute purified samples, the non-spectral matrix effects associated with residual sample and resin-derived organic and inorganic contaminants (Shiel et al., 2009) were limited or avoided. Removal of elements that cause isobaric interferences was confirmed by monitoring eluate cuts prior to analysis. Prior to doping sample Zn, Cd and Pb solutions with their mass bias correcting elements (Cu, Ag and Tl, respectively) for isotopic analysis, each was analyzed on the MC-ICP-MS to ensure their mass bias correcting elements were at levels consistent with the acid blank. This was especially important in this study as Cu, Ag and Tl are all byproducts of Zn and Pb smelting and refining operations in Trail.

Zinc is a special concern for Cd analysis, due to the formation of $ZnAr^+$, which is an isobaric interference on ^{107}Ag and ^{110}Cd. In the majority of the samples, the Zn concentration is much higher than the Cd concentration, the [Zn] is as much as 540× the [Cd] (Table 3.1); thus even a small percentage of Zn in the neighboring Cd eluate cut may have detrimental effects. For the purified Cd samples, the highest relative concentration of Zn to Cd, i.e., [Zn]/[Cd], was ~8.0% and Zn was not detected in the majority of purified Cd samples. In an experiment on the MC-ICP-MS, ~0.1% of Zn was determined to form $ZnAr^+$ (determined by comparing the ^{64}Zn and $^{64}Zn^{40}Ar^+$ ion signal intensities for a 35 μg L^{-1} Cd and 18 μg L^{-1} Ag solution undoped and doped with 30 μg L^{-1} Zn). For the purified Cd sample with the highest [Zn]/[Cd], $^{67}Zn^{40}Ar^+$ and $^{70}Zn^{40}Ar^+$ would result in insignificant changes to the δCd values (affecting the SSB and combined external normalization–SSB delta values in the fourth and third decimal places, respectively).

3.3 Results

3.3.1 Zn, Cd and Pb isotopes

Zinc and Cd concentrations and delta values are reported in Table 3.1 and shown in Fig. 3.2a and b, respectively. Lead concentrations and isotopic ratios are reported in Table 3.2 and shown in Fig. 3.3. The $\delta^{66/64}$Zn, $\delta^{114/110}$Cd and ^{206}Pb/^{207}Pb values of smelting and refining samples are summarized in Fig. 3.1.

3.3.1.1 Zn isotopes

The Zn isotopic composition varies among analyzed samples with a total range of $\delta^{66/64}$Zn = 0.09 to 0.51‰ (see Table 3.1 for the other ratios). The total range represents significant differences in Zn isotopic compositions. The linear data array for Zn ratios in Fig. 3.2a is consistent with mass-dependent fractionation. Zinc ore concentrates (S1) exhibit the lightest Zn isotopic compositions of all smelter samples ($\delta^{66/64}$Zn = 0.09 to 0.17‰; Fig. 3.2a). The Zn isotopic composition of the calcine (S2) is within error of that of the Zn ore concentrates (S1; Fig. 3.2a). The Pb smelter mixed feed (S3), the ZnO fume from Pb smelting operations (S4) and the Zn operations' effluent (S7) exhibit the heaviest Zn isotopic compositions ($\delta^{66/64}$Zn = 0.33 to 0.51‰; Fig. 3.2a). The Zn metal product (S5) has an intermediate Zn isotopic signature ($\delta^{66/64}$Zn = 0.22‰), which can be explained as resulting from the mixing of the isotopically lighter Zn ore concentrates (S1) and the isotopically heavier Zn (S3, S4; Fig. 3.2a) introduced to Zn smelting operations by the Pb smelter mixed feed (P1) via the oxide leaching plant (Z3).

3.3.1.2 Cd isotopes

The Cd isotopic composition varies among analyzed samples with a total range of $\delta^{114/110}$Cd = -0.52 to 0.52‰ (see Table 3.1 for the other ratios). The total range represents significant differences in Cd isotopic compositions. The linear data array for Cd ratios in Fig. 3.2b is consistent with mass-dependent fractionation. Zinc concentrates (S1) have Cd isotopic compositions ranging from $\delta^{114/110}$Cd = -0.13 to 0.18‰ (Fig. 3.2b). The Cd isotopic composition of calcine (S2) is within error of that of the Zn ore concentrates (S1; Fig. 3.2b). The lightest sample Cd isotopic compositions (S3, S4; $\delta^{114/110}$Cd = -0.52 to

-0.38‰) are introduced from the Pb smelter via the oxide leaching plant (Z3). The heaviest Cd isotopic composition is exhibited by the Cd metal product (S6; $\delta^{114/110}$Cd = 0.39 to 0.52‰; Fig. 3.2b). As with Zn, the smelting operations' effluent (S7) exhibits a heavy Cd isotopic composition (Fig. 3.2b). A significant shift in the Cd isotopic signature is observed between the Zn ore concentrates (S1) and the Cd metal product (S6; Fig. 3.2b).

The recycled Cd metal from INMETCO (S8) has a Cd isotopic signature similar to that of the smelter-refined Cd metal product (S6; Fig. 3.2b). The CdS pigment from France (S9), resulting from the calcining of zinc salts, exhibits a Cd isotopic signature within the range of Cd isotopic compositions observed for the Zn ore concentrates (S1) and the smelter-produced calcine (S2; Fig. 3.2b).

3.3.1.3 Pb isotopes

The Pb isotope values of the analyzed samples range from 1.15174 to 1.24642 for ^{206}Pb/^{207}Pb and 2.04842 to 2.10703 for ^{208}Pb/^{206}Pb (see Table 3.2 for the other ratios). The most radiogenic samples are characterized by high ^{206}Pb/^{207}Pb ratios and low ^{208}Pb/^{206}Pb ratios and vice-versa for the least radiogenic samples (Fig. 3.3a). Zinc ore concentrates (S1) exhibit the most radiogenic Pb isotopic values of the analyzed samples (Fig. 3.3a,b). Calcine (S2) has a slightly less radiogenic Pb isotopic composition (Fig. 3.3a,b). The mixed feed (S3) for the Kivcet Pb smelter and the ZnO fume from Pb smelting operations (S4) exhibit the least radiogenic Pb isotopic values (Fig. 3.3a,b). Zinc smelting operations' effluent (S7) has an intermediate Pb isotopic composition. The intermediate Pb isotopic composition of the effluent (S7) may be attributed to mixing of the more radiogenic isotopic compositions of the calcine (S2) and Zn ore concentrates (S1) and the less radiogenic isotopic compositions of the Pb smelter mixed feed (S3) and ZnO fume (S4; Fig. 3.3a,b). Samples form a trend from low Pb concentration and more radiogenic Pb isotopic composition (Zn ore concentrates, S1) to high Pb concentration and less radiogenic Pb isotopic composition (Pb smelter mixed feed, S3; ZnO fume, S4) (inset of Fig. 3.3a).

3.4 Discussion

3.4.1 Fractionation of Zn, Cd and Pb isotopes during Zn refining

3.4.1.1 Zn isotope variation

Zinc ore concentrates (S1; $\delta^{66/64}$Zn = 0.09 to 0.17‰), primarily composed of ZnS, exhibit Zn isotopic compositions that are consistent with those reported in the literature for sphalerites and other ore grade sulfide minerals (Fig. 3.4) (Mason et al., 2005; Sonke et al., 2008; Mattielli et al., 2009) and are within error of the global average Zn isotopic composition ($\delta^{66/64}$Zn = 0.16 ± 0.20‰, 2SD, n = 10 mines) for major ore body sphalerites proposed by Sonke et al. (2008). The $\delta^{66/64}$Zn value for the roaster calcine (S2; $\delta^{66/64}$Zn = 0.17‰) falls within the range of the Zn ore concentrates (S1) included in this study (Fig. 3.4), indicating a near 100% yield from this step. The $\delta^{66/64}$Zn value for the Pb smelter mixed feed (S3; $\delta^{66/64}$Zn = 0.33‰) falls at the heavier end of the range reported for ore grade sulfide minerals (Mason et al., 2005; Sonke et al., 2008; Mattielli et al., 2009) and is heavier than those measured for the Zn ore concentrates included in this study (Fig. 3.4). This discrepancy indicates a significant contribution of relatively heavy Zn to the Pb smelter mixed feed (Fig. 3.4), which may originate from Zn introduced as (1) Pb ore concentrates not included in this study, e.g., from the Cannington mine, Queensland, Australia and/or (2) stockpiled Zn residues, derived from the past processing, sulfide leaching (Z2) and effluent treatment (Z8), of Zn ore concentrates not included in this study, e.g., from the now closed, nearby Sullivan mine, B.C. (see Section 3.4.1.3; personal communication, M. Heximer, Teck Metals Ltd., 2009). This explanation requires the unaccounted ores have Zn isotopic compositions among the heaviest reported (i.e., ZnS: $\delta^{66/64}$Zn ≤ 0.37‰, PbS: $\delta^{66/64}$Zn ≤ 0.25‰; Sonke et al., 2008). The difference between the Zn isotopic compositions of the Pb smelter mixed feed (S3; $\delta^{66/64}$Zn = 0.33‰) and the relatively heavy Zn found in the ZnO fume (S4; $\delta^{66/64}$Zn = 0.43‰) likely reflects variability in the composition of the Pb smelter mixed feed with time, although this is unclear given the measurement uncertainties.

Zinc isotopic fractionation occurring during the processing of Zn ore concentrates (S1) is reflected in the significantly heavy $\delta^{66/64}$Zn values of the Zn operations' effluent

(S7; $\delta^{66/64}$Zn = 0.41 to 0.51‰). This relatively heavy $\delta^{66/64}$Zn value is expected to originate from high temperature roasting (Z1; Fig. 3.1), the primary source of Zn to the effluent, although due to the relatively small Zn loss during roasting, the difference between the Zn isotopic compositions of the Zn ore concentrates (S1) and calcine (S2) is negligible (Fig. 3.2a). Heavy $\delta^{66/64}$Zn values, similar to those found for the Zn operations' effluent (S7; Fig. 3.4), have been observed in smelting and refining polluted lichens (Cloquet et al., 2006a), sediments and soils (Sivry et al., 2008).

Although significant fractionation of Zn isotopes occurs during smelting and refining processes, as observed in the effluent (S7) and particulate atmospheric emissions (as light as $\delta^{66/64}$Zn = -0.73‰; Mattielli et al., 2009), due to the high Zn recovery (~98% overall Zn recovery; personal communication, M. Heximer, Teck Metals Ltd., 2009) the Zn isotopic composition of the Zn metal product (S5) is not significantly different from that of the source material (S1) (Fig. 3.4). The vast majority of the unrecovered Zn (~2%) is lost in Pb operations as ferrous granules. Effluent (0.003%) and atmospheric emissions (0.030%) (calculated from Environment Canada, 2007 and Teck Cominco Ltd., 2008) are isotopically heavy and light, respectively, but represent a very small percentage of the overall Zn budget. Therefore, these losses, although isotopically fractionated relative to the source materials, are not large enough to significantly shift the isotopic composition of the remaining Zn. The Zn isotopic composition of the Zn metal product (S5) can be accounted for by variable mixing of the Zn ore concentrates (S1) and the Pb smelter mixed feed (S3) (Fig. 3.2a). A mixture of 80% and 20% for the Zn ore concentrates (S1) and Pb smelter mixed feed (S3) would account for the observed Zn isotopic composition of the Zn metal product (S5; Fig. 3.1). As a result of this high recovery, variability of the Zn isotopic composition of the Zn metal product is expected to result primarily from isotopic variability inherent to the Zn and Pb ore concentrates used to feed smelting and refining operations rather than from the small Zn losses due to emissions and incomplete recovery of Zn during slag fuming. The relatively small range of Zn isotopic compositions reported for "common" anthropogenic Zn products relative to that reported for ore samples (Fig. 3.4; John et al., 2007) results from smelting and refining operations which homogenize the mixture of Zn ore concentrates (S1) feeding Zn operations (as discussed in Section 3.2.1). The Zn isotopic composition of the Zn metal product (S5;

Fig. 3.4) is consistent with that of "common" anthropogenic Zn (Zn metal and health products, between $\delta^{66/64}Zn = 0.1$ and 0.3‰), including electrochemically refined high purity Zn shot (99.995% purity) from the Canadian Electrolytic Zinc refinery (Salaberry-de-Valleyfield, Québec) and thermal distillation refined Zn metal dust (98.5% purity) (John et al., 2007).

3.4.1.2 Cd isotope variation

The Zn ore concentrates (S1) studied here exhibit Cd isotopic compositions ($\delta^{114/110}Cd = -0.13$ to 0.18‰) consistent with those reported for continental and oceanic sulfides, including sphalerite (ZnS) and greenockite (CdS) minerals (Wombacher et al., 2003; Schmitt et al., 2009) and all $\delta^{114/110}Cd$ values fall within the range of those reported for terrestrial rocks (Wombacher et al., 2003) (Fig. 3.5). The $\delta^{114/110}Cd$ values of the Zn ore concentrates (S1) and the roaster-produced calcine (S2; $\delta^{114/110}Cd = 0.05$‰) cannot be distinguished due to the near 100% yield from roasting (roaster products are separated in a subsequent step of processing). It is therefore unclear from this comparison as to whether roasting fractionates Cd isotopes.

The $\delta^{114/110}Cd$ value of the Pb smelter mixed feed (S3; $\delta^{114/110}Cd = -0.38$‰) is lighter than that of the Zn ore concentrates (S1). Its Cd isotopic composition is within error of the lightest reported for continental sulfides (Wombacher et al., 2003; Schmitt et al., 2009), with a $\delta^{114/110}Cd$ value similar to a greenockite mineral (Schmitt et al., 2009) (Fig. 3.5). It falls within the lighter end of the range reported for oceanic sulfides (Schmitt et al., 2009) and terrestrial rocks (Wombacher et al., 2003) (Fig. 3.5). The relatively light signature of the Pb smelter mixed feed (S3) as compared to the Zn ore concentrates (S1) may reflect, in part, the use of ore concentrates not included in this study (see Section 3.4.1.1 and Section 3.4.1.3; Fig. 3.5). However, given the overall picture constructed by the Cd isotopic compositions of the smelter samples, we suggest the source of light Cd isotopes in the Pb smelter mixed feed (S3) is more likely to be Zn residues resulting from the treatment of roaster-produced calcine in the sulfide leaching plant (Z2). These Zn residues (primarily partially reacted sphalerite particles and $ZnFe_2O_4$) are filtered from the $ZnSO_4$ electrolyte solution in the sulfide leaching plant (Z2) and directed to Pb operations, where they are included in the Pb smelter mixed feed

(S3). Roasting (Z1) is therefore suggested to impart different Cd isotopic compositions to the different mineralogical phases formed.

The ZnO fume (S4) has a light Cd isotopic composition ($\delta^{114/110}$Cd = -0.52‰) within error of that of the Pb smelter mixed feed (S3) (Fig. 3.5). The $\delta^{114/110}$Cd value of the ZnO fume (S4) is similar to that reported for smelting dust (Cloquet et al., 2005) (Fig. 3.5). The Zn operations' effluent (S7) has a relatively heavy Cd isotopic composition, which is expected to result from the high temperature roasting process, similar to Zn. The $\delta^{114/110}$Cd value for the effluent is identical to that reported for Pb–Zn refinery plant slag (Cloquet et al., 2005) and the heaviest of the values observed in smelting and refining polluted sediments (Gao et al., 2008) (Fig. 3.5).

Significant Cd isotopic fractionation results from the refining of Cd as a byproduct of Zn and Pb smelting and refining and is reflected in the Cd isotopic compositions of the effluent (S7), ZnO fume (S4), particulate atmospheric emissions (Cloquet et al., 2005) and Cd metal product (see below). Effluent (0.012%) and atmospheric emissions (0.010%) are isotopically heavy and light (Fig. 3.5), respectively, however, these represent a very small percentage of the overall Cd budget. The loss in heavy Cd isotopes to the effluent during roasting is not significant enough to result in a difference between the Cd isotopic compositions of the Zn ore concentrates and roaster calcine. Although the overall recovery for Cd is not available, it is presumed to be lower than that of Zn, as Cd is recovered as a byproduct and the processing is optimized for recovery of Zn. Cadmium recovery is calculated as 72–92% using the Zn, Cd and Pb contents of Red Dog mine Zn and Pb ore concentrates and annual Zn, Pb and Cd metal production (Fthenakis, 2004; Teck Cominco Ltd., 2008).

The $\delta^{114/110}$Cd value of the Cd metal product (S6; $\delta^{114/110}$Cd = 0.39 to 0.52‰) is heavier than that of the Zn ore concentrates (S1; Fig. 3.2b). Processes occurring in the Cadmium Plant (Z7), mainly the use of vacuum distillation to purify Cd, were considered as potential sources of Cd isotopic fractionation. Evaporation and condensation during fractional distillation have been demonstrated to be sources of Cd isotopic fractionation (Wombacher et al., 2004). However, this explanation is not favored here, as there is not a large loss of Cd associated with the distillation and this explanation does not account for the relatively light isotopic signature of the Pb smelter mixed feed. Rather, a significant

loss of light Cd, by means of a mass loss during Pb operations of Cd originating from both Pb ore concentrates and Zn residues from Zn operations (e.g., Cd is lost to the Pb bullion and ultimately the Cu cake), is expected to account for the relatively heavy isotopic composition of the Cd metal product (S6). In this scenario, the primary source of Cd isotopic fractionation is roasting (Z1), as discussed above, and Zn residues, coming from the sulfide leaching plant (Z2), are expected to account for the light Cd isotopic signature of the Pb smelter mixed feed (S3).

The Cd isotopic signature of the INMETCO recycled Cd metal (S8; $\delta^{114/110}$Cd = 0.23 to 0.34‰) is within error of that of Teck's Cd metal product (S6; Fig. 3.2b), and is expected to vary primarily with that of the Cd recovery plant feed (commercial and consumer Ni-Cd batteries). The ability to assess the Cd isotopic fractionation associated with the thermal recovery of Cd, as part of Ni-Cd battery recycling, is limited due to an unknown Cd loss during processing and the inaccessibility of the plant feed and intermediate products for sampling. The Fragonard CdS pigment (S9) has a $\delta^{114/110}$Cd value consistent with the heaviest Zn ore concentrates (S1a) included in this study, the roaster calcine (S2; Fig 3.2b) and continental and oceanic sulfides (Wombacher et al., 2003; Schmitt et al., 2009) (Fig. 3.5). This similarity suggests that the calcination of zinc salts does not fractionate Cd isotopes and/or the recovery of the process is ~100%, similar to roasting.

3.4.1.3 Pb isotope variation

The three Zn ore concentrates (S1) are the most radiogenic Pb samples included in this study (Fig. 3.3a,b). Those from the Red Dog mine (S1a) exhibit the least radiogenic Pb isotopic signature of the three (Fig. 3.3a,b), with isotope ratios within the range of literature values for ore from the Red Dog mine: $^{206}Pb/^{207}Pb$ = 1.1805 and $^{208}Pb/^{206}Pb$ = 2.0764 (mean calculated by Sangster et al., 2000, from references within). The $^{206}Pb/^{207}Pb$ ratio of the roaster calcine (S2; $^{206}Pb/^{207}Pb$ = 1.16784) is significantly less radiogenic than those of the Zn ore concentrates (S1a,b,c; $^{206}Pb/^{207}Pb$ = 1.17988 to 1.24642), by between -63 and -10‰ (Fig. 3.3a). Therefore, the mixture of Zn ore concentrates used to feed the roasters is presumed to have also included a Zn ore concentrate with a radiogenic Pb isotopic composition not included in this study. The

similarity between the Pb isotopic compositions of the calcine (S2; representative of the mixture of Zn ore concentrates used to feed the roasters) and Zn operations' effluent (S7) corroborates Teck's identification of roasting as the largest source of Zn operations' effluent (personal communication, M. Heximer, Teck Metals Ltd., 2009). The Pb smelter mixed feed (S3) is among the least radiogenic samples included in this study (Fig. 3.3a,b), its Pb isotopic composition requires the mixing of Pb from the Red Dog deposit with Pb from a much less radiogenic source. As Pb ore concentrates were not included in this study, we can not unequivocally identify this less radiogenic source, however, two likely sources are: (1) Pb ore concentrates from the Cannington mine, Queensland, Australia ($^{206}Pb/^{207}Pb$ = ~1.041; Huston et al., 2006) and/or (2) stockpiled Zn residues resulting from the processing of ore concentrates from the nearby Sullivan mine, B.C. (personal communication, M. Heximer, Teck Metals Ltd., 2009). The Sullivan mine was the largest source of Pb ore concentrates to Teck's Trail facility prior to the mine's closure in 2001: $^{206}Pb/^{207}Pb$ = 1.0679 and $^{208}Pb/^{206}Pb$ = 2.1889 (Fig. 3.3a,b; mean calculated by Sangster et al., 2000, from references within). A mixture of Pb and Zn ore concentrates, with 74% and 26% of the total processed Pb originating from the Red Dog and Sullivan mines, respectively, can account for the observed Pb isotopic composition of the Pb smelter mixed feed (S3).

Lead isotopes are not likely to undergo significant mass-dependent fractionation during Zn or Pb smelting operations due to the element's heavy mass and subsequently its small relative mass difference. This is evidenced by: (1) the lack of internal consistency among the delta values per amu calculated for the different Pb isotope ratios (e.g., for the calcine and effluent: $\delta^{206/207}Pb$ = 1.88‰ amu^{-1} and $\delta^{208/206}Pb$ = 0.60‰ amu^{-1} and for the Pb smelter mixed feed and the ZnO fume: $\delta^{206/207}Pb$ = 0.45‰ amu^{-1} and $\delta^{208/206}Pb$ = -0.41‰ amu^{-1}), (2) the discrepancy between the slope of the trend defined by all analyzed samples and that of the mass-dependent fractionation line (Fig. 3.3a) and (3) the extent of the variations observed in Pb isotopes in this study ($\delta^{206/207}Pb$ = 76‰ amu^{-1} for all samples). Kinetic fractionation of Pb would be expected to therefore be smaller than that of Cd due to its heavier mass, a worse case scenario for Pb would be 0.30‰ (this is the total variation, per amu, observed here for Cd), which corresponds to a variation less than the symbol size in Fig. 3.3a (~0.01 for $^{206}Pb/^{207}Pb$ and $^{208}Pb/^{206}Pb$).

In Pb–Pb diagrams (Fig. 3.3a,b), all Pb samples form a mixing trend, where the Pb isotopic compositions of the smelting and refining intermediate products and effluent can be explained by the mixing of Zn and Pb ore concentrates of different origins. Therefore, mixing, rather than mass-dependent fractionation, accounts for the vast majority of the variation among the Pb isotopic compositions of samples. Lead and Zn isotopes agree when the signature reflects the source, departures from this general trend occur when the Zn isotopic composition is fractionated during processing, e.g., Zn operations' effluent (S7; Fig. 3.1). In such cases, pairing the use of Zn and Pb isotopes will allow the assessment of Zn isotopic fractionation and tracing of the source.

3.4.2 Implications for local environmental samples

The implementation of aggressive pollution abatement policies in response to increasingly strict regulations and the availability of new technologies in North America and Western Europe has led to dramatic reductions in the metals (including Zn, Cd, Pb) released into environments neighboring, downstream and downwind of smelters and refineries in these regions. However, high metal levels are expected to persist in environments adjacent to historical polluters. Historical levels of air and water releases from smelting and refining operations in Trail were much higher than today. For example, the direct disposal of granulated slag, resulting from Pb operations (Fig. 3.1), into the Columbia River was ceased in 1995 and this slag is now sold to cement manufacturers (Teck Cominco Ltd., 2007).

The results of this study support the use of Zn and Cd isotopes to trace smelting and refining air emissions and effluent in the local environment, at storage sites and at disposal sites. The use of Pb isotopic signatures may complement the use of Zn and Cd isotopes, because the Pb isotopic signature reflects the source. Several recent studies have used Zn and Cd isotopic signatures to identify the source of enriched metal levels in reservoirs representative of natural environments (e.g., lichens, sediments, soils) that have been affected by historical or modern smelters and refineries (e.g., for Zn: Cloquet et al., 2006a; Sonke et al., 2008; Sivry et al., 2008; Mattielli et al., 2009 and for Cd: Cloquet et al., 2006b; Gao et al., 2008). Distinguishing between historic and recent releases may not be possible, as shifts in the source Zn and Pb ore concentrates over time

may not be accompanied by significant changes in the Zn and Cd isotopic compositions. However, well documented temporal changes in the Pb isotopic composition of ore concentrates consumed by smelters and refineries may allow differentiation between historic and recent Pb smelting emission related depositions in the environment.

3.5 Conclusions

Our investigation of Zn, Cd and Pb isotopic fractionation in smelting and refining processes resulted in the following conclusions:

(1) Significant fractionation of Zn isotopes occurs systematically throughout the hydrometallurgical processing of Zn ore concentrates as evidenced by the significant shift between the Zn isotopic compositions of the Zn ore concentrates and the effluent. The effluent represents only a very small overall loss of Zn during processing; as a result there is no significant difference between the $\delta^{66/64}$Zn values of the Zn ore concentrates and the refined Zn metal. The $\delta^{66/64}$Zn value of the refined Zn metal is therefore expected to reflect the $\delta^{66/64}$Zn value of the ore concentrate feed.
(2) The same observation holds for Cd, where significant fractionation of Cd isotopes results from the metallurgical processing of Zn ore concentrates. This is evidenced by the larger total variation in Cd isotopic composition exhibited by the Zn ore concentrates, Pb smelter mixed feed, ZnO fume, refined Cd metal and effluent.
(3) Recycling of Ni-Cd batteries is not associated with a significant shift in the Cd isotopic composition between the metallic Cd electrode plate (as represented by the refined Cd metal) and the recycled Cd metal product.
(4) No significant fractionation of Pb isotopes results from the smelting and refining of Zn and Pb ore concentrates. Significant Pb isotopic variation between the Zn ore concentrates and the Pb smelter mixed feed reflects the contribution to the latter of various Pb ore concentrates not included in this study and/or stockpiled residues from Zn operations.
(5) The results of this study suggest Zn and Cd isotopes can be used to trace metallurgical processing emissions of these metals in the environment.

3.6 Acknowledgements

We especially want to thank Teck and John F.H. Thompson for providing smelter samples and are grateful to Michael Heximer for his assistance with sample selection and for providing valuable discussion regarding smelting processes. We thank INMETCO, especially Frank Przywarty and Al Hardies, for the recycled Cd metal sample and a description of their Cd recovery process. We are grateful to Jane Barling for comments on this manuscript and for her assistance with the Nu Plasma MC-ICP-MS and to Maureen Soon for her assistance with the Varian 725-ES ICP-OES. We thank James Scoates for comments on this manuscript and his support. We are grateful to Jeroen Sonke and Alla Dolgopolova for their insightful and constructive reviews. We also thank Francis Albarède for providing an aliquot of the "Lyon-JMC" Zn standard solution. This study was funded by NSERC Discovery grants to Dominique Weis and Kristin J. Orians.

Table 3.1. Zinc and Cd contents and isotopic compositions.

Sample ID[a]	Sample	[Zn](%)[b]	$\delta^{66}Zn/^{64}Zn$[c]	$\delta^{67}Zn/^{64}Zn$[c]	$\delta^{68}Zn/^{64}Zn$[c]	n[d]	[Cd](%)[b]	$\delta^{111}Cd/^{110}Cd$[c]	$\delta^{112}Cd/^{110}Cd$[c]	$\delta^{113}Cd/^{110}Cd$[c]	$\delta^{114}Cd/^{110}Cd$[c]	n[d]
	Zinc ore concentrates											
S1a	Red Dog mine	52.2	0.12 ± 0.00	0.19 ± 0.03	0.23 ± 0.07	2	0.302	0.03 ± 0.07	0.08 ± 0.13	0.14 ± 0.17	0.18 ± 0.27	3
S1a	Red Dog mine dup.[e]	52.2	0.17 ± 0.05	0.27 ± 0.18	0.33 ± 0.16	3	0.302	0.05 ± 0.05	0.10 ± 0.07	0.13 ± 0.07	0.17 ± 0.15	3
S1b	Pend Oreille mine	64.2	0.09 ± 0.07	0.13 ± 0.14	0.20 ± 0.17	5	0.118	0.04 ± 0.04	0.08 ± 0.06	0.10 ± 0.04	0.14 ± 0.12	3
S1c	Bolivian blend	51.7	0.12 ± 0.11	0.16 ± 0.11	0.19 ± 0.23	3	0.233	-0.04 ± 0.04	-0.09 ± 0.12	-0.12 ± 0.18	-0.13 ± 0.24	3
	Zinc smelter, Trail, B.C.											
S2	Calcine	58.4	0.17 ± 0.06	0.24 ± 0.13	0.31 ± 0.08	3	0.286	0.02 ± 0.02	0.05 ± 0.02	0.06 ± 0.17	0.05 ± 0.12	2
S5	Refined Zn alloy	95.0	0.22 ± 0.04	0.31 ± 0.13	0.45 ± 0.10	3						
S6	Refined Cd metal[f]						100	0.08 ± 0.01	0.19 ± 0.06	0.30 ± 0.19	0.39 ± 0.18	3
S6	Refined Cd metal dup.[e,f]						100	0.15 ± 0.09	0.27 ± 0.14	0.40 ± 0.19	0.52 ± 0.19	3
S7	Effluent (ppm)	109	0.51 ± 0.02	0.74 ± 0.09	1.02 ± 0.11	2	1.34	0.09 ± 0.02	0.18 ± 0.01	0.24 ± 0.06	0.31 ± 0.07	3
S7	Effluent dup.[e] (ppm)	109	0.41 ± 0.08	0.64 ± 0.13	0.82 ± 0.19	3	1.34	0.12 ± 0.01	0.24 ± 0.00	0.35 ± 0.07	0.46 ± 0.08	2
	Lead smelter, Trail, B.C.											
S3	Mixed feed	8.68	0.33 ± 0.15	n/a[g]	n/a[g]	3	0.155	-0.11 ± 0.07	-0.19 ± 0.12	-0.29 ± 0.20	-0.38 ± 0.25	3
S4	ZnO fume (feed material for Zn operations)	46.3	0.43 ± 0.03	0.63 ± 0.07	0.85 ± 0.08	3	0.354	-0.14 ± 0.03	-0.26 ± 0.02	-0.40 ± 0.03	-0.52 ± 0.02	3
	Inmetco, Inc., Ellwood City, PA											
S8	Recycled Cd metal[f]						100	0.05 ± 0.11	0.12 ± 0.14	0.18 ± 0.32	0.23 ± 0.34	3
S8	Recycled Cd metal dup.[e,f]						100	0.08 ± 0.04	0.17 ± 0.04	0.28 ± 0.13	0.34 ± 0.12	3
	Cadmium products											
S9	CdS yellow pigment	8.5					45.3	0.02 ± 0.04	0.06 ± 0.02	0.12 ± 0.10	0.16 ± 0.01	3

[a]Column 1 identifies sample ID as described in section 3.2 Materials and methods and shown in Fig. 3.1.

[b]Elemental concentration given as % by weight, except where noted.

[c]Ratios are reported as the mean ± 2 standard deviation (SD).

[d]n refers to the number of replicate isotopic measurements.

[e]dup. refers to a full procedural duplicate, inclusive of the analytical separation and isotopic analysis.

[f]Concentrations provided by manufacturer.

[g]Deltas calculated for ratios with masses 67 and 68 in the numerator are omitted due to a Ba^{2+} interference.

Table 3.2. Lead contents and isotopic compositions.

Sample ID[a]	Sample	[Pb](%)[c]	$^{206}Pb/^{204}Pb$[d,e]	$^{207}Pb/^{204}Pb$[d,e]	$^{208}Pb/^{204}Pb$[d,e]	$^{206}Pb/^{207}Pb$[d,e]	$^{208}Pb/^{206}Pb$[d,e]
	Zinc ore concentrates						
S1a	Red Dog mine	2.81	18.4161 ± 0.0008	15.6077 ± 0.0007	38.262 ± 0.002	1.17991 ± 0.00002	2.07766 ± 0.00003
S1a	Red Dog mine dup.[b]	2.81	18.4192 ± 0.0008	15.6112 ± 0.0007	38.269 ± 0.002	1.17988 ± 0.00001	2.07766 ± 0.00004
S1b	Pend Oreille mine	0.779	19.7144 ± 0.0010	15.8166 ± 0.0009	40.383 ± 0.002	1.24642 ± 0.00001	2.04842 ± 0.00003
S1c	Bolivian blend	1.16	18.7984 ± 0.0010	15.6808 ± 0.0009	39.106 ± 0.003	1.19880 ± 0.00002	2.08028 ± 0.00003
	Zinc smelter, Trail, B.C.						
S2	Calcine	2.57	18.1980 ± 0.0010	15.5826 ± 0.0008	38.135 ± 0.002	1.16784 ± 0.00002	2.09553 ± 0.00004
S7	Effluent (ppm)	4.08	18.1760 ± 0.0010	15.5931 ± 0.0009	38.134 ± 0.002	1.16564 ± 0.00001	2.09806 ± 0.00004
	Lead smelter, Trail, B.C.						
S3	Mixed feed	20.6	17.9372 ± 0.0009	15.5668 ± 0.0008	37.794 ± 0.002	1.15226 ± 0.00002	2.10703 ± 0.00003
S4	ZnO fume (feed material for Zn operations)	18.1	17.9243 ± 0.0008	15.5627 ± 0.0008	37.736 ± 0.002	1.15174 ± 0.00001	2.10529 ± 0.00003

[a]Column 1 identifies sample ID as described in section 3.2 Materials and methods and shown in Fig. 3.1.

[b]dup. refers to a full procedural duplicate, inclusive of the analytical separation and isotopic analysis.

[c]Elemental concentration given as % by weight, except where noted.

[d]Ratios are reported as the mean ± 2 standard error (SE).

[e]All data have been normalized to the NIST SRM 981 triple spike Pb ratios of Galer and Abouchami (1998).

Fig. 3.1. Schematic depiction of Zn and Pb operations at Teck's integrated Zn and Pb smelting and refining complex in Trail (B.C., Canada). Processes employed during Zn and Pb operations are indicated by a circle and designated by Z and P, respectively, followed by a number corresponding to the step in the process (Z1, Z2, etc. and P1, P2, etc., respectively). Samples are indicated by a star and are designated by an S followed by a number (S1, S2, etc.). $\delta^{66/64}$Zn, $\delta^{114/110}$Cd and $^{206/207}$Pb values are given for each sample.
This figure is adapted from http://www.metsoc.org/virtualtour/processes/zinclead.asp and personal communication, M. Heximer, Teck Metals Ltd., 2009.

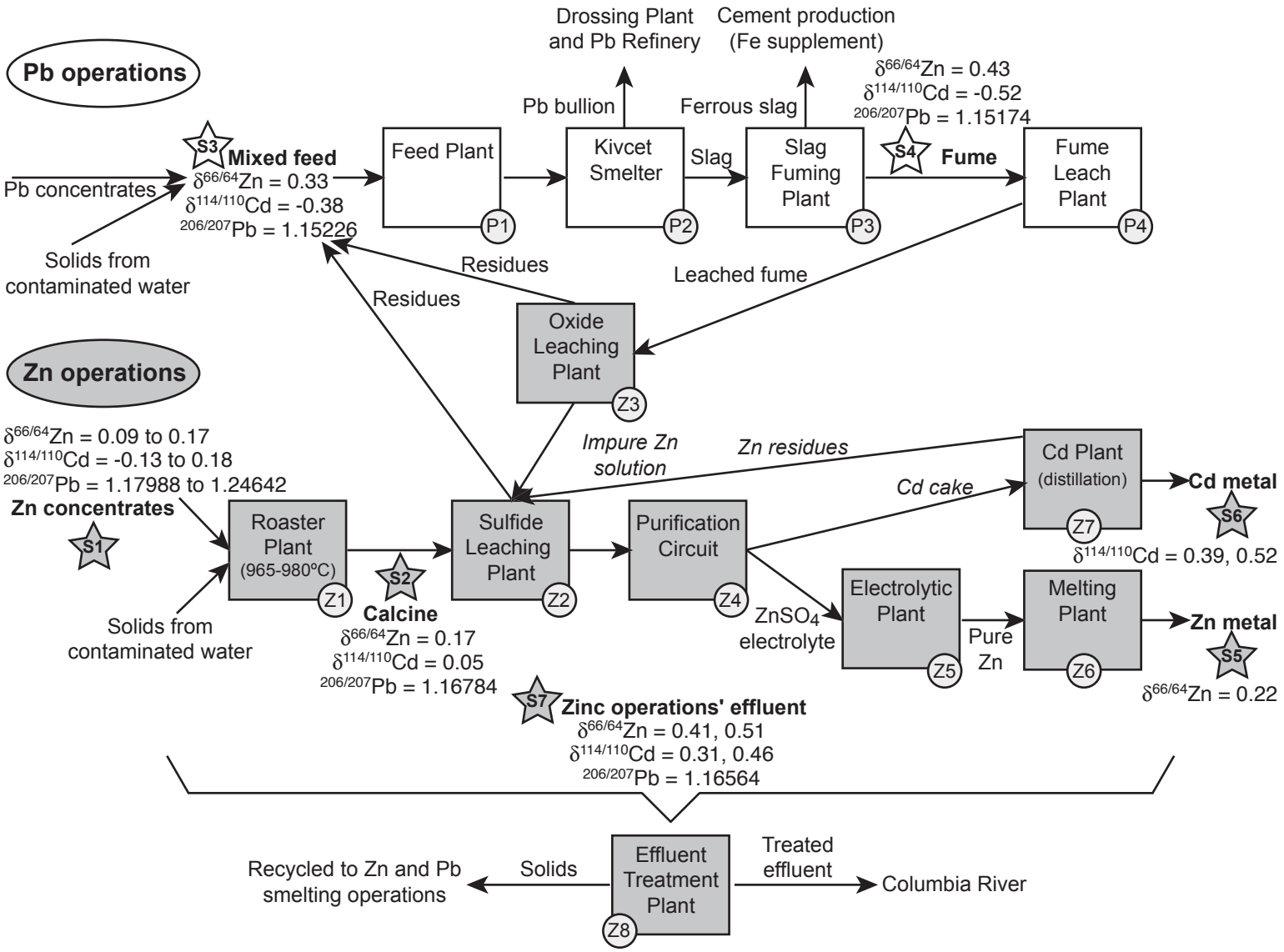
Pb operations
Drossing Plant and Pb Refinery
Cement production (Fe supplement)
Pb bullion
Ferrous slag
δ66/64Zn = 0.43
δ114/110Cd = -0.52
206/207Pb = 1.15174
S3
Mixed feed
δ66/64Zn = 0.33
δ114/110Cd = -0.38
206/207Pb = 1.15226
Pb concentrates
Solids from contaminated water
Feed Plant
P1
Kivcet Smelter
P2
Slag
Slag Fuming Plant
P3
S4
Fume
Fume Leach Plant
P4
Residues
Residues
Leached fume
Oxide Leaching Plant
Z3
Zn operations
δ66/64Zn = 0.09 to 0.17
δ114/110Cd = -0.13 to 0.18
206/207Pb = 1.17988 to 1.24642
Zn concentrates
S1
Roaster Plant (965-980ºC)
Z1
S2
Calcine
δ66/64Zn = 0.17
δ114/110Cd = 0.05
206/207Pb = 1.16784
Solids from contaminated water
Impure Zn solution
Zn residues
Sulfide Leaching Plant
Z2
Purification Circuit
Z4
Cd cake
Cd Plant (distillation)
Z7
Cd metal
S6
δ114/110Cd = 0.39, 0.52
ZnSO4 electrolyte
Electrolytic Plant
Z5
Pure Zn
Melting Plant
Z6
Zn metal
S5
δ66/64Zn = 0.22
S7
Zinc operations' effluent
δ66/64Zn = 0.41, 0.51
δ114/110Cd = 0.31, 0.46
206/207Pb = 1.16564
Effluent Treatment Plant
Z8
Solids
Recycled to Zn and Pb smelting operations
Treated effluent
Columbia River

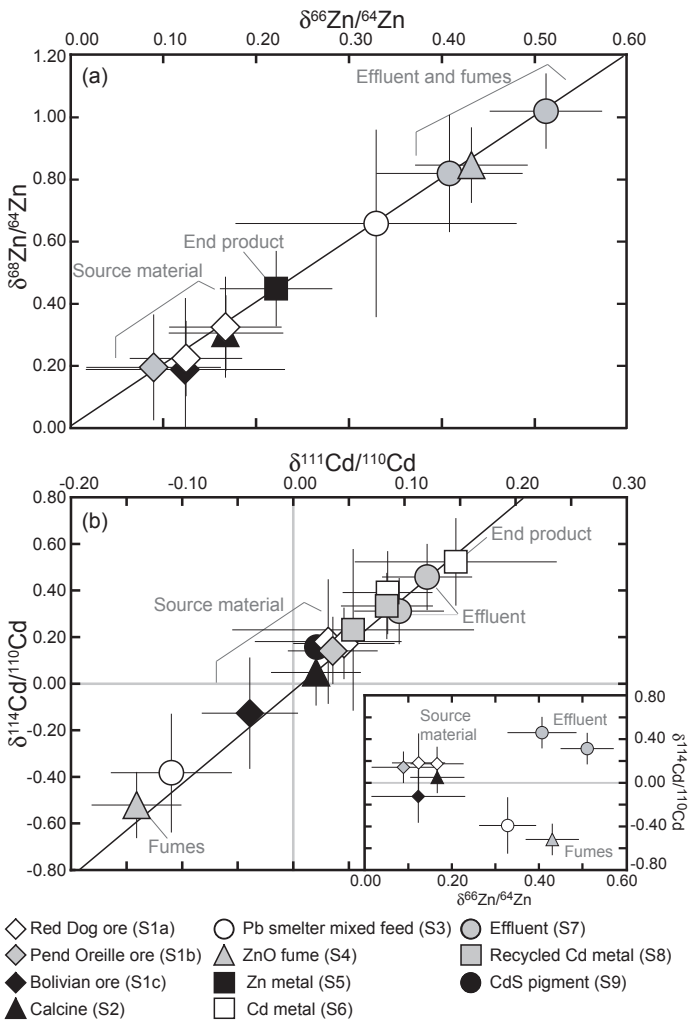

Fig. 3.2. Mass-dependent Zn and Cd isotopic fractionation for all Zn and Cd samples, respectively: (a) $\delta^{68/64}$Zn vs. $\delta^{66/64}$Zn and (b) $\delta^{114/110}$Cd vs. $\delta^{111/110}$Cd. Error bars denote ± 2 standard deviation (SD) on the mean delta value for replicate analyses of each sample. The calculated regression lines (for (a), $r^2 = 0.9953$; for (b), $r^2 = 0.9857$) are coherent with mass-dependent isotopic fractionation, indicating spectral interferences are insignificant with one exception. For (b), the $\delta^{68/64}$Zn value for the Pb smelter mixed feed is biased by a significant Ba^{2+} interference on mass 68, as a result this sample is excluded from the linear regression. The $\delta^{68/64}$Zn value plotted for the Pb smelter mixed feed is calculated from the $\delta^{66/64}$Zn value. Inset shows $\delta^{114/110}$Cd vs. $\delta^{66/64}$Zn for all samples for which both Zn and Cd isotopic measurements were made. Error bars denote ± 2SD on the mean delta value for replicate analyses of each sample, except when this value is less than the long-term reproducibility calculated for the in-house secondary Zn and isotopic standards (Shiel et al., 2009), and then the latter is used. Source material (i.e., Zn ore concentrates) for both Zn and Cd isotopes falls in a narrow range. Processing of Zn ore concentrates through Teck's Trail operations leads to heavier isotopic compositions of both Zn and Cd in the effluent, suggesting a similar mechanism of isotopic fractionation during processing. On the contrary, the Pb smelter mixed feed and ZnO fume are isotopically light for Cd and heavy for Zn, perhaps suggesting the two elements behave differently during roasting.

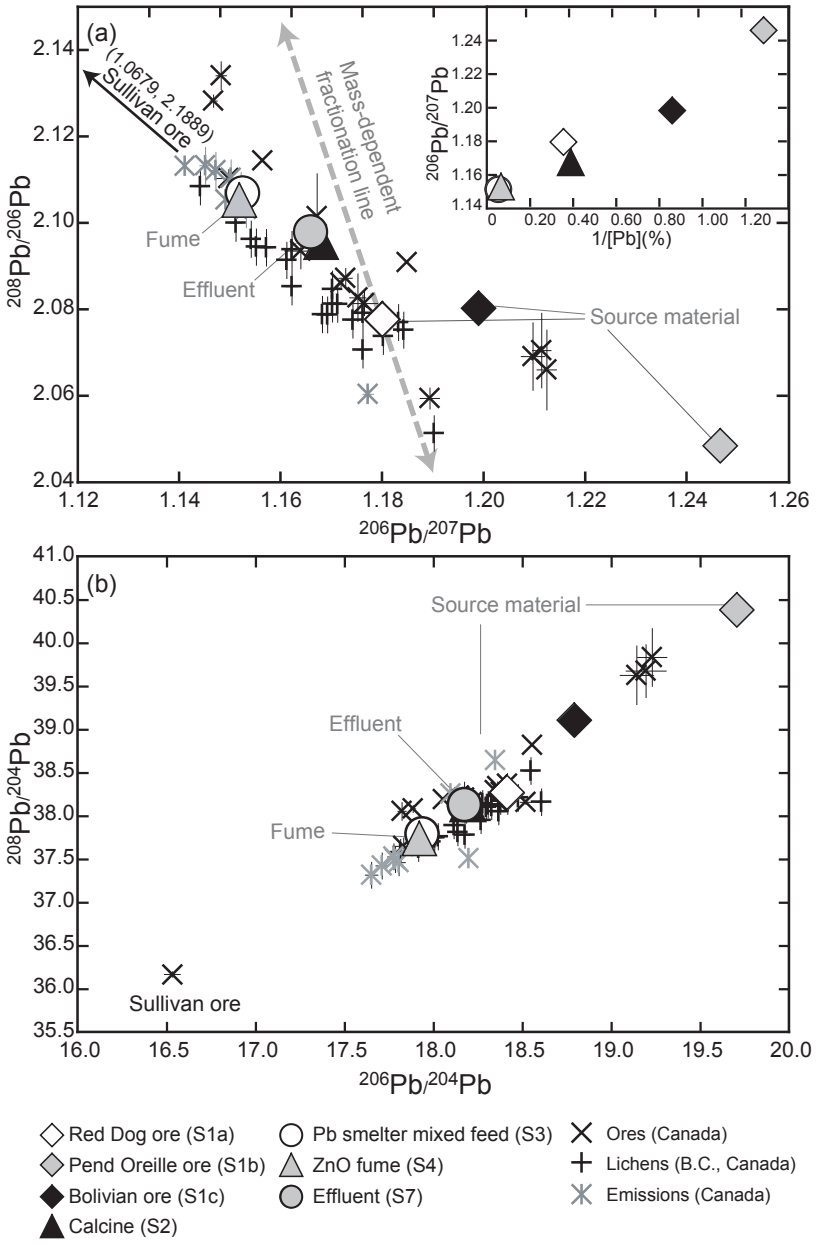

Fig. 3.3. Plots of (a) $^{208}Pb/^{206}Pb$ vs. $^{206}Pb/^{207}Pb$ and (b) $^{208}Pb/^{204}Pb$ vs. $^{206}Pb/^{204}Pb$ for all smelter and refinery Pb samples. For all samples, 2 standard error is smaller than the symbol size. The data are compared with the Pb isotope ratios of Canadian Pb ores including Sullivan mine ore (Sangster et al., 2000), lichens from B.C. (Simonetti et al., 2003) and Canadian emissions (Carignan and Gariépy, 1995; Bollhöfer and Rosman, 2001). Error bars indicate error as reported by referenced authors; in several cases this error is smaller than the symbol size. The dashed line in (a) corresponds to mass-dependent fractionation of Pb isotopes. Inset in (a) shows $^{206}Pb/^{207}Pb$ vs. 1/[Pb](%) for all samples except the effluent.

Fig. 3.4. Variations in Zn isotopic composition of samples from the smelting and refining operations depicted in Fig. 3.1 and published geological and anthropogenic materials. The grey ellipses indicate error as reported by referenced authors; for this study the grey ellipses denote ± 2 standard deviation on the mean $\delta^{66/64}$Zn value for replicate analyses of each sample, except when this value is less than the long-term reproducibility calculated for the in-house secondary Zn isotopic standard, ±0.06‰, and then the latter is used. In several cases the error is smaller than the symbol. Data sources: [1]Sonke et al., 2008; [2]Mason et al., 2005; [3]John et al., 2008; [4]Mattielli et al., 2009; [5]Cloquet et al., 2006a; [6]Sivry et al., 2008; [7]John et al., 2007.

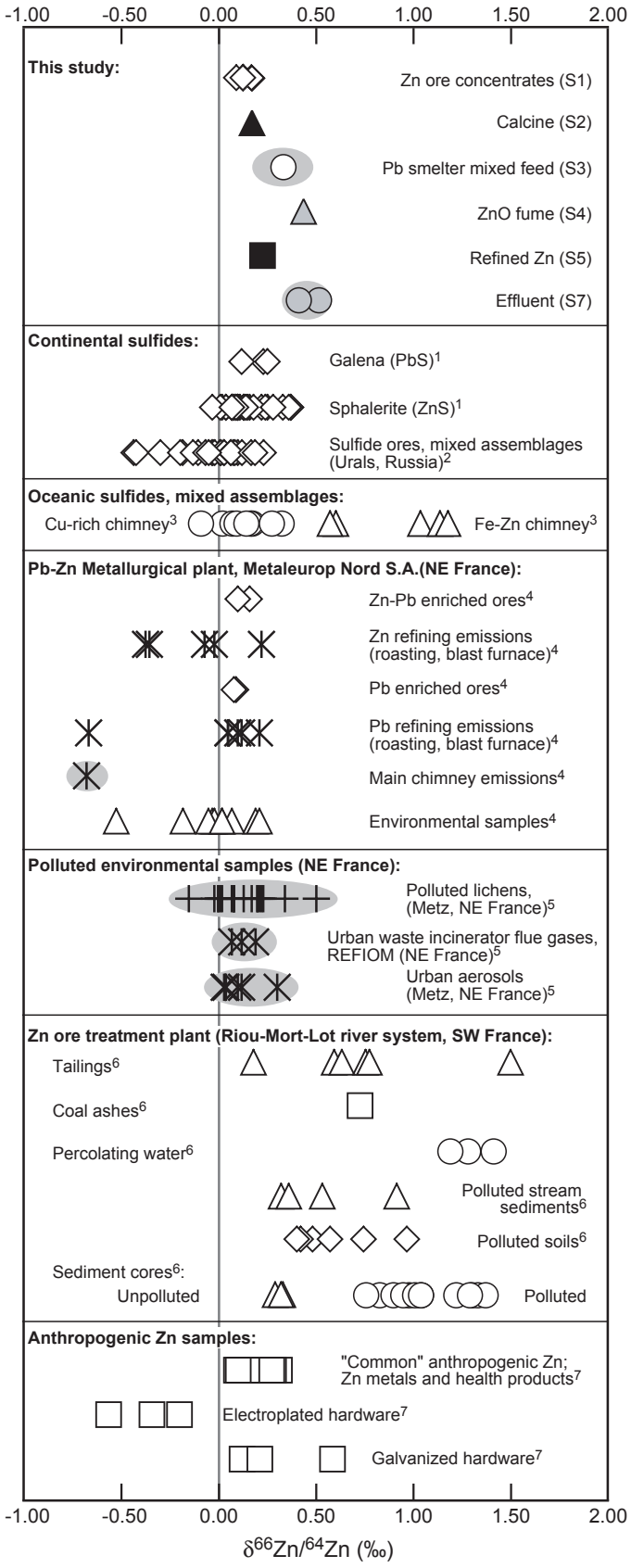
-1.00
-0.50
0.00
0.50
1.00
1.50
2.00
This study:
Zn ore concentrates (S1)
Calcine (S2)
Pb smelter mixed feed (S3)
ZnO fume (S4)
Refined Zn (S5)
Effluent (S7)
Continental sulfides:
Galena (PbS)[1]
Sphalerite (ZnS)[1]
Sulfide ores, mixed assemblages (Urals, Russia)[2]
Oceanic sulfides, mixed assemblages:
Cu-rich chimney[3]
Fe-Zn chimney[3]
Pb-Zn Metallurgical plant, Metaleurop Nord S.A.(NE France):
Zn-Pb enriched ores[4]
Zn refining emissions (roasting, blast furnace)[4]
Pb enriched ores[4]
Pb refining emissions (roasting, blast furnace)[4]
Main chimney emissions[4]
Environmental samples[4]
Polluted environmental samples (NE France):
Polluted lichens, (Metz, NE France)[5]
Urban waste incinerator flue gases, REFIOM (NE France)[5]
Urban aerosols (Metz, NE France)[5]
Zn ore treatment plant (Riou-Mort-Lot river system, SW France):
Tailings[6]
Coal ashes[6]
Percolating water[6]
Polluted stream sediments[6]
Polluted soils[6]
Sediment cores[6]:
Unpolluted
Polluted
Anthropogenic Zn samples:
"Common" anthropogenic Zn; Zn metals and health products[7]
Electroplated hardware[7]
Galvanized hardware[7]
δ66Zn/64Zn (‰)

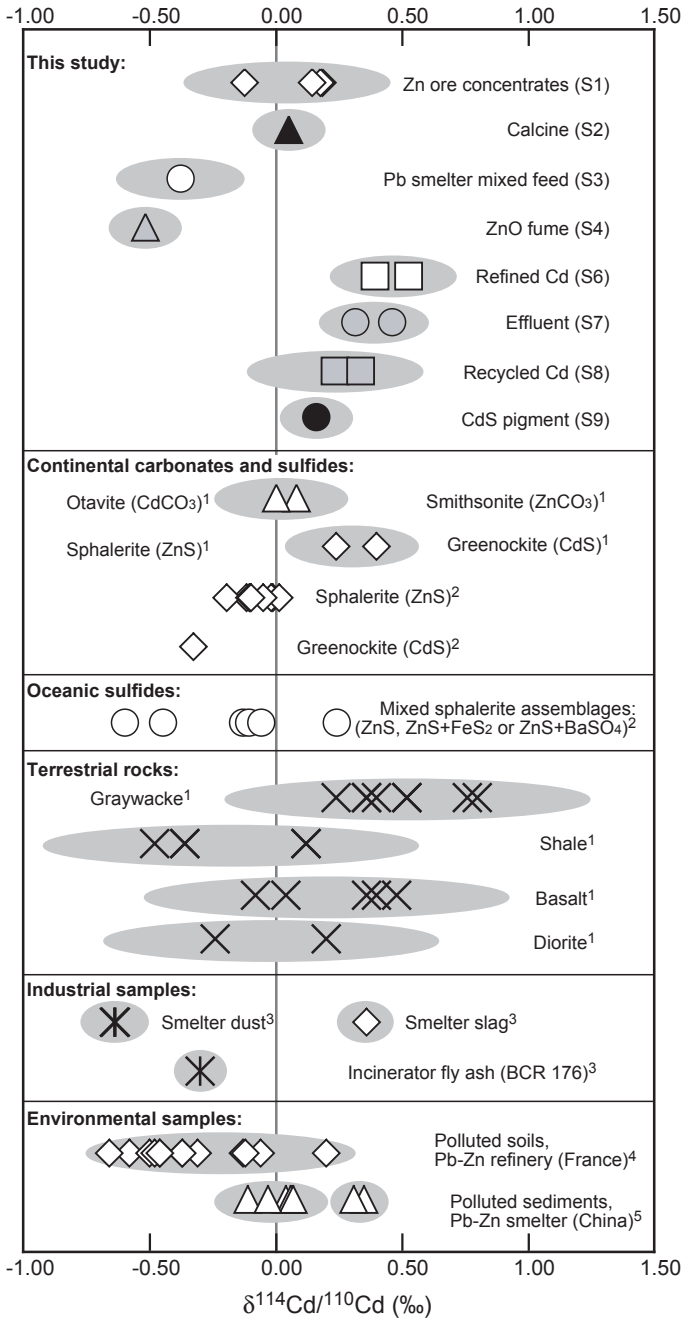

Fig. 3.5. Variations in Cd isotopic composition of samples from the smelting and refining operations depicted in Fig. 3.1, recycled Cd metal, CdS pigment and published geological and anthropogenic materials. The grey ellipses indicate error as reported by referenced authors; for this study the grey ellipses denote ± 2 standard deviation on the mean $\delta^{114/110}$Cd value for replicate analyses of each sample, except when this value is less than the long-term reproducibility calculated for the in-house secondary Cd isotopic standard, ±0.14‰, and then the latter is used. In several cases the error is smaller than the symbol. Data sources: [1]Wombacher et al., 2003; [2]Schmitt et al., 2009; [3]Cloquet et al., 2005; [4]Cloquet et al., 2006b; [5]Gao et al., 2008.

3.7. References

Albarède, F., Beard, B.L. (2004) Analytical methods for non-traditional isotopes. Reviews in Mineralogy and Geochemistry 55: 113–152.

Anbar, A.D., Roe, J.E., Barling, J., Nealson, K.H. (2000) Nonbiological fractionation of iron isotopes. Science 288: 126–128.

Barling, J., Weis, D. (2008) Influence of non-spectral matrix effects on the accuracy of Pb isotope ratio measurement by MC-ICP-MS: implications for the external normalization method of instrumental mass bias correction. Journal of Analytical Atomic Spectrometry 23: 1017–1025.

Böhlke, J.K., de Laeter, J.R., De Bièvre, P., Hidaka, H., Peiser, H.S., Rosman, K.J.R., Taylor, P.D.P. (2005) Isotopic compositions of the Elements, 2001. Journal of Physical and Chemical Reference Data 34: 57–67.

Bollhöfer, A., Rosman, K.J.R. (2001) Isotopic source signatures for atmospheric lead: The Northern Hemisphere. Geochimica et Cosmochimica Acta 65: 1727–1740.

Carignan, J., Gariépy, C. (1995) Isotopic composition of epiphytic lichens as a tracer of the sources of atmospheric lead emissions in southern Quebec, Canada. Geochimica et Cosmochimica Acta 59: 4427–4433.

Cloquet, C., Carignan, J., Libourel, G. (2006a) Isotopic composition of Zn and Pb atmospheric depositions in an urban/periurban area of northeastern France. Environmental Science & Technology 40: 6594–6600.

Cloquet, C., Carignan, J., Libourel, G., Sterckeman, T., Perdrix, E. (2006b) Tracing source pollution in soils using cadmium and lead isotopes. Environmental Science & Technology 40: 2525–2530.

Cloquet, C., Rouxel, O., Carignan, J., Libourel, G. (2005) Natural cadmium isotopic variations in eight geological reference materials (NIST SRM 2711, BCR 176, GSS-1, GXR-1, GXR-2, GSD-12, Nod-P-1, Nod-A-1) and anthropogenic samples, measured by MC-ICP-MS. Geostandards and Geoanalytical Research 29: 95–106.

De Jong, J., Schoemann, V., Tison, J.L., Becquevort, S., Masson, F., Lannuzel, D., Petit, J., Chou, L., Weis, D., Mattielli, N. (2007) Precise measurement of Fe isotopes in

marine samples by multi-collector inductively coupled plasma mass spectrometry (MC-ICP-MS). Analytica Chimica Acta 589: 105–119.

de Laeter, J.R., Böhlke, J.K., De Biévre, P., Hidaka, H., Peiser, H.S., Rosman, K.J.R., Taylor, P.D.P. (2003) Atomic weights of the elements: Review 2000 - (IUPAC technical report). Pure and Applied Chemistry 75: 683–800.

Dolgopolova, A., Weiss, D.J., Seltmann, R., Kober, B., Mason, T.F.D., Coles, B., Stanley, C.J. (2006) Use of isotope ratios to assess sources of Pb and Zn dispersed in the environment during mining and ore processing within the Orlovka-Spokoinoe mining site (Russia). Applied Geochemistry 21: 563–579.

Environment Canada. (2007) Detailed Substance Report for Cadmium (and its compounds) reported by Teck Cominco – Trail Operations, from the National Pollutant Release Inventory: http://www.ec.gc.ca/pdb/querysite.

Faure, G., Mensing, T.M. (2005) Isotopes, Principles and Applications, third edition. Hoboken, New Jersey: John Wiley & Sons, Inc., pp. 928.

Fthenakis, V.M. (2004) Life cycle impact analysis of cadmium in CdTePV production. Renewable & Sustainable Energy Reviews 8: 303–334.

Galer, S.J.G., Abouchami, W. (1998) Practical application of lead triple spiking for correction of instrumental mass discrimination. Mineralogical Magazine 62A: 491–492.

Gao, B., Liu, Y., Sun, K., Liang, X., Peng, P., Sheng, G., Fu, J. (2008) Precise determination of cadmium and lead isotopic compositions in river sediments. Analytica Chimica Acta 612: 114–120.

Graydon, J.W., Kirk, D.W. (1988) A Microscopic Study of the Transformation of Sphalerite Particles During the Roasting of Zinc Concentrate. Metallurgical and Materials Transactions B 19: 141–146.

Greenwood, N.N., Earnshaw, A. (2001) Chemistry of the Elements. Oxford: Butterworth Heinemann, pp. 1341.

Guberman, D.E. (2009) Lead, in Metals and minerals: U.S. Geological Survey Minerals Yearbook 2007. I: 42.1–42.18. (Available at http://minerals.usgs.gov/minerals/pubs/commodity/lead/myb1-2007-lead.pdf.)

Hanewald, R.H., Schweers, M.E., Liotta, J.J. (1996) Recycling Nickel-Cadmium Batteries through the High Temperature Metal Recovery Process and NEW Cadmium Recovery Facility. Battery Conference on Applications and Advances, Eleventh Annual, Jan 9–12 2006: 207–212.

Huston, D.L., Stevens, B., Southgate, P.N., Muhling, P., Wyborn, L. (2006) Australian Zn-Pb-Ag Ore-Forming Systems: A Review and Analysis. Economic Geology 101: 1117–1157.

John, S.G., Park, G., Zhang, Z., Boyle, E.A. (2007) The isotopic composition of some common forms of anthropogenic zinc. Chemical Geology 245: 61–69.

John, S.G., Rouxel, O.J., Craddock, P.R., Engwall, A.M., Boyle, E.A. (2008) Zinc stable isotopes in seafloor hydrothermal vent fluids and chimneys. Earth and Planetary Science Letters 269: 17–28.

Johnson, C.M., Beard, B.L., Albarède, F. (2004) Overview and General Concepts. Reviews in Mineralogy and Geochemistry 55: 1–24.

Maréchal, C.N., Albarède, F. (2002) Ion-exchange fractionation of copper and zinc isotopes. Geochimica et Cosmochimica Acta 66: 1499–1509.

Maréchal, C.N., Télouk, P., Albarède, F. (1999) Precise analysis of copper and zinc isotopic compositions by plasma-source mass spectrometry. Chemical Geology 156: 251–273.

Mason, T.F.D. (2003) High-precision transition metal isotope analysis by plasma-source mass spectrometry and implications for low temperature geochemistry. Ph.D. thesis, University of London, p. 287.

Mason, T.F.D., Weiss, D.J., Chapman, J.B., Wilkinson, J.J., Tessalina, S.G., Spiro, B., Horstwood, M.S.A., Spratt, J., Coles, B.J. (2005) Zn and Cu isotopic variability in the Alexandrinka volcanic-hosted massive sulphide (VHMS) ore deposit, Urals, Russia. Chemical Geology 221: 170–187.

Mattielli, N., Petit, J.C.J., Deboudt, K., Flament, P., Perdrix, E., Taillez, A., Rimetz-Planchon, J., Weis, D. (2009) Zn isotope study of atmospheric emissions and dry depositions within a 5 km radius of a Pb-Zn refinery. Atmospheric Environment 43: 1265–1272.

Peterson, B.J., Fry, B. (1987) Stable isotopes in ecosystem studies. Annual Review of Ecology and Systematics 18: 293–320.

Sangster, D.F., Outridge, P.M., Davis, W.J. (2000) Stable lead isotope characteristics of lead ore deposits of environmental significance. Environmental Reviews 8: 115–147.

Schmitt, A.-D., Galer, S.J.G., Abouchami, W. (2009) Mass-dependent cadmium isotopic variations in nature with emphasis on the marine environment. Earth and Planetary Science Letters 277: 262–272.

Schönbächler, M., Carlson, R.W., Horan, M.E., Mock, T.D., Hauri, E.H. (2007) High precision Ag isotope measurements in geologic materials by multiple-collector ICPMS: An evaluation of dry versus wet plasma. International Journal of Mass Spectrometry 261: 183–191.

Shiel, A.E., Barling, J., Orians, K.J., Weis, D. (2009) Matrix effects on the multi-collector inductively coupled plasma mass spectrometric analysis of high-precision cadmium and zinc isotope ratios. Analytica Chimica Acta 633: 29–37.

Simonetti, A., Gariépy, C., Carignan, J. (2003) Tracing sources of atmospheric pollution in Western Canada using the Pb isotopic composition and heavy metal abundances of epiphytic lichens. Atmospheric Environment 37: 2853–2865.

Sivry, Y., Riotte, J., Sonke, J.E., Audry, S., Schäfer, J., Viers, J., Blanc, G., Freydier, R., Dupré, B. (2008) Zn isotopes as tracers of anthropogenic pollution from Zn-ore smelters The Riou Mort-Lot River system. Chemical Geology 255: 295–304.

Sonke, J.E., Sivry, Y., Viers, J., Freydier, R., Dejonghe, L., André, L., Aggarwal, J.K., Fontan, F., Dupré, B. (2008) Historical variations in the isotopic composition of atmospheric zinc deposition from a zinc smelter. Chemical Geology 252: 145–157.

Teck Cominco Ltd. (2007) Our Commitment: Teck Sustainability Report 2007, Teck Cominco Ltd., Vancouver, B.C., Canada.

Teck Cominco Ltd. (2008) Annual Report 2007, Teck Cominco Ltd., Vancouver, B.C., Canada.

Tolcin, A.C. (2008) Cadmium, in Metals and minerals: U.S. Geological Survey Minerals Yearbook 2007. I: 15.1–15.9. (Available at

http://minerals.usgs.gov/minerals/pubs/commodity/cadmium/myb1-2007-cadmi.pdf.)

Tolcin, A.C. (2009) Zinc, in Metals and minerals: U.S. Geological Survey Minerals Yearbook 2007. I: 84.1–84.18. (Available at http://minerals.usgs.gov/minerals/pubs/commodity/zinc/myb1-2007-zinc.pdf.)

Weis, D., Kieffer, B., Maerschalk, C., Barling, J., De Jong, J., Williams, G.A., Hanano, D., Pretorius, W., Mattielli, N., Scoates, J.S., Goolaerts, A., Friedman, R.M., Mahoney, J.B. (2006) High-precision isotopic characterization of USGS reference materials by TIMS and MC-ICP-MS. Geochemistry Geophysics Geosystems 7, Q08006, doi: 10.1029/2006GC001283.

White, W.M., Albarède, F., Telouk, P. (2000) High-precision analysis of Pb isotope ratios by multi-collector ICP-MS. Chemical Geology 167: 257–270.

Wombacher, F., Rehkämper, M. (2004) Problems and suggestions concerning the notation of cadmium stable isotope compositions and the use of reference materials. Geostandards and Geoanalytical Research 28: 173–178.

Wombacher, F., Rehkämper, M., Mezger, K. (2004) Determination of the mass-dependence of cadmium isotope fractionation during evaporation. Geochimica et Cosmochimica Acta 68: 2349–2357.

Wombacher, F., Rehkämper, M., Mezger, K., Münker, C. (2003) Stable isotope compositions of Cd in geological materials and meteorites determined by multicollector-ICPMS. Geochimica et Cosmochimica Acta 67: 4639–4654.

CHAPTER 4

Tracing cadmium, zinc and lead pollution in bivalves from the coasts of western Canada, the USA and France using isotopes [1]

[1]A version of this chapter will be submitted for publication. Shiel, A.E., Weis, D., Orians, K.J. (2010) Tracing cadmium, zinc and lead pollution in bivalves from the coasts of western Canada, the USA and France using isotopes.

4.1 Introduction

Coastal and marine pollution impact the global environment and have implications for the health of ecosystems and organisms. Marine pollution, including heavy metal pollution, adversely affects local fisheries and associated economies. In some cases, however, high metal concentrations in the environment and resident organisms may not derive from an anthropogenic source. The source of high Cd levels reported in the tissues of oysters (*Crassostrea gigas*) harvested from British Columbia (B.C., western Canada) (e.g., Kruzynski, 2001, 2004; Lekhi et al., 2008; Bendell and Feng, 2009) is unknown but thought to be largely natural. In B.C., the Federal and Provincial Governments have encouraged pursuits in aquaculture as the forest industry and wild fisheries have declined. In 1997, the Provincial Government made plans to double the crown lands available for bivalve aquaculture through the Shellfish Development Initiative (Kruzynski, 2004). In 1999/2000, however, several shipments of B.C. oysters were rejected by Hong Kong for exceeding their import Cd limit of 2 μg g^{-1} wet weight (Kruzynski, 2004). This generated concerns over the potential loss of markets supporting the expanding aquaculture industry as well as health concerns related to the consumption of B.C. shellfish with high Cd levels. The subsequent survey of B.C. oysters, harvested from the western coast of Canada, by the Canadian Food Inspection Agency (CFIA) found a mean Cd concentration of 2.63 μg g^{-1} wet weight (n = 81), with 60% of samples over 2 μg g^{-1} wet weight (Schallié, 2001). Oysters with relatively high Cd levels were not limited to populated areas but rather included those harvested from sparsely inhibited or "pristine" areas. In contrast, a complimentary investigation of oysters (*Crassostrea virginica*) harvested from the eastern coast of Canada found Cd concentrations ranging from 0.07 to 0.56 μg g^{-1} wet weight, with a mean Cd concentration of only 0.33 μg g^{-1} wet weight (n = 18) (Schallié, 2001). Using the Cd concentrations reported for B.C. oysters by the CFIA, Health Canada conducted a formal Health Risk Assessment. Based on this assessment, they recommended consumption be limited to a dozen 40 g oysters per month for an adult (Kruzynski, 2004). However, no consideration was made for nutritional and other risk factors in their assessment. In

addition, major gaps exist in the knowledge related to Cd bioavailability from oysters and potential health effects (Kruzynski, 2004).

Potential sources of Cd to B.C. coastal waters and bivalve molluscs (e.g., oysters and mussels) include natural sources, such as the upwelling of deep oceanic waters or the weathering of mineral outcrops, or anthropogenic sources, such as erosion-related runoff (e.g., in logging areas), municipal storm water, effluent from wastewater treatment, pulp and paper mills or mining. The disparity between the Cd concentrations found in oysters from the Pacific and Atlantic coasts of Canada (with the exception of polluted estuaries on the Atlantic coast) suggests the source of high Cd in the North Pacific region may be natural. Seawater in the North Pacific has higher dissolved Cd concentrations due to the global thermohaline circulation of the ocean. Upwelling of intermediate waters rich in nutrients and nutrient-type trace metals (e.g., Cd and Zn) could bring this water to the regions where oysters are grown. In global thermohaline circulation, deep water forms in the North Atlantic Ocean, sinks, flows south, around Antarctica, moves east through the Indian Ocean, and then northward from the South Pacific Ocean to the North Pacific Ocean, accumulating nutrients and trace metals along the way. Cadmium concentrations of North Pacific deep waters (1.04 nmol kg^{-1} or 117 ng kg^{-1}; Bruland, 1980) are ~3–4× those of the North Atlantic (0.32 nmol kg^{-1} or 36 ng kg^{-1}; Bruland and Franks, 1983). Similarly, Zn concentrations of North Pacific deep waters (9.07 nmol kg^{-1} or 593 ng kg^{-1}; Bruland, 1980) are ~4–6× those of the North Atlantic (1.61 nmol kg^{-1} or 105 ng kg^{-1}, Bruland and Franks, 1983). On the west coast of Vancouver Island, variations in the Cd concentrations of mussel tissues were found to be associated with variations in dissolved Cd related to upwelling events (Lares and Orians, 1997). The US Mussel Watch Program (NOAA, USA) did not find a correlation between high Cd concentrations in oysters and mussels and high human population density; this was in contrast to Pb concentrations, for which a fairly strong correlation with high human population density was reported (O'Connor, 2002). The US Mussel Watch Program reported high Cd concentrations in mussels inhabiting coastal Northern California and suggested coastal upwelling as the source (O'Connor, 2002). Further, Cd concentrations in scallops from Antarctica are high (14–49 μg g^{-1} dry weight); high concentrations in this remote area were suggested to

result from the upwelling of Cd-rich deep-waters (Berkman and Nigro, 1992; Viarengo et al., 1993).

In contrast to Cd and Zn, which have nutrient–type depth profiles in the ocean and increase in concentration as deep waters flow from the Atlantic to the Pacific, Pb has a scavenged-type depth profile (Chester, 2003). Lead concentrations are high at the surface, due to atmospheric input, and decrease with depth and deep water age, as Pb is scavenged onto particles and removed to the sediments. Most Pb in the modern ocean is anthropogenic in origin (Chester, 2003). The worldwide decline in the consumption of leaded gasoline has been associated with significant reductions in the atmospheric deposition of Pb to the surface oceans. In the central North Pacific, Pb concentrations decreased by a factor of ~2 in surface waters from ~65 pmol kg^{-1} (~13 ng kg^{-1}) in 1976 (Schaule and Patterson, 1981) to ~30 pmol kg^{-1} (~6.2 ng kg^{-1}) in 1999 (Boyle et al., 2005), correlated with the phase-out of leaded gasoline in the USA. Similarly, Pb concentrations in surface waters of the western North Atlantic decreased by a factor of ~4 during the 1980s (Boyle et al., 1994), with lead concentrations from ~40 to 60 pmol kg^{-1} (~8.3 to 12 ng kg^{-1}) reported for 1995/6 in surface waters from the western North Atlantic (Wu and Boyle, 1997). A decreasing trend in Pb concentrations continues in the oceans.

Oysters and mussels are bioaccumulators and have much higher metal concentrations than seawater. As sessile organisms, their tissue metal concentrations are representative of time-integrated metal concentrations at the collection site. As a result, these bivalves are used to monitor coastal contamination, including contamination of heavy metals (e.g., Cd, Zn and Pb) in national mussel watch programs such as those of the USA and France. These programs monitor both spatial and temporal trends in chemical concentrations. However, some limitations are associated with the evaluation of chemical contamination using concentrations alone, e.g., it is difficult to differentiate between anthropogenic and natural metal sources or to determine if relatively low metal concentrations represent the natural baseline level, in addition, for some metals, concentrations vary depending on the species. For example, in B.C., estimates of annual coastal Cd loading from local anthropogenic inputs failed to explain observed variations in the Cd concentrations of B.C. oysters (Kruzynski et al., 2002). New geochemical tools, such as Cd and Zn isotopic signatures, may provide strong evidence as to metal sources.

The ionization efficiency needed for the precise measurement of small natural variations in Cd and Zn isotopic composition has been afforded by the introduction of the multi-collector inductively coupled plasma mass spectrometer (MC-ICP-MS). Cadmium and Zn are among a growing number of non-traditional stable isotope systems (i.e., Li, Mg, Ca, Si, Ti, Cr, Fe, Ni, Cu, Ge, Se, Zr, Mo, Ru, Ag, W and Tl) under investigation. These tools may be especially powerful in combination with radiogenic isotope tracers, e.g., Pb, which are used to trace the source.

In this study, we evaluate the use of Cd, Zn and Pb isotopes as tracers of sources of these metals to the marine environment and bivalves. These elements are often found together in solid wastes, wastewaters and emissions from industrial sources, e.g., ore mining, smelting (Shiel et al., 2010) and steelmaking (Ketterer et al., 2001). The correlation of these isotopic tracers from a common source is used to resolve ambiguities encountered with the use of only one of these isotope systems. Our investigation centers on determining the origin of these metals in oysters harvested from sites in B.C. (Canada). In order to gain a broader perspective on Cd and Zn isotopic variability in marine environments, these isotopic compositions are compared to those of bivalve molluscs (i.e., oysters and mussels) from Hawaii, the Atlantic coast of the USA and the Atlantic and Mediterranean coasts of France. This allows the assessment of Cd and Zn isotopic compositions of bivalves from sites impacted, to various degrees, by different natural and anthropogenic sources. Lead isotopes are used to "fingerprint" important anthropogenic sources, narrowing the identified potential anthropogenic sources of Cd and Zn at marine sites. Finally, Pb isotopes are used to determine the relative importance of natural and anthropogenic Pb sources to bivalves post leaded gasoline phase-out.

4.1.1 Cd Zn and Pb emission sources in Canada, the USA and France

Global anthropogenic emissions of Cd and Zn to the atmosphere are estimated to account for the majority (70% for Cd, and 56% for Zn) of total (i.e., sum of natural and anthropogenic) atmospheric emissions of these metals (Pacyna and Pacyna, 2001). Non-ferrous metal smelting and refining is the largest source of Cd and Zn emissions to the atmosphere, accounting for approximately 72–73% of anthropogenic emissions of these metals (Pacyna and Pacyna, 2001). British Columbia is home to one of the world's

largest fully integrated Zn and Pb smelting and refining complexes (Trail, B.C.). In 2008, this facility (Teck) reported the largest on-site releases to air and water of the metals, Cd, Zn and Pb, and their compounds (235 kg, 97 tonnes, 3,065 kg; respectively) (Environment Canada, 2009). Even so, the quantities of Cd, Zn and Pb released from the smelting and refining operations in Trail declined considerably, by ~98–99%, between 1994 and 2008 (in 1994: 11 tonnes, 4,466 tonnes, 246 tonnes; respectively) (Environment Canada, 2009). Decreasing levels of metal emissions from Teck's Trail facility reflect facility upgrades (including the implementation of new technologies, which increased internal recycling between operations) and the vast improvement in efficiency of emission controls employed at the facility in an effort to improve their environmental performance and demonstrate a commitment to environmental sustainability.

B.C. oysters were collected from two regions, Desolation Sound and Barkley Sound, which are located ~540 km northwest and west of the facility in Trail, B.C. Atmospheric emissions from smelting and refining operations in Trail may be a source of Cd, Zn and/or Pb to the oyster farms in Desolation Sound, both currently and more importantly in the past, as the most frequent wind direction near the site (in Powell River, 45 km southeast of Desolation Sound) is east (i.e., toward the west). The oyster farms in Barkley Sound are not likely to receive significant Pb emissions from smelting and refining operations as the most frequent wind direction over the Georgia Strait (separates the B.C. mainland from Vancouver Island) is northwest (i.e., toward the southeast).

Anthropogenic sources account for ~91% of total (sum of natural and anthropogenic) global atmospheric Pb emissions to the environment (Pacyna and Pacyna, 2001). Globally, the major source of atmospheric Pb emissions is the combustion of unleaded and leaded gasoline (the latter being gasoline treated with an organolead compound, most commonly tetraethyl lead), which accounts for approximately 74% of anthropogenic Pb emissions (Pacyna and Pacyna, 2001). Summaries of estimated Pb emissions from the consumption of petroleum products and coal are presented in Table 4.1 (for B.C. in 2008 and Canada in 1970/2008) and Table 4.2 and Fig. 4.1 (for Canada, the USA and France in 2005). In Canada, Pb emissions resulting from the consumption of refined petroleum products and coal in 2008 are estimated to be <1% of those emitted in 1970 (Table 4.1). In 1970, almost 100% of the total Pb emissions from the consumption

of refined petroleum products and coal are attributed to the widespread use of leaded gasoline in motor vehicles (Table 4.1). The phase out of the use of leaded motor gasoline in on-road vehicles began in Canada and the USA in the 1970s and continued through the 1980s, with the introduction of unleaded gasoline in 1975. Leaded gasoline has been prohibited in motor vehicles since 1990 and 1996 in Canada and the USA, respectively. The phase-in of unleaded motor gasoline began in France in 1989 and was completed in 2000. The shift to the use of unleaded gasoline is overwhelmingly responsible for the reduction in Pb emissions over that time. In the wake of the phase-out of leaded motor gasoline, other anthropogenic Pb emission sources are left as dominant Pb contributors, albeit with total anthropogenic Pb emission levels much smaller than those before the phase-out (Table 4.1). The use of aviation gasoline (avgas), which contains the antiknock additive tetra-ethyl lead (TEL), in piston type aircraft engines and the consumption of diesel fuel and heavy fuel oil by the marine transportation sector are now relatively important anthropogenic sources of Pb emissions to the environment (Tables 4.1 and 4.2). In B.C., the most significant Pb sources include Pb emissions from industry (e.g., smelting and refining operations and mining), the combustion of various refined petroleum products (e.g., avgas and diesel fuel oil; Table 4.1) and the storage and handling of large volumes of petroleum products, chemicals and coal.

In 2008, British Columbia (B.C.) was responsible for ~10.6% of Canada's Pb emissions resulting from the consumption of refined petroleum products and coal (Table 4.1). For both Canada and B.C., the consumption of avgas (59.6 and 67.6% of the total Pb emissions, respectively) was the most important of these Pb emissions sources (Table 4.1). Although, the second most important of these Pb emission sources was coal (17.4%) in Canada and diesel fuel oil (16.3%) in B.C. (Table 4.1). Across Canada, the primary use of coal is for the production of electricity, however, in B.C. most electricity is produced using hydroelectric dams and coal is used primarily for industrial purposes (Ménard, 2005). The relative importance of these Pb emissions sources in the USA is strikingly similar to Canada, where avgas accounts for more than half of the total Pb emissions from the consumption of petroleum products (Fig. 4.1). In contrast to Canada and the USA, diesel fuel oil is the most important source of these Pb emissions in France, accounting for almost 50% (Fig. 4.1).

4.2 Materials and methods

Bivalve samples from western Canada (B.C., Fig. 4.2), the USA (Fig. 4.3) and France (Fig. 4.4) were selected to gain an appreciation for the global variability of the Cd, Zn and Pb isotopic compositions recorded in bivalve tissues. Selected sites represent a wide range of coastal health, from relatively "pristine" (i.e., sparsely inhabited) to highly polluted (i.e., populated and/or industrial presence) environments. The majority of bivalve samples were analyzed for both Cd and Pb isotopic compositions, whereas Zn isotopic analyses were performed only on a subset of samples chosen to exemplify total variability and extremes in environmental site conditions (i.e., select sites in B.C. and France). The observed limited variability in Zn isotopic compositions did not justify a more detailed study.

4.2.1 Sample materials and collection

This study includes B.C. oysters (*Crassostrea gigas*) from oyster farming sites within Desolation Sound (B.C. mainland) and Barkley Sound (west coast of Vancouver Island) (Fig. 4.2). These oysters (dried powders) were provided by George M. Kruzynski (Fisheries and Oceans Canada), William Heath (B.C. Ministry of Agriculture & Lands) and Leah I. Bendell (Simon Fraser University). These oysters were collected in early 2004, with the exception of the oyster from Thor's Cove (Desolation Sound) collected late in 2002 (included in the Cd and Zn isotope studies) and one of the two oysters from Seddall Island (Barkley Sound) collected in late 2003 (included in the Pb isotope study). Details regarding sample collection are provided by Kruzynski (2004).

Oyster and mussel tissue samples (dried powders) from the USA and France (Fig 4.3 and 4.4, respectively) have been provided by their respective national Mussel Watch projects; these projects are handled by the National Status and Trends (NS&T) program of the National Oceanic and Atmospheric Administration (NOAA) and the Réseau National d'Observation de la qualité du milieu marin (RNO) of the Institut Français de Recherche pour l'Exploitation de la Mer (IFREMER), respectively. Information about the NOAA (USA) and IFREMER (France) mussel watch projects, including details about the

sampling sites and sample collection are provided by NOAA (1998) and O'Connor and Lauenstein (2006) and Claisse (1989), respectively. The oyster and mussel samples from the USA (Fig. 4.3) were collected between 2003 and 2006. The majority of the oyster and mussel samples from France (Fig. 4.4) were collected in 2004 and 2005. However, archived samples from 1984 (Boyardville, Marennes Oléron basin) and 1987 (La Fosse, Gironde estuary) are also included to provide a temporal dimension to our study. As no one species exists at all sites, the mussel watch programs of both the USA and France use several species of both oysters (*Crassostrea gigas, Crassostrea virginica*, *Ostrea sandvicensis*) and mussels (*Mytilus edulis*, *Mytilus galloprovincialis*). The species of each sample is indicated in Tables 4.3, 4.4 and 4.5.

4.2.2 Sample preparation

Detailed descriptions of the sample preparation, which lead to the dried oyster tissue powders provided for use in this study, are provided by Christie and Bendell (2009) for B.C. samples, NOAA (1998) for the USA samples and Claisse (1989) for the French samples. For B.C., oyster individuals, rather than pooled samples were provided. These individuals were separated into guts contents and the remaining soft tissues. For the USA and France, samples from each site were pooled as 20 oysters or 30 mussels and >10 oysters or >50 mussels, respectively. Small differences in the sampling and processing of bivalves are not expected to affect the results of this study.

4.2.2.1 Reagents

Nitric (HNO_3), hydrochloric (HCl) and hydrofluoric (HF) acids used in this study were purified in-house from concentrated reagent grade acids by sub-boiling distillation. Baseline® hydrobromic (HBr) acid and hydrogen peroxide (H_2O_2) produced by Seastar Chemicals Inc. (Canada) were also utilized. Ultra-pure water (≥ 18.2 MΩ cm), prepared by de-ionization of reverse osmosis water using a Milli-Q® system (Millipore, USA), was used to prepare all solutions.

All labware was washed successively with a ~2% extran® 300 (Merck KGaA, Germany) solution (alkaline cleanser), analytical grade HCl and environmental grade HNO_3. Savillex® PFA vials used for sample digestions and to collect purified Cd and Zn

samples were cleaned in an additional step with ~1.5 M sub-boiled HNO_3. Savillex® PFA vials used to collect purified Pb samples were cleaned in an additional step with ~6 M sub-boiled HCl.

4.2.2.2 Sample digestion

For dried and powdered bivalve tissue samples, 100–600 mg was weighed out into Savillex® PFA vials. Closed-vessel digestion was carried out on a hotplate using successive steps of HNO_3 and HNO_3+H_2O_2. Separate sample digests were used for the purification of sample Cd and Zn and the purification of sample Pb.

4.2.2.3 Anion exchange chromatography

Sample Cd and Zn was isolated using the anion exchange chromatography method of Mason (2003), and is presented in detail in Shiel et al. (2009). In this study, the resin was batch cleaned, prior to loading on the column, using the method of De Jong et al. (2007) and then cleaned on column before loading and purifying samples. Treatment of the purified samples (Cd and Zn eluate cuts) before Cd and Zn isotopic analysis on the mass spectrometer is described by Shiel et al. (2010). Sample Pb was isolated by anion-exchange chromatography using the AG 1-X8 (100–200 mesh) resin (Bio-Rad Laboratories, Inc.), as previously described (Weis et al., 2006; Shiel et al., 2010).

4.2.3 Standards

Standard solutions used for element concentration determination were prepared from 1,000 μg mL^{-1} single-element solutions from High Purity Standards, Inc. (USA) and Specpure® Plasma (Alfa Aesar®, Johnson Matthey Company, USA).

Source information and isotope data for the in-house primary and secondary reference Cd and Zn isotopic standards as well as reference materials are provided by Shiel et al. (2009). The JMC Cd standard (Wombacher et al., 2003; Wombacher and Rehkämper, 2004) and the in-house primary reference Cd standard (PCIGR-1 Cd) are identical within uncertainty ($\delta^{114/110}Cd = -0.03 \pm 0.05‰$, n = 3). The "Lyon-JMC" Zn standard (Maréchal et al., 1999) and the in-house primary reference Zn standard (PCIGR-

1 Zn) are isotopically identical within uncertainty ($\delta^{66/64}$Zn = -0.01 ± 0.22‰, n = 7). The NIST (USA) SRM 981 natural Pb (isotopic) standard is used for monitoring analytical run instrument drift and normalization of all measured Pb isotopic ratios relative to the triple-spike values of Galer and Abouchami (1998).

4.2.4 Data presentation

Cadmium and Zn isotopic compositions are expressed relative to the PCIGR-1 Cd and PCIGR-1 Zn reference standards in the standard delta (δ) per mil (‰) notation as follows:

$$\delta^{j}\text{Cd} = \left(\frac{(^{j}Cd)_{\text{sample}}}{(^{j}Cd)_{\text{standard}}} - 1 \right) \text{x } 1{,}000$$

$$\delta^{k}\text{Zn} = \left(\frac{(^{k}Zn)_{\text{sample}}}{(^{k}Zn)_{\text{standard}}} - 1 \right) \text{x } 1{,}000$$

where j and k are the measured isotope ratios, for Cd j = 111/110, 112/110, 113/110 or 114/110 and for Zn k = 66/64, 67/64 or 68/64. Isotopic compositions for all the ratios mentioned above are reported. However, discussion will revolve around ^{114}Cd/^{110}Cd and ^{66}Zn/^{64}Zn. These isotopes are selected for their high relative isotopic abundances, the large relative mass difference between the isotope pair and to avoid or minimize isobaric interferences.

For Pb, the ^{206}Pb/^{204}Pb, ^{207}Pb/^{204}Pb, ^{208}Pb/^{204}Pb, ^{206}Pb/^{207}Pb and ^{208}Pb/^{206}Pb ratios are reported. However, most discussion will focus on the ^{206}Pb/^{207}Pb and ^{208}Pb/^{206}Pb ratios, to be consistent with the majority of environmental studies, which in the past, have omitted reporting ^{204}Pb values or report values with large errors due to various combinations of the following: limited instrument sensitivity, the low relative isotopic abundance (1.4%; Bölke et al., 2005) of ^{204}Pb and limited Pb availability in samples (Sangster et al., 2000, and references within).

4.2.5 Analytical methods

Experimental work was carried out in metal-free Class 1,000 clean laboratories at the Pacific Centre for Isotopic and Geochemical Research (PCIGR), University of British Columbia (UBC). Sample preparation for elemental and isotopic analyses was performed

in Class 100 laminar flow hoods in the clean labs and instrument rooms. Elemental analysis was carried out on an ELEMENT2 (Thermo Finnigan, Germany) high-resolution inductively coupled plasma mass spectrometer (HR-ICP-MS). The trace element analysis method and instrument set-up are described by Shiel et al. (2009). Isotopic analysis was performed on a Nu Plasma (Nu 021; Nu Instruments, UK) multi-collector inductively coupled plasma mass spectrometer (MC-ICP-MS). The isotopic analysis methods for Cd, Zn and Pb are described in Shiel et al. (2010).

4.3 Results

Cadmium and Zn concentrations and delta values for bivalve samples are reported in Tables 4.3 and 4.4, respectively. Cd concentrations for all samples collected between 2002 and 2006 are given in a histogram (Fig. 4.5). Variations in bivalve Cd tissue concentrations and isotopic composition are shown in Fig. 4.6. Mass dependent fractionation is shown for Cd and Zn isotopes in Fig. 4.7a and b, respectively. Lead concentrations and isotopic ratios are reported in Table 4.5 and shown in Figures 4.8, 4.9 and 4.10 for bivalve samples from B.C. (Canada) and Hawaii (North Pacific Ocean), the USA East Coast (Northwest Atlantic Ocean) and France (Northeast Atlantic Ocean and Mediterranean Sea), respectively.

4.3.1 Cd isotopes

The Cd isotopic composition varies among bivalve samples by 0.99‰ with a total range from $\delta^{114/110}$Cd = -1.08 to -0.09‰ (Fig. 4.6; see Table 4.3 for the other ratios). The total range represents significant differences in Cd isotopic compositions. The linear data array for Cd ratios in Fig. 4.7a is consistent with mass-dependent fractionation.

Oysters from the southern coast of B.C. (Canada) have Cd contents of 2.9 to 13 μg g^{-1} dry weight (tissues) and of 39 to 78 μg g^{-1} dry weight (gut contents) (Table 4.3; Fig. 4.5). Their Cd isotopic compositions range from $\delta^{114/110}$Cd = -0.69 to -0.09‰ (Fig. 4.6). For the three B.C. oysters for which both tissues and gut contents were measured, the $\delta^{114/110}$Cd values of the tissues and gut contents are within error (Appendix H). For the B.C. oysters, the heaviest $\delta^{114/110}$Cd value is exhibited by one of the Barkley Sound (west

coast of Vancouver Island) oyster samples (Seddall Island; $\delta^{114/110}$Cd = -0.09‰), the lightest by one of the Desolation Sound (B.C. mainland) oyster samples (Gorge Harbor; $\delta^{114/110}$Cd = -0.69‰) (Fig. 4.6). The average $\delta^{114/110}$Cd value of Desolation Sound oysters (-0.54‰) is lighter than that of Barkley Sound oysters (-0.31‰). The Hawaiian oyster sample (Honolulu Harbor) has a Cd concentration of 1.0 μg g^{-1} dry weight, which is lower than those of the other Pacific Ocean samples (i.e., B.C. oysters) (Fig. 4.5). The $\delta^{114/110}$Cd valve of the Hawaiian oyster sample (-0.46‰) is comparable to those exhibited by the B.C. oyster samples (Fig. 6). B.C. oysters tend to have the highest Cd tissue concentrations, excluding bivalves from the highly polluted Gironde estuary (Fig. 4.5). Also, their Cd isotopic compositions are among the heaviest exhibited by all bivalve samples (Fig. 4.6).

Oysters and mussels from the USA East Coast have Cd concentrations ranging from 1.5 to 16 μg g^{-1} dry weight (Table 4.3; Fig. 4.5). Their Cd isotopic compositions range from $\delta^{114/110}$Cd = -1.20 to -0.46‰ (Fig. 4.6). For USA East Coast bivalves, the heaviest $\delta^{114/110}$Cd value is exhibited by mussels from Cape Arundel, ME ($\delta^{114/110}$Cd = -0.54‰), the lightest by oysters from Charleston Harbor, SC ($\delta^{114/110}$Cd = -1.20‰) (Fig. 4.6). This is the lightest Cd composition reported, with the exception of values reported for ordinary chondrites and a layered tektite (impact-related rock) (Wombacher et al., 2003).

Oysters from the English Channel and the French Atlantic Coast have Cd concentrations ranging from 1.4 (Abers Benoît, English Channel) to 29 μg g^{-1} dry weight (Gironde estuary, Atlantic Ocean) for samples collected in 2004/5 (Fig. 4.5) and up to 129 μg g^{-1} dry weight (Gironde estuary) including samples collected in 1984/7 (Table 4.3). French mussels have Cd concentrations ranging from 0.37 (Etang du Prevost, Mediterranean Sea) to 5.7 μg g^{-1} dry weight (Etang de Bages, Mediterranean Sea) (Fig. 4.5). Cadmium isotopic compositions of the French bivalve samples range from $\delta^{114/110}$Cd = -1.08 to -0.20‰ (Fig. 4.6). The heaviest $\delta^{114/110}$Cd value (-0.20‰) is exhibited by mussels from Oye Plage (English Channel), the lightest by French oysters from the Atlantic Coast, Les Palles (-1.08‰) and the Gironde estuary (-0.99 to -1.06‰, includes oysters collected both in 1987 and 2005) (Fig 4.6). For French bivalves, $\delta^{114/110}$Cd values vary from –0.88 to –0.20‰ for sites on the English Channel, from –1.08 to –0.62‰ for

sites on the Atlantic Coast and from –0.52 to –0.29‰ for sites on the Mediterranean Coast (Fig. 4.6). The Cd isotopic values exhibited by bivalves from the Marennes-Oléron basin and Gironde estuary (Atlantic Coast) are among the lightest of the whole study (Fig. 4.7a). For bivalves collected from Boyardville (Atlantic Coast) in 1984, the Cd concentration of the oyster sample is ~6.3× that of the mussel sample, while an insignificant difference is observed between their $\delta^{114/110}$Cd values (Fig. 4.6).

4.3.2 Zn isotopes

The Zn isotopic composition varies among bivalve samples by only 0.18‰ with a total range of $\delta^{66/64}$Zn = 0.28 to 0.46‰, except for the significantly heavier oyster samples from the Gironde estuary (Atlantic Coast; 1987/2005), which are as heavy as 1.15‰ (Fig. 4.7b; see Table 4.4 for the other ratios). The narrow total range in Zn isotopic composition exhibited by the majority of the bivalve samples is much smaller than that reported for seawater and plankton tow samples (Bermin et al., 2006; John, 2007) (Fig. 4.11b, 4.12b). The much heavier Zn isotopic compositions of the oysters from the Gironde estuary (Atlantic Coast) are consistent with compositions from smelter tailings (Sivry et al., 2008) and polluted sediments (Sonke et al., 2008) (Fig. 4.12b). The linear data array for Zn ratios in Fig. 4.7b is consistent with mass-dependent fractionation.

Oysters from the southern coast of B.C. (Canada) have Zn contents of 390 to 490 μg g^{-1} dry weight (tissues). There is no significant difference between the $\delta^{66/64}$Zn values of oysters from Desolation Sound (B.C. mainland) and Barkley Sound (west coast of Vancouver Island) (total range of 0.28 to 0.36‰; Table 4.4).

Oysters from the English Channel and the Atlantic Coast of France have Zn concentrations ranging from 1320 (Abers Benoît, English Channel) to 3570 μg g^{-1} dry weight (Gironde estuary, Atlantic Coast) for samples collected in 2005 and up to 8350 μg g^{-1} dry weight (Gironde estuary) for samples collected in 1987 (Table 4.4). Mussels from the French Mediterranean Coast have Zn concentrations ranging from 90.0 (Etang de Bages) to 116 μg g^{-1} dry weight (Etang du Prévost) (Table 4.4). Zinc isotopic compositions of the French bivalve samples range from $\delta^{66/64}$Zn = 0.39 to 1.15‰ (Fig. 4.7b). The lightest $\delta^{66/64}$Zn value is exhibited by the oyster sample from the English Channel (Abers Benoît; 0.39‰) (Fig. 4.7b). The heaviest $\delta^{66/64}$Zn values are exhibited by

the oysters from the Gironde estuary on the Atlantic Coast (1.03 to 1.15‰, for oysters collected both in 1987 and 2005) (Fig. 4.7b). For French bivalves, $\delta^{66/64}$Zn values vary from 0.39 to 1.15‰ for sites on the English Channel and Atlantic Coast and from 0.43 to 0.46‰ for sites on the Mediterranean Coast (Fig. 4.7b). The Zn isotopic compositions of the oysters from the Gironde estuary (Atlantic Coast) are by far the heaviest of the whole study. Due to the limited overall variation in the Zn isotopic compositions of bivalves, with the exception of the oysters from the highly polluted Gironde estuary, the USA samples were excluded from the Zn isotopic composition study.

4.3.3 Pb isotopes

The Pb isotope values of the bivalve samples range from 1.14832 to 1.21783 for $^{206}Pb/^{207}Pb$ and 2.03564 to 2.10931 for $^{208}Pb/^{206}Pb$ (Table 4.5). The most radiogenic samples are characterized by high $^{206}Pb/^{207}Pb$ and low $^{208}Pb/^{206}Pb$ ratios.

Oysters from the southern coast of B.C. (Canada) have Pb contents of 0.05 to 0.22 μg g^{-1} dry weight. Their Pb isotopic compositions range from $^{206}Pb/^{207}Pb$ = 1.14832 to 1.17442, within the range of those reported for B.C. lichens (Simonetti et al., 2003) (Fig. 4.8). The lowest $^{206}Pb/^{207}Pb$ value is exhibited by one of the Desolation Sound (B.C. mainland) oyster samples (Gorge Harbor; $^{206}Pb/^{207}Pb$ = 1.14832), the highest by one of the Barkley Sound (west coast of Vancouver Island) oyster samples (Seddall Island; $^{206}Pb/^{207}Pb$ = 1.17442). In general, the oysters from Desolation Sound (B.C. mainland) have higher Pb contents and lower $^{206}Pb/^{207}Pb$ values than those from Barkley Sound (west coast of Vancouver Island) (Fig. 4.8). The Hawaiian oyster sample (Honolulu Harbor) has a much higher Pb concentration (5.7 μg g^{-1} dry weight) than those of the other Pacific Ocean samples (i.e., B.C. oysters) (Table 4.5). Despite this, the $^{206}Pb/^{207}Pb$ value of the Hawaiian oyster sample (1.16521 ± 0.00001) is within the range of those measured for the B.C. oysters (Fig. 4.8).

Oysters and mussels from the USA East Coast have Pb concentrations ranging from 0.11 to 2.2 μg g^{-1} dry weight (Table 4.5). The Pb isotopic compositions of these bivalves range from $^{206}Pb/^{207}Pb$ = 1.17949 to 1.21783 over a range similar to that of North American coals (Fig. 4.9). The lowest of these $^{206}Pb/^{207}Pb$ values is exhibited by oysters from Charleston Harbor (SC), the highest by oysters from Mobile Bay (AL) (Fig. 4.9).

Despite the difference between the Pb concentrations of the Chesapeake Bay (MD) oysters (the Bodkin Point oyster sample has a Pb concentration 2.6× that of the Choptank River oyster sample), the Pb isotopic compositions of the oysters are almost within error (Fig. 4.9).

Bivalve samples from the coasts of France have Pb concentrations ranging from 0.40 (Etang de Bages, Mediterranean Coast) to 3.1 μg g^{-1} dry weight (Gironde estuary, Atlantic Coast) for samples collected in 2004/2005 and up to 34 μg g^{-1} dry weight (Gironde estuary) for samples collected in 1984/7 (Table 4.5). Lead isotopic signatures of the same bivalve samples range from $^{206}Pb/^{207}Pb$ = 1.16076 to 1.18134, intermediate between those of French aerosols and pre-industrial sediments (Fig. 4.10). The lowest $^{206}Pb/^{207}Pb$ value is exhibited by Loire estuary (Atlantic Coast) mussels ($^{206}Pb/^{207}Pb$ = 1.16076 to 1.18134), the highest by Gironde estuary (Atlantic Coast) oysters ($^{206}Pb/^{207}Pb$ = 1.18134; 2005 sample) (Fig. 4.10). For French bivalves, $^{206}Pb/^{207}Pb$ values vary from 1.16355 to 1.17534 for sites on the English Channel, from 1.16076 to 1.18134 for sites on the Atlantic Coast and from 1.17374 to 1.18064 for sites on the Mediterranean Coast (Fig. 4.10). A shift is observed between the Pb isotopic compositions of bivalves sampled in 1984/7 and 2004/5 from the Gironde estuary and Marennes-Oléron basin (Fig 4.10). For bivalves collected from Boyardville in 1984, the Pb concentration and isotopic composition of oysters (Fig. 4.10) is similar but not identical to that of mussels (1.97 μg g^{-1} dry weight, $^{206}Pb/^{207}Pb$ = 1.17739 and 1.76 μg g^{-1} dry weight, $^{206}Pb/^{207}Pb$ = 1.17433; respectively).

4.4 Discussion

4.4.1 Isotopic variations in bivalves from the Pacific Coast of Canada and Hawaii

4.4.1.1 Cd isotope systematics

B.C. oyster tissues ($\delta^{114/110}Cd$ = -0.55 to -0.29‰) and associated gut contents ($\delta^{114/110}Cd$ = -0.64 to -0.26‰) exhibit Cd isotopic signatures within the range of the lightest reported for North Pacific seawater (Lacan et al., 2006; Ripperger et al., 2007) (Fig. 4.11a). The Cd isotopic compositions of the B.C. oysters and their gut contents

($\delta^{114/110}$Cd = -0.69 to -0.09‰) are within error (Appendix H). An evaluation of the importance of preferential uptake of light Cd by phytoplankton (as observed in phytoplankton culture experiments, $\Delta\delta^{114/110}$Cd = -1.35 between culture media and phytoplankton cultures; Lacan et al., 2006) in determining the Cd isotopic compositions of oysters in the North Pacific is not possible given the scale of this study and the poorly constrained Cd isotopic compositions of local waters. We expect small variations in the relative contributions of Cd sources through time (e.g., seasonally variable upwelling of deep nutrient-rich waters or shifts in the relative contributions of anthropogenic Cd emissions) to be reflected in subtle differences between the $\delta^{114/110}$Cd values of the gut contents (potentially transient Cd source) and the oyster tissues (Cd is accumulated over time).

The relatively light Cd isotopic compositions of the oysters from Desolation Sound (B.C. mainland), as compared to those of oysters from Barkley Sound (west coast of Vancouver Island), are attributed to the mixing of seawater Cd with anthropogenic Cd emissions characterized by a light Cd isotopic composition (Cloquet et al., 2005; Shiel et al., 2010) (Fig. 4.11a). Alternatively, differences between the Cd isotopic compositions of oysters from Desolation Sound and Barkley Sound may potentially reflect natural differences between the Cd isotopic compositions of waters in the Strait of Georgia and along the west coast of Vancouver Island. However, mixing with a light Cd source related to anthropogenic emissions is strongly supported by the positive correlation between the $\delta^{114/110}$Cd and ^{206}Pb/^{207}Pb values of B.C. oysters (inset of Fig. 4.7a), where increasing values reflect an increasing contribution of natural Cd and Pb and decreasing values reflect an increasing contribution from anthropogenic sources of Cd and Pb (see Section 4.4.1.3). The Hawaiian oyster sample from Honolulu Harbor exhibits a Cd isotopic composition within the range of those of B.C. oysters (Fig. 4.6), indicating a common natural Cd source across the Northwest Pacific Ocean.

4.4.1.2 Zn isotope systematics

The $\delta^{66/64}$Zn values of B.C. oysters (0.28 to 0.36‰) from Desolation Sound (B.C. mainland) and Barkley Sound (west coast of Vancouver Island) are within error (Fig. 4.11b). The limited range of $\delta^{66/64}$Zn values exhibited by B.C. oysters falls within the

range reported for North Pacific seawater and plankton tows (-0.16 to 0.62‰ and 0.08 to 0.57‰, respectively; John, 2007) (Fig. 4.11b). As natural Zn concentrations are much higher than those of Cd in bivalve tissues (e.g., for two B.C. oysters, the Zn concentration is 68× or 94× higher than the Cd concentration; Tables 4.3 and 4.4), any anthropogenic contribution will need to be correspondingly larger to be recorded in the Zn isotopic signature. Therefore, it is not surprising that the Zn isotopic compositions exhibited by B.C. oysters are within error (Fig. 4.11b), despite the total variability observed in the Cd isotopic compositions.

4.4.1.3 Pb isotope systematics

In Pb–Pb diagrams (Fig. 4.8), the Pb isotopic ratios of bivalve samples from the Pacific Coast of B.C. and Hawaii form a linear trend, between several modern anthropogenic Pb emissions (discussed in detail below) and natural Pb (e.g., Chinese loess; Jones et al, 2000). The Pb isotopic compositions of the oysters can be explained by mixing of these end-members. Unlike Cd and Zn, Pb isotopes are not likely to undergo significant mass dependent fractionation during anthropogenic processing due to the element's heavy mass and as a consequent its small relative mass difference (Shiel et al., 2010). The Pb contents of oysters from both Desolation Sound (B.C. mainland) and Barkley Sound (west coast of Vancouver Island) are comparably low (0.05-0.22 μg g^{-1} dry weight) and below the median concentration of Pb in oysters from the USA established by the US Mussel Watch Program (0.5 μg g^{-1} dry weight in 1993; Beliaeff et al., 1998). However, oysters from Desolation Sound (B.C. mainland) are characterized by lower $^{206}Pb/^{207}Pb$ and higher $^{208}Pb/^{206}Pb$ ratios than those from Barkley Sound (west coast of Vancouver Island). The Pb isotopic composition of the Hawaiian oyster sample from Honolulu Harbor is comparable to those of the oysters from Barkley Sound, however, the Pb content of this sample is significantly greater (5.7 μg g^{-1} dry weight) than those of the B.C. oysters or the median concentration for oysters from the USA (0.5 μg g^{-1} dry weight in 1993; Beliaeff et al., 1998).

The relatively radiogenic Pb isotopic signatures of the oysters from Barkley Sound are consistent with those of road dust from highways in the lower mainland (representative of the average modern Pb isotopic signature of unleaded gasoline

consumed by passenger automobiles and diesel fuel consumed by trucks mixed with local natural Pb; Preciado et al., 2007). The Pb isotopic signature of B.C. mainland oysters is attributed to a relatively large contribution of anthropogenic Pb emissions from a source that is characteristically unradiogenic (low $^{206}Pb/^{207}Pb$). This unradiogenic anthropogenic Pb source is suggested to be Pb ore from Mt. Isa (Australia) and/or the Sullivan mine (B.C., Canada), although the latter has become increasing less important as a source over time as the mine was closed in 2001. Two plausible mechanisms for the dispersion of this unradiogenic Pb source in the B.C. lower mainland are (1) Pb emissions resulting from the smelting and refining operations in Trail, B.C. (1,563 kg Pb released to the air in 2008; Environment Canada, 2009) of ore concentrates from the Cannington mine (Mt. Isa inlier, Eastern Succession, Australia; $^{206}Pb/^{207}Pb$ 1.041; Huston et al., 2006) and the Sullivan mine (B.C.; $^{206}Pb/^{207}Pb$ 1.0679; Sangster et al., 2000, and references within) (Shiel et al., 2010) (Fig. 4.8), and (2) Pb emissions resulting from the consumption of avgas (responsible for an estimated 4,860 kg Pb emissions in B.C.; Table 4.1) in small general aircrafts (e.g., personal aircrafts, seaplanes, crop dusters and bush planes). Avgas, similar to leaded motor gasoline, uses the antiknock additive, TEL, which is now manufactured by only a few companies worldwide. Much of the Pb used to produce TEL originates from Australia (Mt. Isa and Broken Hill) and formerly B.C., Canada (Sullivan mine) (Monna et al., 1995, 1997), i.e., relatively old terrains, with distinctly unradiogenic Pb isotopic compositions. Further testing is needed to determine the Pb isotopic composition of locally consumed avgas; this is especially important as there is a part of the general aviation fleet that can not use existing alternative fuels and will continue to use avgas until an alternative is available. Atmospheric emissions of Pb (1,563 kg Pb in 2008; Environment Canada, 2009) from smelting and refining operations in Trail are thought to be an important source of Pb to the lower B.C. mainland and by extrapolation, to the oyster farms in Desolation Sound as the most frequent wind direction near the site is east. Historic releases of Pb from smelting and refining in Trail were much greater than current Pb releases and therefore historically these operations were responsible for a relatively larger contribution of Pb pollution to the B.C. lower mainland. Historical releases of Pb from operations in Trail decreased substantially in the late-1990s and early 2000s; e.g., total on-site Pb emissions in 2008 were ~1.2% of those released in 1994

(Environment Canada, 2009). The positive correlation between the $\delta^{114/110}$Cd and ^{206}Pb/^{207}Pb values of B.C. oysters (inset of Fig. 4.7a), suggests a source that exhibits both a light Cd isotopic composition and an unradiogenic Pb isotopic composition (e.g., emissions from smelting and refining operations in Trail; see 4.4.1.1). The similarity between the Pb isotopic compositions of oysters from B.C. and Hawaii suggests comparable anthropogenic Pb sources across the NE Pacific, i.e., the consumption of petroleum products, such as unleaded motor gasoline and diesel fuel, characterized by comparable Pb isotopic compositions.

The use of diesel fuel oil and heavy fuel oil by container ships, cargo ships, ferries and cruise ships represents another important source of modern anthropogenic Pb emissions in B.C. (Table 4.1). The Pb isotopic composition of these fuels is not well constrained and will vary with that of the crude oil source (few studies have measured the Pb isotopic composition of crude oils; e.g., Dreyfus et al., 2007). In addition, an evaluation needs to be made of other significant provincial Pb polluters, including the Vancouver Wharves (released 1,602 kg Pb to the air and 129 kg Pb to the water in 2008), wastewater treatment facilities (1,064 kg released to waters in 2008 by facilities serving the Greater Vancouver area, Victoria and Nanaimo) and smaller Pb polluters located adjacent to the oyster collection sites, e.g., pulp and paper mills located in Elk Falls (released 89 kg Pb to the air and water in 2008) and Port Alberni (released 11 kg Pb to the air and water in 2008) (Environment Canada, 2009). Testing of the Pb isotopic signatures of these emissions is needed to confirm their relative importance in B.C. oysters.

4.4.2 Isotopic variations in bivalves from the USA Atlantic Coast

4.4.2.1 Cd isotope systematics

Significant variability in the Cd isotopic compositions is exhibited among bivalves from the USA East Coast and δCd values of these samples include values among the lightest ever reported. The bivalves from the USA East Coast are enriched in light Cd relative to those from the North Pacific (i.e., B.C. and Hawaii) (Fig. 4.6). Cadmium concentrations in the USA East Coast bivalves likely result from the significantly denser

industrial presence on the USA East Coast. This is in contrast to the attribution of comparable Cd concentrations in North Pacific oysters to natural sources. The relatively light isotopic compositions of the USA East Coast bivalves suggest contributions of light Cd enriched emissions from anthropogenic processes, e.g., smelting (e.g., Cloquet et al., 2005; Shiel et al., 2010). Primary and secondary smelting and refining of non-ferrous metals and iron and steel mills report the largest Cd emissions regionally (US EPA, 2010); the variable importance of anthropogenic emissions from these facilities between sites is expected to account for the majority of the variability observed in the Cd isotopic compositions of the USA East Coast bivalves. As compared to bivalves from the Northwest Pacific, bivalves from the North Atlantic have lower natural Cd contents and as a result, similar contributions from anthropogenic sources will be more apparent in the Cd isotopic signatures of North Atlantic bivalves than in Northwest Pacific bivalves.

An overall positive correlation exists between the $\delta^{114/110}$Cd and ^{206}Pb/^{207}Pb values of bivalves from the USA East Coast (inset of Fig. 4.7a), similar to the one observed for B.C. oysters, but displaced towards lower $\delta^{114/110}$Cd values. For oyster and mussel samples, the NS&T Program Mussel Watch found that Cd tissue concentrations were not statistically correlated to human population density (O'Connor, 2002), rather high Cd concentrations may represent natural enrichments of this element, as observed in the Northwest Pacific. For the oyster and mussel samples included in this study, there is no clear relationship between the Cd concentration and isotopic composition of tissues.

Mussels from Cape Arundel (Gulf of Maine) are characterized by both the lowest Cd concentration (1.5 μg g^{-1} dry weight) and the heaviest Cd isotopic composition of the USA East Coast bivalve samples (Fig. 4.12a), closest to those of Atlantic Ocean seawater (Ripperger et al., 2007), ferromanganese nodules (Schmitt et al., 2009) and terrestrial rocks and minerals (Wombacher et al., 2003). All other USA East Coast bivalves (Fig. 4.3) are collected from sites more proximal to industries reporting significant Cd releases (Fig. 4.3). Steelmaking, using electric arc and blast furnaces, needs to be evaluated as a source of Cd isotopic fractionation. Iron and steel mills populate the USA East Coast; mills are located (near bivalve collection sites) in, e.g., Baltimore (MD), Charleston (SC), Tuscaloosa (AL) and Axis (AL) (Fig. 4.3). Baltimore Harbor, which feeds into Chesapeake Bay, receives metal pollution from local industries including a local iron and

steel mill (Fig. 4.3; US EPA, 2010). In Chesapeake Bay, the Cd concentration of the oyster sample from Bodkin Point (located where Baltimore Harbor enters Chesapeake Bay) is ~3.5× that of the oyster sample from the mouth of the Choptank River (a major tributary of Chesapeake Bay located ~60 km south of Baltimore Harbor). In addition to having the higher Cd concentration, the oyster sample from Bodkin Point has a lighter Cd isotopic composition ($\delta^{114/110}$Cd = -0.74‰) than that of the oyster sample from Choptank River ($\delta^{114/110}$Cd = -0.56‰). A similarly light $\delta^{114/110}$Cd value is exhibited by the oyster sample from Mobile Bay (-0.78‰; Fig. 4.6) suggesting contributions of light Cd enriched atmospheric emissions from the nearby secondary smelter or iron and steel mills (Fig. 4.3).

The Cd concentrations (2.1 and 4.2 μg g^{-1} dry weight) of the oyster samples from Charleston Harbor (SC) are higher than the average concentration reported for the state (NOAA, 2010). Bivalves from Charleston Harbor (SC) exhibit the lightest Cd isotopic signatures ($\delta^{114/110}$Cd = -1.20 and -1.05‰) of this study. The relatively light Cd isotopic compositions of these bivalves suggest contributions from a Cd emission source that is characterized by a light isotopic composition (Fig. 4.12a), e.g., emissions from Zn smelting and refining operations (Cloquet et al., 2005; Shiel et al., 2010) in Clarksville, TN (Fig. 4.3; discussed in Section 4.4.2.2).

4.4.2.2 Pb isotope systematics

A strong correlation between Pb concentration and human population density exists for oyster and mussel tissues collected as apart of the NS&T program Mussel Watch (O'Connor, 2002). The Pb isotopic compositions of these bivalves (Fig. 4.9) are consistent with values measured for NE USA emissions (Bollhöfer and Rosman, 2001; Carignan et al, 2002). The range in Pb isotopic compositions of the bivalves from the USA East Coast suggests significant contributions from varied and regional industrial Pb emission sources and corroborates the lighter Cd isotopic signatures. Post-leaded gasoline phase-out, facilities that release significant quantities of Pb are shown to dictate the Pb isotopic signature of local environments. The relative contribution of Pb emissions from the combustion of coal, to the total Pb emissions from fuel consumption (Table 4.2), is similar for the USA (21.9%) and Canada (18.9%). Combustion of coal therefore is

expected to be a significant Pb source to bivalves from the USA East Coast. B.C. is in strong contrast to the rest of the Canada and the USA, as there is a much smaller contribution of Pb emissions from coal combustion (Table 4.1) and this source is therefore not a significant contributor of Pb to the B.C. oysters. The importance of Pb emissions from coal combustion on the USA East Coast is reflected in the Pb isotopic compositions of the USA East Coast bivalves, which are largely overlapping with those of North American coals (Díaz-Somoano et al., 2009). The electric power sector is the largest USA consumer of coal (US EIA, 2010) and therefore the largest source of these Pb emissions.

On the USA East Coast, significant Pb releases are reported by several industries, e.g., primary Zn and Pb smelting and refining of non-ferrous metals, secondary smelting and refining of lead (e.g., car batteries, ammunition, electric arc furnace dust from steel mills) and steelmaking (Fig. 4.3). The range of Pb isotopic compositions exhibited by USA East Coast bivalves suggests mixing with a Pb emission source characterized by a radiogenic signature such as that of SE Missouri Pb ore ($^{206}Pb/^{207}Pb = 1.3390$; calculated by Sangster et al., 2000, from references within) (Fig. 4.9). There was an increase in the usage of SE Missouri Pb ore in primary Pb production post-1980 in the USA (Shirahata et al., 1980; Ketterer et al., 2001). Primary Pb smelting operations in Herculaneum, MO (Doe Run Co. Herculaneum Smelter), reported the highest quantity of air emissions of Pb compounds (17,501 kg, sum of on-site point source and fugitive emissions) in the USA in 2008 (US EPA, 2010). Secondary Pb smelting and refining operations may be in part or wholly responsible for the radiogenic Pb found in the surrounding areas. A secondary Pb smelting facility in Iron, MO (Buick Resource Recycling Facility), which processes car batteries and ammunition, reported significant air emissions of Pb compounds (11,487 kg, sum of on-site point source and fugitive emissions) in 2008, second only to the primary Pb smelting operations in Herculaneum (MO) (US EPA, 2010). This radiogenic Pb component is seen most significantly in the oyster sample from Alabama (Fig. 4.9). Secondary Pb smelting operations in Troy (AL) and/or Baton Rouge (LA) may be significant sources of Pb emissions deposited at this site. The iron and steel mills populating the USA East Coast may be another important source of radiogenic Pb in the USA East Coast bivalves, as regional steel mill electric arc furnace dust is expected to

have a radiogenic Pb isotopic signature (for electric arc furnace process materials, $^{206}Pb/^{207}Pb = 1.214$; Ketterer et al., 2001) (Fig. 4.9).

Oysters from Charleston Harbor (SC) are characterized by the lowest $^{206}Pb/^{207}Pb$ values of the USA East Coast bivalves (Fig. 4.9). Identification of the dominant Pb sources to the sites in Charleston Harbor (Shutes Folly and Fort Johnson) is especially important as an increasing temporal trend in Pb concentration was identified at these sites (O'Connor and Lauenstein, 2006). The Pb isotopic composition of these bivalves, in combination with their relatively light Cd isotopic composition, is consistent with emissions from primary smelting of ores with less radiogenic Pb compositions (i.e., relatively low $^{206}Pb/^{207}Pb$) (Fig. 4.9), e.g., Zn smelting and refining in Clarksville, TN (~802 km NW on Charleston Harbor) of ores from Australia (e.g., Broken Hill: $^{206}Pb/^{207}Pb = 1.0407$, Mount Isa: $^{206}Pb/^{207}Pb = 1.0431$), Central and South America (e.g., for Argentina $^{206}Pb/^{207}Pb = 1.1530$ to 1.1535) and Ireland ($^{206}Pb/^{207}Pb = 1.1581$ to 1.1717 for 20th century producing mines) (Sangster et al., 2000, and references within; Nyrstar, 2010).

4.4.3 Isotopic variations in bivalves from the Atlantic and Mediterranean Coasts of France

4.4.3.1 Cd isotope systematics

Bivalves from the French coasts (Fig. 4.4) exhibit the most overall variation in $\delta^{114/110}Cd$ (Fig. 4.6), from relatively light isotopic compositions, such as those observed in bivalves from sites within the polluted Marennes-Oléron basin and the Gironde estuary (Atlantic Coast), to relatively heavy isotopic compositions, such as observed in bivalves from Oye Plage (English Channel) and Etang du Prévost (Mediterranean Sea). This range in isotopic composition reflects the large variability of coastal health and anthropogenic inputs among French sites included in this study.

For bivalve samples collected from the English Channel, increasing Cd concentrations correspond to increasing light Cd compositions (Fig. 4.6). The mussel sample from Oye Plage (English Channel) has the lowest Cd concentration and exhibits the heaviest Cd isotopic composition of the French bivalves ($\delta^{114/110}Cd = -0.20‰$), closest

to that of Atlantic seawater (Ripperger et al., 2007; Fig. 4.12a). In contrast, mussels from the Seine estuary have the highest Cd concentration and exhibit the lightest Cd isotopic composition for the English Channel samples (Fig. 4.6). The Seine River and estuary receive wastewater and industrial effluents from neighboring urban areas including Paris, Rouen and Le Havre (Fig. 4.4). Cadmium contamination in the estuary is largely attributed to the disposal (banned in 1992) of calcium sulfate (high Cd content), a waste byproduct produced by phosphoric acid plants located near Rouen and Le Havre (Fig. 4.4), into the Seine River and estuary (Nakhlé et al., 2007).

The Cd isotopic compositions ($\delta^{114/110}$Cd = -1.08 to -0.62‰) of the bivalves from the Atlantic coast of France reflect the relatively large anthropogenic presence near the collection sites (Fig. 4.6). The heaviest Cd isotopic composition of the French Atlantic Coast bivalves is that of the mussels collected from the Loire estuary ($\delta^{114/110}$Cd = -0.62‰); however, this isotopic composition is still relatively light when compared to those of bivalves from the other coasts studied here. The Gironde estuary and the adjacent Marennes Oléron basin are famous for their oysters, the latter being the location of the largest oyster farming area in Europe. As a result, concern exists over the documented history of metal contamination from local industries (e.g., mining, smelting, foundries, battery manufacturing) along the Garonne River and its tributaries (especially the Lot River), which feed into the Gironde estuary (Grousset et al., 1999; Audry et al., 2004). Cadmium contamination is primarily attributed to smelting activities (1842 to 1987) near Decazeville (Audry et al., 2004). Cadmium, Zn and Pb concentrations of oysters from the Gironde estuary show a marked decrease between 1987 and 2005, corresponding to the shutdown of the smelter near Decazeville. Despite the significant decrease in the Cd concentrations over this time (from 129.1 to 28.7 μg g^{-1} dry weight), the Cd isotopic signatures ($\delta^{114/110}$Cd = -1.02, -1.03‰) of the oyster samples are still within error of each other and of smelting dust (from the Metaleurop Pb smelter and refinery in Noyelles-Godault, Northeast France, closed in 2003; Cloquet et al., 2005) (Fig. 4.4, 4.12a). This suggests the dominant source of Cd pollution in the Gironde estuary remains historical Cd emissions from the now-closed, metallurgical industry (Jouanneau et al., 1990) likely via remobilization of sediments and associated metals by, e.g., flooding, riverbed dredging and other anthropogenic activities, especially from the

Lot River (Audry et al., 2004). Although the Cd concentrations of bivalves from the nearby sites in the Marennes-Oléron basin, La Moucliere and Les Palles, (1.1 and 2.8 μg g^{-1} dry weight, respectively) are much lower than those of the oyster sample from the Gironde estuary (28.7 μg g^{-1} dry weight), their Cd isotopic compositions are within error, suggesting the dominant source of Cd is also historic smelting emissions (Fig. 4.6).

Both oyster and mussel samples from Boyardville (1984) were included in this study. Cadmium metal concentrations in bivalves for this collection year are the highest reported for this site (IFREMER, 2010), reflecting the strength of local industrial Cd emissions at the time (discussed above). Consistent with previous findings that significant differences exist between the accumulation of Cd in oyster verses mussel tissues in contaminated environments (Claisse et al., 1989), the Cd concentration of the Boyardville oyster is ~6.3× that of the mussel. Despite this difference in Cd concentration, the $\delta^{114/110}$Cd values of the oyster and mussel samples are within error (Fig. 4.6), suggesting that differences in Cd uptake among bivalve species do not affect the Cd isotopic composition of the accumulated Cd.

The French Mediterranean sites are coastal lagoons and will therefore have the tendency to accumulate pollutants with time. The significantly higher Cd concentration of the mussels from Etang de Bages (5.7 μg g^{-1} dry weight), as compared to those from Etang du Prévost (0.4 μg g^{-1} dry weight), is accompanied by a significantly lighter Cd isotopic composition ($\delta^{114/110}$Cd = -0.51 as compared to -0.29‰, respectively). The Cd contamination at Etang de Bages is attributed largely to Cd emissions associated with Cd pigment plant activities in the nearby city of Narbonne (Fig. 4.4), which ceased in the early 1990s (Claisse, 1989). In contrast, the Cd isotopic composition of mussels collected from Etang du Prévost is consistent with the lightest δCd values reported for Mediterranean seawater (Lacan et al., 2006) (Fig. 4.12a).

4.4.3.2 Zn isotope systematics

French bivalves from the English Channel and the Mediterranean Coast have Zn isotopic compositions within error of each other and seawater from the English Channel and Atlantic Ocean (Bermin et al., 2006; John, 2007) (Fig. 4.12b). Oysters from the polluted Gironde estuary have distinctly heavier Zn isotopic compositions, which are

consistent with a large Zn contribution from local smelting operations as demonstrated by the similarity between the $\delta^{66/64}$Zn of these oyster samples (1.03‰) and smelting polluted sediments and mine tailings (Sonke et al., 2008) (Fig. 4.12b). Similar to Cd, for the Gironde estuary oyster samples from 1987 and 2005, despite the significant decrease in the Zn concentrations over time (from 8350 to 3570 μg g^{-1} dry weight, respectively), the Zn isotopic signatures ($\delta^{66/64}$Zn = 1.15 and 1.03‰, respectively) are within error, suggesting that the dominant source of Zn pollution in the Gironde estuary remains historical Zn emissions from the now-closed, metallurgical industry (Fig. 4.12b).

4.4.3.3 Pb isotope systematics

All French bivalve samples have Pb isotopic compositions consistent with industrial, as opposed to automotive (leaded gasoline, which in Europe is less radiogenic), Pb sources as defined by Deboudt et al. (1999). Lead deposited in the environment from the use of leaded gasoline (banned in France in 2000) is characterized by a low radiogenic Pb isotopic signature (e.g., auto exhaust collected in 1987 before the introduction of unleaded gasoline in France in 1989; Monna et al., 1995) (Fig. 4.10). This is because the TEL additive was produced primarily from Pb ores from the Broken Hill and Mt. Isa (Australia) and Sullivan (B.C.) mines (Monna et al., 1995), which all exhibit unradiogenic Pb isotopic signatures. In Europe, the decrease in the Pb concentration of aerosols, associated with the progressive phase-out of leaded gasoline, is linked with a systematic change in ^{206}Pb/^{207}Pb, i.e., increasing since 1979 (Grousset et al., 1994). Nationally, diesel fuel oil (18,194 kg Pb in 2005) and avgas (~13,750 kg Pb in 2005) are the two most important sources of Pb emissions from the consumption of petroleum products and coal (Fig. 4.1). Industrial facilities that report significant Pb emissions (of a similar magnitude to those produced by fuel consumption) proximal to the bivalve collection sites are discussed below.

Bivalve samples from Northeast France (Oye Plage and Ambleteuse) and the Seine and Loire estuaries are characterized by relatively low ^{206}Pb/^{207}Pb values as compared to other French bivalve samples. Although the Metaleurop Pb smelter in Noyelles-Godault (Northeast France) closed in 2003, Pb emissions (~29,000 kg Pb in 2002; DRIRE Nord Pas-de-Calais, 2003) from the smelter are expected to represent a

significant contribution of Pb to the bivalves collected in 2004 at proximal sites. A nearby iron and steel mill (Sollac Atlantique, now ArcelorMittal Dunkerque, Northeast France) emitted a similar magnitude of Pb, 15,319 kg in 2002 (DRIRE Nord Pas-de-Calais, 2003). A mixture of Pb emissions from these two facilities may be largely responsible for the Pb isotopic signatures exhibited by the bivalve samples from the Northeast French coast. The Pb isotopic signature of the oyster sample from Abers Benoît (English Channel) is closer to that of the radiogenic pre-industrial sediments (Sun, 1980) endmember than to those of the other bivalves sampled from the English Channel (Fig. 4.10), indicating a larger contribution of natural Pb at Abers Benoît.

The Pb isotopic compositions of the bivalves from the Atlantic Coast of France (Fig. 4.10) plot with the values for the Garonne River and its tributaries (SPM and sediments) in the late 1990s, which are not different from those reported for waters collected by Elbaz-Poulichet et al. (1986) in the same area in the mid-1980s. Lead in oysters from the Gironde estuary and the Marennes-Oléron basin (Atlantic Coast) is suggested to derive largely from local industries, e.g. mining and smelting operations (closed in 1987; Audry et al., 2004). A shift in the Pb isotopic composition toward the radiogenic natural endmember (pre-industrial river sediments; Elbaz-Poulichet et al., 1986) is observed between the mid-1980s and 2004/5 for samples from both the Gironde estuary and the Marennes-Oléron basin (Fig. 4.10). However, insignificant change is observed in the Pb concentrations of the bivalve tissues over the same time (Table 4.5). This shift is consistent with increasing contributions from a natural endmember and results from the banning of Pb addition to gasoline in France (Grousset et al., 1994). This is in contrast to the insignificant change observed in the Cd and Zn isotopic compositions of bivalve tissues over that time (see sections 4.4.3.1 and 4.4.3.2), which indicate the dominant Cd and Zn sources to those oysters have not changed. This striking difference between the reaction rates to environmental changes of Pb versus Cd and Zn isotopic signatures is a strong argument for the combined use of these isotope systems to trace the sources, fate and behavior of these metals in the environment.

For French Mediterranean collection sites (coastal lagoons/semi-enclosed basin) the Pb concentration increases as the Pb isotopic compositions become less radiogenic (Table 4.5; Fig. 4.10). This trend indicates increasing relative contributions from

anthropogenic Pb sources and decreasing contributions from natural Pb sources (e.g., pre-industrial sediments; Sun, 1980). Mussels from the coastal lagoon, Etang du Prévost, have the highest Pb concentrations and least radiogenic Pb signatures of these sites, indicating the largest anthropogenic input, likely resulting from metal pollution associated with harbor operations accumulating due to the enclosed nature of the site. These results are consistent with the Pb isotopic compositions for recent and ancient shells (the latter being relatively radiogenic) of Mediterranean mussels (Labonne et al., 1998).

4.5 Conclusions

Our investigation of Cd, Zn and Pb isotopic signatures in oysters and mussels from the western coast of Canada, the USA and France resulted in the following conclusions:

(1) High Cd levels in B.C. oysters are largely attributed to the natural upwelling of nutrient (and Cd) rich deep waters in the North Pacific as the Cd isotopic composition of B.C. oysters falls within the light end of those reported for North Pacific seawater. Variability in the Cd isotopic compositions of B.C. oysters is attributed to variable Cd contributions from anthropogenic emission sources (e.g., smelting). We suggest limiting consumption of B.C. oysters to ensure dietary Cd remains within safe limits. The Zn isotopic compositions of B.C. oysters fall within a narrow range of those reported for North Pacific seawater, indicating a primarily natural Zn source.
(2) For B.C. oysters, Pb isotopic signatures identify unleaded gasoline and diesel fuel as the primary Pb sources, despite low Pb concentrations (lowest of the study). The Pb isotopic composition of the oyster from Hawaii falls within the range of those of B.C. oysters (despite its much higher Pb concentration) suggesting a common Pb source for the North Pacific. Pb isotopic signatures of B.C. mainland oysters reveal, in comparison to those of the west coast of Vancouver Island and Hawaii, additional contributions from a characteristically unradiogenic source such as Pb emissions from B.C. smelting and refining operations.

(3) The Cd isotopic compositions of the USA East Coast bivalves include some of the lightest compositions ever measured, and reflect significant anthropogenic Cd inputs (e.g., primary/secondary smelting or steelmaking).

(4) Lead isotopic signatures of USA East Coast bivalves are consistent with those of US coals and industrial Pb emission sources (e.g., primary/secondary smelting or steelmaking).

(5) Significant variation in Cd concentrations, as well as $\delta^{114/110}$Cd values, exists between coastal sites of France, from relatively pristine (relatively heavy $\delta^{114/110}$Cd; e.g., Oye Plage) to heavily polluted (relatively light $\delta^{114/110}$Cd; e.g., Marennes-Oléron basin and Gironde estuary). For the smelting polluted sites in the Marennes-Oléron basin and the Gironde estuary, decreases in the Cd concentrations between 1984/7 and 2004/5 are not accompanied by a shift toward natural isotopic compositions suggesting the dominant Cd source remains historical smelting activities. The Zn isotopic composition of French bivalves falls within a narrow range of that of seawater and plankton tows, with the exception of the oysters from the smelting polluted Gironde estuary, which exhibit characteristically heavy Zn isotopic compositions.

(6) The Pb isotopic compositions of French bivalves are consistent with industrial as oppose to automotive Pb sources. Shifts are observed in the Pb isotopic compositions of French bivalves between 1984/7 and 2004/5 related to the complete phase-out of leaded gasoline in automobiles in France.

(7) The results of this study demonstrate the effective use of Cd isotopes, and to a lesser extent Zn isotopes, to trace industrial emissions of these metals in the environment. The combined use of Cd and Pb isotopes allows the assessment of Cd isotopic fractionation and tracing (fingerprinting) of the source.

4.6 Acknowledgements

We especially want to thank George M. Kruzynski (Fisheries and Oceans Canada) and William Heath (B.C. Ministry of Agriculture & Lands) for providing the B.C. oyster samples and are grateful to them for numerous valuable discussions. We thank Didier Claisse and Daniel Cossa at IFREMER and Gunnar Lauenstein at NOAA for providing

the bivalve samples for France and the USA, respectively. We want to especially thank Daniel Cossa for providing helpful comments and suggestions. We are grateful to Jane Barling for her assistance with the Nu Plasma MC-ICP-MS and to Bert Mueller for his assistance with the ELEMENT2 HR-ICP-MS. This study was funded by NSERC Discovery grants to Dominique Weis and Kristin J. Orians.

Table 4.1. Estimated Pb emissions from the consumption of petroleum products and coal in B.C. (2008) and all of Canada (1970 and 2008).

Fuel	B.C. 2008	Canada 2008	Canada 1970	Pb fraction emitted	B.C. 2008	Canada 2008	Canada 1970	B.C. 2008	Canada 2008	Canada 1970
Petroleum product[a,b]	**Fuel Pb (kg)**				**Pb emissions (kg)**			**Pb emissions , % of total**		
Avgas[c,d]	6480	53760		0.75-1.00[e]	4860	40320		67.57	58.89	
Leaded gasoline[d,f]	312	668	11585620	0.75-1.00[e]	234	501	8689215	3.25	0.73	99.87
Unleaded gasoline										
Premium[g]	333	2618		0.75-1.00[e]	250	1963		3.47	2.87	
Mid-grade[g]	74	376		0.75-1.00[e]	56	282		0.77	0.41	
Regular[g]	395	3766		0.75-1.00[e]	296	2824		4.12	4.12	
Diesel fuel oil[h]	1232	9322	2772	0.95[i]	1170	8856	2634	16.27	12.93	0.03
Heavy fuel oil[j]	4041	25586	44672	0.045[k]	182	1151	2010	2.53	1.68	0.02
Light fuel oil[l]	3	152	448	NA[m]						
Jet fuel[n]	11	45	14	0.75-1.00[e]	8	33	11	0.12	0.05	<0.01
Coal[b,o,p]										
	7194	660000	341836	0.019[q]	137	12540	6495	1.90	18.31	0.07
TOTAL	**20075**	**756291**	**11975362**		**7192**	**68471**	**8700364**			

[a]Consumption of petroleum products in B.C. and Canada in 2008; Statistics Canada, 2010.

[b]Consumption of petroleum products and coal in Canada in 1970; Quirin, 1999.

[c]Aviation gasoline [Pb], 100 low lead (100LL); ConocoPhillips, 2007.

[d]Leaded gasoline for 1970 inlcudes both motor vehicle and aircraft consumption; reference[b].

[e]Fraction Pb emitted for both motor and aviation gasolines assumed to be between the historically used, US EPA esimate of 0.75 and 1. The same fraction is assumed for jet fuel. In the following columns, 0.75 is used to calculate Pb emissions.

[f]Median [Pb] of range used to calculate values in the following columns; Quickert et al., 1972; Jungers et al., 1975; Parekh et al., 2002.

[g]Mid-grade value assumed to be the average of the Pb concentrations given for premium and regular gasolines; Sanders, 1998.

[h]Average [Pb] of diesel samples used to calculate values in the following columns; Reyes and Campos, 2005.

[i]Fraction Pb emitted for diesel calculated from Pb consumption rate and emission rate for diesel engines; Wang et al., 2003.

[j]Low sulfur fuel [Pb] used to calculate values in the following columns; Miller et al., 1996.

[k]Fraction Pb emitted for heavy fuel oil calculated from emission rate of 0.182 kg Pb/million L fuel consumed (1.5×10^{-3} lb/1000 US gallon fuel consumed); US EPA, 1998.

[l][Pb] from Miller et al., 1996.

[m]Fraction Pb emitted not available for light fuel oil; Pb emissions are not calculated due to uncertainty. Small relative contributions are expected.

[n]Median [Pb] of range used to calculate values in the following columns; Shumway, 2000, in Murphy et al., 2007.

[o]Coal consumption is given for 2007, 2008 data is unavailable; no significant change is expected for 2008; Stone, 2009.

[p]Average [Pb] for North American coals (143 samples); Chow and Earl, 1972.

[q]Fraction Pb emitted for coal calculated from emission factor of 0.21 mg Pb/1 kg coal feed (2.1 x 10-4 kg Pb/1 Mg coal feed); US EPA, 1998.

Table 4.2. Estimated Pb emissions from the consumption of petroleum products and coal in Canada, the USA and France (2005).

Fuel	Canada 2005	USA 2005	France 2005	Pb fraction emitted	Canada 2005	USA 2005	France 2005	Canada 2005	USA 2005	France 2005
Petroleum product[a]	**Fuel Pb (kg)**				**Pb emissions (kg)**			**Pb emissions , % of total**		
Avgas[b]	52500	805833	18333	0.75-1.00[c]	39375	604375	13750	56.58	62.01	34.68
Motor gasoline[d]	7328	95673	2619	0.75-1.00[c]	5496	71755	1964	7.90	7.36	4.95
Diesel fuel oil[e]	10395	78860	19151	0.95[f]	9875	74917	18194	14.19	7.69	45.89
Heavy fuel oil[g]	37416	213546	27420	0.045[h]	1684	9610	1234	2.42	0.99	3.11
Jet fuel[i]	45	633	54	0.75-1.00[c]	34	475	40	0.05	0.05	0.10
Coal[a,J]										
	690646	11236170	234938	0.019[k]	13122	213487	4464	18.86	21.90	11.26
TOTAL	**798330**	**12430715**	**302515**		**69586**	**974618**	**39646**			

[a]US EIA, 2008.

[b]Aviation gasoline [Pb], 100 low lead (100LL); ConocoPhillips, 2007.

[c]Fraction Pb emitted for both motor and aviation gasolines assumed to be between the historically used, US EPA esimate of 0.75 and 1. The same fraction is assumed for jet fuel. In the following columns, 0.75 is used to calculate Pb emissions .

[d]Calculated motor gasoline [Pb] calculated based on those of premium and regular gasolines and the estimated relative consumption of each; Sanders, 1998.

[e]Average [Pb] of diesel samples used to calculate values in the following columns; Reyes and Campos, 2005.

[f]Fraction Pb emitted for diesel calculated from Pb consumption rate and emission rate for diesel engines; Wang et al., 2003.

[g]Low sulfur fuel [Pb] used to calculate values in the following columns; Miller et al., 1996.

[h]Fraction Pb emitted for heavy fuel oil calculated from emission rate of 0.182 kg Pb/million L fuel consumed (1.5×10^{-3} lb/1000 US gallon fuel consumed); US EPA, 1998.

[i]Median [Pb] of range used to calculate values in the following columns; Shumway, 2000, in Murphy et al., 2007.

[j]Average [Pb] for North American coals (143 samples); Chow and Earl, 1972.

[k]Fraction Pb emitted for coal calculated from emission factor of 0.21 mg Pb/1 kg coal feed (2.1 x 10-4 kg Pb/1 Mg coal feed); US EPA, 1998.

Table 4.3. Cadmium concentrations (μg g^{-1} dry weight) and isotopic compositions of bivalve tissues.

Sample collection site[a], year		Bivalve species	[Cd]	$\delta^{111}Cd/^{110}Cd$[b]	$\delta^{112}Cd/^{110}Cd$[b]	$\delta^{113}Cd/^{110}Cd$[b]	$\delta^{114}Cd/^{110}Cd$[b]	n[c]
Western Canada [d]								
Desolation Sound, B.C.								
Gorge Harbor	2004	*C. gigas*	7.3	-0.17 ± 0.03	-0.36 ± 0.01	-0.51 ± 0.03	-0.69 ± 0.01	2
Redonda Bay	2004	*C. gigas*	4.6	-0.14 ± 0.03	-0.28 ± 0.07	-0.42 ± 0.12	-0.55 ± 0.14	3
Redonda Bay*	2004	*C. gigas*	78	-0.17 ± 0.08	-0.35 ± 0.07	-0.43 ± 0.24	-0.64 ± 0.28	3
Teakerne Arm	2004	*C. gigas*	13	-0.17 ± 0.06	-0.32 ± 0.11	-0.47 ± 0.05	-0.64 ± 0.20	3
Thor's Cove	2002	*C. gigas*	5.5	-0.09 ± 0.03	-0.17 ± 0.11	-0.24 ± 0.19	-0.34 ± 0.25	3
Trevenen Bay	2004	*C. gigas*	11	-0.11 ± 0.07	-0.21 ± 0.07	-0.28 ± 0.19	-0.38 ± 0.14	3
Barkley Sound, B.C.								
Effingham Inlet	2004	*C. gigas*	2.9	-0.08 ± 0.04	-0.15 ± 0.04	-0.21 ± 0.14	-0.29 ± 0.15	3
Effingham Inlet*	2004	*C. gigas*	39	-0.07 ± 0.09	-0.13 ± 0.10	-0.25 ± 0.09	-0.26 ± 0.07	3
Fatty Basin	2004	*C. gigas*	6.5	-0.11 ± 0.07	-0.17 ± 0.11	-0.24 ± 0.18	-0.33 ± 0.13	3
Poett Nook	2004	*C. gigas*	6.0	-0.11 ± 0.11	-0.20 ± 0.10	-0.30 ± 0.19	-0.37 ± 0.18	3
Poett Nook*	2004	*C. gigas*	40	-0.14 ± 0.12	-0.26 ± 0.23	-0.40 ± 0.34	-0.52 ± 0.41	3
Seddall Island	2004	*C. gigas*	5.2	-0.05 ± 0.06	-0.06 ± 0.12	-0.10 ± 0.18	-0.09 ± 0.23	4
France [e]								
English Channel								
Oye plage, Dunkerque-Calais	2004	*M. edulis*	0.48	-0.09 ± 0.13	-0.10 ± 0.16	-0.21 ± 0.25	-0.20 ± 0.22	3
Ambleuteuse-Boulogne	2004	*M. edulis*	0.57	-0.15 ± 0.07	-0.28 ± 0.16	-0.34 ± 0.31	-0.49 ± 0.36	3
Cap de la Hève, Seine estuary	2004	*M. edulis*	2.2	-0.22 ± 0.08	-0.44 ± 0.11	-0.68 ± 0.16	-0.88 ± 0.23	3
Aber Benoît, North Brittany[f]	2005	*C. gigas*	1.4	-0.15 ± 0.11	-0.29 ± 0.17	-0.49 ± 0.06	-0.63 ± 0.14	2
Aber Benoît, North Brittany dup.[f,g]	2005	*C. gigas*	1.4	-0.14 ± 0.10	-0.25 ± 0.19	-0.42 ± 0.18	-0.52 ± 0.31	3
Atlantic Ocean								
Pointe de Chemoulin, Loire estuary	2004	*M. edulis*	1.8	-0.15 ± 0.05	-0.31 ± 0.06	-0.47 ± 0.21	-0.62 ± 0.20	3
Boyardville, Marennes-Oléron basin[h]	1984	*C. gigas*	12	-0.13 ± 0.07	-0.33 ± 0.21	-0.51 ± 0.24	-0.63 ± 0.35	3
Boyardville, Marennes-Oléron basin[h]	1984	*M. edulis*	1.9	-0.20 ± 0.10	-0.36 ± 0.14	-0.62 ± 0.23	-0.72 ± 0.21	3
La Mouclière, Marennes-Oléron basin	2004	*M. edulis*	1.1	-0.22 ± 0.06	-0.45 ± 0.08	-0.70 ± 0.04	-0.92 ± 0.07	3
Les Palles, Marennes-Oléron basin	2004	*C. gigas*	2.8	-0.28 ± 0.05	-0.55 ± 0.05	-0.81 ± 0.12	-1.08 ± 0.09	3
La Fosse, Gironde estuary[f]	1987	*C. gigas*	129	-0.27 ± 0.06	-0.51 ± 0.02	-0.74 ± 0.13	-0.99 ± 0.12	4
La Fosse, Gironde estuary dup.[f,g]	1987	*C. gigas*	129	-0.27 ± 0.04	-0.52 ± 0.13	-0.81 ± 0.31	-1.06 ± 0.30	3
La Fosse, Gironde estuary[f]	2005	*C. gigas*	29	-0.26 ± 0.04	-0.52 ± 0.05	-0.79 ± 0.12	-1.03 ± 0.17	5
Mediterranean Sea								
Etang de Bages, Roussillon[f]	2005	*M. galloprovincialis*	5.7	-0.14 ± 0.08	-0.25 ± 0.05	-0.40 ± 0.04	-0.51 ± 0.11	5
Etang de Bages, Roussillon dup.[f,g]	2005	*M. galloprovincialis*	5.7	-0.13 ± 0.13	-0.26 ± 0.14	-0.41 ± 0.07	-0.51 ± 0.20	3
Etang du Prévost, Thau[f]	2005	*M. galloprovincialis*	0.37	-0.09	-0.17	-0.19	-0.27	1
USA [e]								
Atlantic Ocean								
Kennebunkport, Cape Arundel, ME	2005	*M. edulis*	1.5	-0.15 ± 0.08	-0.30 ± 0.15	-0.40 ± 0.15	-0.54 ± 0.21	2
Arnolds Point Shoal, Delaware Bay, NJ	2005	*C. virginica*	12	-0.19 ± 0.05	-0.41 ± 0.13	-0.63 ± 0.24	-0.81 ± 0.32	3
ırnolds Point Shoal, Delaware Bay, NJ dup.[g]	2005	*C. virginica*	12	-0.22 ± 0.09	-0.45 ± 0.16	-0.67 ± 0.30	-0.91 ± 0.36	3
Bodkin Point, Chesapeake Bay, MD	2005	*C. virginica*	16	-0.19 ± 0.07	-0.37 ± 0.11	-0.55 ± 0.23	-0.74 ± 0.26	4
Choptank River, Chesapeake Bay, MD	2005	*C. virginica*	4.6	-0.13 ± 0.05	-0.29 ± 0.04	-0.41 ± 0.05	-0.56 ± 0.10	2
Fort Johnson, Charleston Harbor, SC	2006	*C. virginica*	2.1	-0.33 ± 0.04	-0.60 ± 0.05	-0.87 ± 0.21	-1.20 ± 0.27	2
Shutes Folly Island, Charleston Harbor, SC	2006	*C. virginica*	4.2	-0.29	-0.56	-0.82	-1.05	1
Dog River, Mobile Bay, AL	2006	*C. virginica*	3.9	-0.18 ± 0.06	-0.41 ± 0.11	-0.62 ± 0.09	-0.78 ± 0.19	3
Pacific Ocean								
Keehi Lagoon, Honolulu Harbor, HI	2004	*O. sandvicensis*	1.0	-0.13 ± 0.10	-0.25 ± 0.10	-0.36 ± 0.18	-0.46 ± 0.12	3

[a]Sample collection sites labelled to be consistent with those assigned by the NS&T (NOAA, USA) and the RNO (IFREMER, France), where appropriate.
[b]Ratios are reported permil (‰) as the mean ± 2 standard deviation (SD).
[c]n refers to the number of replicate isotopic measurements.
[d]B.C. oyster samples are soft tissues of individuals, exclusive of the gut contents, except where guts are indicated (*) and these samples include only the gut and its contents.
[e]Bivalve samples from France and the USA are pooled samples rather than individuals (see Section 4.2.2).
[f][Cd] provided by the RNO (IFREMER).
[g]dup. refers to a full procedual duplicate, inclusive of the analytical separation and isotopic analysis.

Table 4.4. Zinc concentrations (µg g^{-1} dry weight) and isotopic compositions of bivalve tissues.

Sample collection site[a], year		Bivalve species	[Zn]	$\delta^{66}Zn/^{64}Zn$[b]	$\delta^{67}Zn/^{64}Zn$[b]	$\delta^{68}Zn/^{64}Zn$[b]	n[c]
Western Canada [d]							
Desolation Sound, B.C.							
Thor's Cove	2002	*C. gigas*	390	0.28 ± 0.05	0.45 ± 0.16	0.59 ± 0.17	2
Barkley Sound, B.C.							
Fatty Basin	2004	*C. gigas*	439	0.36 ± 0.13	0.55 ± 0.22	0.74 ± 0.26	5
Seddall Island	2004	*C. gigas*	490	0.30 ± 0.15	0.47 ± 0.14	0.62 ± 0.29	3
France [e,f]							
English Channel							
Aber Benoît, North Brittany	2005	*C. gigas*	1320	0.39 ± 0.04	0.60 ± 0.07	0.78 ± 0.07	3
Atlantic Ocean							
La Fosse, Gironde estuary	1987	*C. gigas*	8350	1.15 ± 0.10	1.73 ± 0.12	2.27 ± 0.12	3
La Fosse, Gironde estuary	2005	*C. gigas*	3570	1.03 ± 0.04	1.54 ± 0.08	2.05 ± 0.08	3
Mediterranean Sea							
Etang de Bages, Roussillon	2005	*M. galloprovincialis*	90.0	0.43 ± 0.06	0.62 ± 0.10	0.85 ± 0.07	4
Etang du Prévost, Thau	2005	*M. galloprovincialis*	116	0.46 ± 0.07	0.69 ± 0.16	0.91 ± 0.13	3

[a]Sample collection sites are labelled to be consistent with those assigned by the RNO (IFREMER, France), where appropriate.
[b]Ratios are reported permil (‰) as the mean ± 2 standard deviation (SD).
[c]n refers to the number of replicate isotopic measurements.
[d]B.C. oyster samples are soft tissues of individuals, exclusive of the gut content.
[e]Bivalve samples from France are pooled samples rather than individuals (see Section 4.2.2).

Table 4.5. Lead concentrations (μg g^{-1} dry weight) and isotopic compositions of bivalve tissues.

Sample collection site[a], year		Bivalve species	[Pb]	$^{206}Pb/^{204}Pb$	2SE[b,c]	$^{207}Pb/^{204}Pb$	2SE[b,c]	$^{208}Pb/^{204}Pb$	2SE[b,c]	$^{206}Pb/^{207}Pb$	2SE[b,c]	$^{208}Pb/^{206}Pb$	2SE[b,c]
Western Canada [d]													
Desolation Sound, B.C.													
Gorge Harbor	2004	*C. gigas*	0.13	17.8791	7	15.5702	6	37.625	3	1.14832	2	2.10447	3
Redonda Bay	2004	*C. gigas*	0.05	17.9159	12	15.5708	11	37.697	3	1.15061	2	2.10409	5
Teakerne Arm	2004	*C. gigas*	0.09	17.9232	9	15.5771	8	37.731	2	1.15059	2	2.10522	4
Barkley Sound, B.C.													
Effingham Inlet	2004	*C. gigas*	0.22	18.1930	13	15.5946	11	38.024	3	1.16659	2	2.09001	4
Fatty Basin	2004	*C. gigas*	0.11	18.2745	15	15.5965	12	38.070	3	1.17167	2	2.08312	6
Fatty Basin rep.[c]	2004	*C. gigas*	0.11	18.2707	15	15.5940	15	38.065	4	1.17165	3	2.08343	7
Poett Nook	2004	*C. gigas*	0.05	18.0245	12	15.5857	12	37.822	3	1.15649	2	2.09831	6
Poett Nook*	2004	*C. gigas*	0.10	18.0816	16	15.5857	15	37.875	4	1.16020	3	2.09465	6
Seddall Island	2003	*C. gigas*	0.16	18.0302	15	15.5842	18	37.787	3	1.15695	2	2.09567	5
Seddall Island*	2003	*C. gigas*	0.11	18.2433	23	15.5850	21	37.997	5	1.17059	4	2.08271	10
Seddall Island	2004	*C. gigas*	0.14	18.3149	9	15.5947	9	38.089	2	1.17442	2	2.07973	4
France [f]													
English Channel													
Oye plage, Dunkerque-Calais	2004	*M. edulis*	1.8	18.2015	10	15.6226	9	38.176	2	1.16508	1	2.09742	4
Oye plage, Dunkerque-Calais rep.[c]	2004	*M. edulis*	1.8	18.2009	9	15.6220	7	38.175	2	1.16509	2	2.09743	4
Ambleuteuse-Boulogne	2004	*M. edulis*	1.4	18.2225	11	15.6262	11	38.206	3	1.16615	2	2.09662	4
Cap de la Hève, Seine estuary	2004	*M. edulis*	5.7	18.1819	6	15.6271	7	38.194	2	1.16355	1	2.10053	3
Cap de la Hève, Seine estuary rep.[c]	2004	*M. edulis*	5.7	18.1837	6	15.6277	6	38.197	2	1.16358	1	2.10046	3
Aber Benoît, North Brittany[g]	2005	*C. gigas*	0.90	18.3787	9	15.6390	7	38.351	2	1.17518	1	2.08670	3
Aber Benoît, North Brittany dup.[g,h]	2005	*C. gigas*	0.90	18.3798	12	15.6378	12	38.350	3	1.17534	2	2.08657	4
Atlantic Ocean													
Pointe de Chemoulin, Loire estuary	2004	*M. edulis*	1.5	18.1476	8	15.6343	8	38.150	2	1.16076	1	2.10223	3
Boyardville, Marennes-Oléron basin	1984	*C. gigas*	2.0	18.4302	6	15.6536	5	38.828	1	1.17739	2	2.10673	3
Boyardville, Marennes-Oléron basin	1984	*M. edulis*	1.8	18.3860	6	15.6567	6	38.782	1	1.17433	1	2.10931	4
La Mouclière, Marennes-Oléron basin	2004	*M. edulis*	1.6	18.4534	7	15.6636	6	38.742	2	1.17810	1	2.09943	3
Les Palles, Marennes-Oléron basin	2004	*C. gigas*	1.2	18.4639	6	15.6571	6	38.729	2	1.17927	1	2.09758	3
La Fosse, Gironde estuary[g]	1987	*C. gigas*	3.4	18.3920	9	15.6556	9	38.478	3	1.17479	1	2.09209	4
La Fosse, Gironde estuary rep.[c,g]	1987	*C. gigas*	3.4	18.3917	10	15.6547	9	38.477	2	1.17485	2	2.09202	3
La Fosse, Gironde estuary dup.[g,h]	1987	*C. gigas*	3.4	18.3917	8	15.6536	7	38.474	2	1.17488	2	2.09190	4
La Fosse, Gironde estuary	2004	*C. gigas*	2.6	18.4855	7	15.6636	6	38.596	2	1.18019	1	2.08789	3
La Fosse, Gironde estuary[g]	2005	*C. gigas*	3.1	18.5035	12	15.6623	10	38.678	3	1.18134	2	2.09047	4
Mediterranean Sea													
Etang de Bages, Roussillon[g]	2005	*M. galloprovincialis*	0.40	18.4924	10	15.6630	9	38.488	2	1.18064	1	2.08130	4
Etang du Prévost, Thau[g]	2005	*M. galloprovincialis*	1.7	18.3733	6	15.6523	5	38.432	2	1.17385	1	2.09169	4
Etang du Prévost, Thau dup.[g,h]	2005	*M. galloprovincialis*	1.7	18.3716	12	15.6522	11	38.429	3	1.17374	1	2.09175	3
Anse de Carteau, Golfe de Fos	2004	*M. galloprovincialis*	1.1	18.4451	8	15.6580	6	38.446	2	1.17801	1	2.08435	3
USA [f]													
Atlantic Ocean													
Kennebunkport, Cape Arundel, ME	2005	*M. edulis*	2.0	18.8412	9	15.6585	6	38.574	2	1.20326	1	2.04734	3
Dover Point, Great Bay, NH	2005	*M. edulis*	2.2	18.8415	7	15.6629	6	38.594	2	1.20295	1	2.04838	3
Arnolds Point Shoal, Delaware Bay, NJ	2005	*C. virginica*	0.65	18.9200	16	15.6783	15	38.754	4	1.20675	2	2.04829	4
Bodkin Point, Chesapeake Bay, MD	2005	*C. virginica*	0.29	18.7752	11	15.6712	11	38.582	3	1.19810	2	2.05488	4
Choptank River, Chesapeake Bay, MD	2005	*C. virginica*	0.11	18.7642	11	15.6559	9	38.577	2	1.19854	2	2.05591	4
Cape Hatteras, Pamlico Sound, NC	2006	*C. virginica*	0.56	18.9586	7	15.6713	7	38.867	2	1.20976	1	2.05031	3
Fort Johnson, Charleston Harbor, SC	2006	*C. virginica*	0.75	18.4078	8	15.6066	8	38.155	2	1.17949	2	2.07269	4
Shutes Folly Island, Charleston Harbor, SC	2006	*C. virginica*	0.72	18.5151	11	15.6140	11	38.284	3	1.18580	1	2.06773	3
Dog River, Mobile Bay, AL	2006	*C. virginica*	0.27	19.0807	12	15.6681	9	38.842	2	1.21783	2	2.03564	4
Pacific Ocean													
Keehi Lagoon, Honolulu Harbor, HI	2004	*O. sandvicensis*	5.7	18.1721	8	15.5959	7	37.933	2	1.16521	1	2.08734	3

[a]Sample collection sites labelled to be consitent with those assigned by the NS&T (NOAA, USA) and the RNO (IFREMER, France), where appropriate.
[b]Ratios are reported as the mean ± 2 standard error (SE). Reported error values are the ten-thousandth ($^{206}Pb/^{204}Pb$, $^{207}Pb/^{204}Pb$), thousandth ($^{208}Pb/^{204}Pb$) or hundred-thousandth ($^{206}Pb/^{207}Pb$, $^{208}Pb/^{206}Pb$) decimal digit.
[c]All data have been normalized to the NIST SRM 981 triple spike Pb ratios of Galer and Abouchami, 1998.
[d]B.C. oyster samples are soft tissues of individuals, exclusive of the gut contents, except where guts are indicated (*) and these samples include only the gut and its contents.
[e]rep. refers to a replicate analysis of the Pb sample solution.
[f]Bivalve samples from France and the USA are pooled samples rather than individuals (see Section 4.2.2).
[g][Pb] provided by the RNO (IFREMER).

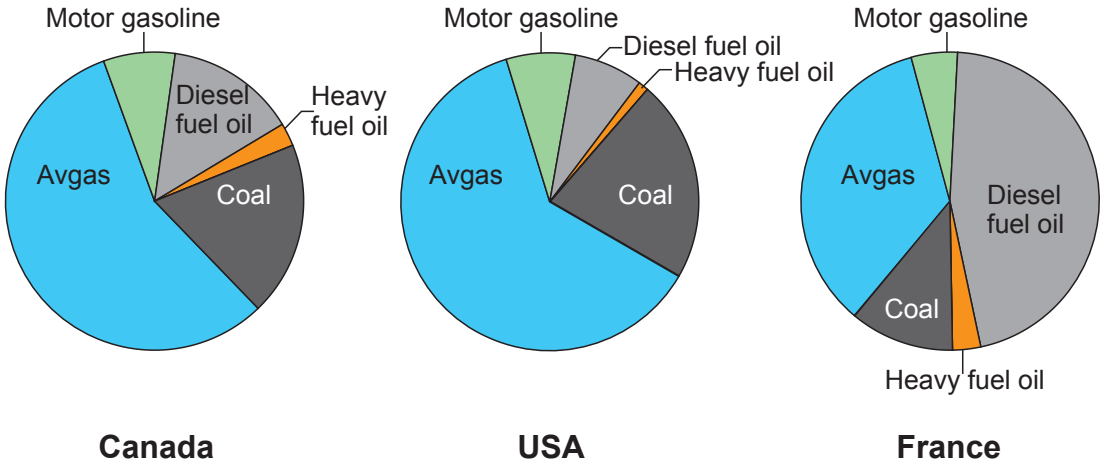

Fig. 4.1. Pie charts of the relative Pb emission contributions from petroleum products and coal consumption in Canada, the USA and France in 2005. Table 4.2 includes the references for data used to calculate these contributions.

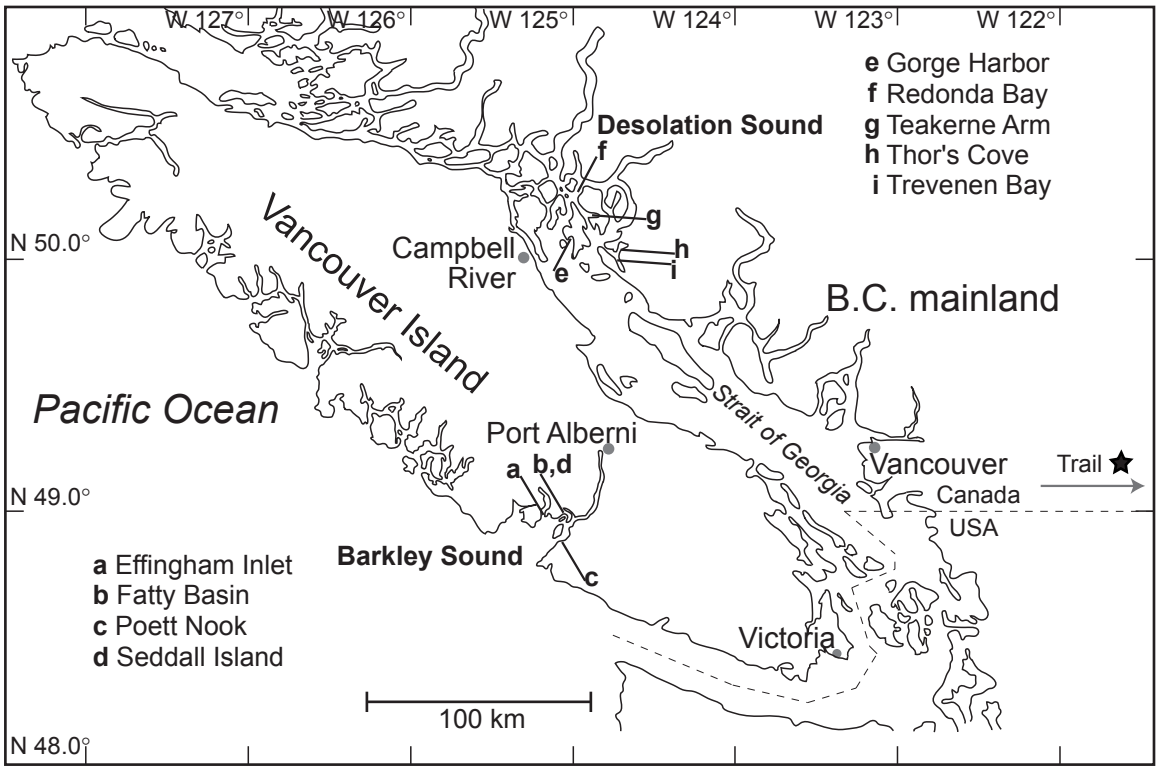

Fig. 4.2. Map of SW British Columbia showing the locations of sampling sites. The integrated Zn and Pb smelting and refining complex (black star) in Trail is located ~400 km from Vancouver.

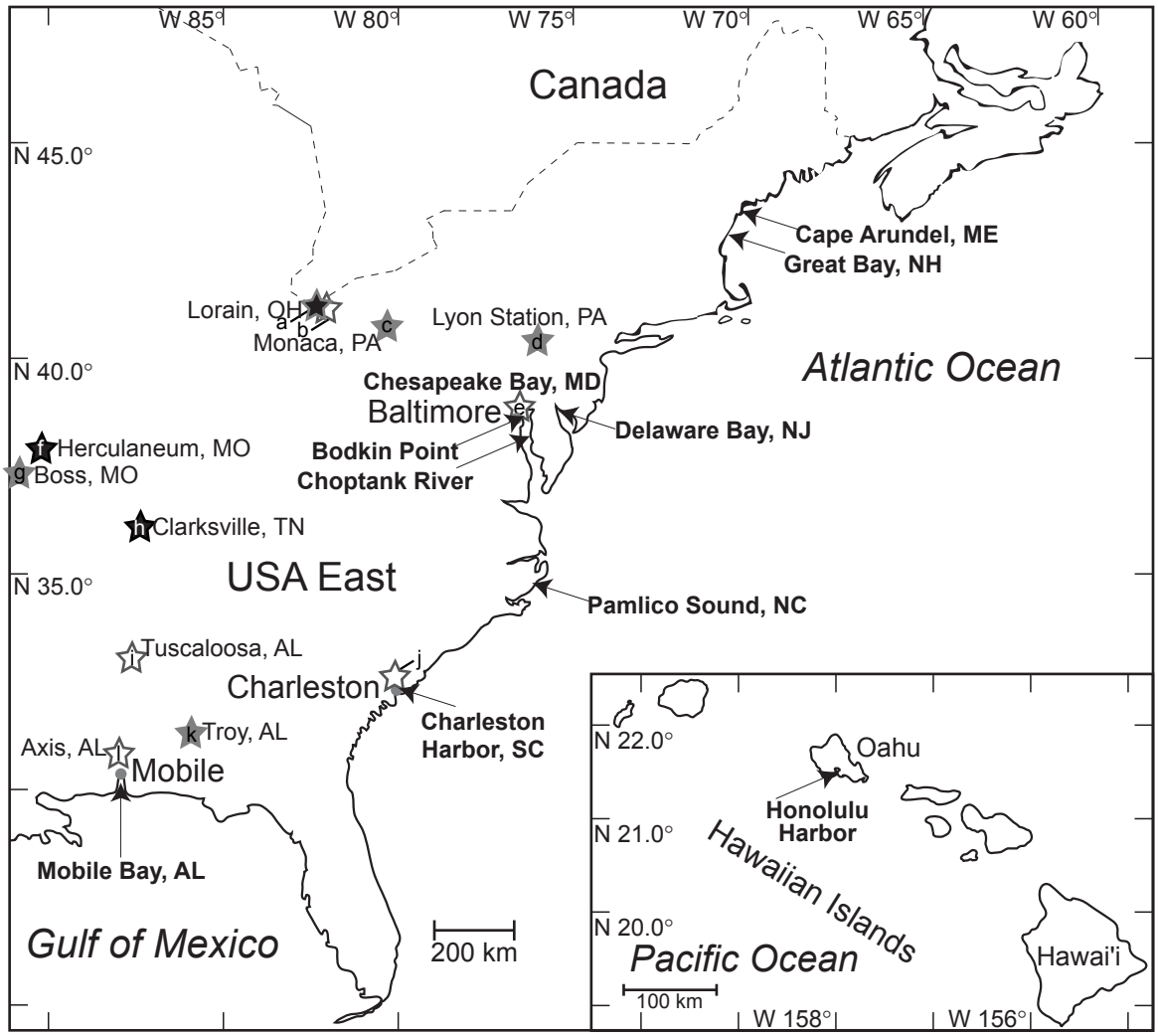

Fig. 4.3. Map of the USA East Coast and Hawaii (inset) showing the locations of sampling sites. Facilities (not comprehensive) reporting emissions which are relevant in the discussion of Cd and Pb sources to the bivalve samples are indicated by stars; a and b: Lorain, OH; c: Monaca, PA; d: Lyon Station, PA; e: Baltimore, MD; f: Herculaneum, MO; g: Boss, MO; h: Clarksville, TN; i: Tuscaloosa, AL; j: Charleston, SC; k: Troy, AL; l: Axis, AL. Black star: primary smelting of non-ferrous metals; black star, grey border: copper foundry; white star: iron and steel mill; grey star: secondary smelter.

Fig. 4.4. Map of France showing the locations of sampling sites. The sites along the French Mediterranean coast are unique in that they are coastal lagoons (Etang de Bages and Etang du Prévost) and a semi-enclosed basin (Anse de Carteau). Note the Marennes-Oléron basin and Anse de Carteau are sites of major oyster and mussel production, respectively. Facilities of significance in the discussion are shown here. Black star: smelting and refining of Pb and Zn near Noyelles-Godault and of Zn near Decazeville (both now closed); white star: iron and steel mill near Dunkerque; grey star: Cd pigment plant near Narbonne (now closed).

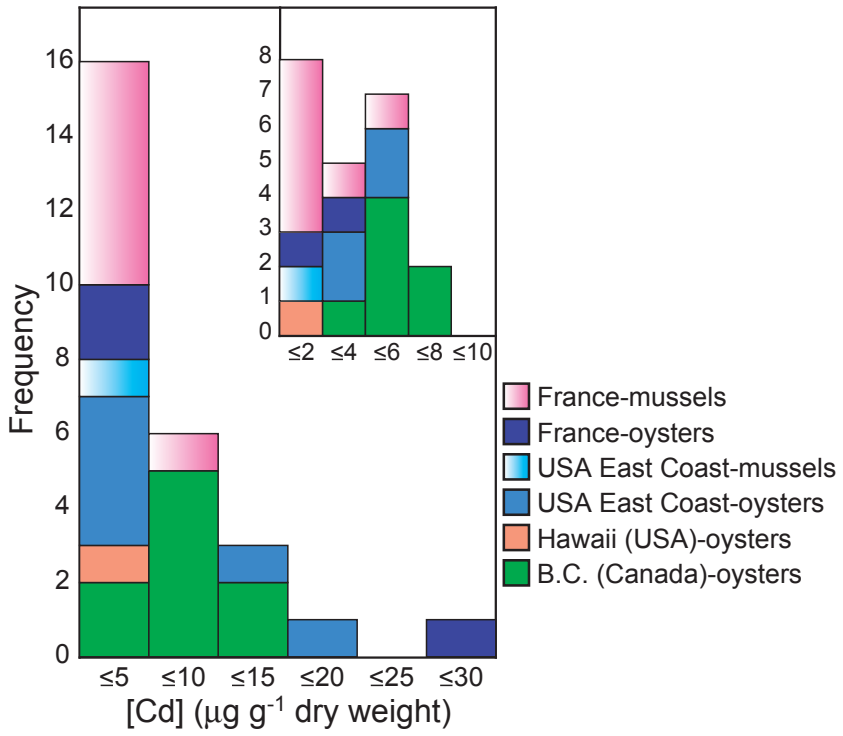

Fig. 4.5. Histogram of the Cd concentrations of oyster and mussel soft tissue samples collected between 2002 and 2006. Oyster (solid color) and mussel (color gradient) samples are differentiated, as significant differences in Cd accumulation exist between the two species in polluted environments (Boutier et al., 1989). Unlike the bivalve samples from the USA and France, the B.C. oyster samples do not include gut contents. Due to the high relative Cd concentration of gut contents, B.C. whole oysters (inclusive of the gut) will have somewhat higher Cd concentrations than those shown here. B.C. whole oyster Cd concentrations are reported to range from 3.78 to 22.1 µg g^{-1} dry weight for oyster farming areas (Bendell and Feng, 2009). The data is also given in Table 4.3.

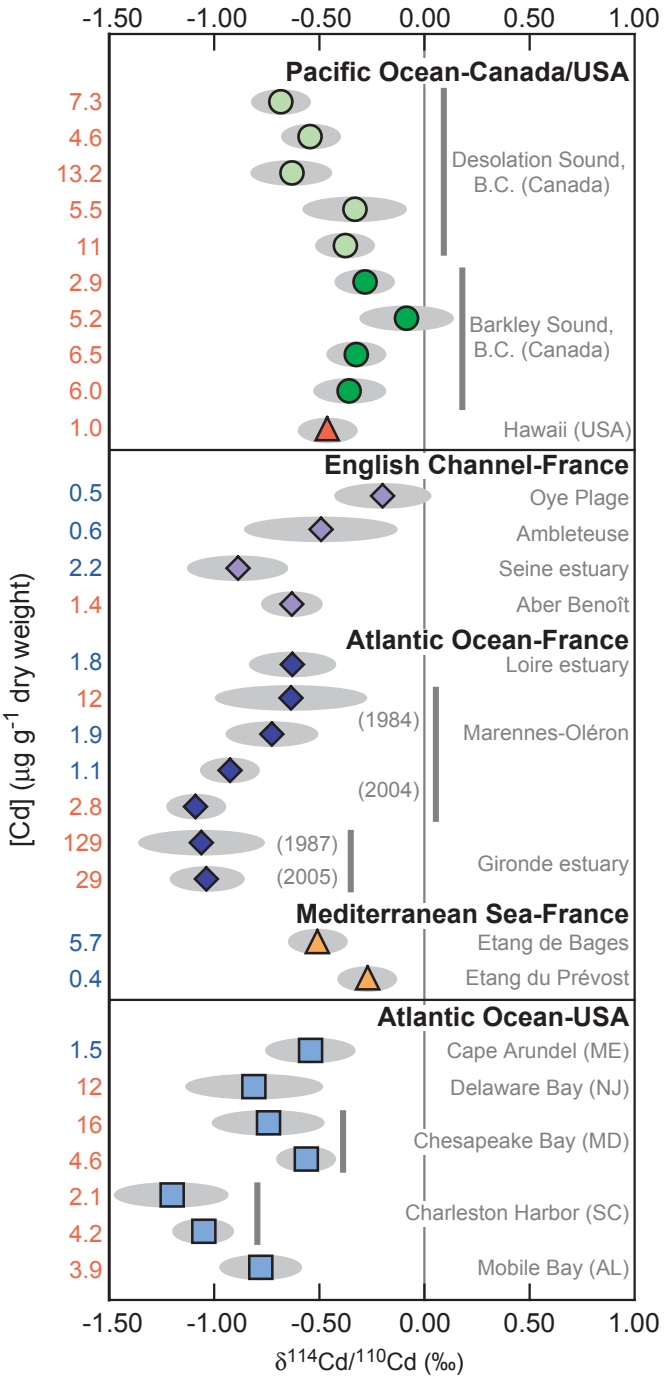

Fig. 4.6. Plot of variations in the Cd isotopic composition of bivalve samples, inclusive of those from western Canada (B.C.), Hawaii, the USA East Coast and France. The grey ellipses denote 2 standard deviation on the mean Cd value, except when this value is less than the long-term reproducibility calculated for the in-house secondary standards (±0.14‰), and then the latter is used. Cadmium concentrations in bivalve tissues are given on the left in red (oysters) and blue (mussels). For the Marennes-Oléron, samples collected in 1984 are from Boyardville and in 2004 are from La Mouclière (top) and Les Palles (bottom). The data is also given in Table 4.3.

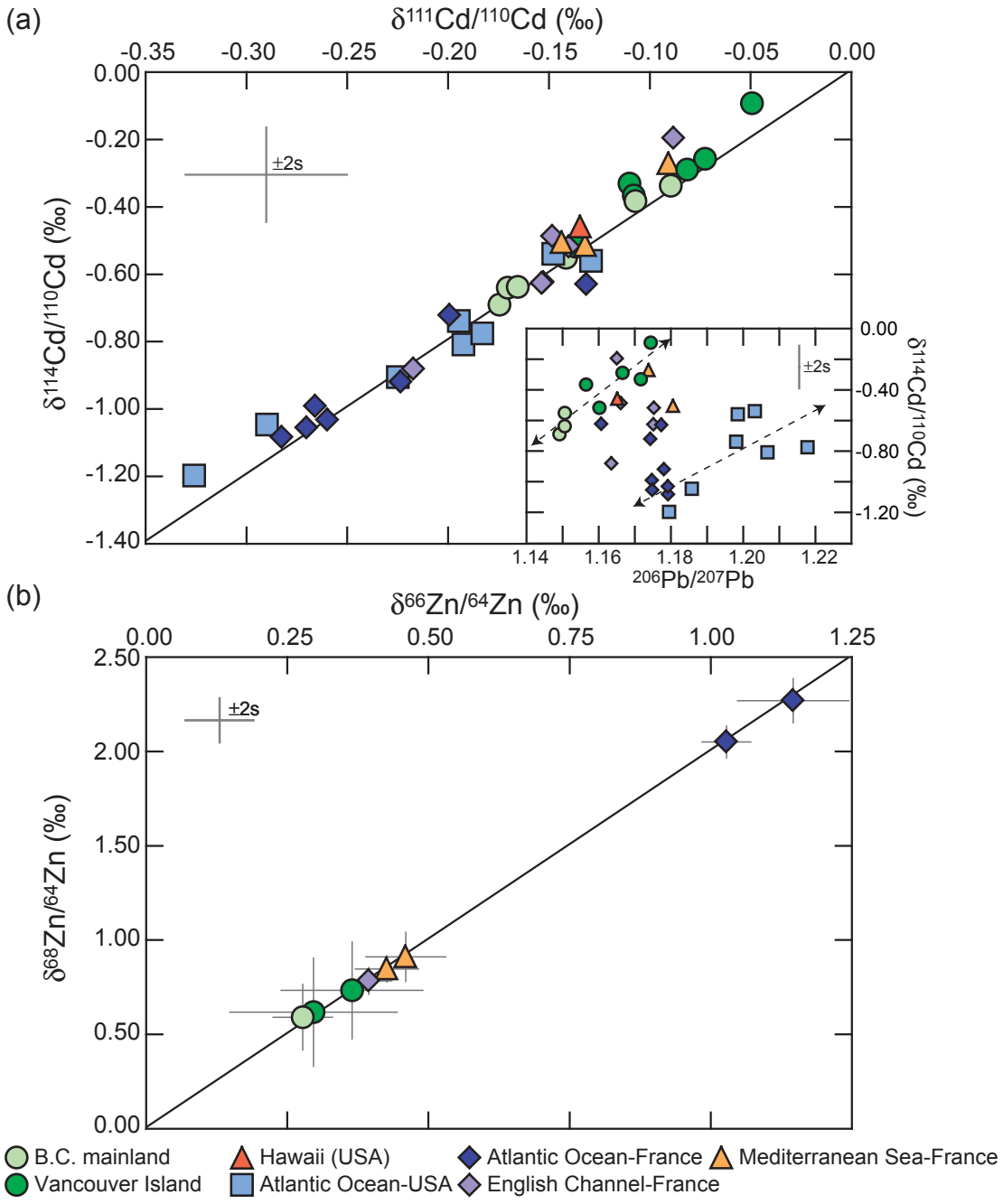

Fig. 4.7. Mass-dependent Cd and Zn isotopic fractionation for all bivalve samples: (a) $\delta^{114/110}$Cd vs. $\delta^{111/110}$Cd and (b) $\delta^{68/64}$Zn vs. $\delta^{66/64}$Zn. The calculated regression lines (for (a), r^2=0.9624; for (b), r^2=0.9995) are coherent with mass-dependent isotopic fractionation, indicating spectral interferences are insignificant. Inset in (a) shows $\delta^{114/110}$Cd vs. ^{206}Pb/^{207}Pb; best fit lines are shown for the B.C oysters and USA East Coast bivalves. The error on each sample is not shown in (a) for clarity; in (b), error bars denote 2 standard deviation (SD) on the mean δZn value for replicate analyses of each sample. The long-term reproducibility, calculated as the 2SD on the mean δCd and δZn values for the in-house secondary Cd and Zn isotopic standards (Shiel et al., 2009), is shown. For Pb, the error (2SE) is smaller than the symbol size. Note that in (a) for Aber Benoît (English Channel-France) and the Loire estuary (Atlantic Ocean-France), the values (-0.15‰, -0.63‰ and -0.15‰, -0.62‰, respectively) overlap.

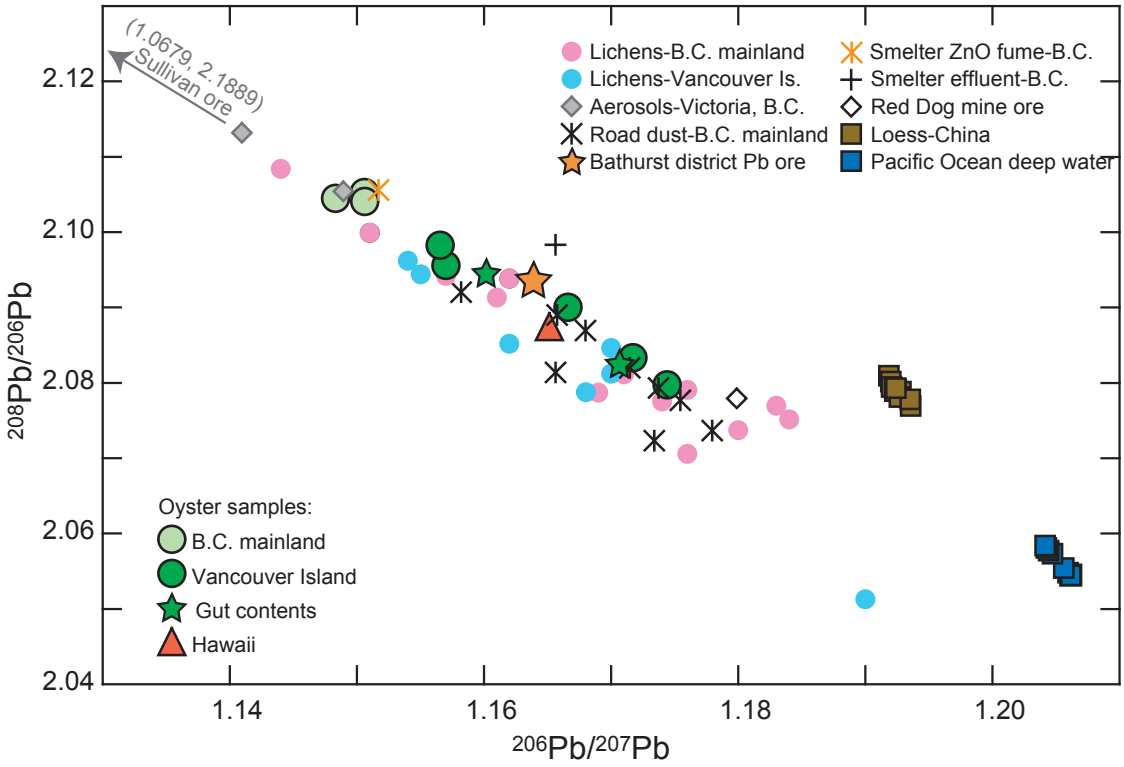

Fig. 4.8. Plot of $^{208}Pb/^{206}Pb$ vs. $^{206}Pb/^{207}Pb$ for the B.C. and Hawaiian oysters. These Pb isotope ratios are compared with those of B.C. lichens (representative of atmospheric Pb fall-out, collected in 1995-7; Simonetti et al., 2003); aerosols from Victoria (collected in 1998/9; Bollhöfer and Rosman, 2001); road dust from the lower B.C. mainland (Preciado et al., 2007); B.C. smelter ZnO fume and effluent (Shiel et al., 2010); Red Dog mine (AK) ore (Shiel et al., 2010); Bathurst district ore (representative of Canadian leaded gasoline) and Sullivan mine (B.C.) ore (Sangster et al., 2000, and references within); loess-China (Jones et al., 2000); Pacific Ocean deep water (ferromanganese crust from the N. Pacific Ocean, last 2 Ma years of time series shown; van de Flierdt et al., 2003). For this study, the error (2SE) is smaller than the symbol size.

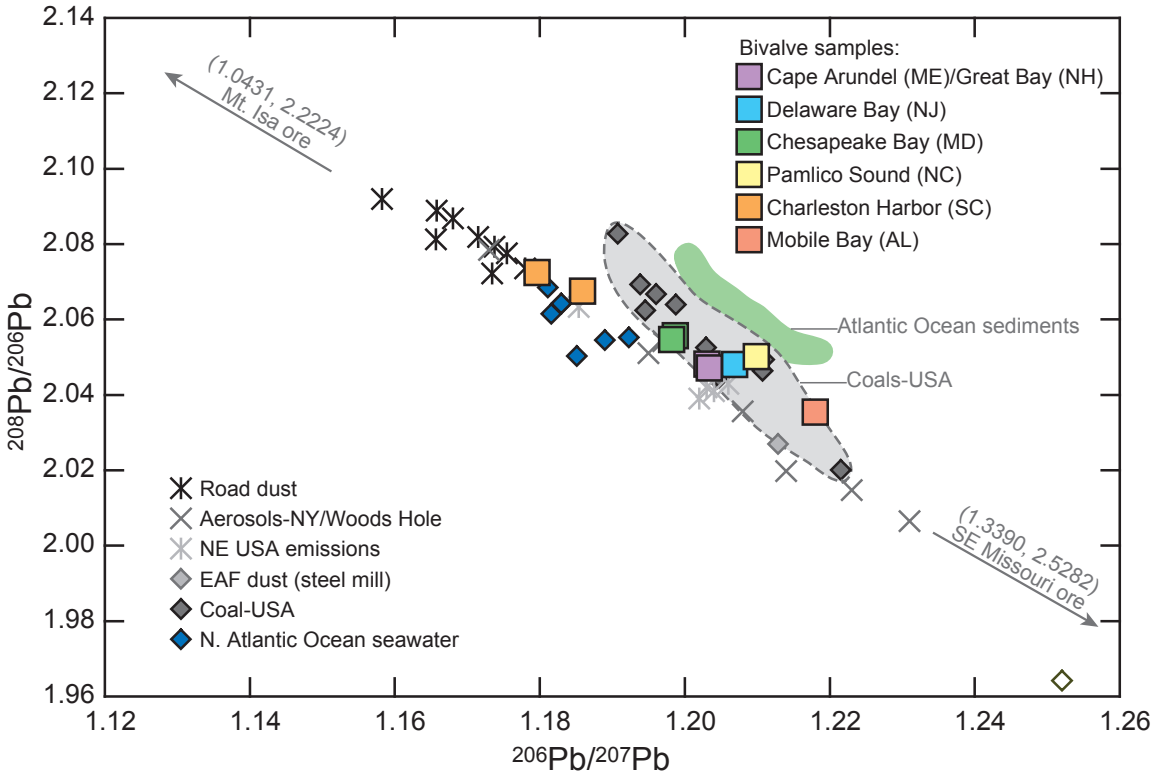

Fig. 4.9. Plot of $^{208}Pb/^{206}Pb$ vs. $^{206}Pb/^{207}Pb$ for the USA East Coast bivalves. The data are compared with the Pb isotope ratios of road dust from the lower B.C. mainland (collected in 2002/3; Preciado et al., 2007), aerosols from New York and Woods Hole (collected in 1997/8; Bollhöfer and Rosman, 2001), NE USA lichens (representative of atmospheric Pb fall-out, collected in 1994-6; Carignan et al., 2002), electric arc furnace (EAF) dust (steel mill; Ketterer et al., 2001), US coal samples (Díaz-Somoano et al., 2009), Mt. Isa and SE Missouri Pb ores (Sangster et al., 2000, and references within), N. Atlantic Ocean seawater (collected in 1988; Véron et al., 1994) and Atlantic Ocean sediments (Sun, 1980). For this study, the error (2SE) is smaller than the symbol size.

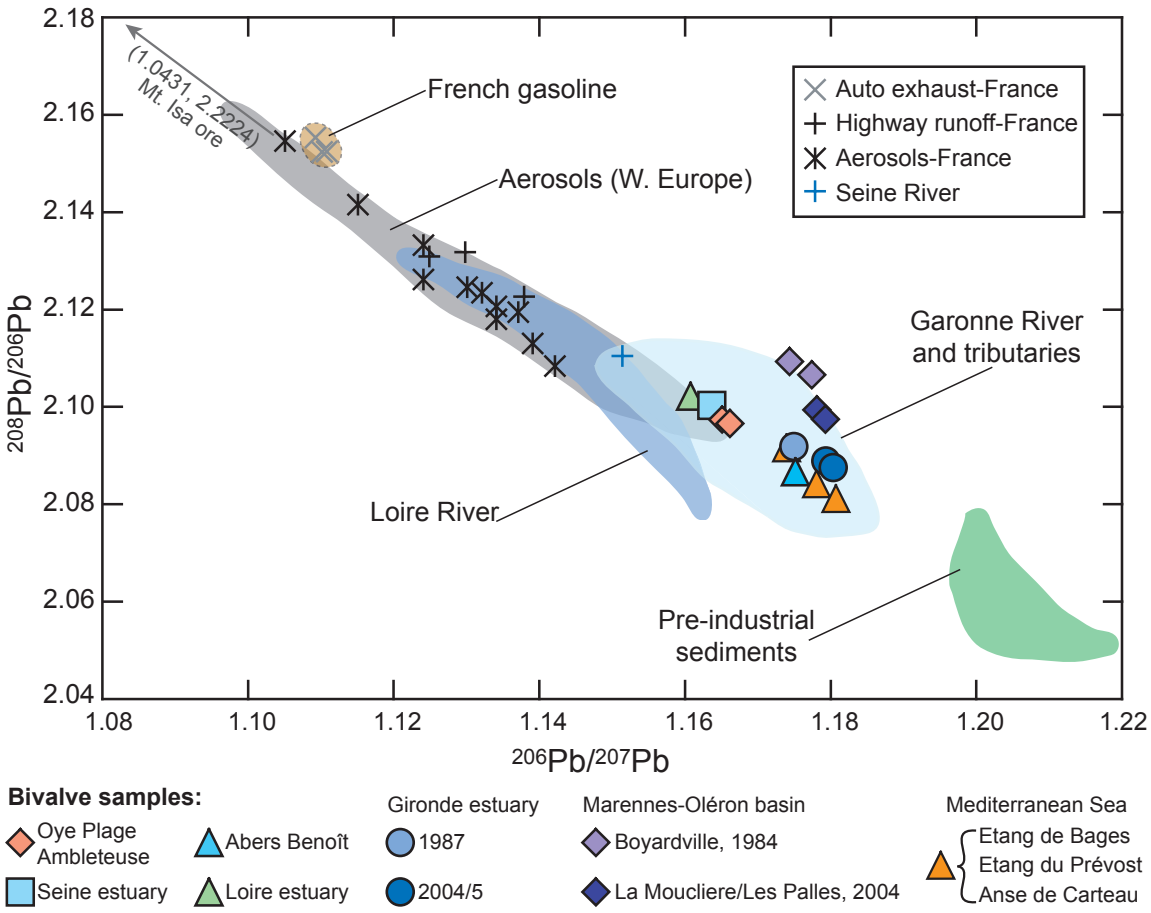

Fig. 4.10. Plot of $^{208}Pb/^{206}Pb$ vs. $^{206}Pb/^{207}Pb$ for the French bivalves. These Pb isotope ratios are compared with those of pre-industrial sediments (Sun, 1980; Elbaz-Poulichet et al., 1986), Garonne River and its tributaries (Elbaz-Poulichet et al., 1986; Grousset et al., 1999), Seine and Loire Rivers (Elbaz-Poulichet et al., 1986), aerosols from western Europe and France (1994-1998; Bollhöfer and Rosman, 2001), auto exhaust (1987) and highway runoff (1992/3) (France; Monna et al., 1995) and Mt. Isa Pb ores (Sangster et al., 2000, and references within). There is an insignificant difference between the Pb isotope ratios of the Garonne River and its tributaries collected in the early 1980s and the late 1990s (Elbaz-Poulichet et al., 1986; Grousset et al., 1999). For this study, the error (2SE) is smaller than the symbol size.

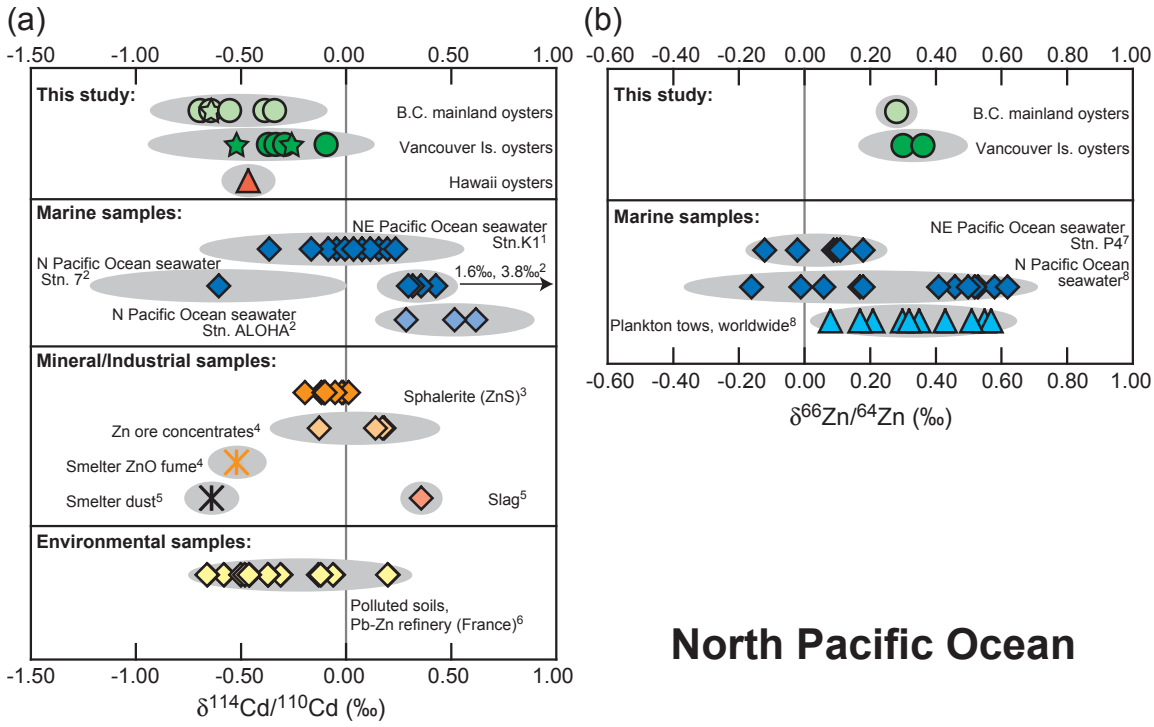

Fig. 4.11. Variations in the (a) Cd and (b) Zn isotopic compositions of oysters (oyster gut contents indicated by a star) from the North Pacific Ocean, seawater, plankton, geological and anthropogenic materials. The grey ellipses indicate error as reported by referenced authors; for this study the grey fields denote 2 standard deviation on the mean Cd value in (a) or Zn value in (b) for replicate analyses of each sample except when this value is less than the long-term reproducibility calculated for the in-house secondary standards (for (a), ±0.14‰; for (b), ±0.06‰), and then the latter is used. In several cases the error is smaller than the symbol and so no grey field is shown. Data sources: [1]Lacan et al., 2006; [2]Ripperger et al., 2007; [3]Schmitt et al., 2009; [4]Shiel et al., 2010; [5]Cloquet et al., 2005; [6]Cloquet et al., 2006b; [7]Bermin et al., 2006; [8]John, 2007.

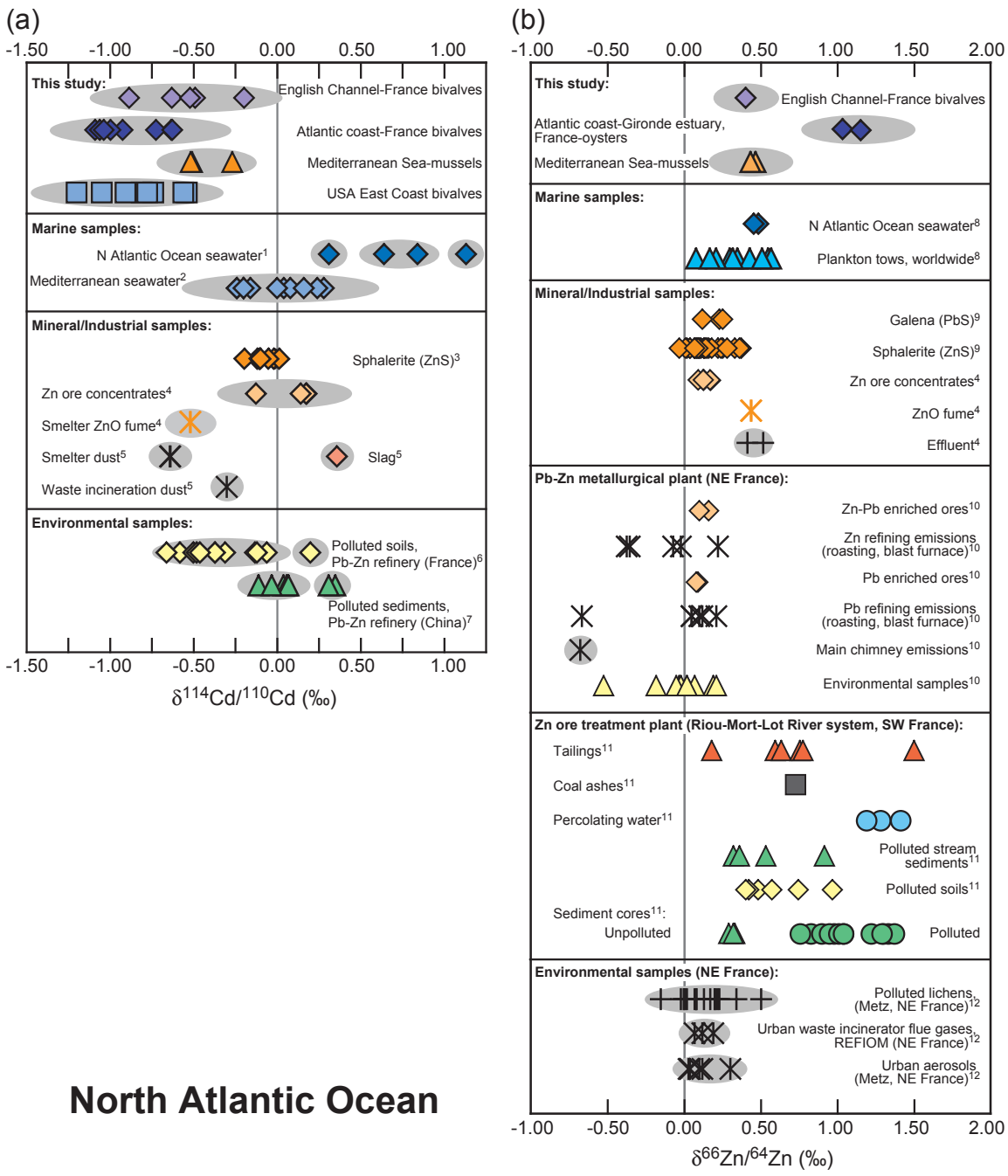

Fig. 4.12. Variations in the (a) Cd and (b) Zn isotopic compositions of bivalves from the North Atlantic Ocean, seawater, plankton, geological and anthropogenic materials. The grey ellipses indicate error as reported by referenced authors; for this study the grey fields denote 2 standard deviation on the mean Cd value in (a) or Zn value in (b) for replicate analyses of each sample except when this value is less than the long-term reproducibility calculated for the in-house secondary standards (for (a), ±0.14‰; for (b), ±0.06‰), and then the latter is used. In several cases the error is smaller than the symbol and so no grey field is shown. Data sources: [1]Ripperger et al., 2007; [2]Lacan et al., 2006; [3]Schmitt et al., 2009; [4]Shiel et al., 2010; [5]Cloquet et al., 2005; [6]Cloquet et al., 2006a; [7]Gao et al., 2008; [8]John, 2007; [9]Sonke et al., 2008; [10]Mattielli et al., 2009; [11]Sivry et al., 2008; [12]Cloquet et al., 2006a.

4.7 References

Audry, S., Blanc, G., Schafer, J. (2004) Cadmium transport in the Lot-Garonne River system (France) - temporal variability and a model for flux estimation. Science of the Total Environment 319: 197–213.

Bendell, L.I., Feng, C. (2009) Spatial and temporal variations in cadmium concentrations and burdens in the Pacific oyster (*Crassostrea gigas*) sampled from the Pacific north-west. Marine Pollution Bulletin 58: 1137–1143.

Berkman, P.A., Nigro, M. (1992) Trace-Metal Concentrations in Scallops around Antarctica - Extending the Mussel Watch Program to the Southern-Ocean. Marine Pollution Bulletin 24: 322–323.

Bermin, J., Vance, D., Archer, C., Statham, P.J. (2006) The determination of the isotopic composition of Cu and Zn in seawater. Chemical Geology 226: 280–297.

Böhlke, J.K., de Laeter, J.R., De Bievre, P., Hidaka, H., Peiser, H.S., Rosman, K.J.R., Taylor, P.D.P. (2005) Isotopic compositions of the elements, 2001. Journal of Physical and Chemical Reference Data 34: 57–67.

Bollhöfer, A., Rosman, K.J.R. (2001) Isotopic source signatures for atmospheric lead: The Northern Hemisphere. Geochimica et Cosmochimica Acta 65: 1727–1740.

Boyle, E.A., Bergquist, B.A., Kayser, R.A., Mahowald, N. (2005) Iron, manganese, and lead at Hawaii Ocean Time-series station ALOHA: Temporal variability and an intermediate water hydrothermal plume. Geochimica et Cosmochimica Acta 69: 933–952.

Boyle, E.A., Sherrell, R.M., Bacon, M.P. (1994) Lead Variability in the Western North-Atlantic Ocean and Central Greenland Ice - Implications for the Search for Decadal Trends in Anthropogenic Emissions. Geochimica et Cosmochimica Acta 58: 3227–3238.

Bruland, K.W. (1980) Oceanographic Distributions of Cadmium, Zinc, Nickel, and Copper in the North Pacific. Earth and Planetary Science Letters 47: 176–198.

Bruland, K.W. and R.P. Franks. (1983) Mn, Ni, Cu, Zn, and Cd in the Western North Atlantic. In: Wong, C.S, Bruland, K.W., Boyle, E., Burton, D., Goldberg, E.D.

(Eds.) Trace Metals in Seawater. NATO Conference Series IV; Marine Sciences, pp. 395–414.

Carignan, J., Simonetti, A., Gariepy, C. (2002) Dispersal of atmospheric lead in northeastern North America as recorded by epiphytic lichens. Atmospheric Environment 36: 3759–3766.

Chow, T.J., Earl, J.L. (1972) Lead Isotopes in North American Coals. Science 176: 510–511.

Christie, J.C., Bendell, L.I. (2009) Sources of dietary cadmium to the Pacific oyster *Crassostrea gigas*. Marine Environmental Research 68: 97–105.

Claisse, D. (1989) Chemical Contamination of French Coasts - the Results of a 10 Years Mussel Watch. Marine Pollution Bulletin 20: 523–528.

Cloquet, C., Carignan, J., Libourel, G. (2006a) Isotopic composition of Zn and Pb atmospheric depositions in an urban/periurban area of northeastern France. Environmental Science & Technology 40: 6594–6600.

Cloquet, C., Carignan, J., Libourel, G., Sterckeman, T., Perdrix, E. (2006b) Tracing source pollution in soils using cadmium and lead isotopes. Environmental Science & Technology 40: 2525–2530.

Cloquet, C., Rouxel, O., Carignan, J., Libourel, G. (2005) Natural cadmium isotopic variations in eight geological reference materials (NIST SRM 2711, BCR 176, GSS-1, GXR-1, GXR-2, GSD-12, Nod-P-1, Nod-A-1) and anthropogenic samples, measured by MC-ICP-MS. Geostandards and Geoanalytical Research 29: 95–106.

DRIRE Nord Pas-de-Calais. (2003) L'Industrie au Regard de l'Environnement, édition 2003. http://www.nord-pas-de-calais.drire.gouv.fr/environnement/ire.html.

De Jong, J., Schoemann, V., Tison, J.L., Becquevort, S., Masson, F., Lannuzel, D., Petit, J., Chou, L., Weis, D., Mattielli, N. (2007) Precise measurement of Fe isotopes in marine samples by multi-collector inductively coupled plasma mass spectrometry (MC-ICP-MS). Analytica Chimica Acta 589: 105–119.

Deboudt, K., Flament, P., Weis, D., Mennessier, J.P., Maquinghen, P. (1999) Assessment of pollution aerosols sources above the Straits of Dover using lead isotope geochemistry. Science of the Total Environment 236: 57–74.

Diaz-Somoano, M., Kylander, M.E., Lopez-Anton, M.A., Suarez-Ruiz, I., Martinez-Tarazona, M.R., Ferrat, M., Kober, B., Weiss, D.J. (2009) Stable Lead Isotope Compositions In Selected Coals From Around The World And Implications For Present Day Aerosol Source Tracing. Environmental Science & Technology 43: 1078–1085.

Dreyfus, S., Pecheyran, C., Lienemann, C.P., Magnier, C., Prinzhofer, A., Donard, O.F.X. (2007) Determination of lead isotope ratios in crude oils with Q-ICP/MS. Journal of Analytical Atomic Spectrometry 22: 351–360.

Elbaz-Poulichet, F., Holliger, P., Martin, J.M., Petit, D. (1986) Stable Lead Isotopes Ratios in Major French Rivers and Estuaries. Science of the Total Environment 54: 61–76.

Emsley, J. (1998) The Elements, third edition. New York: Oxford University Press, pp. 292.

Environment Canada. (2009) National Pollutant Release Inventory, Pollution Data Library, 2008 Revised Facility Data Release: http://www.ec.gc.ca/npri/.

Galer, S.J.G., Abouchami, W. (1998) Practical application of lead triple spiking for correction of instrumental mass discrimination. Mineralogical Magazine 62A: 491–492.

Gao, B., Liu, Y., Sun, K., Liang, X.R., Peng, P., Sheng, G., Fu, J. (2008) Precise determination of cadmium and lead isotopic compositions in river sediments. Analytica Chimica Acta 612: 114–120.

Grousset, F.E., Jouanneau, J.M., Castaing, P., Lavaux, G., Latouche, C. (1999) A 70 year record of contamination from industrial activity along the Garonne River and its tributaries (SW France). Estuarine Coastal and Shelf Science 48: 401–414.

Grousset, F.E., Quetel, C.R., Thomas, B., Buatmenard, P., Donard, O.F.X., Bucher, A. (1994) Transient Pb Isotopic Signatures in the Western-European Atmosphere. Environmental Science & Technology 28: 1605–1608.

Huston, D.L., Stevens, B., Southgate, P.N., Muhling, P., Wyborn, L. (2006) Australian Zn-Pb-Ag ore-forming systems: A review and analysis. Economic Geology 101: 1117–1157.

John, S.G. (2007) The Marine Biogeochemistry of Zinc Isotopes. Ph.D. thesis, Massachusetts Institute of Technology, pp. 142.

John, S.G., Park, G., Zhang, Z., Boyle, E.A. (2007) The isotopic composition of some common forms of anthropogenic zinc. Chemical Geology 245: 61–69.

Johnson, K. (2010) The Periodic Table of Elements in the Ocean. The MBARI Chemical Sensor Program: http://www.mbari.org/chemsensor/pteo.htm.

Jones, C.E., Halliday, A.N., Rea, D.K., Owen, R.M. (2000) Eolian inputs of lead to the North Pacific. Geochimica et Cosmochimica Acta 64: 1405–1416.

Jouanneau, J.M., Boutier, B., Chiffoleau, J.F., Latouche, C., Philipps, I. (1990) Cadmium in the Gironde Fluvioestuarine System - Behavior and Flow. Science of the Total Environment 97-8: 465–479.

Jungers, R.H., Lee Jr., R.E., von Lehmden, D.J. (1975) The EPA National Fuels Surveillance Network. 1. Trace Constituents in Gasoline and Commercial Gasoline Fuel Additives. Environmental Health Perspectives 10: 143-150.

Ketterer, M.E., Lowry, J.H., Simon, J., Humphries, K., Novotnak, M.P. (2001) Lead isotopic and chalcophile element compositions in the environment near a zinc smelting-secondary zinc recovery facility, Palmerton, Pennsylvania, USA. Applied Geochemistry 16: 207–229.

Kruzynski, G.M. (2001) Cadmium in BC farmed oysters: a review of available data, potential sources, health considerations, and research needs. In: Kruzynski, G.M., Addison, R.F., MacDonald, R.W. (Eds.) (2002) Proceedings of a workshop on possible pathways of cadmium into the Pacific oyster *Crassostrea gigas* as cultured on the coast of British Columbia, Institute of Ocean Sciences, Mar. 6–7, 2001, pp. 21–22. Canadian Technical Report of Fisheries and Aquatic Science 2405: pp. 65.

Kruzynski, G.M. (2004) Cadmium in oysters and scallops: the BC experience. Toxicology Letters 148: 159-169.

Kruzynski, G.M., Addison, R.F., MacDonald, R.W. (2002) Proceedings of a workshop on possible pathways of cadmium into the Pacific oyster *Crassostrea gigas* as cultured on the coast of British Columbia, Institute of Ocean Sciences, Mar. 6–7,

2001, pp. 21–22. Canadian Technical Report of Fisheries and Aquatic Science 2405: pp. 65. (Available at http://www.dfo-mpo.gc.ca/Library/262960.pdf)

Labonne, M., Ben Othman, D., Luck, J.M. (1998) Recent and past anthropogenic impact on a Mediterranean lagoon: Lead isotope constraints from mussel shells. Applied Geochemistry 13: 885–892.

Lacan, F., Francois, R., Ji, Y., Sherrell, R.M. (2006) Cadmium isotopic composition in the ocean. Geochimica et Cosmochimica Acta 70: 5104–5118.

Lares, M.L., Orians, K.J. (1997) Natural Cd and Pb variations in *Mytilus californianus* during the upwelling season. Science of the Total Environment 197: 177–195.

Lekhi, P., Cassis, D., Pearce, C.M., Ebell, N., Maldonado, M.T., Orians, K. (2008) Role of dissolved and particulate cadmium in the accumulation of cadmium in cultured oysters (*Crassostrea gigas*). Science of the Total Environment 393: 309–325.

Maréchal, C.N., Télouk, P., Albarède, F. (1999) Precise analysis of copper and zinc isotopic compositions by plasma-source mass spectrometry. Chemical Geology 156: 251–273.

Mason, T.F.D. (2003) High-precision transition metal isotope analysis by plasma-source mass spectrometry and implications for low temperature geochemistry. Ph.D. thesis, University of London, pp. 287.

Mattielli, N., Petit, J.C.J., Deboudt, K., Flament, P., Perdrix, E., Taillez, A., Rimetz-Planchon, J., Weis, D. (2009) Zn isotope study of atmospheric emissions and dry depositions within a 5 km radius of a Pb-Zn refinery. Atmospheric Environment 43: 1265–1272.

Ménard, M. (2005) Canada, a Big Energy Consumer: A Regional Perspective. Catalogue no.: 11-621-M. (Available at http://www.statcan.gc.ca/pub/11-621-m/11-621-m2005023-eng.htm).

Miller, C.A., Ryan, J.V., Lombardo, T. (1996) Characterization of air toxics from an oil-fired firetube boiler. Journal of the Air & Waste Management Association 46: 742–748.

Monna, F., Benothman, D., Luck, J.M. (1995) Pb Isotopes and Pb, Zn and Cd Concentrations in the Rivers Feeding a Coastal Pond (Thau, Southern France) -

Constraints on the Origin(S) and Flux(Es) of Metals. Science of the Total Environment 166: 19–34.

Monna, F., Lancelot, J., Croudace, I.W., Cundy, A.B., Lewis, J.T. (1997) Pb isotopic composition of airborne particulate material from France and the southern United Kingdom: Implications for Pb pollution sources in urban areas. Environmental Science & Technology 31: 2277–2286.

Murphy, D.M., Hudson, P.K., Cziczo, D.J., Gallavardin, S., Froyd, K.D., Johnston, M.V., Middlebrook, A.M., Reinard, M.S., Thomson, D.S., Thornberry, T., Wexler, A.S. (2007) Distribution of lead in single atmospheric particles. Atmospheric Chemistry and Physics Discussions 7: 3763-3804.

NOAA (National Oceanic and Atmospheric Administration). (1998) Sampling and Analytical Methods of the National Status and Trends Program Mussel Watch Project: 1993–1996 Update. Lauenstein, G.G., Cantillo, A. Y. (Eds.) NOAA Technical Memorandum NOS ORCA 130. pp. 234.

Nogawa K., Ishizaki, A. (1979) comparison between cadmium in rice and renal effects among inhabitants of the Jinzu River basin, Environ. Res. 18: 410–420.

Nozaki, Y. (1997) A Fresh Look at Element Distribution in the North Pacific Eos, Electronic Supplement. American Geophysical Union.

Nystar. (2010) Clarksville: http://www.nyrstar.com/nyrstar/en/operations/usa/clarksville/.

O'Connor, T.P. (2002) National distribution of chemical concentrations in mussels and oysters in the USA. Marine Environmental Research 53: 117–143.

O'Connor, T.P., Lauenstein, G.G. (2006) Trends in chemical concentrations in mussels and oysters collected along the US coast: Update to 2003. Marine Environmental Research 62: 261–285.

Pacyna J.M.; Pacyna E.G. (2001) An assessment of global and regional emissions of trace metals to the atmosphere from anthropogenic sources worldwide. Environmental Reviews, 9: 269–298.

Parekh, P.P., Khwaja, H.A., Khan, A.R., Naqvi, R.R., Malik, A., Khan, K., Hussain, G. (2002) Lead content of petrol and diesel and its assessment in an urban environment. Environmental Monitoring and Assessment 74: 255–262.

Preciado, H.F., Li, L.Y. (2006) Evaluation of metal loadings and bioavailability in air, water and soil along two highways of British Columbia, Canada. Water Air and Soil Pollution 172: 81-108.

Preciado, H.F., Li, L.Y., Weis, D. (2007) Investigation of past and present multi-metal input along two highways of British Columbia, Canada, using lead isotopic signatures. Water Air and Soil Pollution 184: 127–139.

Quickert, N., Zdrojewski, A., Dubois, L. (1972) The analysis of lead in commercial gasolines from the Ottawa area. Science of the Total Environment 1: 309–313.

Quirin, G.D. (1999) Section Q: Energy and Electric Power in Statistics Canada. In: Statistics Canada. Historical Statistics of Canada. Catalogue no.: 11-516-X. (Available at http://www.statcan.gc.ca/pub/11-516-x/sectionq/4057756-eng.htm)

Reyes, M.N.M., Campos, R.C. (2005) Graphite furnace atomic absorption spectrometric determination of Ni and Pb in diesel and gasoline samples stabilized as microemulsion using conventional and permanent modifiers. Spectrochimica Acta Part B-Atomic Spectroscopy 60: 615–624.

Ripperger, S., Rehkämper, M., Porcelli, D., Halliday, A.N. (2007) Cadmium isotope fractionation in seawater - A signature of biological activity. Earth and Planetary Science Letters 261: 670–684.

Sanders, J. (1998) the determination of lead in unleaded gasoline using the SpectrAA 55 atomic absorption spectrophotometer. Varian AA Application Notes, pp. 3. (Available at http://www.varianinc.com/media/sci/apps/a-aa12.pdf)

Sangster, D.F., Outridge, P.M., Davis, W.J. (2000) Stable lead isotope characteristics of lead ore deposits of environmental significance. Environmental Reviews 8: 115–147.

Schallié, K. (2001) Results of the 2000 survey of cadmium in B.C. oysters. In: Kruzynski, G.M., Addison, R.F., MacDonald, R.W. (Eds.) (2002) Proceedings of a workshop on possible pathways of cadmium into the Pacific oyster *Crassostrea gigas* as cultured on the coast of British Columbia, Institute of Ocean Sciences, Mar. 6–7, 2001, pp. 31–32. Canadian Technical Report of Fisheries and Aquatic Science 2405: pp. 65.

Schaule, B.K., Patterson, C.C. (1981) Lead Concentrations in the Northeast Pacific - Evidence for Global Anthropogenic Perturbations. Earth and Planetary Science Letters 54: 97–116.

Schmitt, A.D., Galer, S.J.G., Abouchami, W. (2009) Mass-dependent cadmium isotopic variations in nature with emphasis on the marine environment. Earth and Planetary Science Letters 277: 262–272.

Shiel, A.E., Barling, J., Orians, K.J., Weis, D. (2009) Matrix effects on the multi-collector inductively coupled plasma mass spectrometric analysis of high-precision cadmium and zinc isotope ratios. Analytica Chimica Acta 633: 29–37.

Shiel, A.E., Weis, D., Orians, K.J. (2010) Evaluation of zinc, cadmium and lead isotope fractionation during smelting and refining. Science of the Total Environment 408: 2357–2368.

Shirahata, H., Elias, R.W., Patterson, C.C., Koide, M. (1980) Chronological Variations in Concentrations and Isotopic Compositions of Anthropogenic Atmospheric Lead in Sediments of a Remote Subalpine Pond. Geochimica et Cosmochimica Acta 44: 149–162.

Shumway, L.A. (2000) Trace element and polycyclic aromatic hydrocarbon analyses of jet engine fuels: Jet A, JP5, and JP8, Technical Report 1845, SPAWAR Systems Center, San Diego.

Simonetti, A., Gariepy, C., Carignan, J. (2003) Tracing sources of atmospheric pollution in Western Canada using the Pb isotopic composition and heavy metal abundances of epiphytic lichens. Atmospheric Environment 37: 2853–2865.

Sivry, Y., Riotte, J., Sonke, J.E., Audry, S., Schäfer, J., Viers, J., Blanc, G., Freydier, R., Dupré, B. (2008) Zn isotopes as tracers of anthropogenic pollution from Zn-ore smelters The Riou Mort-Lot River system. Chemical Geology 255: 295–304.

Sonke, J.E., Sivry, Y., Viers, J., Freydier, R., Dejonghe, L., André, L., Aggarwal, J.K., Fontan, F., Dupré, B. (2008) Historical variations in the isotopic composition of atmospheric zinc deposition from a zinc smelter. Chemical Geology 252: 145–157.

Statistics Canada (2010) The Supply and Disposition of Refined Petroleum Products in Canada – October 2009, Catalogue no.: 45-004-X, 64:10, pp. 89.

Stone, K. (2008) Coal In: ed. Godin, E. Canadian Minerals Yearbook 2008. Catalogue no.: M38-5/57E-PDF. (Available at http://www.nrcan.gc.ca/smm-mms/busi-indu/cmy-amc/2008revu/htm-com/coa-cha-eng.htm)

Sun, S.S. (1980) Lead Isotopic Study of Young Volcanic-Rocks from Mid-Ocean Ridges, Ocean Islands and Island Arcs. Philosophical Transactions of the Royal Society of London Series a-Mathematical Physical and Engineering Sciences 297: 409–445.

van de Flierdt, T., Frank, M., Halliday, A.N., Hein, J.R., Hattendorf, B., Gunther, D., Kubik, P.W. (2003) Lead isotopes in North Pacific deep water - implications for past changes in input sources and circulation patterns. Earth and Planetary Science Letters 209: 149–164.

Veron, A.J., Church, T.M., Patterson, C.C., Flegal, A.R. (1994) Use of Stable Lead Isotopes to Characterize the Sources of Anthropogenic Lead in North-Atlantic Surface Waters. Geochimica et Cosmochimica Acta 58: 3199–3206.

Viarengo, A., Canesi, L., Mazzucotelli, A., Ponzano, E. (1993) Cu, Zn and Cd Content in Different Tissues of the Antarctic Scallop Adamussium-Colbecki - Role of Metallothionein in Heavy-Metal Homeostasis and Detoxication. Marine Ecology-Progress Series 95: 163–168.

Wang, Y.F., Huang, K.L., Li, C.T., Mi, H.H., Luo, J.H., Tsai, P.J. (2003) Emissions of fuel metals content from a diesel vehicle engine. Atmospheric Environment 37: 4637–4643.

Wombacher, F., Rehkämper, M. (2004) Problems and suggestions concerning the notation of cadmium stable isotope compositions and the use of reference materials. Geostandards and Geoanalytical Research 28: 173–178.

Wombacher, F., Rehkämper, M., Mezger, K. (2004) Determination of the mass-dependence of cadmium isotope fractionation during evaporation. Geochimica et Cosmochimica Acta 68: 2349–2357.

Wombacher, F., Rehkämper, M., Mezger, K., Munker, C. (2003) Stable isotope compositions of cadmium in geological materials and meteorites determined by multiple-collector ICPMS. Geochimica et Cosmochimica Acta 67: 4639–4654.

Wu, J.F., Boyle, E.A. (1997) Lead in the western North Atlantic Ocean: Completed response to leaded gasoline phaseout. Geochimica et Cosmochimica Acta 61: 3279–3283.

US EIA (Energy Information Administration). (2008) International Energy Annual 2006. (Available at http://www.eia.doe.gov/iea/)

US EIA (Energy Information Administration). (2010) Quarterly Coal Report: October-December 2009. pp. 55. (Available at http://www.eia.doe.gov/cneaf/coal/quarterly/qcr.pdf)

US EPA (Environmental Protection Agency). (1998) Chapter 1: External Combustion Sources in AP 42, fifth edition, Compilation of Air Pollutant Emission Factors, Volume 1: Stationary Point and Area Sources. (Available at http://www.epa.gov/ttnchie1/ap42/ch01/index.html)

US EPA (Environmental Protection Agency). (2010) Toxics Release Inventory (TRI) Explorer: Release reports: http://www.epa.gov/triexplorer/chemical.htm.

CHAPTER 5

Conclusions

5.1 Introduction

Metal emissions to the natural environment from anthropogenic sources may be much larger than those from natural sources as is the case for atmospheric emissions of Cd, Zn and Pb globally; Pacyna and Pacyna, 2001). This can disturb the natural cycles for these metals. For many metals anthropogenic emissions have lead to higher levels than occur naturally even in remote regions, such as Greenland and Antarctica (Pacyna and Pacyna, 2001). Both the health of ecosystems and humans depend on achieving sustainable metal emission levels. The accomplishment of this goal requires diligent environmental monitoring, implementation of increasingly efficient industrial processes and improved emission controls and a reduction of our dependence on fossil fuels. Globally, non-ferrous metal smelting is the largest contributor to anthropogenic atmospheric emissions of Cd and Zn (Pacyna and Pacyna, 2001). This study has demonstrated Cd and Zn isotopes to be effective tracers of Cd and Zn emissions in the environment, as the isotopic compositions of these metal emissions are fractionated relative to source materials (i.e., ores). The use of the stable isotope systematics of Cd and Zn (and potentially those of other heavy elements) to evaluate the relative strength and extent of metal emissions to the environment from anthropogenic sources, and clearly demonstrate their impact on environmental health has the potential to:

(1) establish the need for stricter regulations for polluting industries;
(2) put pressure on reluctant facilities to invest in more efficient technologies and emission control;
(3) determine the impact of anthropogenic emissions from laxly regulated industrial sources, even when emissions cross political borders;
(4) demonstrate the effectiveness of remediation strategies in industrially impacted environments or the successful natural recovery of ecosystem health when strategies are emplaced to reduce metal emissions.

The efficiency of Cd and Zn isotopes as new tools will improve with the expansion of the natural and anthropogenic materials' isotopic compositions database and knowledge regarding sources and mechanisms of isotopic fractionation.

5.2 Key findings of this study

This study began with the successful establishment of a technique to measure Cd and Zn isotopes in bivalve molluscs, environmental and anthropogenic samples. The development of this technique facilitated the evaluation of Cd and Zn isotopes as a tool for the identification of natural and anthropogenic metal sources and assessment of their relative contributions in the environment. A multi-tracer approach is used to resolve ambiguities inherent to the interpretation of single element stable isotope data (similar to light stable isotope studies; Peterson and Fry, 1987). The combined use of Pb isotopes, along with the Cd and Zn isotopes, allows the processes contributing metals to be identified through "fingerprinting". Cadmium and Zn stable isotope systematics are successfully used to trace the source of natural and anthropogenic emissions of these elements. The major contributions of this study are the following: (1) establishment of smelting and refining processes as sources of Cd and Zn isotopic fractionation; (2) characterized Cd, Zn and Pb isotopic end members — providing a link to ore sources; (3) characterized the Cd and Zn isotopic compositions of smelter effluent and fumes as different from those of source materials; (4) demonstrated the overall closed nature of the integrated smelting and refining facility in Trail due to internal recycling between operations; (5) established high Cd concentrations of B.C. oysters as mostly natural with some local variability due to anthropogenic sources; (6) identified greater anthropogenic contributions of Cd in USA East Coast bivalves due to high prevalence of industry; (7) documented relatively large variability among bivalves from the coasts of France resulting from the large variability of environmental health at collection sites; (8) established oysters and mussels from sites in the Marennes-Oléron basin and Gironde estuary (French Atlantic Coast) as having the largest anthropogenic Cd contribution of French sites (this region is the largest oyster farming area in Europe and produces some of the most prized in the world!). This study has contributed substantially to our understanding of Cd and Zn cycling and distribution processes in the environment and the relative importance of natural and anthropogenic sources.

A summary of each chapter including major contributes follows:

Matrix effects on the multi-collector inductively coupled plasma mass spectrometric analysis of high-precision cadmium and zinc isotope ratios

Resin-derived contaminants added to samples during column chemistry are shown to cause matrix effects that lead to inaccuracy in multi-collector inductively coupled plasma mass spectrometry (MC-ICP-MS) measurement of small variations in Cd and Zn isotopic compositions observed among terrestrial samples. These matrix effects were evaluated by comparing pure Cd and Zn standards and standards doped with bulk column blank from the anion exchange chromatography procedure. Doped standards exhibit signal enhancements (Cd, Ag, Zn and Cu), instrumental mass bias changes and inaccurate isotopic compositions relative to undoped standards, all of which are attributed to the combined presence of resin-derived organics and inorganics. The matrix effect associated with the inorganic component of the column blanks was evaluated separately by doping standards with metals at the trace levels detected in the column blanks. Mass bias effects introduced by the inorganic column blank matrix are smaller than for the bulk column blank matrix but can still lead to significant changes in ion signal intensity, instrumental mass bias and isotopic ratios. Chemical treatment with refluxed HNO_3 or $HClO_4/HNO_3$ removes resin-derived organic components resulting in matrix effects similar in magnitude to those associated with the inorganic component of the column blank.

Mass bias correction using combined external normalization-SSB does not correct for these matrix effects because the instrumental mass biases experienced by Cd and Zn are decoupled from those of Ag and Cu, respectively. These results demonstrate that ion exchange chromatography and associated resin-derived contaminants can be a source of error (up to 0.23‰ amu^{-1} for $\delta^{114/110}Cd_{Ag\text{-}corrected}$ and 0.28‰ amu^{-1} for $\delta^{66/64}Zn_{Cu\text{-}corrected}$) in MC-ICP-MS measurement of heavy stable element isotopic compositions. As a result of these experiments, all samples were loaded on to anion exchange chromatography columns in sufficient quantities to allow significant dilution of the purified samples (and resin-derived matrix) in the analyzed solutions, thus minimizing the associated matrix effects. In addition, purified samples (i.e., Cd and Zn eluate cuts) were dried and close-

vessel digested on a hotplate using HNO_3 and H_2O_2 in an effort to remove any resin-derived organics before bringing the samples up in dilute HNO_3 for isotopic analysis.

Evaluation of zinc, cadmium and lead isotope fractionation during smelting and refining

To evaluate metallurgical processing as a source of Zn and Cd isotopic fractionation and to potentially trace their distribution in the environment, high-precision MC-ICP-MS Zn, Cd and Pb isotope ratio measurements were made for samples from the integrated Zn–Pb smelting and refining complex in Trail, B.C., Canada. Significant fractionation of Zn and Cd isotopes during processing of ZnS and PbS ore concentrates is demonstrated by the total variation in $\delta^{66/64}$Zn and $\delta^{114/110}$Cd values of 0.42‰ and 1.04‰, respectively, among all smelter samples.

No significant difference is observed between the isotopic compositions of the Zn ore concentrates ($\delta^{66/64}$Zn = 0.09 to 0.17‰; $\delta^{114/110}$Cd = -0.13 to 0.18‰) and the roasting product, calcine ($\delta^{66/64}$Zn = 0.17‰; $\delta^{114/110}$Cd = 0.05‰), due to ~100% recovery from roasting. The overall Zn recovery from metallurgical processing is ~98%, thus the refined Zn metal ($\delta^{66/64}$Zn = 0.22‰) is not significantly fractionated relative to the starting materials despite significantly fractionated fume ($\delta^{66/64}$Zn = 0.43‰) and effluent ($\delta^{66/64}$Zn = 0.41 to 0.51‰). Calculated Cd recovery from metallurgical processing is 72–92%, with the majority of the unrecovered Cd lost during Pb operations ($\delta^{114/110}$Cd = -0.38‰). The refined Cd metal is heavy ($\delta^{114/110}$Cd = 0.39 to 0.52‰) relative to the starting materials. In addition, significant fractionation of Cd isotopes is evidenced by the relatively light and heavy isotopic compositions of the fume ($\delta^{114/110}$Cd = -0.52‰) and effluent ($\delta^{114/110}$Cd = 0.31 to 0.46‰). In contrast to Zn and Cd, Pb isotopes are homogenized by mixing of Pb sources during processing. The total variation observed in the Pb isotopic compositions of smelter samples is attributed to mixing of ore sources, with different radiogenic signatures, during processing.

Tracing cadmium, zinc and lead in bivalves from the coasts of western Canada, the USA and France using isotopes

In a multi-tracer study, Cd, Zn and Pb isotopic compositions (MC-ICP-MS) and elemental concentrations (HR-ICP-MS) are used to distinguish between natural and anthropogenic sources of these metals in bivalves collected from western Canada (B.C.), Hawaii, the USA East Coast and France.

B.C. oyster tissues and gut contents have identical Cd isotopic compositions ($\delta^{114/110}$Cd = -0.69 to -0.09‰) that fall within the light end of the range reported for North Pacific seawater, suggesting the high Cd levels in these oysters primarily results from natural upwelling of Cd-rich deep-waters in the North Pacific. We suggest limiting consumption of B.C. oysters to ensure Cd intake remains within safe levels. Variability in the Cd isotopic compositions of B.C. oysters is attributed to variable contributions from anthropogenic sources; the lightest of these oysters are from the B.C. mainland. The range of Zn isotopic composition exhibited by B.C. oysters ($\delta^{66/64}$Zn = 0.28 to 0.36‰) is consistent with that of North Pacific seawater. Despite relatively low Pb levels in B.C. oysters (0.05 to 0.22 μg g^{-1} tissue dry weight), their Pb isotopic compositions reflect primarily anthropogenic sources, likely mixing between Pb emissions from the consumption of unleaded automotive gasoline and diesel fuel (high ^{206}Pb/^{207}Pb) and smelting (potentially historical) of Pb ores in Trail, B.C. (low ^{206}Pb/^{207}Pb source). Both the Cd and Pb isotopic compositions of the Hawaiian oysters fall within the range exhibited by the oysters from Vancouver Island suggesting similar metal sources.

All bivalve samples from the Atlantic coasts exhibit Cd isotopic compositions lighter than reported for North Atlantic seawater suggesting the widespread importance of anthropogenic sources. USA East Coast bivalves exhibit relatively light Cd isotopic compositions ($\delta^{114/110}$Cd = -1.20 to -0.54‰) due to the high prevalence of industry on this coast. The $\delta^{114/110}$Cd values of USA East Coast bivalves include the lightest ever reported for terrestrial materials (with the exception of that reported for a tektite sample, i.e., in a completely different set of conditions). The Pb isotopic compositions of bivalves from the USA East Coast indicate Pb emissions from the combustion of coal are an important source of Pb; this is consistent with the high consumption of coal for power production on this coast.

The large variability of environmental health among coastal areas in France is reflected in the broad range of Cd isotopic compositions exhibited by French bivalves ($\delta^{114/110}$Cd = -1.08 to -0.20‰). Oysters and mussels from the Marennes-Oléron basin and Gironde estuary have the lightest Cd isotopic compositions of the French oysters consistent with significant historical Cd emissions from the now-closed proximal Zn smelter. In these bivalves, significant declines in the Cd levels between 1984/7 and 2004/5 are not accompanied by a shift in the Cd isotopic composition toward natural values. The Mediterranean samples have isotopic compositions within error of the lighter end of the range reported for Mediterranean seawater. The Zn isotopic compositions of French oysters and mussels ($\delta^{66/64}$Zn = 0.39 to 0.46‰) are identical to those reported for North Atlantic seawater, with the exception of the much heavier compositions of oysters ($\delta^{66/64}$Zn = 1.03 to 1.15‰) from the polluted Gironde estuary. The French bivalves exhibit Pb isotopic compositions that indicate primarily industrial (as opposed to automotive) sources; this is consistent with the collection of most of the French bivalve samples in 2004, after the complete phase-out of leaded gasoline in France.

This study demonstrates the effective use of Cd and Zn isotopes to trace anthropogenic sources in the environment and the benefit of combining these tools with Pb isotope "fingerprinting" techniques to identify processes contributing metals.

5.3 Suggestions for future research

This work represents significant contributions to our understanding of Cd and Zn isotopes as source tracers and provides direction for future research. Measurement of the small differences observed in the isotopic compositions of heavy stable elements has only been possible in recent years, primarily with the MC-ICP-MS. Improved techniques and instrumentation are expected to facilitate increasingly precise measurement of these small differences. Potential applications for heavy stable isotopes are early in their development. Prospective research includes:

(1) The evaluation of isotopic fractionation for other metals during smelting and refining and the potential use of these elemental isotopes

for tracing emissions in the environment. For example, an investigation of Cu, Ni and/or Sb isotope fractionation (depending on starting materials processed by the facility) during Cu smelting and refining to produce Cu and Ni metals and associated byproducts, e.g., Sb.

(2) The evaluation of isotopic fractionation for heavy metals during various anthropogenic processes and the assessment of the potential to trace those anthropogenic metal emission sources. For example, an investigation of isotopic fractionation of Cd, Cr, Cu, Hg and/or Zn during waste incineration, which contributes between 1 and 5% of total global atmospheric emissions of these metals (mid-1990s; Pacyna and Pacyna, 2001). Initial investigation of the Cd isotopic composition of urban waste incineration fly ash suggests incineration may fractionate Cd isotopes (Cloquet et al., 2005).

In addition, this study has exposed several opportunities for Pb "fingerprinting" or the combined use of Cd and Pb isotopes to trace these metals in the environment. Prospective research includes:

(1) A thorough investigation of anthropogenic metal sources in the Greater Vancouver area, focusing on Pb. The consumption of petroleum products accounts for substantial contributions to total atmospheric Pb emissions in B.C. (e.g., consumption of avgas by small planes and diesel and heavy fuel oils by boats). An investigation of the Pb isotopic signatures of these emissions would allow the precise determination of their relative importance as anthropogenic Pb sources in Southwestern B.C. In particular, the impact of significant Pb emissions, resulting from the consumption of avgas (accounts for ~68% of total Pb emissions from the consumption of fossil fuels in B.C.; Table 4.1), on local environmental health needs to be assessed.

(2) An evaluation of the historical evolution of Pb pollution in the Vancouver area and its sources through a tracer study of Pb in

available environmental archives, such as tree cores (Stanley Park is home to trees that are hundreds of years old) or peat cores (a core from Burns Bog, located within the Greater Vancouver area, could provide a record of thousands of years).

(3) Regional studies of Cd and Pb isotope systematics in bivalves and other environmental samples in order to provide clear links between high metal levels and anthropogenic sources; e.g., oysters from Charleston Harbor exhibit Cd isotopic compositions among the lightest in the study–a regional study of broader scope may allow the precise identification of the important anthropogenic sources.

5.4 References

Cloquet, C., Rouxel, O., Carignan, J., Libourel, G. (2005) Natural cadmium isotopic variations in eight geological reference materials (NIST SRM 2711, BCR 176, GSS-1, GXR-1, GXR-2, GSD-12, Nod-P-1, Nod-A-1) and anthropogenic samples, measured by MC-ICP-MS. Geostandards and Geoanalytical Research 29: 95–106.

Pacyna, J.M., Pacyna, E.G. (2001) An assessment of global and regional emissions of trace metals to the atmosphere from anthropogenic sources worldwide. Environmental Reviews 9: 269–298.

Peterson, B.J., Fry, B. (1987) Stable isotopes in ecosystem studies. Annual Review of Ecology and Systematics 18: 293–320.

Appendices

Appendix A List of publications and presentations during Ph.D.

Peer-reviewed publications

Shiel, A.E., D. Weis and K.J. Orians. Tracing cadmium, zinc and lead pollution in oysters from the coasts of western Canada, the USA and France using isotopes (in preparation).

Shiel, A.E., D. Weis and K.J. Orians (2010) Evaluation of zinc, cadmium and lead isotope fractionation during smelting and refining. Science of the Total Environment 408: 2357-2368.

Shiel A.E., J. Barling, K.J. Orians and D. Weis (2009) Matrix effects on the multi-collector inductively coupled plasma mass spectrometric analysis of high-precision cadmium and zinc isotope ratios. Analytica Chimica Acta 633: 29-37.

Conference abstracts

Oral presentations

Shiel, A.E., K.J. Orians, D. Cossa and D. Weis (2008) Sourcing Metals in Bivalves Using Combined Pb, Zn and Cd Isotopic Compositions. Geochimica et Cosmochimica Acta 72(12) Supplement 1: A859.

Shiel, A.E., K.J. Orians, D. Cossa and D. Weis (2007) Anthropogenic contamination of bivalves revealed by Cd isotopes. Geochimica et Cosmochimica Acta 71(15) Supplement 1: A928.

Posters

Shiel, A.E., D. Weis and K.J. Orians. (2010) Pb, Cd and Zn Isotopes as Source Tracers in Pacific/Atlantic Bivalves. Geochimica et Cosmochimica Acta 74(11) Supplement 1: A952.

Torchinsky, A., **A.E. Shiel,** M. Price and D. Weis. (2010) Pb, Cd and Zn Isotopes as Source Tracers in Pacific/Atlantic Bivalves. Geochimica et Cosmochimica Acta 74(11) Supplement 1: A1050.

Verheyden, S., C. Maerschalk, **A.E. Shiel** and N. Mattielli (2007) Single column procedure for quantitative separation and recovery of Cd for high precision isotope analysis by MC-ICP-MS. Geochimica et Cosmochimica Acta 71(15): Supplement 1: A1063.

Shiel, A.E., D. Weis, J. Barling and K.J. Orians (2006) Matrix effects on the MC-ICP-MS Analysis of Zn and Cd isotopes. Eos Trans. AGU, 87(52), Fall Meet. Suppl., Abstract V21B-0583.

Barling, J., **A.E. Shiel** and D. Weis (2006) The Influence of Non-spectral Matrix Effects on the Accuracy of Isotope Ratio Measurement by MC-ICP-MS. Eos Trans. AGU, 87(52), Fall Meet. Suppl., Abstract V21B-0584.

Barling, J., **A.E. Shiel**, B. Mueller and D. Weis (2006) An Investigation of Non-Spectral Matrix Effects on the Accuracy of Non-Traditional Stable Isotope Measurements by MC-ICP-MS. Geophysical Research Abstracts, 8, 10261.

Shiel, A.E., J. Barling, D. Weis and K.J. Orians (2005) Potential Use of Cadmium Isotopes to Source Cadmium in Oysters, Eos Trans. AGU, 86(52), Fall Meet. Suppl., Abstract OS51C-0574.

Appendix B Cd and Zn separation chemistry, designed by Mason (2003).

Eluent	Acid Volume (ml)	Eluted
2 mL AG MP-1M resin, 100-200 mesh size, chloride form (Bio-Rad Laboratories, Inc.)[a]		
Resin cleaning		
1 M HNO3	10	
≥18.2 MΩ cm water	2	
1 M HNO3	10	
≥18.2 MΩ cm water	2	
1 M HNO3	10	
≥18.2 MΩ cm water	10	
Resin conditioning		
7 M HCl	10	
Load sample solution		
7 M HCl	1	
Elution sequence		
7 M HCl	10	Matrix (e.g. Mg, Al, Ca, Cr)
7 M HCl	20	Cu
8 M HF+2 M HCl	10	Fe, Mo, Sn
0.1 M HBr+0.5 M HNO_3	10	Zn
0.5 M HNO_3	10	Cd

[a]Resin was loaded into single use, acid washed PolyPrep® columns (Bio-Rad Laboratories, Inc.).

Appendix C Column matrix effects on Cd and Ag ion-signal intensities and delta Cd values. Table includes values shown in Fig. 2.2.

		Change in ion-signal (%)		Sample-standard bracketing					External normalization with sample-standard bracketing				
Sample	Volume (%)	^{110}Cd	^{109}Ag	$\delta^{111/110}Cd_{SSB}$/ amu	$\delta^{112/110}Cd_{SSB}$/ amu	$\delta^{113/110}Cd_{SSB}$/ amu	$\delta^{114/110}Cd_{SSB}$/ amu	$\delta^{114/110}Cd_{SSB}$	$\delta^{111/110}Cd_{Ag\text{-}corr.}$/ amu	$\delta^{112/110}Cd_{Ag\text{-}corr.}$/ amu	$\delta^{113/110}Cd_{Ag\text{-}corr.}$/ amu	$\delta^{114/110}Cd_{Ag\text{-}corr.}$/ amu	$\delta^{114/110}Cd_{Ag\text{-}corr.}$
Blank 1													
	2	8.28	7.48	-0.07	-0.05	-0.06	-0.04	-0.16	-0.08	-0.08	-0.08	-0.07	-0.27
	10	21.30	24.45	-0.09	-0.10	-0.12	-0.12	-0.46	-0.11	-0.11	-0.13	-0.11	-0.45
	20	14.11	19.04	0.03	0.01	0.03	0.01	0.04	-0.09	-0.10	-0.09	-0.10	-0.40
	50	13.94	21.99	0.12	0.14	0.15	0.14	0.57	-0.17	-0.14	-0.14	-0.14	-0.57
Blank 2													
	2	6.58	7.51	0.01	0.00	0.01	0.01	0.05	-0.05	-0.06	-0.04	-0.04	-0.18
	10	11.92	14.50	0.03	0.01	0.00	0.00	0.00	-0.03	-0.07	-0.08	-0.08	-0.30
	50	16.18	3.63	0.16	0.21	0.24	0.22	0.90	-0.18	-0.15	-0.12	-0.13	-0.52
Blank 3													
	2	0.69	-0.16	0.02	-0.03	-0.03	-0.03	-0.11	-0.02	-0.05	-0.06	-0.06	-0.23
	10	8.20	12.36	0.04	0.03	0.00	0.02	0.07	-0.08	-0.08	-0.10	-0.09	-0.36
	50	9.85	23.50	0.03	0.02	0.03	0.02	0.09	-0.19	-0.19	-0.19	-0.19	-0.77
Blank 4													
	50	10.45	26.36	-0.13	-0.10	-0.10	-0.11	-0.44	-0.25	-0.22	-0.23	-0.23	-0.92
Blank 5 (fluxed HNO_3 treatment, run during same analytical session as Blank 2)													
	2	3.95	4.10	-0.07	-0.08	-0.09	-0.08	-0.31	-0.03	-0.05	-0.05	-0.04	-0.14
	10	12.52	15.95	-0.01	0.00	0.01	0.00	-0.02	-0.06	-0.06	-0.04	-0.05	-0.21
	50	15.04	23.29	0.12	0.11	0.10	0.11	0.43	-0.09	-0.11	-0.10	-0.10	-0.39
Blank 6 ($HClO_4$ treatment; run during same analytical session as Blank 4)													
	50	11.47	25.62	0.08	0.08	0.10	0.09	0.37	-0.11	-0.11	-0.10	-0.10	-0.41
$HClO_4$ acid blank (run during same analytical session as Blank 4)													
	50	13.10	22.48	0.10	0.09	0.10	0.10	0.38	-0.10	-0.11	-0.09	-0.08	-0.34
Blank 7 (A-type skimmer)													
	2	4.10	-0.90	-0.01	-0.01	0.02	0.00	0.00	-0.02	-0.03	0.01	-0.02	-0.08
	10	6.34	8.18	0.05	0.04	0.05	0.05	0.19	-0.11	-0.10	-0.09	-0.09	-0.36
	50	10.25	17.09	0.06	0.06	0.04	0.06	0.24	-0.15	-0.15	-0.16	-0.15	-0.60

Appendix D Column matrix effects on Zn and Cu ion-signal intensities and delta Zn values. Table includes values shown in Fig. 2.1.

		Change in ion-signal (%)		Sample-standard bracketing					External normalization with sample-standard bracketing				
Sample	**Run #**	**^{64}Zn**	**^{63}Cu**	$\delta^{66/64}Zn_{SSB}$/ amu	$\delta^{67/64}Zn_{SSB}$/ amu	$\delta^{68/64}Zn_{SSB}$/ amu	$\delta^{68/66}Zn_{SSB}$/ amu	$\delta^{66/64}Zn_{SSB}$	$\delta^{66/64}Zn_{Cu\text{-}corr.}$/ amu	$\delta^{67/64}Zn_{Cu\text{-}corr.}$/ amu	$\delta^{68/64}Zn_{Cu\text{-}corr.}$/ amu	$\delta^{68/66}Zn_{Cu\text{-}corr.}$/ amu	$\delta^{66/64}Zn_{Cu\text{-}corr.}$
Blank 1													
	0.2	8.86	3.14	-0.02	0.02	-0.02	-0.01	-0.04	-0.14	-0.10	-0.14	-0.13	-0.28
	2	16.28	9.62	0.01	0.05	0.01	0.02	0.01	-0.28	-0.24	-0.27	-0.25	-0.56
	10	25.98	25.56	0.10	0.13	0.10	0.11	0.20	-0.16	-0.12	-0.15	-0.14	-0.33
	50	26.20	31.87	0.10	0.22	0.14	0.18	0.21	-0.24	-0.12	-0.19	-0.15	-0.49
Blank 2													
	50	14.98	25.06	0.15	0.42	0.27	0.39	0.30	-0.12	0.16	0.00	0.12	-0.24
Blank 3 (fluxed HNO_3 treatment; run during same analytical session as Blank 1)													
	2	10.73	12.61	0.05	0.05	0.04	0.04	0.10	-0.03	-0.03	-0.03	-0.03	-0.06
	10	-16.23	21.73	0.10	0.17	0.12	0.13	0.20	0.01	0.07	0.02	0.03	0.01
	50	-10.30	28.17	0.02	0.29	0.10	0.17	0.05	0.04	0.29	0.11	0.18	0.08
Blank 4 ($HClO_4$ treatment; run during same analytical session as Blank 1)													
	2	10.28	11.22	0.04	0.05	0.04	0.04	0.08	-0.20	-0.19	-0.20	-0.20	-0.40
	10	18.34	25.64	0.04	0.08	0.05	0.06	0.08	-0.22	-0.18	-0.21	-0.20	-0.44
	50	-13.56	35.66	0.05	0.29	0.13	0.21	0.10	-0.20	0.04	-0.12	-0.05	-0.40
Blank 5 ($HClO_4$ treatment; run during same analytical session as Blank 2-not shown in Fig. 2.2)													
	50	3.07	15.92	0.09	0.37	0.22	0.34	0.18	-0.14	0.14	-0.03	0.11	-0.28

Appendix E Inorganic column-derived matrix effects on Cd and Ag ion-signal intensities and delta Cd values. Table includes values given in the Results section.

		Change in ion-signal (%)		Sample-standard bracketing					External normalization with sample-standard bracketing				
Sample	**Run #**	**^{110}Cd**	**^{109}Ag**	$\delta^{111/110}Cd_{SSB}$/ amu	$\delta^{112/110}Cd_{SSB}$/ amu	$\delta^{113/110}Cd_{SSB}$/ amu	$\delta^{114/110}Cd_{SSB}$/ amu	$\delta^{114/110}Cd_{SSB}$	$\delta^{111/110}Cd_{Ag\text{-}corr.}$/ amu	$\delta^{112/110}Cd_{Ag\text{-}corr.}$/ amu	$\delta^{113/110}Cd_{Ag\text{-}corr.}$/ amu	$\delta^{114/110}Cd_{Ag\text{-}corr.}$/ amu	$\delta^{114/110}Cd_{Ag\text{-}corr.}$
Mg-doped													
	1	4.66	4.53	-0.08	-0.04	-0.04	-0.04	-0.17	-0.02	0.00	0.01	0.00	0.00
	2	6.78	6.20	-0.09	-0.07	-0.05	-0.05	-0.22	-0.03	-0.01	0.01	0.01	0.03
	3	10.29	14.87	-0.04	-0.03	-0.03	-0.03	-0.11	-0.01	-0.01	0.00	0.00	0.00
Mock Col Inorg													
	1	8.58	9.46	0.00	-0.03	-0.03	-0.03	-0.12	0.08	0.06	0.06	0.06	0.24
	2	12.93	13.98	0.03	0.04	0.00	0.01	0.06	0.10	0.12	0.07	0.09	0.37
	3	11.26	15.74	0.00	-0.04	0.00	-0.01	-0.02	-0.06	-0.07	-0.07	-0.07	-0.26
	4	8.55	14.77	0.14	0.12	0.11	0.12	0.47	0.04	0.02	0.01	0.03	0.10

Appendix F Matrix effects from metallic elements on Cd and Ag ion-signal intensities and delta Cd values. Table includes values shown in Figs. 2.2(a) and 2.4(a).

		Change in ion-signal (%)		Sample-standard bracketing					External normalization with sample-standard bracketing				
Doping Element	**Volume (%)**	**^{110}Cd**	**^{109}Ag**	$\delta^{111/110}Cd_{SSB}$/ amu	$\delta^{112/110}Cd_{SSB}$/ amu	$\delta^{113/110}Cd_{SSB}$/ amu	$\delta^{114/110}Cd_{SSB}$/ amu	$\delta^{114/110}Cd_{SSB}$	$\delta^{111/110}Cd_{Ag\text{-}corr.}$/ amu	$\delta^{112/110}Cd_{Ag\text{-}corr.}$/ amu	$\delta^{113/110}Cd_{Ag\text{-}corr.}$/ amu	$\delta^{114/110}Cd_{Ag\text{-}corr.}$/ amu	$\delta^{114/110}Cd_{Ag\text{-}corr.}$
Al													
	1	-24.12	9.14	0.16	0.18	0.19	0.19	0.76	-0.13	-0.12	-0.12	-0.11	-0.45
	2	-22.30	12.67	-0.19	-0.17	-0.18	-0.17	-0.69	-0.30	-0.30	-0.31	-0.31	-1.22
	3	-23.86	10.34	-0.10	-0.07	-0.07	-0.07	-0.28	-0.26	-0.24	-0.23	-0.23	-0.93
	4	-9.58	17.56	-0.26	-0.24	-0.22	-0.23	-0.92	-0.39	-0.37	-0.36	-0.36	-1.44
Zn[1]													
	1	5.46	12.12	-0.10	-0.09	-0.09	-0.09	-0.35	-0.17	-0.17	-0.16	-0.17	-0.67
	2	3.92	10.48	-0.10	-0.10	-0.10	-0.09	-0.37	-0.14	-0.13	-0.13	-0.12	-0.48
	3	2.18	27.62	-0.10	-0.08	-0.08	-0.08	-0.32	-0.19	-0.17	-0.18	-0.17	-0.68
	4	2.50	11.70	-0.12	-0.09	-0.09	-0.08	-0.32	-0.19	-0.16	-0.16	-0.15	-0.59
Rb													
	1	-1.55	8.12	-1.91	-1.93	-1.98	-1.96	-7.84	-0.35	-0.37	-0.43	-0.43	-1.70
	2	7.12	16.36	-0.17	-0.16	-0.18	-0.17	-0.67	-0.07	-0.06	-0.07	-0.07	-0.27
Sr													
	1	-10.72	35.48	-0.26	-0.29	-0.31	-0.31	-1.25	0.10	0.08	0.06	0.06	0.22
	2	4.48	-3.40	-0.21	-0.20	-0.17	-0.19	-0.76	-0.06	-0.05	-0.03	-0.04	-0.16
	3	11.09	26.55	-0.30	-0.32	-0.31	-0.33	-1.33	0.11	0.09	0.10	0.08	0.32
Cs													
	1	1.03	12.94	-2.23	-2.20	-2.30	-2.23	-8.92	-0.33	-0.35	-0.43	-0.40	-1.60
	2	2.73	12.88	-0.62	-0.64	-0.66	-0.65	-2.58	-0.15	-0.18	-0.19	-0.18	-0.71
	3	17.57	33.18	-0.22	-0.22	-0.21	-0.20	-0.82	-0.19	-0.19	-0.18	-0.18	-0.72
	4	-6.74	-1.09	-0.04	-0.06	-0.07	-0.07	-0.27	-0.08	-0.09	-0.09	-0.09	-0.38
Ba													
	1	8.87	14.73	-0.71	-0.73	-0.73	-0.74	-2.95	-0.25	-0.28	-0.27	-0.29	-1.17
	2	2.00	8.45	-0.47	-0.46	-0.47	-0.47	-1.89	-0.35	-0.34	-0.34	-0.35	-1.40
	3	7.29	12.24	-0.15	-0.15	-0.15	-0.15	-0.58	-0.16	-0.17	-0.17	-0.16	-0.66
Lu													
	1	15.98	13.48	-0.19	-0.23	-0.20	-0.21	-0.85	-0.10	-0.16	-0.14	-0.15	-0.58
	2	-1.01	53.37	-0.07	-0.09	-0.08	-0.08	-0.32	-0.22	-0.22	-0.21	-0.21	-0.85
	3	11.64	-8.59	0.03	0.03	0.02	0.01	0.05	0.02	0.01	0.01	-0.01	-0.03
	4	8.77	-7.64	-0.06	-0.10	-0.14	-0.12	-0.48	0.01	-0.02	-0.03	-0.03	-0.10
Ir													
	1	0.71	4.66	0.32	0.37	0.38	0.38	1.53	-0.24	-0.21	-0.20	-0.19	-0.76
Pb													
	1	8.22	10.63	-0.39	-0.41	-0.40	-0.40	-1.62	-0.10	-0.11	-0.11	-0.11	-0.43
	2	5.21	1.03	0.12	0.11	0.09	0.10	0.40	0.02	0.02	0.03	0.02	0.07

[1]Based on comparison of the delta values of $^{114/110}$Cd with interference free ratio $^{114/111}$Cd, it is estimated that the contribution of $ZnAr^+$ on mass 110 is 0.046 mV for a run with 1.593724 V on mass 110 and that this contributes -0.03‰ to the observed $\delta^{114/110}Cd_{SSB}$ = -0.32‰. Assuming that the zinc argides are present roughly in proportion to the isotopic abundances of Zn, then the $ZnAr^+$ contribution on ^{107}Ag would be approximately 0.316 mV on a 3.676206 V beam. Fractionation correction using f(Ag) results in $\delta^{114/110}Cd_{Ag\text{-}corr.}$ = -0.59‰, removing the $^{67}Zn^{40}Ar^+$ contribution on ^{107}Ag results in $\delta^{114/110}Cd_{Ag\text{-}corr.}$ = -0.72‰.

Appendix G Matrix effects from metallic elements on Zn and Cu ion-signal intensities and delta Zn values. Table includes values shown in Figs. 2.3(b) and 2.4(b).

		Change in ion-signal (%)		Sample-standard bracketing					External normalization with sample-standard bracketing				
Doping Element	**Run #**	**^{64}Zn**	**^{63}Cu**	$\delta^{66/64}Zn_{SSB}$/ amu	$\delta^{67/64}Zn_{SSB}$/ amu	$\delta^{68/64}Zn_{SSB}$/ amu	$\delta^{68/66}Zn_{SSB}$/ amu	$\delta^{66/64}Zn_{SSB}$	$\delta^{66/64}Zn_{Cu\text{-}corr.}$/ amu	$\delta^{67/64}Zn_{Cu\text{-}corr.}$/ amu	$\delta^{68/64}Zn_{Cu\text{-}corr.}$/ amu	$\delta^{68/66}Zn_{Cu\text{-}corr.}$/ amu	$\delta^{66/64}Zn_{Cu\text{-}corr.}$
Al[1]													
	1	0.92	12.66	-0.28	-0.01	-0.27	-0.26	-0.57	-0.33	-0.05	-0.31	-0.30	-0.65
	2	-2.68	14.46	-0.34	0.14	-0.33	-0.33	-0.68	-0.56	-0.08	-0.55	-0.54	-1.12
Ca													
	1	4.60	6.50	-0.32	-0.33	-0.33	-0.34	-0.65	-0.73	-0.74	-0.73	-0.72	-1.46
	2	3.12	0.31	-0.27	-0.26	-0.26	-0.26	-0.54	-0.72	-0.69	-0.70	-0.69	-1.44
Sr[2]													
	1	6.90	4.30	-4.73	-3.21	-2.46	-0.18	-9.46	-3.27	-1.77	-1.02	1.24	-6.54
	2	10.68	13.26	-5.69	-3.86	-2.96	-0.23	-11.37	-4.46	-2.63	-1.75	0.98	-8.93
Cd													
	1	4.56	0.92	-0.24	-0.24	-0.25	-0.25	-0.48	-0.72	-0.71	-0.71	-0.71	-1.43
	2	4.82	-0.89	-0.23	-0.24	-0.24	-0.24	-0.46	-0.75	-0.75	-0.75	-0.74	-1.50
Ba[3]													
	1	4.85	3.48	6.10	693.04	371.31	727.64	12.21	-15.29	629.08	320.61	677.21	-30.58
	2	8.91	9.81	5.19	616.32	330.01	648.07	10.38	-12.89	566.46	289.81	608.17	-25.77
Pb													
	1	4.00	-2.73	-0.14	-0.15	-0.14	-0.14	-0.29	-0.51	-0.51	-0.50	-0.49	-1.02
	2	3.26	-3.30	-0.03	-0.04	-0.02	-0.01	-0.05	-0.65	-0.66	-0.63	-0.62	-1.30

[1]Changes in the calculated delta value for $^{67}Zn/^{64}Zn$ are in part due to the formation of $AlAr^{+}$ (m/z = 67).

[2]Changes in the intensities of ^{63}Cu and ^{64}Zn and the calculated delta values are in part due to the formation of $SrAr^{2+}$ (m/z = 63, 64).

[3]Changes in the calculated delta values are in part due to the formation of significant Ba^{2+} (m/z = 65, 66, 67, 68).

Appendix H Plot of $\delta^{114/110}$Cd vs. $\delta^{111/110}$Cd for B.C. oyster soft tissues and gut contents. The error bars denote 2 standard deviation (2SD) on the mean δCd value for replicate analyses of each sample.

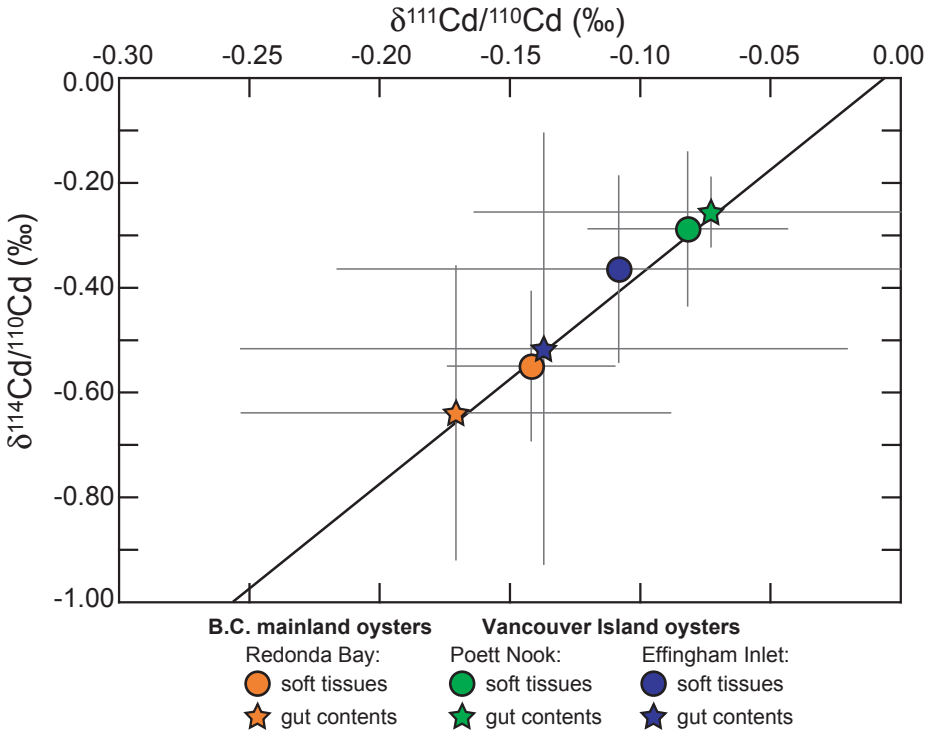

Appendix I Method for the measurement of Cd isotopes in environmental and geological samples.

These methods are appropriate for the preparation of biological, environmental and geological samples for Cd isotope MC-ICP-MS analysis. Small modifications to the procedure will be necessitated by differences between sample materials.

1. Sample preparation:
    a. Homogenize sample material. For B.C. oyster samples, homogenization is accomplished by processing tissues in a commercial blender equipped with an acid-washed polycarbonate container and a stainless steel blade.
    b. Dry sample material in a drying oven or freeze-dryer.
    c. Weigh out dry sample material into digestion vessels.
    d. Digest sample material using closed-vessel hot-plate techniques or microwave digestion. For dried and powdered bivalve tissue samples, 100–600 mg sample is weighed out into Savillex® PFA vials. Closed-vessel digestion is carried out on a hotplate using successive steps of HNO_3 and HNO_3+H_2O_2. To determine the appropriate amount of sample material to be digested and loaded onto anion exchange chromatography columns the following must be considered:
        i. The quantity of analyte needed for the MC-ICP-MS isotopic analysis and trace element concentration determination. To avoid non-spectral matrix effects related to the presence of resin-derived organics and inorganic elements, sufficient quantities of sample material need to be loaded on the column so that no more than 20% of the Cd eluate cut is in the analyzed solution.
        ii. The column capacity for the analyte and matrix elements.
    e. Isolation of the analyte, i.e., Cd. The anion exchange chromatography procedure is given in Appendix B. The digested sample is loaded in 7 M HCl after being centrifuged to ensure undigested material is removed. Small volumes of the eluent (e.g., 2 mL) are loaded on the column to reduce the flow

rate of the solvent through the column and achieve better chromatographic separations. In addition, eluent volumes larger than those listed in Appendix B are used in some cases to ensure that the matrix elements and analytes are properly separated. For bivalve tissue samples, where [Zn]>>[Cd], ~16 mL of the eluent 0.1 M HBr+0.5 M HNO_3 is added 2 mL at a time, to ensure ~100% of the Zn is eluted before eluting the Cd and minimizing the quantity of Zn found in the Cd eluate cut. Cadmium is typically eluted using 14–16 mL of 0.5 M HNO_3 to ensure ~100% Cd recovery.

f. Cadmium eluate cuts were dried dry in Savillex® PFA vials. Dried eluate cuts are treated with HNO_3+H_2O_2, close-vessel digested overnight in an effort to digest any resin-derived organics and then dried again, driving off any traces of eluent acids (i.e., trace HCl, HF or HBr) and redissolved in 1 mL of 0.05 M HNO_3 in preparation for isotopic analysis.

2. Isotope analysis:
    a. Isotope ratios are measured by multi-collection on a Nu Plasma MC-ICP-MS (Nu 021; Nu Instruments, UK) using the DSN-100 (Nu Instruments, UK) membrane desolvator for sample introduction.
    b. The standard dry plasma cones (type B; Nu Instruments, UK) are used.
    c. A standard SSB measurement protocol is followed, where samples are run alternately with standards.
    d. The Cd isotope measurement method was adapted from Wombacher et al. (2003) and consists of a dynamic run with main and interference cycles that enable collection of masses 106 to 118 (isotopes of Cd, Ag and Sn). Correction of the Sn interference on ^{112}Cd, ^{114}Cd and ^{116}Cd is enabled by measurement of ^{118}Sn. An analysis comprises 2 blocks of 15 × 5 s integrations with a 20 s ESA deflected baseline before each block.
    e. Each sample is measured at least three times during at least two analytical sessions. Each analytical session is preceded by the measurement of (1) a zero-delta, by back-to-back analysis of the PCIGR-1 Cd standard (batch run of ≥7 runs, often run overnight), and (2) the PCIGR-2 Cd standard (n≥3). The

PCIGR-2 Cd standard is measured several more times during the analytical session, typically as every fourth sample.

f. The presence of matrix elements in analyzed solutions is routinely monitored to ensure any spectral and non-spectral matrix effects are minimal. Particular attention is paid to potential isobaric interferences on isotopes of the analyte of singly and doubly charged elements and polyatomic species. Analyzed Cd solutions are monitored for $ZnAr^+$ by measuring the intensity at mass 104 ($^{64}Zn^{40}Ar^+$; ^{64}Zn is the most abundant Zn isotope).

References

Wombacher, F., Rehkämper, M., Mezger, K., Munker, C. (2003) Stable isotope compositions of cadmium in geological materials and meteorites determined by multiple-collector ICPMS. Geochimica et Cosmochimica Acta 67: 4639–4654.

Appendix J Stanley Park trees

Introduction

Stanley Park was established in 1888 and is the largest and most visited park in Vancouver, B.C. Windstorms during the winter of 2006–2007 resulted in the loss of more than 10,000 trees (between 5 and 10% of all trees) in Stanley Park. Three fallen trees from Stanley Park were sampled in order to reconstruct the history of Pb pollution for the Vancouver area. Lead isotope ratios of the annual growth rings of these trees will be used to identify the sources of atmospheric lead through time.

Sample selection

Alyssa E. Shiel obtained permission for the sampling of fallen trees in Stanley Park from Jim Lowden and Yuna Flewin. Trees were selected for sampling by Alyssa E. Shiel with the assistance of Paul Lawson (Forest Manager, Malcolm Knapp Research Forest, UBC) on April 11, 2007. Samples were selected from the north side of Stanley Park near Prospect Point (Appendix K), which suffered moderate to severe forest damage during the 2006–2007 winter storms. Three trees were selected for sampling: (1) a Western Hemlock, (2) a Douglas Fir (located closest to Prospect Point, adjacent to a parking lot) and (3) a Western Red Cedar. Cookie samples (Appendix L) were taken using chainsaws, April 12 and 13, 2007, by park staff (Eric Meagher, Supervisor, Stanley Park Maintenance). Samples were picked up from the park and transported to UBC on April 13, 2007 and left to dry (exposed to rainwater and hosed off at the park prior to pick up). Photographs of the fallen trees in Stanley Park and of sample selection are shown in Appendix M.

Sample preparation and analytical methods

Cookie samples of each tree were quartered and then cut down to manageable sizes (core samples) using a band saw (Appendix M) with the help of Dr. Kyu-Young Kang (Department of Forestry, UBC). Core samples were scanned to create a digital record of each before processing. Tree-ring counting was used to determine the age of each tree and was accomplished by direct observation and using the digital images. Tree-

rings of the Western Hemlock (tree 1) and the Western Red Cedar (tree 3) were formed between 1881 and 2006 (over 125 years) and between 1801 and 2006 (over 205 years), respectively. Photographs of sample preparation are shown in Appendix M.

The core was separated into tree-ring samples, representing between one and nine years (depending on the size of the individual rings), using a stainless steel knife. Samples were blown off with N_2 gas, transferred to pre-weighed vials (cleaned with Citranox® detergent and 1 M HCl, analytical grade), freeze-dried and weighed. Selected samples were transferred to savillex® vials and then close-vessel digested on a hotplate using successive treatments of HNO_3 and HNO_3+H_2O_2. An aliquot of each sample was set aside for Pb concentration determination. Sample Pb was isolated from the remaining sample by anion exchange chromatography using the AG 1-X8 (100–200 mesh) resin (Bio-Rad Laboratories, Inc.).

Experimental work was carried out in metal-free Class 1,000 clean laboratories at the Pacific Centre for Isotopic and Geochemical Research (PCIGR), University of British Columbia (UBC). Sample preparation for elemental and isotopic analyses was performed in Class 100 laminar flow hoods in the clean labs and instrument rooms. Elemental analysis was carried out on an ELEMENT2 (Thermo Finnigan, Germany) high-resolution inductively coupled plasma mass spectrometer (HR-ICP-MS). The trace element analysis method and instrument set-up are described in Section 2.2.4.1. Isotopic analysis was performed on a Nu Plasma (Nu 021; Nu Instruments, UK) multi-collector inductively coupled plasma mass spectrometer (MC-ICP-MS). The isotopic analysis method for Pb is described in Section 3.2.5.2.2.

Results

Preliminary results for the Western Hemlock (tree 1) and the Western Red Cedar (tree 3) are in Appendices N and O. Lead concentration data needs to be interrupted with caution as growth rate of the tree-rings can influence the concentration of elements in the wood. Neighboring trees should display similar radial (i.e., across the tree-rings) patterns in Pb concentration and isotopic composition. Differences observed between the temporal records in Pb isotopic composition (Appendices N and O) of the Western Hemlock (tree 1) and the Western Red Cedar (tree 3) may be attributed to the movement of Pb in a

radial direction. Further study is needed to determine if the temporal record of Pb pollution is preserved in the annual tree-rings of the three sampled Stanley Park trees.

Recommendations for future work

1. Combust tree-ring samples prior to digestion.
2. Compare temporal trends recorded in the tree-rings of the Douglas Fir (tree 2) with the results for the Western Hemlock (tree 1) and the Western Red Cedar (tree 3).
3. Compare the Pb distribution patterns recorded in several radial cores of the same tree sample.
4. Calculate Pb enrichment factors in the tree-rings by measuring the ratio of Pb and a lithogenic element (e.g., Sc). Critically evaluate the significance of trends in Pb enrichment factors and [Pb].

Appendix K Stanley Park trees, sampling locations of three trees are indicated by green stars and identified as tree 1 (Western Hemlock), tree 2 (Douglas Fir) and tree 3 (Western Red Cedar).

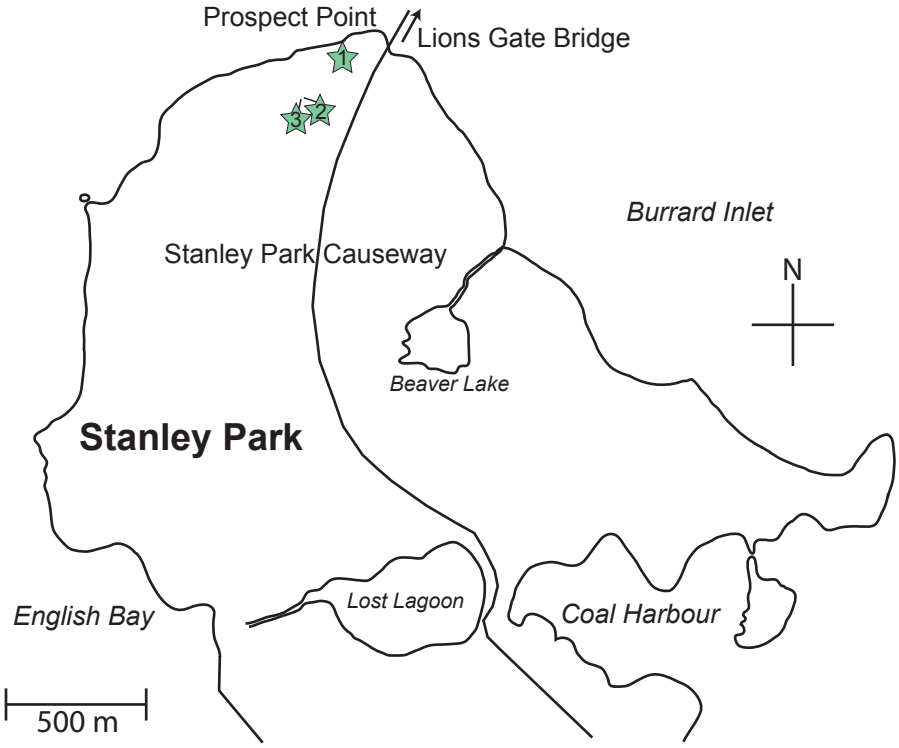

Appendix L Stanley Park trees, core sampling of the fallen trees. Fallen trees (a) were sampled first as cookies or disks (b). These cookie samples (b) were then quatered (c). A straight cut was made across each of the cookie quarters (c) creating boards (d). These boards (d) were then cut into strips (e), where each strip (e) is the equivalent of a core, which samples across the tree rings.

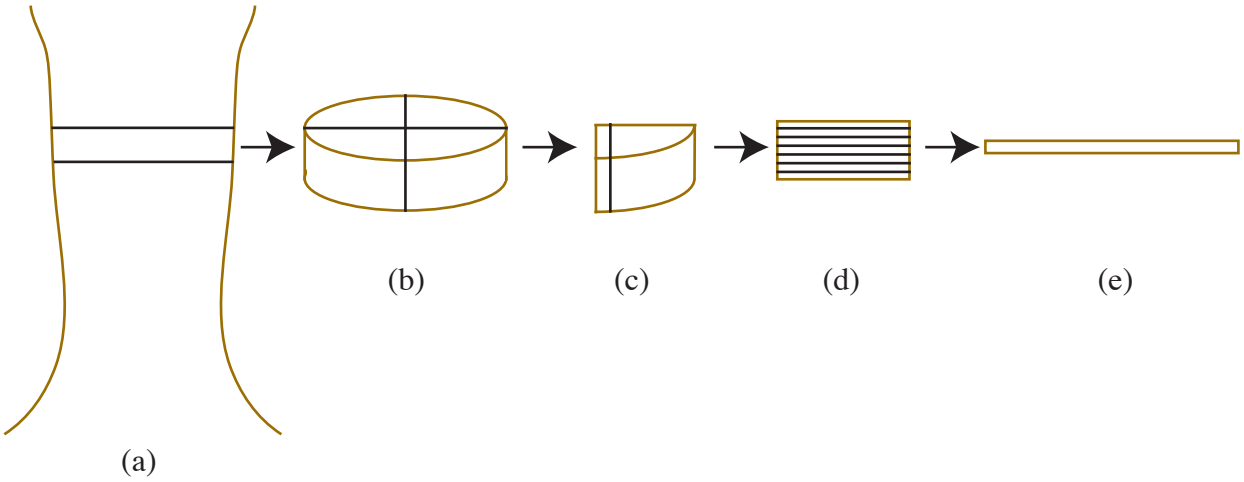

Appendix M Stanley Park trees, photographs of fallen trees, sample selection and preparation.

Appendix N Stanley Park trees, Pb concentrations and isotopic compositions of tree-ring samples.

Tree-ring years		[Pb] ppm[a]	$^{206}Pb/^{204}Pb$	2SE[b,c]	$^{207}Pb/^{204}Pb$	2SE[b,c]	$^{208}Pb/^{204}Pb$	2SE[b,c]	$^{206}Pb/^{207}Pb$	2SE[b,c]	$^{208}Pb/^{206}Pb$	2SE[b,c]
Western Red Cedar (tree 3)												
1917	1920	0.02	17.7462	49	15.5333	45	37.544	14	1.14252	6	2.11575	11
1928	1932		17.8309	19	15.5477	14	37.600	4	1.14687	2	2.10872	6
1936	1940	0.04	17.8766	20	15.5480	19	37.640	5	1.14972	3	2.10558	7
1950	1953	0.07	17.7624	9	15.5506	11	37.512	3	1.14227	2	2.11179	5
1964	1972		17.7375	7	15.5501	7	37.499	2	1.14065	1	2.11408	4
1979	1984	2.3	17.6517	8	15.5452	7	37.406	2	1.13550	1	2.11909	4
1991	1994	5.7	17.6856	8	15.5480	7	37.444	2	1.13748	1	2.11723	3
2002	2006	0.27	17.7180	7	15.5506	6	37.481	2	1.13936	1	2.11546	3
Western Hemlock (tree 1)												
1930	1933		17.4911	7	15.5434	8	37.255	2	1.12528	1	2.12997	4
1949	1953		17.5624	8	15.5426	7	37.325	2	1.12994	1	2.12535	3
1960	1963		17.5616	8	15.5412	9	37.324	2	1.12998	1	2.12536	3
1971	1971		17.5453	6	15.5436	7	37.325	2	1.12878	2	2.12738	4
1972	1972		17.5834	6	15.5492	7	37.370	4	1.13085	2	2.12518	4
1980	1981		17.6153	7	15.5538	7	37.392	2	1.13253	2	2.12270	4
1990	1990		17.6029	13	15.5505	13	37.382	3	1.13193	3	2.12369	4
1991	1991		17.6114	8	15.5537	7	37.396	2	1.13229	1	2.12341	4
2002	2006		17.7279	45	15.5601	45	37.532	10	1.13922	5	2.11707	4

[a]Pb concentrations were measured for a subset of samples.

[b]Ratios are reported as the mean ± 2 standard error (SE). Reported error values are the ten-thousandth ($^{206}Pb/^{204}Pb$, $^{207}Pb/^{204}Pb$), thousandth ($^{208}Pb/^{204}Pb$) or hundred-thousandth ($^{206}Pb/^{207}Pb$, $^{208}Pb/^{206}Pb$) decimal digit.

[c]All data have been normalized to the NIST SRM 981 triple spike Pb ratios of Galer and Abouchami, 1998.

Appendix O Stanley Park trees, Pb concentrations and $^{206}Pb/^{207}Pb$ values for tree-ring samples. For tree-ring year, (youngest tree-ring year + oldest tree-ring year) /2 is plotted. The error (2SE) on the $^{206}Pb/^{207}Pb$ value is smaller than the symbol size.